

THE EFFECTS OF MECHANICAL  
STIMULATION ON THE ORGANISATION  
AND EXPRESSION OF CYTOSKELETAL  
ELEMENTS AND EXTRACELLULAR  
MATRIX METABOLISM IN BOVINE  
INTERVERTEBRAL DISC CELLS

Siyuan Li BM MSc

A thesis submitted to Cardiff University in accordance with the  
requirements for the degree of Doctor of Philosophy in the school of  
Biosciences

May 2009

UMI Number: U585214

All rights reserved

INFORMATION TO ALL USERS

The quality of this reproduction is dependent upon the quality of the copy submitted.

In the unlikely event that the author did not send a complete manuscript and there are missing pages, these will be noted. Also, if material had to be removed, a note will indicate the deletion.



UMI U585214

Published by ProQuest LLC 2013. Copyright in the Dissertation held by the Author.  
Microform Edition © ProQuest LLC.

All rights reserved. This work is protected against  
unauthorized copying under Title 17, United States Code.



ProQuest LLC  
789 East Eisenhower Parkway  
P.O. Box 1346  
Ann Arbor, MI 48106-1346

## DECLARATION


This work has not previously been accepted in substance for any degree and is not concurrently submitted in candidature for any degree.

Signed.......... (candidate)

Date .....03/07/2009.....

## STATEMENT 1

This thesis is being submitted in partial fulfilment of the requirements for the degree of PhD in the School of Biosciences, Cardiff University.

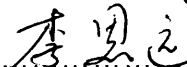
Signed.......... (candidate)

Date .....03/07/2009.....

## STATEMENT 2

This thesis is the result of my own independent work/investigation, except where otherwise stated.

Other sources are acknowledged by explicit references.

Signed.......... (candidate)

Date .....03/07/2009.....

## STATEMENT 3

I hereby give consent for my thesis, if accepted, to be available for photocopying and for inter-library loan, and for the title and summary to be made available to outside organisations.

Signed.......... (candidate)

Date .....03/07/2009.....

*Dedicated to my wife*

*Dr. Xiaoli Jia*

*In appreciation of her unconditional love, support*

*and encouragement throughout*

## **Acknowledgements**

*First and foremost I would like to thank my supervisors Prof. Vic Duance and Dr. Emma Blain for navigating me on this most difficult, sometimes despairing but eventually the most enjoyable study in my life – a Ph.D in the UK. Thanks a lot for your unconditional support and encouragement during my study, not only for helping with my experiments, but also with day-to-day life. Especially, I want to thank you both for your patience in correcting my “ugly English” in writing up. Without your help, it is almost a mission impossible for myself! Big thanks to the DHPA funding which gave me the opportunity to study in the UK and complete this challenging and interesting project.*

*To the member of Lab C5.11 –a big thank-you to Drs. Debbie Mason, Sophie Gilbert, Rhian Thomas and Sim Singhrao and Rebecca Harrison, for kindly helping me troubleshoot during my experiments, and of course the sharing of the daily coffee and cake time which gradually become my habit here. To Dr. Anthony Hayes, thanks a lot for assistance with the scanning confocal microscope.*

*A big thank-you to Prof. Bruce Caterson and Dr. Clare Hughes – for the kind invitation for my first trip to the sea side, the delicious Sunday Roast and of course the support for my continuous study and work here. To Prof. Jungling Cao, thank you very much for your support and help throughout my PhD.*

*I would like to acknowledge the support received from CTBL and the friendships forged over the 3 years – particularly Iris Chung. Thanks to Dr. Alvian Kwan who introduced me to the exercise of Kungfu which gives me a lot of fun. A big thank-you to Drs. Shane Wainwright, Claire Gealy, Radha Nair-Roberts, and Amy Wright for your support during my writing up.*

*Thanks a lot for the friendships and support from Drs. Yadan Zhang and Shanshan Huang, Wentao Sun, Tingting Wang, Liangge Chen, Jia Sun, Xuedong Zhao, Na Li and Martin Weinel, who share the daily happiness with me.*

*Finally, I would like to acknowledge the self-giving support and encouragement from my parents, my wife Dr. Xiaoli Jia and my daughter Niuniu. Without you, I could not have done it alone in the UK.*

***Thank you all with much appreciation.***

## Abbreviations

ADAM	a protein with a disintegrin and metalloprotease domain
ADAMTS	ADAM with a thrombospondin-like motif
ADP	adenosine diphosphate
ATP	adenosine triphosphate
AF	annulus fibrosus
AJ	apophyseal joint
BCA	bicinchoninic acid
BSA	bovine serum albumin
bp	Base pair
CC	coccygeal disc
cDNA	complementary deoxyribonucleic acid
CEP	cartilaginous endplates
CILP	cartilage intermediate layer protein
COMP	cartilage oligomeric matrix protein
CS	chondroitin sulfate
Ct	threshold cycle
CTS	cyclic tensile strain
	complement C1r/C1s-urchin epidermal growth factor-bone
CUB	morphogenetic protein-1 domain
Cys	cysteine-rich domain
Da	dalton
dH <sub>2</sub> O	distilled water
Dis	disintegrin-like domain
DMEM	Dulbecco's Modified Eagle Medium
DNA	deoxyribonucleic acid
dNTP	deoxy-ribonucleotide triphosphate
DTT	dithiothreitol
EBSS	Earle's Balanced Salt Solution

ECL	enhanced chemiluminescence
ECM	extracellular matrix
ERK	extracellularly related kinase
F-actin	filament actin
FBS	fetal bovine serum
Fn	fibronectin
g	gram
G-actin	globular actin
GAPDH	glyceraldehyde 3-phosphate dehydrogenase
Hz	hertz
IAF	inner annulus fibrosus
IF	Intermediate filament
IgG	Immunoglobulin G
IPTG	isopropyl $\beta$ -D-1-thiogalactopyranoside
ITS	insulin-transferrin-sodium selenite
IVD	intervertebral disc
KS	keratan sulfate
LDH	lactate dehydrogenase
MAPK	mitogen-activated protein kinase
mHBSS	modified Hank's balanced salt solution
MMP	matrix metalloproteinase
MPa	mega pascals
mRNA	message ribonucleic acid
N	Newtons
NC	non-collagenous
NF- $\kappa$ B	nuclear factor kappa-light-chain-enhancer of activated B cells
NO	nitric oxide
NP	nucleus pulposus
NR	nerve root
OA	osteoarthritis
OAF	outer annulus fibrosus

PBS	phosphate buffered saline
PCR	polymerase chain reaction
PLAC	proteinase and lacunin domain
PVDF	polyvinylidene fluoride
RNA	ribonucleic acid
RNase	ribonuclease
ROCK	Rho-dependent kinase
ROK $\alpha$	RhoA-binding kinase $\alpha$
rpm	revolutions per minutes
SC	spinal cord
SDS	Sodium dodecyl sulphate
SDS-PAGE	sodium dodecyl sulphate-polyacrylamide gel electrophoresis
SLRPs	small leucine-rich proteoglycans
SP	signal peptide
TBS	tris buffered saline
TEMED	tetramethylethylenediamine
TGF $\beta$	transforming growth factor $\beta$
TIMP	tissue inhibitor of matrix metalloproteinase
TM	transmembrane domain
TS	thrombospondin type I motif
U	unit
V	volt
v/v	volume/volume
w/v	weight/volume
VB	vertebral body
X-gal	5-bromo-4-chloro-3-indolyl- $\beta$ -D-galactosidase



## Abstract

**Introduction:** Disc degeneration is the primary cause of low back pain. Due to the main function of the spine, mechanical stimuli play a pivotal role in the development of disc degeneration. Previous studies have shown that cytoskeletal elements are involved in the mechanotransduction pathways between the extracellular matrix (ECM) and cell nucleus. However, the precise mechanism of this mechano-induced signalling is not clear in the intervertebral disc (IVD). Therefore, the effects of tensile strain and compression on the organisation and expression of cytoskeletal elements in bovine disc cells and on ECM metabolism molecules were investigated using confocal microscopy, real-time PCR, Western blotting, gelatin zymography and reverse gelatin zymography.

**Results:** (i) **In situ:** F-actin filaments were punctate and distributed beneath the cell membrane in both nucleus pulposus (NP) and outer annulus fibrosus (OAF). There was higher  $\beta$ -actin expression in the OAF than NP.  $\beta$ -tubulin filaments formed a meshwork distributed throughout the cytoplasm with more  $\beta$ -tubulin gene and protein expression in the NP. Vimentin filaments formed a meshwork distributed throughout the cytoplasm with lower vimentin protein content in the OAF. There was less vimentin protein, but an increase in partially degraded vimentin in OAF with maturity. (ii) **Cyclic tensile strain (CTS):** CTS promoted the reorganisation of F-actin and  $\beta$ -tubulin networks and increased both their mRNA and protein expression, whilst reducing vimentin levels. CTS differentially-regulated mRNA expression levels of MMPs and TIMPs suggesting accelerated ECM remodelling processes in IVD cells. OAF cells are more responsive to tensile strain than NP cells. Stretch-induced mechano-responses in IVD cells are age and strain-dependent. Age delayed the cell's response to tensile force. Low (5%) and medium (10%) strains induced anabolic effects but high strain (15%) induced more catabolic responses. (iii) **Compressive loading:** Compressive loading (10%, 1Hz) altered the architecture of F-actin,  $\beta$ -tubulin and vimentin filaments, along with an increase in  $\beta$ -tubulin mRNA and a decrease in vimentin and vinculin gene expression. Compressive loading increased transcription of matrix molecules and decreased mRNA levels of catabolic enzymes in IVD cells, suggesting an overall anabolic effect of physiological compression on IVD cell metabolism. Ageing delayed or reversed these mechano-responses in mature IVD cells.

**Conclusion:** Cytoskeletal elements including  $\beta$ -actin,  $\beta$ -tubulin and vimentin are involved in strain-induced and compression-induced mechanotransduction in IVD cells. NP and OAF cells respond differently to the type of mechanical stimulus applied. However physiological loads induce matrix synthesis in NP and OAF cells, whilst non-physiological strains promote a catabolic phenotype. Ageing can delay the cell's response to mechanical load which may induce "abnormal" ECM remodelling events, and increase the potential risk of a loss of tissue homeostasis and the likelihood of disc degeneration.

**CHAPTER 1.....1**

1.1 Intervertebral Disc .....	1
1.1.1 IVD structure.....	1
1.1.1.1 Annulus Fibrosus .....	1
1.1.1.2 Nucleus Pulposus.....	3
1.1.1.3 Cartilaginous Endplate.....	3
1.1.2 IVD Development .....	4
1.1.3 Cells of the IVD .....	5
1.1.3.1 Nucleus Pulposus.....	5
1.1.3.2 Inner Annulus fibrosus.....	6
1.1.3.3 Outer Annulus Fibrosus .....	6
1.1.4 Extracellular matrix components of the IVD.....	7
1.1.4.1 Water.....	7
1.1.4.2 Proteoglycans of the IVD.....	8
1.1.4.2.1 Aggrecan.....	9
1.1.4.2.2 Versican .....	10
1.1.4.2.3 Small leucine-rich proteoglycans (SLRPs).....	11
1.1.4.3 Collagens of the IVD .....	12
1.1.4.3.1 Types I and II collagen .....	13
1.1.4.3.2 Minor collagen components.....	13
1.1.4.3.3 Type VI Collagen.....	15
1.1.4.3.4 Type X collagen .....	15
1.1.4.3 Other Matrix Components of the IVD.....	15
1.2 IVD metabolism related enzymes.....	16
1.2.1 Matrix Metalloproteinases .....	17
1.2.2 Aggrecanases .....	18
1.2.3 Tissue Inhibitors of Metalloproteinases .....	20
1.3 Cytoskeleton in the IVD.....	21
1.3.1 Actin Microfilaments.....	22
1.3.2 Intermediate filaments .....	23
1.3.3 Microtubules .....	26
1.3.4 Cytoskeleton-associated proteins in IVD .....	27
1.3.4.1 Paxillin .....	27
1.3.4.2 Vinculin.....	28
1.4. The biomechanics of the IVD.....	29
1.4.1 IVD structure and biomechanical function.....	29
1.4.1.1 Annulus fibrosus.....	29
1.4.1.2. Nucleus pulposus.....	30
1.4.2. Forces acting on the IVD.....	31
1.4.2.1 Compression.....	31
1.4.2.2. Tension.....	32
1.4.2.3 Shear .....	33
1.4.3 Mechanical damage to the intervertebral disc.....	34
1.4.3.1 Compression.....	34
1.4.3.2 Compression and bending.....	35
1.4.3.3. Repetitive loading.....	35

1.5 Biomechanics and biochemical changes of IVD .....	35
1.5.1 Compression.....	36
1.5.2. Tensile forces .....	37
1.6 Ageing and IVD degeneration.....	37
1.6.1 Macroscopic Changes with Increasing Age.....	37
1.6.2 Changes in Matrix Components with Age.....	38
1.6.3 Changes in Matrix Turnover and Catabolism with Age.....	38
1.7 Pathology of low back pain .....	39
* 1.8 Hypothesis .....	43
* 1.9 Project Aims .....	43

## **CHAPTER 2..... 44**

2.1 Background.....	45
→ 2.2 Materials and Methods.....	47
2.2.1 Source of Bovine Intervertebral Discs.....	47
2.2.2 Analysis of cytoskeletal element organisation using confocal microscopy.....	47
2.2.3 Analysis of cytoskeletal element gene expression using quantitative polymerase chain reaction.....	49
2.2.3.1 Total RNA extraction.....	49
2.2.3.2 cDNA synthesis .....	50
2.2.3.3 Generation of plasmid standards for real-time PCR.....	50
2.2.3.3.1 Amplification of target gene by PCR.....	50
2.2.3.3.2 PCR product clean up.....	50
2.2.3.3.3 pGEM <sup>®</sup> -T Easy Vector ligation .....	51
2.2.3.3.4 Transformation of competent <i>E. Coli</i> cells with the ligated pGEM <sup>®</sup> -T Easy Vector.....	52
2.2.3.3.5 Plasmid extraction and purification.....	52
2.2.3.4 Real-time PCR.....	53
2.2.3.4.1 Real-time PCR background .....	53
2.2.3.4.2 Setting up a standard curve using plasmid DNA .....	53
2.2.3.4.3 Real-time PCR .....	54
2.2.3.4.4 Method of quantification for real-time PCR.....	56
2.2.4 Determination of protein concentration using the BCA assay....	59
2.2.5 Determination of total cell number and cell viability using the lactate dehydrogenase assay .....	60
2.2.6 Determination of total cell number according to DNA concentration.....	60
2.2.7 Analysis of proteins using Western Blotting .....	61
2.2.7.1 Sample preparation .....	61
2.2.7.2 Sodium dodecyl sulphate-polyacrylamide gel electrophoresis .....	62
2.2.7.3 Preparation of transfer membrane .....	62
2.2.7.4 Transfer of proteins from SDS-PAGE gel to PVDF membrane.....	63
2.2.7.5 Immuno-probing of membrane.....	63

2.2.7.6	Detection of immunoreactive bands .....	65
2.2.8	Statistical Analysis .....	65
2.3	Results .....	66
2.3.1	Normalisation methods .....	66
2.3.2	Confirmation of successful separation of nucleus pulposus from outer annulus fibrosus of the disc .....	66
2.3.3	Differential F-actin organisation and $\beta$ -actin mRNA and protein expression in IVD .....	69
2.3.3.1	F-actin organisation differs between NP and OAF .....	69
2.3.3.2	Increased $\beta$ -actin mRNA and protein expression in OAF .....	69
2.3.4	Differential $\beta$ -tubulin mRNA and protein expression in IVD ....	75
2.3.4.1	$\beta$ -tubulin organisation does not alter between NP and OAF .....	75
2.3.4.2	Increased $\beta$ -tubulin mRNA and protein expression in NP .....	75
2.3.5	Differential vimentin organisation, mRNA and protein expression in IVD .....	79
2.3.5.1	Vimentin organisation differs between NP and OAF .....	79
2.3.5.2	Differential vimentin mRNA and protein expression in NP and OAF .....	81
2.4	Discussion .....	84
2.5	Conclusions .....	87

## **CHAPTER 3..... *Effect of cyclic stretching on cyto of IV disc* ..... 89**

3.1	Background .....	90
3.2	Materials and Methods .....	94
3.2.1	Cell isolation and cell culture .....	94
3.2.2	Application of cyclic tensile strain .....	95
3.2.3	Determination of cell viability using the LDH assay .....	96
3.2.4	Analysis of cytoskeletal element organisation using confocal microscopy .....	96
3.2.5	Analysis of cytoskeletal element gene expression using quantitative PCR .....	97
3.2.6	Analysis of protein expression within cells using Western Blotting .....	102
3.2.7	Analysis of MMPs using gelatin zymography .....	102
3.2.7.1	Sample preparation .....	102
3.2.7.2	Gelatin zymography analysis .....	104
3.2.7.3	Activation of MMPs .....	104
3.2.7.4	Staining and destaining of the gel .....	105
3.2.8	Analysis of TIMPs using reverse gelatin zymography .....	105
3.2.8.1	Sample preparation .....	105
3.2.8.2	SDS-PAGE gel electrophoresis .....	105
3.2.8.3	Activation of MMPs .....	106
3.2.8.4	Staining and destaining of the gel .....	106
3.2.9	Statistical Analysis .....	106

3.3 Results	107
3.3.1 Effect of stretching on cell viability	107
3.3.2 Characterisation of the phenotype of IVD cells in monolayer culture	107
3.3.3 The effect of tensile force on $\beta$ -actin filaments	110
3.3.3.1 Tensile force alters the organisation of F-actin in IVD cells	110
3.3.3.2 CTS promoted $\beta$ -actin gene and protein expression in IVD cells	111
3.3.3.2.1 Tensile strain promotes $\beta$ -actin gene expression in NP and OAF cells	111
3.3.3.2.2 Tensile strain promotes $\beta$ -actin protein expression in both NP and OAF cells	115
3.3.4 CTS altered actin-binding protein gene expression in IVD cells	115
3.3.5 The effect of tensile force on $\beta$ -tubulin filaments	118
3.3.5.1 Tensile force altered the organisation of $\beta$ -tubulin in IVD cells	118
3.3.5.2 Tensile strain promoted $\beta$ -tubulin gene and protein expression in OAF cells	121
3.3.5.2.1 Tensile strain promoted $\beta$ -tubulin gene expression in OAF cells	121
3.3.5.2.2 Tensile strain promoted $\beta$ -tubulin protein expression in OAF cells	121
3.3.6 The effect of tensile force on vimentin filaments	124
3.3.6.1 Tensile force did not alter the organisation of vimentin in IVD cells	124
3.3.6.2 Tensile strain inhibited vimentin gene and protein expression in OAF cells	127
3.3.6.2.1 Tensile strain decreased vimentin gene expression in OAF cells	127
3.3.7 Effect of CTS on the metabolism of ECM components	130
3.3.8 Effect of CTS on the metabolism of ECM-degrading enzymes	132
3.3.8.1 CTS altered ECM-degrading enzymes gene expression in OAF cells	132
3.3.8.2. CTS did not alter pro MMP-2 expression in culture media	134
3.3.9 CTS altered TIMPs-1 and 2 expression in IVD cells	134
3.3.9.1 CTS did not affect TIMPs-1, 2 or 3 gene expression in IVD cells	134
3.3.9.2 CTS altered TIMP-1 and 2 protein expression in IVD cells	134
3.3.9.3 CTS inhibited TIMP-2 protein expression in IVD cells	135
3.3.10 Summary	138
3.4.1 Effect of CTS on the cytoskeletal elements in NP and OAF cells	140
3.4.2 Effect of CTS on ECM synthesis	144
3.4.3 Effect of CTS on ECM remodelling proteases and inhibitors	145

**CHAPTER 4.....155**

4.1 Background.....	150
4.2 Materials and Methods.....	152
4.2.1 Cell isolation and cell culture.....	152
4.2.2 Application of cyclic tensile strain.....	152
4.2.3 Analysis of cytoskeletal element organisation using confocal microscopy.....	153
4.2.4 Analysis of cytoskeletal element gene expression using quantitative PCR.....	153
4.2.5 Determination of total cell number using the lactate dehydrogenase assay.....	153
4.2.6 Analysis of protein expression within cells using Western Blotting.....	154
4.2.7 Determination of MMP expression and activation using gelatin zymography.....	154
4.2.8 Determination of TIMP expression using reverse gelatin zymography.....	154
4.2.9 Statistical Analysis.....	155
4.3 Results.....	156
4.3.1 Characterisation of the phenotype of IVD cells in monolayer culture.....	156
4.3.2 The effect of tensile force on $\beta$ -actin filaments.....	158
4.3.2.1 Tensile force alters the organisation of F-actin in IVD cells.....	158
4.3.2.2 Tensile force alters $\beta$ -actin mRNA levels in IVD cells.....	161
4.3.2.3 Tensile force alters $\beta$ -actin protein expression in IVD cells.....	161
4.3.3 The effect of tensile force on $\beta$ -tubulin filaments.....	164
4.3.4 The effect of tensile force on vimentin filaments.....	170
4.3.4.1 Tensile force did not alter the organisation of vimentin in IVD cells.....	170
4.3.5 The effect of CTS on markers of ECM metabolism.....	176
4.3.6 The effect of CTS on ECM remodelling enzymes.....	179
4.3.7 Tensile force altered MMP-2 protein expression in IVD cells.....	183
4.3.8 Tensile force altered TIMPs expression in IVD cells.....	185
4.3.8.1 Tensile force altered TIMPs-1 and 2 mRNA expression in IVD cells.....	185
4.3.8.2 Tensile force did not alter TIMPs-1 and 2 protein expression in IVD cells.....	188
4.3.9 Summary.....	188
4.4 Discussion.....	190
4.4.1 Effect of CTS on the cytoskeletal elements in NP and OAF cells.....	190
4.4.2 Effect of CTS on ECM synthesis.....	192
4.4.3 Effect of CTS on ECM remodelling proteases and inhibitors.....	193
4.4.4 Conclusion.....	196

**CHAPTER 5.....202**

5.1 Background.....	198
5.2 Materials and methods .....	201
5.2.1 Cell isolation .....	201
5.2.2 Cell culture in agarose gel .....	201
5.2.3 Application of cyclic compressive loading.....	202
5.2.4 Live-dead cell assay .....	204
5.2.5 Analysis of cytoskeletal element organisation using confocal microscopy.....	204
5.2.6 RNA extraction from agarose-cell plugs .....	204
5.2.7 Analysis of gene expression using quantitative PCR.....	205
5.2.8 Statistical Analysis .....	206
5.3 Results .....	207
5.3.1 Cell viability did not change after compressive loading .....	207
5.3.2 Characterisation of the IVD cell phenotype in an agarose gel.....	209
5.3.3 The effect of cyclic compressive loading on the organisation and gene expression of F-actin in IVD cells .....	210
5.3.3.1 Compressive loading altered F-actin organisation .....	210
5.3.3.2 Compressive loading did not change $\beta$ -actin gene expression .....	214
5.3.4 Compressive loading altered vinculin gene expression in IVD cells .....	214
5.3.5 Compressive loading did not change actin-related protein gene expression in IVD cells .....	216
5.3.6 The effect of cyclic compressive loading on the organisation and gene expression of $\beta$ -tubulin filaments in the IVD cells.....	216
5.3.6.1 Compressive loading did not change $\beta$ -tubulin organisation .....	216
5.3.6.2 Compressive loading altered $\beta$ -tubulin gene expression.....	219
5.3.7 The effect of cyclic compressive loading on the organisation and gene expression of vimentin filaments in the IVD cells .....	219
5.3.7.1 Compressive loading changed vimentin organisation .....	219
5.3.7.2 Compressive loading altered vimentin gene expression .....	223
5.3.8 Compressive loading altered types I and II collagen and aggrecan gene expression.....	223
5.3.9 Compressive loading altered ECM degradative enzymes gene expression .....	227
5.3.10 Compressive loading altered TIMP-1 and TIMP-2 gene expression in IVD cells .....	230
5.3.11 Summary .....	230
5.4 Discussion.....	233
5.4.1 IVD cells remain their phenotypes in 3D culture system .....	233
5.4.2 Effect of compression on the cytoskeletal elements in IVD cells .....	235
5.4.3 Effect of compression on ECM remodelling proteases and inhibitors.....	239

5.5 Conclusion.....	241
<b><i>BIBLIOGRAPHY.....</i></b>	<b>262</b>
<b><i>APPENDICES.....</i></b>	<b>295</b>
Appendix 1.....	290
Appendix 2.....	291
Appendix 3.....	292
Appendix 4.....	293
<b><i>PUBLICATIONS.....</i></b>	<b>289</b>



# List of Figures

## Chapter 1

Figure 1-1. A schematic view of a spinal segment and the intervertebral disc.....	2
Figure 1-2. Diagram showing the lamellae structure of collagen fibres in the annulus fibrosus.....	2
Figure 1-3. The relative proportions of the extracellular matrix composition in normal human adult intervertebral disc and endplate.....	8
Figure 1-4 A structural model of aggrecan.....	10
Figure 1-5. A structural model of versican.....	12
Figure 1-6 The domain structure of MMPs ( <i>Adapted from Lemaitre V, D'Armiento J. Birth Defects Res C Embryo Today. 2006, 78(1):1-10</i> ).....	18
Figure 1-7 Domain arrangements of ADAMTS, ADAMs and MMPs.....	20
Figure 1-8. Schematic representation of cytoskeletal element structures and assembly.....	25
Figure 1-9. A comparison between data of Nachemson (Nachemson and Morris, 1964) and those of Wilke (Wilke et al., 1999).....	33
Figure 1-10. The three different types of annulus tears in the intervertebral disc.....	40
Figure 1-11. Different types of herniation in the intervertebral disc.....	41

## Chapter 2

Figure 2-1. Experimental setup for producing a standard curve for real-time PCR.....	55
Figure 2-2 Representative reaction conditions and dissociation curve for real-time PCR.....	57
Figure 2-3 Illustration of the theory behind standard curve quantification.. <b>Error! Bookmark not defined.</b>	
Figure 2-4 Schematic layout of transfer sandwich in Western Blotting.....	64

Figure 2-5 Investigation of the correlations between DNA concentration and LDH levels, as well as DNA concentration and protein levels.....	68
Figure 2-6 Western blot for types I and II collagen in protein extracted from young and mature bovine IVD.....	70
Figure 2-7 Immunofluorescent localisation of F-actin in young and mature bovine IVD.....	71
Figure 2-8 $\beta$ -actin mRNA and protein expression in young and mature nucleus pulposus and outer annulus fibrosus.....	74
Figure 2-9. Immunofluorescent localisation of $\beta$ -tubulin in young and mature bovine intervertebral disc.....	76
Figure 2-10 $\beta$ -tubulin mRNA and protein expression in young and mature nucleus pulposus and outer annulus fibrosus.....	78
Figure 2-11 Immunofluorescent localisation of vimentin in young and mature bovine intervertebral disc.....	80
Figure 2-12 Vimentin mRNA and protein expression in young and mature nucleus pulposus and outer annulus fibrosus.....	83

### Chapter 3

Figure 3-1 Explanatory diagram of the calculation of the fold-change in mRNA levels.....	103
Figure 3-2 Effect of stretch on cell viability.....	108
Figure 3-3 Zonal differences in ECM component gene expression in unstretched IVD cells.....	109
Figure 3-4 Localisation of F-actin filaments in nucleus pulposus cells cultured on type I collagen as a monolayer.....	114
Figure 3-5 $\beta$ -actin gene expression in bovine intervertebral disc cells subjected to tensile strain.....	114
Figure 3-6 $\beta$ -actin protein expression in NP and OAF cells subjected to cyclic tensile strain.....	116
Figure 3-7 Actin-binding protein gene expression in bovine intervertebral disc cells subjected to tensile strain.....	117

Figure 3-8. Localisation of $\beta$ -tubulin in nucleus pulposus cells cultured on type I collagen as a monolayer.....	121
Figure 3-9 $\beta$ -tubulin gene expression in bovine intervertebral disc cells subjected to tensile strain.....	122
Figure 3-10 $\beta$ -tubulin protein expression in NP and OAF cells subjected to cyclic tensile strain.....	123
Figure 3-11. Localisation of vimentin in nucleus pulposus cells cultured on type I collagen as a monolayer.....	127
Figure 3-12 Vimentin gene expression in bovine intervertebral disc cells subjected to tensile strain. ....	128
Figure 3-13 Vimentin protein expression in NP and OAF cells subjected to cyclic tensile strain.....	129
Figure 3-14. ECM component mRNA levels in NP and OAF cells subjected to cyclic tensile strain.....	131
Figure 3-15. ECM-degrading enzymes mRNA levels in NP and OAF cells subjected to cyclic tensile strain.....	133
Figure 3-16. TIMP-1 levels in NP and OAF cells.....	136
Figure 3-17 TIMP-2 levels in NP and OAF cells.....	137

## Chapter 4

Figure 4-1 Zonal and age-related differences in types I and II collagen and aggrecan mRNA levels in bovine IVD cells. ....	157
Figure 4-2. Localisation of F-actin filaments in nucleus pulposus and outer annulus fibrosus cells cultured on type I collagen as a monolayer. ....	161
Figure 4-3. $\beta$ -actin mRNA expression in IVD cells subjected to different magnitudes of cyclic tensile force.. ....	162
Figure 4-4. $\beta$ -actin protein expression in IVD cells after being subjected to different magnitudes of cyclic tensile force. ....	163
Figure 4-5. Localisation of $\beta$ -tubulin filaments in nucleus pulposus and outer annulus fibrosus cells in monolayer cultured on type I collagen.. ....	167
Figure 4-6. $\beta$ -tubulin mRNA expression in IVD cells subjected to different magnitudes of cyclic tensile force.. ....	168

Figure 4-7. $\beta$ -tubulin protein expression in IVD cells after being subjected to different magnitudes of cyclic tensile force.....	169
Figure 4-8. Localisation of vimentin filaments in nucleus pulposus and outer annulus fibrosus cells cultured on type I collagen as a monolayer.....	173
Figure 4-9. Vimentin mRNA expression in IVD cells after being subjected to different magnitudes of cyclic tensile force.....	174
Figure 4-10 Vimentin protein expression in IVD cells after being subjected to different magnitudes of cyclic tensile force.....	175
Figure 4-11 mRNA expression levels for ECM-markers in IVD cells subjected to different magnitudes of cyclic tensile force.....	178
Figure 4-12. ECM remodelling enzyme mRNA expression in IVD cells subjected to different magnitudes of cyclic tensile force.....	182
Figure 4-13 Pro MMP-2 in culture media from bovine NP and OAF cells subjected to tensile strain .....	184
Figure 4-14 TIMP-1 and TIMP-2 mRNA expression in IVD cells subjected to different magnitudes of cyclic tensile force.....	187

## Chapter 5

Figure 5-1. Custom-built compressive loading apparatus.....	203
Figure 5-2. Live-dead cell assay results after compressive loading.....	208
Figure 5-3 Maintenance of NP and OAF phenotypes after seeding cells in a 3-D environment.....	211
Figure 5-4 The organisation of F-actin filaments within cells subjected to compressive loading.....	214
Figure 5-5 Vinculin gene expression in intervertebral disc cells subjected to compressive loading.....	215
Figure 5-6 The organisation of $\beta$ -tubulin filaments within cells subjected to compressive loading.....	219
Figure 5-7 $\beta$ -tubulin gene expression in intervertebral disc cells subjected to compressive loading.....	220
Figure 5-8 The organisation of vimentin filaments within cells subjected to compressive loading.....	223

Figure 5-9 Vimentin gene expression in intervertebral disc cells subjected to compressive loading. ....	224
Figure 5-10 ECM component gene expression in intervertebral disc cells subjected to compressive loading. ....	226
Figure 5-11 ECM degradative enzyme mRNA in intervertebral disc cells subjected to compressive load. ....	237
Figure 5-12 TIMP-1 and TIMP-2 mRNA in intervertebral disc cells subjected to compressive loading. ....	232

## List of Tables

Table 2-1. PCR reaction mixture composition.....	51
Table 2-2. pGEM®-T Easy Vector ligation reaction components.....	51
Table 2-3 Real-time PCR reaction components.....	54
Table 2-4. Primer sequences for real-time quantitative PCR .....	58
Table 2-5 Reagents used to make up resolving and stacking gels required for ...	64
Table 3-1. Primer sequences for real-time quantitative PCR .....	98
Table 3-2 Reagents used to make up resolving and stacking gels required for gelatin zymography.....	104
Table 3-3 Reagents used to make up resolving and stacking gels required for reverse gelatin zymography .....	106
Table 3-4. The effects of CTS (10% elongation, 1Hz) on bovine IVD cells.....	139
Table 4-1 Summary for the effects of cyclic tensile force on bovine intervertebral disc cells .....	189
Table 5-1 Summary of mechanoresponsive genes in intervertebral disc cells ..	232

# CHAPTER 1.

Introduction

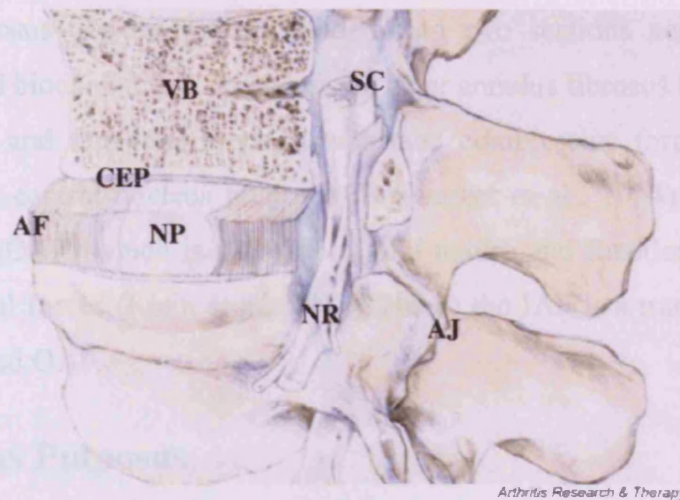


Figure 1-1. A schematic view of a spinal segment and the intervertebral disc. The figure shows the organisation of the disc with the nucleus pulposus (NP) surrounded by the lamellae of the annulus fibrosus (AF) and separated from the vertebral bodies (VB) by the cartilaginous end-plate (CEP). The figure also shows the relationship between the intervertebral disc and the spinal cord (SC), the nerve root (NR), and the apophyseal joints (AJ). Taken with permission from Urban et al. *Arthritis Res Ther* 2003 5:120

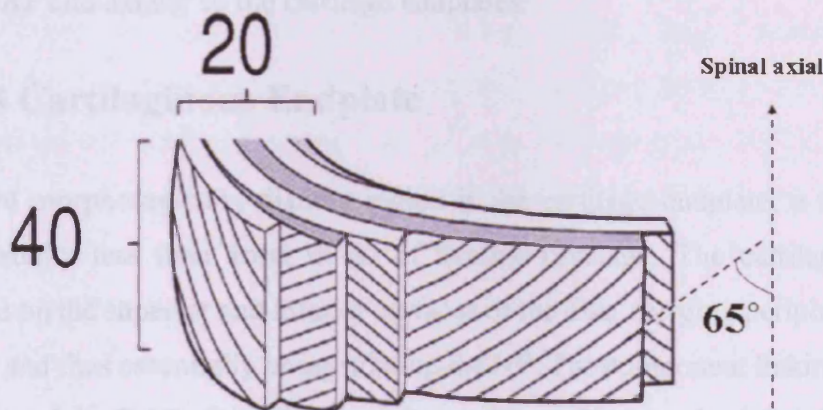


Figure 1-2. Diagram showing the lamellae structure of collagen fibres in the annulus fibrosus. The collagen fibres in the lamellae of the annulus fibrosus display an alternating direction, and form a 65° angle with the spinal axis. Typical values are given of the number of lamellae in the annulus and the number of collagen fibre bundles in a lamella. Adapted from Adams, M.A., and Roughley, P.J. 2006. *Spine*. 31:2151-61.

The annulus fibrosus can be further divided into two sections according to the morphological and biochemical differences: the inner annulus fibrosus (IAF), which is fibrocartilaginous and functions more to withstand compressive forces forming an interface with the central nucleus pulposus (Schwarzer et al., 1994), and the outer annulus fibrosus (OAF) which is more fibrous in nature and functions primarily to withstand tensional forces (Klein et al., 1983). Hence the IAF is a transitional region between the NP and OAF.

### **1.1.1.2 Nucleus Pulposus**

The NP is a highly hydrated structure, containing a large amount of proteoglycan and relatively few collagen fibres with sparse cells randomly distributed through the matrix (Meachim and Cornah, 1970). Although the NP exists as a discrete entity in the young, with ageing the interface with the inner annulus merges. The central NP contains collagen fibres, which are organized randomly, and elastin fibres (sometimes up to 150µm in length), which are arranged radially from the centre of the nucleus towards the disc periphery (Yu et al., 2002). The NP acts to dissipate compressive loads radially to the OAF and axially to the cartilage endplates.

### **1.1.1.3 Cartilaginous Endplate**

The third morphologically distinct region is the cartilage endplate, a thin horizontal layer, usually less than 1mm thick, of hyaline cartilage. The cartilage endplate is localised on the superior and inferior surfaces of the disc, merging peripherally with the annulus and thus essentially encapsulating the NP. The component linking the cartilage endplate and the OAF of the disc are collagen fibres. They run horizontally and parallel to the vertebral bodies continuously from the disc and thereby encapsulate these different components into an intact structure (Roberts et al., 1989). They are important shock absorbers protecting the vertebral body from axial loads and preventing the nucleus from bulging into the vertebral body. They are also important for disc nutrition.



## 1.1.2 IVD Development

Spinal column formation starts in the third week in the embryo from the central notochord and surrounding mesenchyme. The mesenchymal tissue forms the surrounding AF, whereas the notochord gives rise to the NP of the disc. Mesenchymal cells in the peripheral regions of the disc arrange themselves in a lamellar fashion and differentiate into fibroblasts, forming the OAF (Anderson and Tannoury, 2005). The notochordal cells in the central regions of the forming disc deposit a proteoglycan rich substance to form the extracellular matrix (ECM) of the NP (Walmsley, 1953). Therefore, the embryonic disc can be divided into two distinct parts according to the structure and composition: the fluid-like NP, rich in notochordal cells and proteoglycan, and the fibrous annulus fibrosus, rich in fibroblast-like cells as well as collagen. Above and below the embryonic discs is the forming cartilaginous endplates of the vertebrae, which are formed by the mesenchymal cells. The existence of notochordal cells in the embryonic disc persists till birth in the human being, and then slowly decline and are replaced by chondrocyte-like cells by age ten (Aguiar et al., 1999) through apoptosis or terminal differentiation (Roughley, 2004). In contrast, the notochordal cells persist through most of the adult life in some species (e.g., rodents, cats and non-chondrodystrophoid dogs). In other species such as horse and bovine disc, the notochordal cells disappear at the time of birth (Horner et al., 2002). It is presently uncertain the relationship between the notochordal cells and the chondrocyte-like cells in the NP. Some researchers believe that the chondrocytic cell phenotype is originally derived from the continued (possibly terminal) differentiation of the notochordal cells (Hunter et al., 2003). However, others believe that they are derived from the cells in cartilaginous endplates or AF, which subsequently invade the NP after the programmed death (apoptosis) of the notochordal cells (Hunter et al., 2003). The function of notochordal cells in the disc is not very clear, although some studies suggest that the notochordal cells can proliferate and synthesise extracellular matrix components, and stimulate matrix production (Cappello et al., 2006).

### **1.1.3 Cells of the IVD**

There is a very low cell density in IVD compared to most tissues especially in the NP, where cells make up approximately 1-2% of the tissue volume (Roberts et al., 2006). Cell density in the OAF is significantly higher than that of the NP. A fourfold increase in cell density was found proceeding from the NP to the OAF (Hastreiter et al., 2001).

Cell metabolism and synthesis of ECM molecules are essential to the maintenance of a healthy, functioning IVD. Disc cells are also responsible for ECM turnover and remodelling through the production of catabolic enzymes. The balance between catabolism and anabolism is crucial for ECM homeostasis. If excess enzymes are produced, there would be deleterious effects on the functional properties of the matrix. Moreover, there are at least two populations localised in different regions of the disc with distinct cell phenotypes.

#### **1.1.3.1 Nucleus Pulposus**

The cells in the NP are described as chondrocyte-like. They have a round or oval appearance and are surrounded by a distinct capsule. This whole entity is sometimes termed a 'chondron', and is mainly composed of type III and VI collagen (Roberts et al., 1991a; Roberts et al., 1991c). In addition to morphology, NP cell metabolism is also similar to articular chondrocytes. For example, the NP cells exhibit a catabolic response to the stimulation of lipopolysaccharide, with down-regulation of aggrecan synthesis and an increase in aggrecan degradation (Aota et al., 2006). However, the NP cells do exhibit some functional differences from cartilage chondrocytes (Johnson et al., 1986). For example, cartilage chondrocytes have a decreasing rate of glycolysis at low oxygen concentrations (Lee and Urban, 1997). In contrast, disc cells exhibit an increasing glycolytic rate when the oxygen tension falls (Holm et al., 1981; Ishihara and Urban, 1999). Moreover, bovine NP cells generally produce significantly more proteoglycan than articular chondrocytes or cells from other areas of the disc. These differences may be due to the different environment of the cells and the different nutritional pathways between cartilage and intervertebral disc.

The notochordal cell is another distinct cell population within the NP of the intervertebral disc. It is believed to originate from the notochord during embryogenesis and is involved in the formation of the primitive NP (Hayes et al., 2001). During development, the NP is densely populated with large notochordal cells, which recede with maturation and are thought to be replaced by chondrocyte-like cells from the annulus. The functions of notochordal cells are not clear. Previous studies have suggested that notochordal cells can synthesise ECM components such as sulphate-containing proteoglycan and type IIA collagen (Zhu et al., 2001; Cappello et al., 2006). In addition, they modify the behaviour of other cells by secreting matrix metalloproteinases and growth factors, and maintain the hydration of the NP (Oegema, 2002). However, due to the poor understanding of the function of notochordal cells in normal, healthy discs during development and in young adults, it is uncertain whether the disappearance of notochordal cells in humans with ageing is an initial factor for the degeneration of intervertebral disc.

There is also a very small number of fibroblast-like cells in the NP, but their function is not clear (Johnson et al., 1986).

### **1.1.3.2 Inner Annulus fibrosus**

Similar to the cells in the nucleus pulposus, most cells in the IAF region are round or oval in appearance. Towards the centre of the disc, the cell density decreases so the cells take on a more rounded shape. There are also some elongated cells in this region (Hastreiter et al., 2001), and their function is also unclear.

### **1.1.3.3 Outer Annulus Fibrosus**

The cells in the OAF are thin, elongated, fibroblast-like cells that lie parallel to the collagen fibres. In young individuals these cells lie within a small lacunar space, predominantly in sheets between the lamellar bundles, whereas in the mature human disc clonal cell clusters form. The cells are interspersed throughout the lamellar bundles, which themselves have become more irregular, with numerous bifurcations and interdigitations. This heterogeneity may arise in response to the loading history of

the disc (Gruber and Hanley, 1998). All of the OAF cells have a polarised organisation with cell nuclei localising close to the membrane and the other cell components (rough endoplasmic reticulum, Golgi, and secretory vesicles) occupying the opposite side of the cell from the nuclei when compared with NP cells. This distribution of cell organelles may be a result of directed secretion of ECM components such as proteoglycan and collagen by the OAF cells (Gruber et al., 2007). It is likely that the morphology of the OAF cell is the result of entrapment by the surrounding matrix, as they assume a more rounded or oval shape if released from the extracellular matrix (Roberts et al., 1991b).

### **1.1.4 Extracellular matrix components of the IVD**

The major constituents of the extracellular matrix of the IVD are collagens, proteoglycans, and water (Figure 1-3). The collagens and proteoglycans are the principal components conferring the mechanical properties to the tissue. The fibrous collagen network provides the necessary tensile component, whilst the proteoglycans retain the water necessary for the disc to withstand compressive forces. Besides the components above, there are also some glycoproteins in the matrix. The functions of these glycoproteins are not very clear to date, but in other tissues, they function as mediators of interactions between matrix components and connective tissue cells and are therefore important in matrix organisation and integrity.

#### **1.1.4.1 Water**

Water is the main constituent in the disc, making up 65 to 90% of the tissue volume, depending on age and disc region (Figure 1-3). With ageing and degeneration, the water content in the IVD gradually declines, which also correlates with the decreasing quantity of proteoglycan in the matrix (Pearce and Grimmer, 1983; Pearce et al., 1987). The amount of water also varies depending on the load applied. When load is applied to the disc, there is significant water loss from the NP. Less water is lost in the intermediate region but there is only marginal water loss in the OAF (Kingma et al., 2000).

### 1.1.4.2 Proteoglycans of the IVD

One of the major components in the matrix of the IVD is the proteoglycan aggrecan, which can absorb water and provides the swelling pressure for resisting compression. It represents around 10% per cent of the dry weight of the OAF with an increasing proportion towards the IAF and NP where proteoglycans constitute approximately 50% of the dry weight (Eyre, 1979).

Proteoglycans can be divided into large aggregating and small leucine-rich proteoglycans (SLRPs). These are two members of the large aggregating proteoglycans: aggrecan and versican. For the SLRPs, at least four members have been identified: biglycan, decorin, lumican and fibromodulin (Bayliss, 1992; Johnstone et al., 1993).

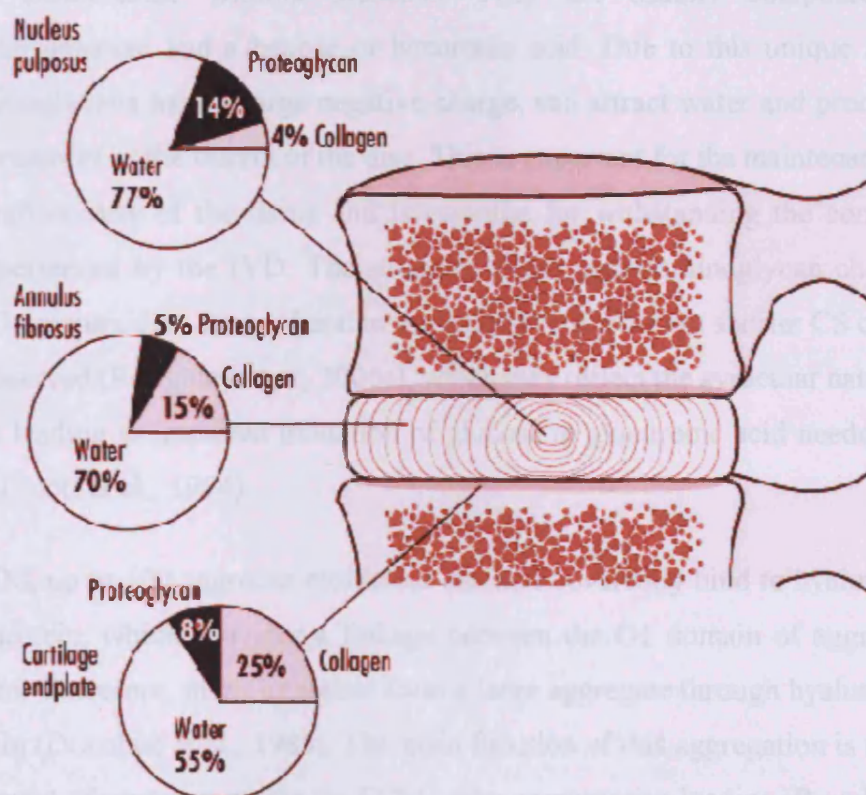


Figure 1-3. The relative proportions of the extracellular matrix composition in normal human adult intervertebral disc and endplate. *Adapted from Urban and Roberts.* <http://www.ilo.org/encyclopedia/?print&nd=857400144>

### 1.1.4.2.1 Aggrecan

Aggrecan is the archetypal large aggregating proteoglycan with an approximate molecular weight of 230 kDa (Doege et al., 1991). It contains a core protein with many glycosaminoglycan side chains attached to it (Figure 1-4). Three globular domains are present on the newly synthesised aggrecan: the G1 and G2 globular domains are located at the N-terminus, whereas the G3 domain localises at the C-terminus of the core protein. The G1 and G2 domains are separated by a short interglobular domain, whereas the G2 and G3 domains are separated by a long extended region, to which three adjacent glycosaminoglycan-attachment domains are attached: one keratan sulphate-rich domain and two chondroitin sulphate (CS)-rich domains (CS1 and CS2) (Caterson et al., 1995). Glycosaminoglycans are polysaccharides consisting of a repeating disaccharide without branches. They are usually composed of an N-acetyl-hexosamine and a hexose or hexuronic acid. Due to this unique structure, glycosaminoglycans have a large negative charge, can attract water and produce high osmotic pressures in the matrix of the disc. This is important for the maintenance of the high hydration state of the tissue and is essential for withstanding the compressive forces experienced by the IVD. The structure of the glycosaminoglycan chains vary with age. In mature disc, longer keratan sulphate (KS) chains but shorter CS chains are usually observed (Roughley et al., 2006a), which may reflect the avascular nature of the adult disc leading to impaired oxidation of glucose to glucuronic acid needed for CS synthesis (Scott et al., 1994).

In the ECM, up to 100 aggrecan molecules can non-covalently bind to hyaluronan via the link protein, which provides a linkage between the G1 domain of aggrecan and hyaluronan. Therefore, many aggrecan form a large aggregate through hyaluronan and link protein (Donohue et al., 1988). The main function of this aggregation is to restrict the movement of aggrecan within the ECM under compressive loading (Roughley et al., 2006a). Therefore, the ability of IVD to resist compressive loading is dependent on the concentration of aggregating aggrecan in the ECM (Roughley et al., 2006b). However, there is also a significant proportion of the aggrecan that is non-aggregating. In human IVD, about 50% of aggrecan is aggregated in the OAF but decreases to 20% in the NP (Adams et al., 1977; Johnstone and Bayliss, 1995). The origin of the non-aggregating

proteoglycans is unclear, and one possible explanation is that they are derived from aggrecan by proteolysis (Roughley et al., 2006b). In cartilage, when aggrecan is broken down by metalloproteinases, the degradative products are usually lost into the synovial fluid. However, the unique fibrocartilaginous organisation in IVD allows the accumulation of proteolytic degradation products of aggrecan irrespective of hyaluronan interaction (Roughley et al., 2006a). This may explain the increased proportion of non-aggregating aggrecan in IVD.

#### 1.1.4.2.3 Small leucine-rich proteoglycans (SLRPs)

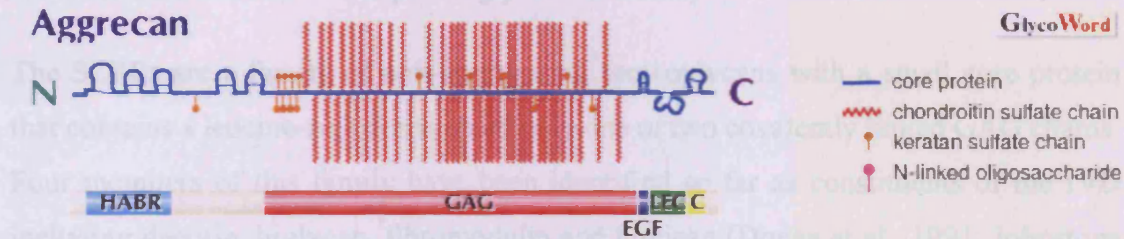


Figure 1-4 A structural model of aggrecan. The schematic representation above shows the organisation of peptide domains in aggrecan. HABR: hyaluronic acid-binding region; GAG: glycosaminoglycan-attachment domain; EGF: epidermal growth factor-like repeat; LEC: C-type lectin-like module; C: complement regulatory protein-like module.

Adapted from Toshikazu Yada <http://www.glycoforum.gr.jp/science/word/teoglycan/PG.A03E.html>

#### 1.1.4.2.2 Versican

Versican is a large chondroitin sulphate proteoglycan (>1000 kDa) widely expressed in many tissues. Versican consists of a 500 kDa core protein bound with 12-16 chondroitin sulphate chains. Similar with aggrecan, versican can bind to hyaluronan through its hyaluronic acid-binding region (Dours-Zimmermann and Zimmermann, 1994) (Figure 1-5). Versican is distributed in the anterior longitudinal ligament and pericellular matrix of the OAF, with less towards the IAF and NP (Melrose et al., 2001). The precise function of versican in the IVD is not known, but it may attach adjacent

annular lamellae to one another via elastic fibres or networks because of its colocalisation with elastic fibres (Roark et al., 1995; Melrose et al., 2001). In addition, the positive staining of versican in the trans-lamellar cross-bridge of mature but not young ovine intervertebral discs, suggests that versican may represent an adaptation to the complex biomechanical forces occurring in the annulus fibrosus (Melrose et al., 2008). Furthermore, using bovine intervertebral disc cells cultured *in vitro*, versican was found to promote both NP and OAF cell adhesion and proliferation (Yang et al., 2003).

### **1.1.4.2.3 Small leucine-rich proteoglycans (SLRPs)**

The SLRPs are a family of non-aggregating proteoglycans with a small core protein that contains a leucine-rich domain and only one or two covalently linked GAG chains. Four members of this family have been identified so far as constituents of the IVD including decorin, biglycan, fibromodulin and lumican (Doege et al., 1991; Johnstone et al., 1993). The SLRPs are distributed throughout the different regions of the IVD but with some variations. Most information is available for decorin and biglycan, which have been found at high levels in the OAF and cartilage endplate, and to a lesser extent in the NP (Gotz et al., 1997). Decorin appears to be distributed in the interterritorial matrix, particularly in the NP and endplate, whereas biglycan is located more in the pericellular domain (Gotz et al., 1997; Benjamin and Ralphs, 2004). The functions of the SLRPs in the disc are not clear to date. They contribute very little to the overall negative charge and therefore have minimal effect on the compressive properties. Many of the SLRPs are known to bind growth factors such as transforming growth factor  $\beta$  (TGF $\beta$ ) (Naito, 2005), which may play some roles in homeostasis/remodelling. A recent study has shown that biglycan and fibromodulin accumulated near the lesion zone in the OAF of a sheep model of disc degeneration, suggesting a close relationship of SLRPs with ECM remodelling (Melrose et al., 2007). Furthermore, increased decorin and biglycan gene expression in degenerative IVD induced by scoliosis illustrated that these two SLRPs participate in ECM turnover induced by long-term mechanical stimulation (Bertram et al., 2006).



1.1.4.2.1 Types I and II collagen

The fibrous matrix in the IVD is predominantly collagen. Interchanging gradients from mostly type I collagen in the OAF to mostly type II collagen in the NP (Byers and Leary, 1974). The NP is a type II collagen in the

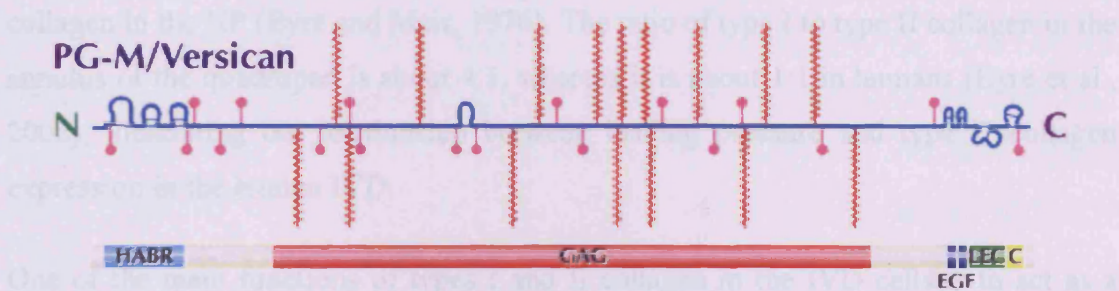


Figure 1-5. A structural model of versican. The schematic representation shows the organisation of peptide domains in versican. HABR: hyaluronic acid-binding region; GAG: glycosaminoglycan-attachment domain; EGF: epidermal growth factor-like repeat; LEC: C-type lectin-like module; C: complement regulatory protein-like module.

Adapted from Toshikazu Yada <http://www.glycoforum.gr.jp/science/word/proteoglycan/PGA03E.html>

1.1.4.2.2 Minor collagen components

**1.1.4.3 Collagens of the IVD**

The OAF contains collagen types II, V and XI, and relatively minor components of

Collagen is a major component of the IVD comprising over 50% of the dry weight of the OAF and 15-20% of the NP (Ayad S, 1986). In a normal young IVD the OAF is reported to contain collagen types I, II, III, V, VI, IX, X, XI, XII and XIV, and the NP contains collagen types I, II, III, VI, IX, X, XI and XII (Duance and Roberts, 2004). Collagens comprise 25% of the whole dry weight of the OAF in normal adult human disc, whereas it declines to 4% in the NP (Figure 1-3).

1981). The expression of type III collagen in human IVD appears to be age-dependent.

Type III collagen is expressed around a few cells in the young disc, and by all of the cells in old disc, but type III collagen expression is absent in disc specimens that remain undecalcified (Bard et al., 1981). The function of type III collagen in the

### **1.1.4.3.1 Types I and II collagen**

The fibrillar matrix in the IVD is predominantly collagen types I and II, with interchanging gradients from mostly type I collagen in the OAF to mostly type II collagen in the NP (Eyre and Muir, 1976). The ratio of type I to type II collagen in the annulus of the quadruped is about 4:1, whereas it is about 1:1 in humans (Eyre et al., 2002), illustrating the relationship between loading pressure and type II collagen expression in the human IVD.

One of the main functions of types I and II collagen in the IVD cells is to act as a scaffold, thereby restricting the movement of matrix components, especially proteoglycans, when mechanical forces are applied to the disc. Therefore, the amount of types I and II collagen in the matrix will directly influence the features of the ECM. With age, type II collagen is elevated in the OAF when compared with the new born disc (Beard et al., 1980), although the relative proportions of collagen types I and II in the OAF of human IVD do not change (Eyre and Muir, 1977), suggesting the migration of type II collagen from NP to OAF with age. Histological analysis has shown that there is increased fraying and fragmentation of collagen with age, suggesting increased collagen degradation (Hollander et al., 1996).

### **1.1.4.2.2 Minor collagen components**

The other fibrillar collagens, types III, V and XI, are relatively minor components of the IVD. However, these minor constituents play important roles in modifying the fibrillar architecture and fibril surface properties, thus influencing the structural and mechanical properties of the tissue.

In the normal adult human IVD, type III collagen is mainly localised in the pericellular matrix of NP and IAF cells (Beard et al., 1981). It composes the 'capsule' matrix around the cell of the disc along with other collagens such as type VI (Roberts et al., 1991c). The expression of type III collagen in human IVD appears to be age-dependent. Type III collagen is expressed around a few cells in the young disc, and in all of the cells in old disc, but type III collagen expression is absent in disc specimens from humans aged under four (Beard et al., 1981). The function of type III collagen in the

IVD is not clear. Immunohistochemical studies on scoliotic discs suggested that there was increased expression of type III collagen in the intercellular matrix (Beard et al., 1981) which may be caused by abnormal mechanical stimulation in the deformed disc. Type III collagen is often found to be colocalised with type I collagen within the same fibril (Fleischmajer et al., 1981), suggesting that type III collagen may modulate the size of type I collagen fibrils because of the smaller diameter of these self-assembled fibrils (Fleischmajer et al., 1990). Type III collagen is primarily located in the territorial matrix of the IAF and NP of the disc. Thus, type III collagen is associated with type II collagen fibrils in the NP, and co-localises to type I collagen fibrils in the AF.

Type V collagen is a fibrillar collagen widely distributed as a minor component in tissues that contain types I and III collagen. The functions and molecular interactions of type V collagen in the pericellular matrix are unclear. Studies have shown that type V collagen adsorbed on a surface binds heparin/heparan sulphate with an apparently higher affinity than do collagen types I, II, III, IV or VI, fibronectin or laminin (LeBaron et al., 1989). Therefore, type V collagen may act as an anchor for proteoglycans in the ECM and function as a substrate for glycosaminoglycan-mediated cell attachment. Type V collagen is generally associated with type I collagen. *In vitro* fibrillogenesis studies have shown that type V collagen may function to regulate the diameter of the major fibrillar collagens and thus influence their mechanical properties (Wenstrup et al., 2004).

Type XI collagen consists of three genetically distinct polypeptide chains:  $\alpha 1(XI)$ ,  $\alpha 2(XI)$ , and over-glycosylated  $\alpha 1(II)$  chains, and is typical of the fibrillar class of collagens having a 300-nm triple helical domain (Burgeson and Hollister, 1979). Type XI collagen is associated with type II collagen fibrils. It retains a globular domain at the N-terminal end of the molecule which is believed to be located on the fibril surface with the triple-helical domain buried within the type II collagen. Therefore, type XI collagen is important in the regulation of fibril diameter and in maintaining tissue integrity and cohesion (Eikenberry, 1992). An interaction between type XI and heparan sulphate glycosaminoglycan has been shown in the matrix, which may contribute to cell surface-matrix interactions (Vaughan-Thomas et al., 2001).

#### **1.1.4.2.3 Type VI Collagen**

Type VI collagen is an unusual collagen that aggregates to form beaded filaments. It has been found in the OAF, NP and the cartilage endplate. In the bovine disc it is a major collagenous constituent representing 20% dry weight of the NP and 5% of the AF (Wu et al., 1987). Immunolocalisation studies indicate that type VI collagen is located around the cells of IVD, being particularly prominent in the NP (Roberts et al., 1991a). There is some evidence that type VI collagen functions as a link between the cell surface and the fibrillar ECM (Pfaff et al., 1993), because it contains a number of amino acid motifs that are recognised by many of the integrins, the cell surface receptors for ECM ligands. This pivotal link has important functions in maintaining tissue homeostasis, and in the cell's response to mechanically-induced tissue damage and degeneration.

#### **1.1.4.2.4 Type X collagen**

Type X collagen belongs to the family of short-chain collagens. It has a short triple helical region, compared to the major fibrillar collagens such as types I and II. This triple helical region is flanked by two non-collagenous (NC) domains, NC2 at the amino terminus and a much larger NC1 at the carboxyl terminus. Type X collagen is present in hypertrophic chondrocytes of the growth plate and endplate, as well as in the NP of the IVD (Schmid and Linsenmayer, 1985). There is a close relationship between type X collagen expression and age (Aigner et al., 1998). The function of type X collagen in disc is not very clear to date, but it has been suggested that type X collagen production may be a response of disc tissue cells to a stimulus, such as altered loading (Aigner et al., 1998).

#### **1.1.4.3 Other Matrix Components of the IVD**

Cartilage intermediate layer protein (CILP) was originally identified in articular cartilage and is also present in the IVD (Tsuruha et al., 2001). This protein has been linked to an increased incidence of lumbar disc disease (Seki et al., 2005), although a recent study indicated that there is no association between CILP and symptoms of lumbar disc herniation in the Finish and Chinese population (Virtanen et al., 2007).

Cartilage oligomeric matrix protein (COMP) is mainly localising in cartilage but also found in bone, tendon, ligament and IVD (Ishii et al., 2006). COMP can bind to collagen type IX, therefore it may play a role in regulating collagen fibril assembly and maintaining collagen network stability (Heinegard et al., 2002). COMP which is distributed in both NP and OAF of IVD is more highly expressed in the OAF (Ishii et al., 2006). COMP presents a lamellar distribution pattern in the OAF in rat disc (Ishii et al., 2006) and the expression of COMP is age-dependent, with higher COMP content in old tissue (Lee et al., 2007a). This suggests that COMP is involved in the structure and maturation of IVD.

Elastin is a highly insoluble protein that is very extensible and highly elastic. Elastin has been reported to occur in all IVD making up 1-10% of the total dry weight (Buckwalter et al., 1976). The distribution of elastin in IVD varies with the different regions. In the NP, it occurs as large, more irregularly shaped fibrils (Yu et al., 2005a), which may serve to resist the radial tensile force when the load is transmitted to the OAF from the NP (Yu et al., 2005a). In the OAF, elastin fibres are distributed between the collagen lamellae (Yu et al., 2005a). This may reflect the different mechanical environment between the NP and OAF. When the spine is bent or flexed, there is sliding between the adjacent collagen lamellae because of the disc deformation. During this process, the elastic fibre network lying between the lamellae may contribute greatly to the recovery of annular lamellae after deformation, and thus help to maintain annulus integrity.

## **1.2 IVD metabolism related enzymes**

As with cartilage, ECM turnover in the IVD is very important for its function. During the process of degeneration, the IVD shows a progressive and significant reduction in height due to tissue resorption. Many enzymes such as matrix metalloproteinases (MMPs), aggrecanases (ADAMTSs) and tissue inhibitor of matrix metalloproteinases (TIMPs) are assumed to play a pivotal role in ECM turnover and remodelling as well as in disc tissue degradation and resorption.

## 1.2.1 Matrix Metalloproteinases

MMPs are a family of enzymes that are capable of degrading the major structural components of the IVD, and therefore are involved in both the normal turnover and the pathological degradation of the ECM in several connective tissues including the IVD.

MMPs belong to the metzincin superfamily of metalloproteinases which includes astacins, ADAMs (a protein with a disintegrin and metalloprotease domain) and ADAM with a thrombospondin-like motif (ADAMTS) proteases. MMPs are zinc and calcium-dependent enzymes, and different MMPs share a common domain structure. The three common domains are the pro-peptide, the catalytic domain and the haemopexin-like C-terminal domain which is linked to the catalytic domain by a flexible hinge region (Figure 1-6). The catalytic domain contains an active site where there is a catalytically important  $Zn^{2+}$  ion.

According to the molecular weight and substrates, MMPs can be divided into six groups: collagenase, gelatinase, stromelysin, matrilysins, membrane-bound and other types of MMPs (Lemaitre and D'Armiento, 2006).

The collagenases include MMPs-1, 8, 13 and 18, which are able to cleave the triple helical part of the fibrillar collagens types I, II, and III. In degenerate discs, the number of cells immunopositive for MMPs-1, 8 and 13 increase with the severity of degeneration (Haro et al., 1999; Le Maitre et al., 2004). The resultant fragments can be cleaved further by the gelatinases: MMPs 2 and 9, levels of which have been found to be elevated in degenerate discs (Crean et al., 1997). MMP-7 expression and activity also appear to be increased in diseased disc (Le Maitre et al., 2006). Similarly, stromelysin (MMP-3) was also increased in the matrix of degraded intervertebral discs, especially in the initial stage of disc degeneration (Nemoto et al., 1997). Like the gelatinases, MMP-3 can further degrade the collagenase-cleaved collagens and is also involved in breaking down other structural components such as proteoglycans and fibronectin (Crean et al., 1997).

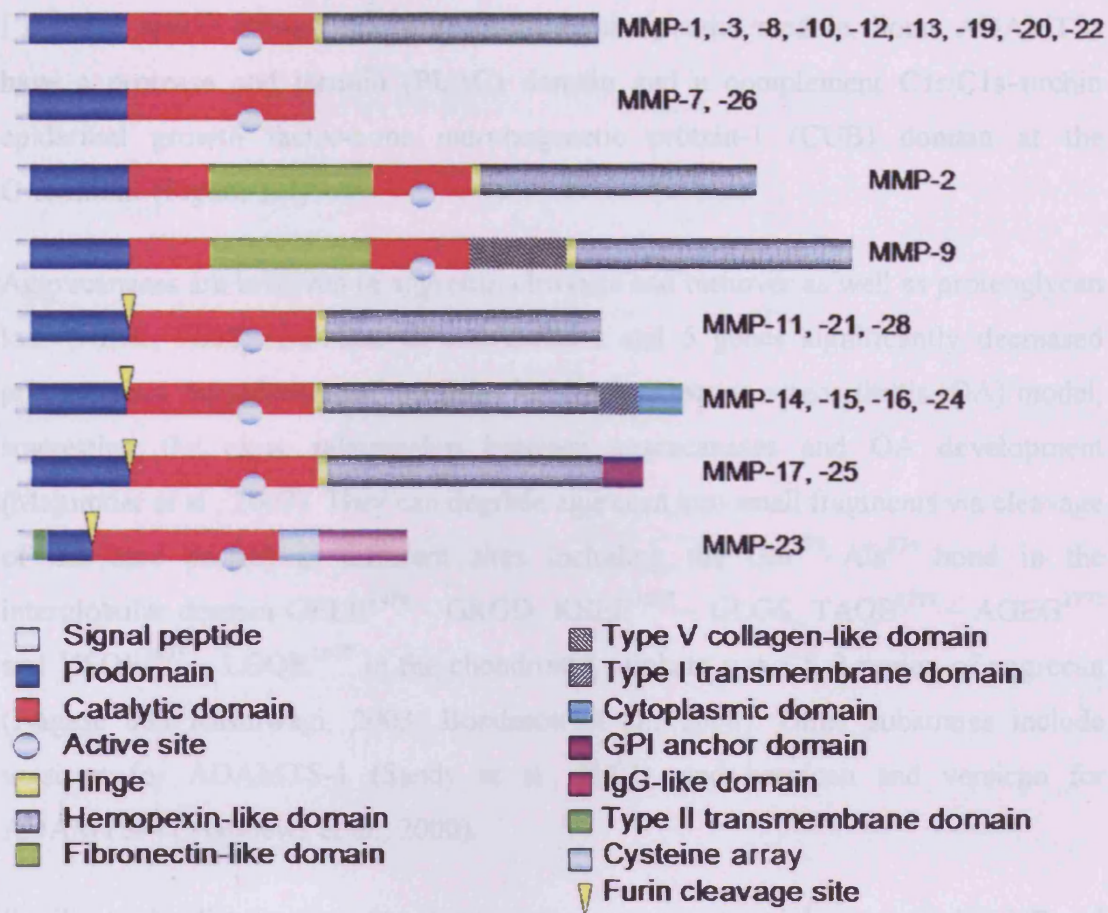


Figure 1-6 The domain structure of MMPs (*Adapted from Lemaitre V, D'Armiento J. Birth Defects Res C Embryo Today. 2006, 78(1):1-10*)

## 1.2.2 Aggrecanases

Aggrecanase was first reported in 1999 (Tortorella et al., 1999). Several aggrecanases have since been identified including aggrecanase-1 and 2, which belong to the ADAMTS family, and are therefore named ADAMTS-4 and ADAMTS-5 respectively. ADAMTS proteins are related to ADAMs which are type I transmembrane proteins with extracellularly located N-termini, but lack a transmembrane domain (Figure 1-7).

The ADAMTS protein comprises several domains including a signal peptide, a pro-domain, a metalloproteinase domain, a disintegrin domain, a thrombospondin type

I motif, a spacer domain, and a second thrombospondin module. Some ADAMTSs have a protease and lacunin (PLAC) domain and a complement C1r/C1s–urchin epidermal growth factor-bone morphogenetic protein-1 (CUB) domain at the C-terminus (Figure 1-7).

Aggrecanases are involved in aggrecan cleavage and turnover as well as proteoglycan loss (Arner, 2002). Deletion of ADAMTS-4 and 5 genes significantly decreased proteoglycan degradation and cartilage lesions in a mouse osteoarthritis (OA) model, suggesting the close relationship between aggrecanases and OA development (Majumdar et al., 2007). They can degrade aggrecan into small fragments via cleavage of the core protein at different sites including the Glu<sup>373</sup>–Ala<sup>374</sup> bond in the interglobular domain GELE<sup>1480</sup> ~ GRGD, KEEE<sup>1667</sup> ~ GLGS, TAQE<sup>1771</sup> ~ AGE<sup>1772</sup> and VSQE<sup>1871</sup> ~ LGQR<sup>1872</sup> in the chondroitin sulphate-rich CS-2 region of aggrecan (Nagase and Kashiwagi, 2003; Bondeson et al., 2008). Other substrates include versican for ADAMTS-1 (Sandy et al., 2001), and brevican and versican for ADAMTS-4 (Matthews et al., 2000).

Similar to the distribution of aggrecan, aggrecanases are mainly expressed in NP and IAF, with little distribution in the OAF (Patel et al., 2007). Aggrecanase-1 was found to have low expression in cells from non-degenerate discs (Le Maitre et al., 2004). In contrast, significantly more aggrecanase-1 was observed in degenerative discs, illustrating the close relationship between aggrecanase-1 and disc degeneration (Le Maitre et al., 2004; Patel et al., 2007; Pockert et al., 2009). There was a tissue-specific difference in the aggrecanase-generated aggrecan fragments in disc with age, i.e. an increase in aggrecan fragments was observed in the OAF with age, which levelled off in adulthood. In contrast, aggrecan fragments were present in the greatest abundance in young NP, but decreased to very low levels with age (Sztrolovics et al., 1997), suggesting an age-related decline in the repair process in the ECM.



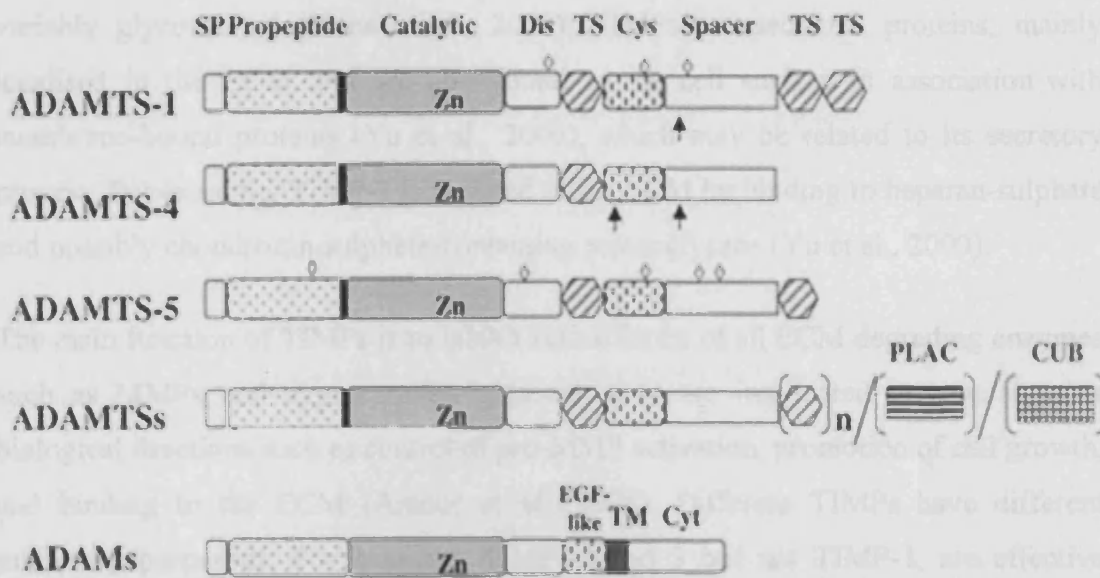


Figure 1-7 Domain arrangements of ADAMTS, ADAMs and MMPs. N-linked glycosylation sites ( $\diamond$ ) and post-translational processing sites of ADAMTS-1 and ADAMTS-4 ( $\uparrow$ ) are indicated. Some ADAMTSs have PLAC and CUB domain at the C terminus. ADAMs are type I membrane proteins but ADAMTSs lack a transmembrane domain.

SP, signal peptide; Dis, disintegrin-like domain; TS, thrombospondin type I motif; Cys, cysteine-rich domain; PLAC, proteinase and lacunin domain; CUB, complement C1r/C1s-urchin epidermal growth factor-bone morphogenetic protein-1 domain; TM, transmembrane domain; Fn, fibronectin. *Adapted from Nagase H, Kashiwagi M. Arthritis Res Ther. 2003; 5(2): 94-103*

### 1.2.3 Tissue Inhibitors of Metalloproteinases

TIMPs are the major cellular inhibitors of the MMP and aggrecanases. There are four identified mammalian TIMPs including TIMPs-1, 2, 3 and 4 to date. They have similar structure, but distinctive biochemical properties and expression patterns. For example, TIMPs-1 and 2 mainly inhibit the activity of collagenases but TIMP-3 inhibits aggrecanases (Brew et al., 2000). TIMPs have molecular weights of 21 ~28 kDa and are

variably glycosylated (Brew et al., 2000). TIMPs are secreted proteins, mainly localised in the ECM, but are also found at the cell surface in association with membrane-bound proteins (Yu et al., 2000), which may be related to its secretory process. For example, TIMP-3 is secreted to the ECM by binding to heparan-sulphate and possibly chondroitin-sulphate-containing proteoglycans (Yu et al., 2000).

The main function of TIMPs is to inhibit active forms of all ECM degrading enzymes such as MMPs and aggrecanases, although they are implicated in several other biological functions such as control of pro-MMP activation, promotion of cell growth, and binding to the ECM (Amour et al., 1998). Different TIMPs have different inhibitory properties. For example, TIMPs-2 and 3 but not TIMP-1, are effective inhibitors for the membrane-type MMPs (MT-MMPs); TIMP-3 but not TIMPs-1, -2 or -4, is a good inhibitor for tumour necrosis factor-K converting enzyme and aggrecanases (Amour et al., 1998; Kashiwagi et al., 2001).

The imbalance between MMPs, aggrecanases and TIMPs greatly contribute to disc degeneration. In a rabbit model (rabbits underwent an annular stab with a 16-gauge needle to the L2-L3, L3-L4, and L4-L5 discs), TIMP-1 expression fell dramatically to one tenth of the baseline and levels remained low throughout the degenerative process (Sobajima et al., 2005). However, MMP-3 levels were strongly elevated in both early and late degeneration (Sobajima et al., 2005). In human disc degeneration, there was an increase in the number of cells immunopositive for MMPs, although this increase was accompanied by an increase in TIMPs-1 and 2 (Le Maitre et al., 2004). However, there was also an increase in ADAMTS-4 but not TIMP-3 expression with increasing degeneration (Le Maitre et al., 2004). This suggests that an imbalance between the expression of the matrix degrading enzymes and TIMPs may be involved in the pathogenesis of disc degeneration.

### **1.3 Cytoskeleton in the IVD**

The cytoskeleton is a cellular "scaffold" or "skeleton" within the cytoplasm. It is a dynamic structure involved in maintaining cell shape, cell motion, intra-cellular transport, cell division and signal transduction. There are three kinds of cytoskeletal

components in IVD, namely actin microfilaments, intermediate filaments and microtubules.

### 1.3.1 Actin Microfilaments

Actin microfilaments are approximately 7 nm in diameter (Fuchs and Cleveland, 1998), and are formed by the head-to-tail polymerisation (Figure 1-8) of the actin monomers (namely globular actin or G-actin). The subunits in an actin fibre are referred to as filamentous actin (or F-actin). There are three isoforms of G-actin,  $\alpha$ ,  $\beta$  and  $\gamma$  (Rubenstein, 1990). The  $\alpha$  actin composes the major constituent of the contractile apparatus in muscle cells. The  $\beta$  and  $\gamma$  actins co-exist in most cell types to polymerise the actin filaments. The functional difference between  $\beta$  and  $\gamma$  isoforms is not clear, but it is believed that there is a close relationship between the actin isoform and the cell phenotype (Gerstenfeld et al., 1985). F-actin is formed by polymerisation of G-actin, which is coupled with ATP. ATP-loaded G-actin monomers are able to add to one end of the filament to maintain its elongation (called the fast growing or barbed end) (Straub and Feuer, 1989). Actin polymerisation is associated with the hydrolysis of the actin-bound ATP moiety to ADP and  $P_i$ . ADP-bound actin is more prone to dissociation and recycles back to the monomer pool. Therefore, there is a continuous disassociation of ADP-bound G-actin at the other end of F-actin (called slow growing or pointed end). The association and disassociation of actin monomers maintain the filament at a constant length, which is referred to as “treadmilling” (Straub and Feuer, 1989). Two parallel F-actin strands rotate 166 degrees to form a double helix and gives rise to the actin microfilament (Fuchs and Cleveland, 1998). Actin polymerisation, depolymerisation and organised assembly of filaments in cells are regulated by a large amount of actin-binding proteins, which can be divided into four groups according to their functional differences (Blain, 2009): (i) proteins that can promote actin nucleation, such as the Arp2/3 complex, which can bind to the side of ATP-F-actin near the growing barbed end of the filament, promoting nucleation of a new F-actin branch (Mullins et al., 1998); (ii) proteins that affect actin filament depolymerisation, such as cofilin. Cofilin causes depolymerisation at the pointed end of actin filaments, thereby preventing actin reassembly (Van Troys et al., 2008); (iii) proteins that associate with monomeric G-actin such as thymosin  $\beta_4$ , which can sequester

ATP-coupled G-actin, holding it in a form that is unable to polymerise (Atkinson et al., 2004); (iv). proteins that cap the filament ends such as gelsolin, which can bind to a actin filament and sever it into two by weakening the non-covalent bonds between actin molecules (Sun et al., 1999). These actin-binding proteins co-ordinately integrate together to regulate actin polymerisation, for participation in a series of tightly controlled cell signalling pathways (Pullikuth and Catling, 2007).

Both hydrostatic pressure (Parkkinen et al., 1995) and cyclic compression (Campbell et al., 2007) can cause actin remodelling in isolated articular chondrocytes. In addition, actin remodelling was also observed in chondrocytes in response to mechanical distortion (Horoyan et al., 1990) and osmotic loading (Erickson et al., 2003). Some evidence shows that the actin filament is involved in the pathogenesis of osteoarthritis (OA) (Kouri et al., 1998; Blain, 2009). However, the mechanism of how actin transduces the mechanical signal between the ECM and cell is not clear to date, although some evidence shows that stretch-activated ion channels, integrins and deformation of intracellular organelles may be involved (Morachevskaya et al., 2007).

Compared with the OAF, there is an abundant distribution of cytoplasmic actin filaments in NP cells (Maldonado and Oegema, 1992), which may be related to the higher compressive loading experienced by the NP relative to the OAF. Therefore, it is reasonable to deduce that actin filaments may be involved in transducing mechanical signals between the cell and the ECM in the IVD. Hyperosmotic stress induces a volume change in IVD cells, and increases the concentration of intracellular calcium which is an actin-dependent mechanism (Pritchard and Guilak, 2004). In addition, cyclic hydrostatic pressure decreases  $\alpha 5$  integrin and actin expression in porcine lumbar intervertebral disc cells (Yu et al., 2005b). This limited information illustrates that actin plays a pivotal role in mechanotransduction and facilitates communication between the cell and the ECM environment.

### **1.3.2 Intermediate filaments**

Intermediate filaments (IFs) are 8-10 nm in diameter and consist of five major types including keratin, vimentin, glial fibrillary acidic protein, desmin and neurofilament

proteins (Ishikawa et al., 1968), in which vimentin is the major IF proteins in the IVD. Vimentin is a highly elongated fibrous molecule and consists of an N-terminal head and a C-terminal tail connected by an alpha helical rod domain. Two vimentin molecules form a coiled coil structure via the interaction of the alpha helical rod domain, and the N-and C-terminals of each filament become aligned. These dimers then form staggered tetramers that line up head to tail and the final 10 nm filament is a helical array of these tetramers (Figure 1-8). The vimentin filament network is a highly dynamic process, and its assembly/disassembly is regulated by phosphorylation and dephosphorylation at serine and threonine residues of vimentin (Blain, 2009). When phosphorylation occurs, the vimentin filaments depolymerise and generate a pool of soluble vimentin subunits. After dephosphorylation, there is a re-polymerisation of vimentin monomers which always accompanies a reorganisation of the vimentin network (Herrmann and Aebi, 2000). During this process, vimentin molecules provide a good substrate for second messenger protein kinases in numerous signal transduction pathways including the MAP kinases ERK 1/2 (Perlson et al., 2006), various 14-3-3 signalling protein isoforms and apoptotic factors (Kim and Coulombe, 2007)..

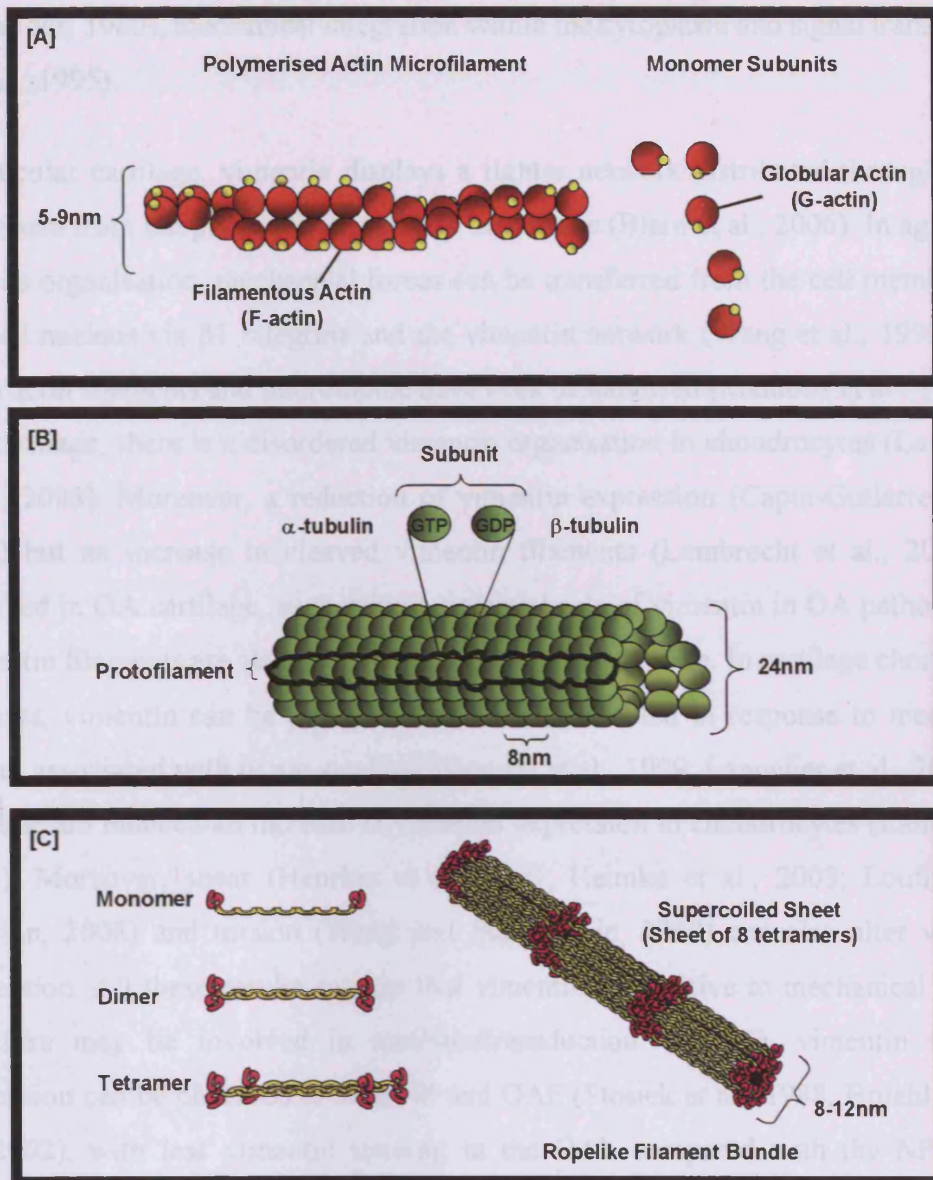


Figure 1-8. Schematic representation of cytoskeletal element structures and assembly. [a] actin filament; [B] microtubule filament and [C] intermediate filament. *Adapted from Blain EJ. Int J Exp Pathol 90, 1-15.*

Vimentin is a 57 kDa intermediate filament protein and is widely expressed in many mesenchymal cell types including the chondrocyte. Vimentin is attached to the cell nucleus, endoplasmic reticulum and mitochondria, therefore playing an important role in anchoring the position of the organelles within the cytoplasm (Katsumoto et al., 1990). Vimentin is also implicated in the spatial coordination of mechanical events

(Lazarides, 1980), mechanical integration within the cytoplasm and signal transduction (Traub, 1995).

In articular cartilage, vimentin displays a tighter network distributed throughout the cytoplasm from the plasma to the nuclear membrane (Blain et al., 2006). In agreement with its organisation, mechanical forces can be transferred from the cell membrane to the cell nucleus via  $\beta 1$  integrins and the vimentin network (Wang et al., 1993), even when actin filaments and microtubule have been destabilised (Maniotis et al., 1997). In OA cartilage, there is a disordered vimentin organisation in chondrocytes (Lambrecht et al., 2008). Moreover, a reduction of vimentin expression (Capin-Gutierrez et al., 2004) but an increase in cleaved vimentin filaments (Lambrecht et al., 2008) are observed in OA cartilage, suggesting a potential role of vimentin in OA pathogenesis. Vimentin filaments are also involved in mechanotransduction. In cartilage chondrocyte explants, vimentin can be disassembled and reassembled in response to mechanical stimuli associated with tissue swelling (Durrant et al., 1999; Langelier et al., 2000). 10% cyclic strain induced an increase in vimentin expression in chondrocytes (Lahiji et al., 2004). Moreover, shear (Henrion et al., 1997; Helmke et al., 2003; Loufrani and Henrion, 2008) and torsion (Wang and Stamenovic, 2000) can also alter vimentin expression. All these results suggest that vimentin is sensitive to mechanical stimuli, therefore may be involved in mechanotransduction. In IVD, vimentin filament expression can be observed in both NP and OAF (Stosiek et al., 1988; Bruehlmann et al., 2002), with less vimentin staining in the OAF compared with the NP. These distributions are in accordance with the idea that regions of higher compressive stress display more organised intermediate filaments (Setton and Chen, 2004). The organisation and expression of vimentin in IVD in response to mechanical load is unknown. However, an increased expression of vimentin mRNA and polymerisation of vimentin subunits was observed in OAF cells following periods of static compression (Chen et al., 2004).

### **1.3.3 Microtubules**

Microtubules (MTs) are filamentous structures within cells and are involved in many processes including mitosis (Mitchison et al., 1986), ciliary movement (Gibbons, 1981),

cytokinesis (Farquharson et al., 1999) and vesicular transport (Vale, 1987). The diameter of a MT is about 25nm and their length is variable from 200nm to 25µm (Figure 1-8).

Microtubule filaments are polymers of two monomeric isoforms:  $\alpha$ -tubulin and  $\beta$ -tubulin (55 kDa).  $\alpha$ - and  $\beta$ -tubulin can bind together to form a heterodimer which is the basic structural unit of microtubules. The tubulin dimers can bind together in an end to end fashion to form protofilaments. The protofilaments then arrange themselves in a helix to form a hollow cylindrical filament, with one turn of the helix containing 13 tubulin dimers which are all from a different protofilament (Figure 1-8).

In articular cartilage chondrocytes, MTs form a loose, basket-like mesh spanning throughout the cytoplasm (Langelier et al., 2000), extending from the innermost parts of the cell to the cell periphery and are particularly abundant around the nucleus (Zwicky and Baici, 2000). This structure is in agreement with the intracytoplasmic transport functions associated with MTs. In addition, the suggestion that MTs serve as stabilising elements for other cytoskeletal systems (Janmey et al., 1991) is compatible with the MT organisation in cartilage. Meanwhile, in a rat OA model, a 20.1% reduction in tubulin labelled chondrocytes was observed compared with normal (Capin-Gutierrez et al., 2004), suggesting that substantial changes in the tubulin cytoskeleton of chondrocytes might be involved in OA pathogenesis. Under hydrostatic cyclical pressure, the distribution of tubulin in normal and OA cells appeared to be different (Fioravanti et al., 2003), which confirmed the results described in the rat model. This suggests that tubulin filaments are indeed implicated in OA pathogenesis and have a close relationship with mechanotransduction in chondrocytes. Unfortunately, little information has been acquired about tubulin in the IVD.

### **1.3.4 Cytoskeleton-associated proteins in IVD**

#### **1.3.4.1 Paxillin**

Paxillin mainly localises at focal adhesions which are plaque-like structures between the cell and ECM. These sites act as ‘anchors’ for maintaining cell shape and are



important for cell movement (Wang, 2007). A focal adhesion serves as a connector between actin filaments and integrins which bind to the ECM. Therefore it is a structural link between the ECM and the actin cytoskeleton which are important sites for signal transduction (Orend and Chiquet-Ehrismann, 2000; Loeser, 2002).

Paxillin is a 68-kDa protein comprising numerous structural domains which are involved in multiple protein-protein interactions. Paxillin localises to focal adhesions through its LIM domains, possibly through a direct association with  $\beta$ -integrin tails (Brown and Turner, 2004). One of the main functions of paxillin is to integrate and disseminate the signals from integrins and growth factor receptors into the cell nucleus. The integrins are important chondrocyte mechano-receptors, especially  $\alpha 5 \beta 1$  integrin which has been confirmed to be a mechanoreceptor in cartilage (Millward-Sadler et al., 1999). When mechanical stimulation is applied, a signal cascade is activated in chondrocytes including the transient activation of paxillin (Lee et al., 2000b; Salter et al., 2001), thereby implicating paxillin in chondrocytes mechanotransduction. This function may be actin network-dependent, because paxillin binds to many proteins such as vinculin that are involved in effecting changes in the organisation of the actin cytoskeleton (Turner, 2000). However, to date, little is known about the function of paxillin in the IVD.

### **1.3.4.2 Vinculin**

Vinculin is a membrane-bound cytoskeletal protein involved in cell adhesion (Critchley, 2000). It is approximately 130 kDa and consists of a globular head domain connected to an elongated tail region by a proline-rich domain. There are cytoskeletal protein binding sites for  $\alpha$ -actinin and talin in the head region, and binding sites for actin and paxillin in the tail region. As vinculin is located at focal adhesion sites, it is likely to play an important role in mechanotransduction. Vinculin expression increases in tendon cells when under cyclic tensile loading (Ralphs et al., 2002). Although the precise mechanism is not clear, recent studies have shown that mechanical stimulation induced activation and reorganisation of the cytoskeleton which may be involved in this event (Lee et al., 2007b; del Rio et al., 2009).

### **1.3.4.3 Talin**

Talin is an actin and  $\beta$ -integrin binding protein and is essential for integrin activation and focal adhesion formation. Talin is a 270KDa protein containing a globular head domain and an elongated rod domain, and usually exists as a homodimer (Nayal et al., 2004). The globular talin head can bind to  $\beta$ -integrin cytodomains and phosphatidylinositol-4, 5-bisphosphate and the rod domain can directly bind to vinculin and actin (Critchley, 2004). Therefore talin provides a link between integrins and the actin filaments. Previous studies have shown that talin plays an important role in integrin activation and focal adhesion formation. During this process, talin recruits the PIP2-synthesising enzyme phosphatidylinositol-4-phosphate 5-kinases type I  $\gamma$  isoform to activate PIP2. This in turn, regulates vinculin activity and the actin binding protein Arp2/3, therefore connecting adhesion and actin polymerisation (Critchley, 2004).

## **1.4. The biomechanics of the IVD**

The main movements applied on the spine during our life are flexion, extension, lateral bending and axial rotation. These movements produce different forces on the components of the spine. The IVDs lie between the vertebrae and their primary function is to transfer compressive forces evenly from one vertebral body to the next, while allowing small intervertebral movement. In order to complete these, the tissue of the disc must be stiff and strong, but in order to allow movement, the tissue must be pliable. These two features are contradictory, but the special structure of the IVD ensures that this biomechanical function is fulfilled.

### **1.4.1 IVD structure and biomechanical function**

#### **1.4.1.1 Annulus fibrosus**

The AF consists of 10-20 concentrically arranged sheets of collagen fibres named lamellae, tightly packed together around the periphery of the disc. A single lamella is too weak to sustain compressive loading. However, when packed together, these lamellae are stiff enough to sustain the considerable loads applied. Another

characteristic of the AF is that the collagen fibre bundles in the lamellae are arranged in alternate directions (Figure 1-2). The fibres in each successive lamella are orientated in an opposite direction, with one layer inclined to the left, the next layer to the right. This special arrangement of the lamellae in AF has two benefits: firstly, it can prevent tearing through the annulus, through which nuclear material might seep or burst, which is crucial for the integrity of the disc. More importantly, this alternating orientation allows the annulus to resist tension in a variety of directions. Sliding movements between the vertebral bodies are resisted by the collagen fibres that are inclined in the direction of movement. Similarly, twisting movements are resisted by the collagen fibres aligned in the OAF. Although the lamellae of the AF can transfer compressive loads from one vertebral body to another, there are still some problems. Firstly, the collagen fibre bundles of the lamellae are too stiff, and they have little shock absorbing properties, therefore they cannot transfer the compression evenly. Secondly, the stiffness of the lamellae of the AF comes from the ordered arrangement of the collagen fibre bundles. If they buckle, they will lose their stiffness and will be unable to resist the compressive loads. Therefore, the AF alone is not well suited to resist high compressive loads, bending, shearing or twisting forces acting on the spine.

### **1.4.1.2. Nucleus pulposus**

The NP contains a large amount of proteoglycan, which can absorb and retain large amounts of water; it acts like a hydrated gel which is very important to the function of the disc. The water ensures that the tissue has very low rigidity, so it is easy to deform in any direction and can equalise the stress applied to it (Adams et al., 1996). When compressed, the semi-fluid mass expands radially and equilibrates the compressive forces both horizontally and vertically across the NP. These forces are resisted by the surrounding AF and endplate, therefore part of the compressive load will be absorbed by the NP and part will be converted to a tensional force and absorbed by the deformation of the AF. The other forces will remain in the NP and will be transferred to the adjacent IVDs through the stiff vertebral body. The expansion also braces the AF from the inside, thereby preventing it from buckling inwards and losing its stiffness. Cooperatively, the NP and OAF maintain the stiffness of the disc against the compressive load, and allow some degree of movement between the vertebral bodies.

## 1.4.2. Forces acting on the IVD

The forces acting on the lumbar spine come from the effect of gravity on the upright body, muscle contraction, the stretching of the fascia and ligaments and the intra-abdominal pressures. Due to the daily movement of the spine, the primary function of the IVD is to resist compressive loading, although there are other forces acting on the IVD disc including tension, shear and torsion.

### 1.4.2.1 Compression

It is not surprising that compressive loading is the main force acting on the intervertebral disc, because the spine is compressed for most of the time, day and night. Measuring the amount of compressive load on the IVD originally came from Nachemson, who inserted a pressure-sensitive needle into the L3-4 disc of conscious volunteers (Nachemson and Morris, 1964). His experiment and subsequent experiments in Japan (Sato et al., 1999) indicate that the compressive force on the lumbar spine rises from 150-250N when lying, to 500-800N when standing erect, 700-1000N when sitting erect, and 1900N when stooping to lift a 10kg weight. However, recent studies using a similar method reported that there may be lower intradiscal pressure in sitting compared with the results from Nachemson (Wilke et al., 1999). Despite this minor difference, all the results suggest that the intradiscal pressure of the lumbar disc varies significantly with body position and manoeuvre, with pressure being greatest in positions where participants held 10-kg weights and lowest in a lying position (Figure 1-9).

The NP exhibits a pressure of approximately 0.05MPa in a cadaveric vertebral body-disc-vertebral body unit when it is unloaded. Pressure will increase in the NP when a compressive load is applied. Low level muscle activity in living subjects lying prone raises the NP pressure to 0.08-0.15 MPa (Sato et al., 1999). Limited knowledge has been acquired about the compressive load applied on the OAF *in vivo*. Using a porcine model, it was demonstrated that the pressure in the NP is much higher (6.3-fold) than that in the OAF (Lee et al., 2004). However, this result came from an *in vitro* experiment, so care needs to be taken in extrapolating to humans *in vivo*.

### 1.4.2.2. Tension

Tensional force acting on the IVD primarily comes from the deformation of the NP caused by compressive loading on the spine, as well as the movement of the adjacent vertebral bodies, which is usually induced by daily movements such as bending, extension and torsion.

The tensional force applied to the NP is usually equal to the compressive force acting on the tissue, due to its highly hydrated gel-like material properties (Adams et al., 1986). The tension in the NP comes from the loose collagen network, which resists forces generated by the swelling of the proteoglycans where a lot of water is retained. Therefore, nuclear swelling pressure, lamellar collagen viscoelasticity, and interstitial fluid permeation were found to be crucial for the tensile properties in the NP (Hsieh et al., 2005).

Tensile tests performed on small samples of the OAF show that adjacent lamellae are only weakly bound together and can be pulled apart with a tensile stress of 0.2-0.3 MPa (Fujita et al., 1997). This result suggests that the lamellae are held together by the proteoglycans, elastin fibres and maybe a small amount of collagen. If samples of the AF are stretched horizontally very slowly (0.01% per second), then failure occurs at a stress of 1-3 MPa (strain of 10-25%) with the anterior annulus being stronger than the posterolateral, and the OAF stronger than the IAF (Ebara et al., 1996). At faster strain rates, the stress at failure rises to 3.5 MPa in the horizontal direction and 10 MPa in the direction of the collagen fibres (Galante, 1967). Due to technical issues, it is difficult to determine the tensional force acting on the AF *in situ*. Previous studies suggest that the average vertical tensile strength of the outer annulus may be 4-9 MPa (Adams, 2006).

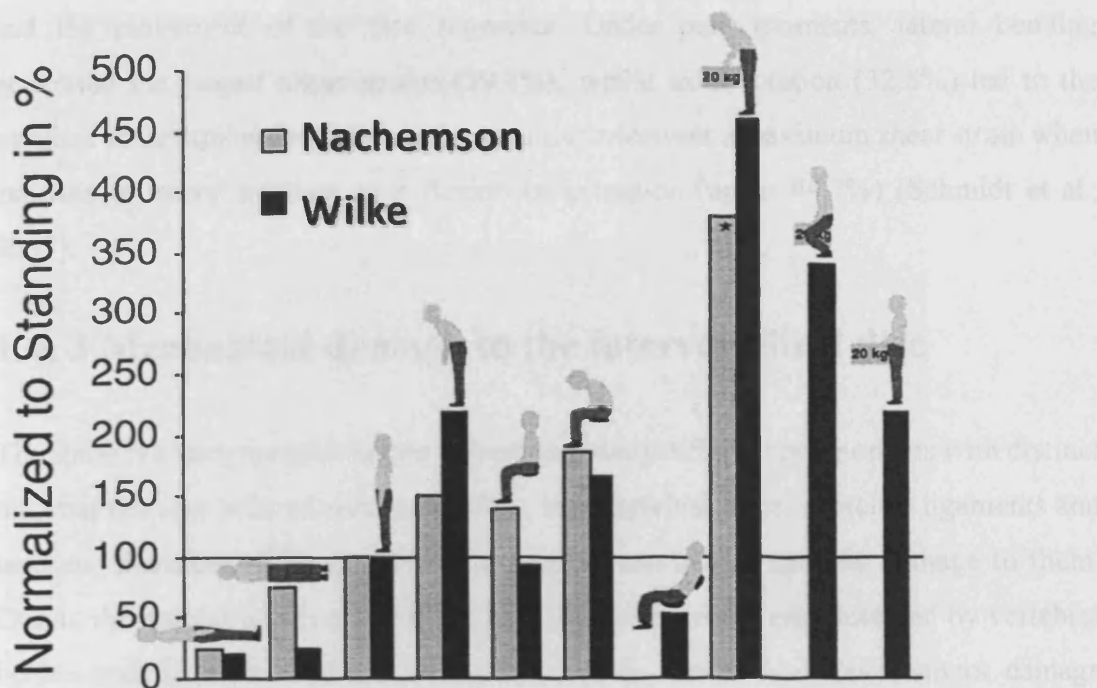


Figure 1-9. A comparison between data of Nachemson (Nachemson and Morris, 1964) and those of Wilke (Wilke et al., 1999) regarding intradiscal pressure in common postures and activities, normalised to standing. *Adapted from Wilke et al. Spine 24, 755-62.*

### 1.4.2.3 Shear

The definition of “shear” is the force which acts parallel to the transverse plane of the IVD, and is at 90° to the compressive force. Shear comes from the torsion movement between the adjacent vertebral bodies, which is mainly resisted by ligaments and muscles especially the zygapophysial joints. Therefore it can be assumed that the IVD only endures a small amount of shear during daily life. Compressive loading also contributes to its formation, therefore shear is greater in the lower lumbar spine. Shear force in the IVD has never been accurately measured *in vivo* due to the technical difficulty. However, anterior shear forces at L5–S1 have been measured at up to 2000 N, and the maximum shear strain was located between the annulus and the inferior endplate (van Dieen et al., 2006). There is a close relationship between the shear stress

and the movement of the disc segments. Under pure moments, lateral bending generated the largest shear strains (39.7%), whilst axial rotation (32.8%) led to the smallest shear strains. In addition, the annulus underwent a maximum shear strain when exposed to lateral bending plus flexion or extension (up to 44.7%) (Schmidt et al., 2007).

### **1.4.3 Mechanical damage to the intervertebral disc**

The spine is a very complex organ comprising many different components with distinct material features such as vertebral bodies, intervertebral discs, muscles, ligaments and tendons; therefore, different mechanical forces can induce specific damage to them. Due to the special position of the IVDs in the spine, which are protected by vertebral bodies and ligaments and are almost immovable, mechanical force cannot damage them directly unless other components around the IVD are firstly damaged. However, mechanical forces can indirectly induce IVD failure after short-term or long-term stimulation through different mechanisms described below:

#### **1.4.3.1 Compression**

As described above, the lamellae of the annulus fibrosus is an unstable structure. When they are arranged in an orderly fashion, the lamellae are stiff enough to resist compressive loading; however, if it buckles, the stiffness will decrease and it will be less able to resist the load. Compressive damage to vertebra allows the endplate to bulge into the vertebral body, therefore increasing the volume of the NP and resulting in a large and immediate drop in NP pressure (Adams et al., 2000). The decompressed NP resists less of the applied compressive force, so more of the load falls upon the AF. The vertical lamellae of the OAF are more severely compressed than before but they receive less radial stress support from the NP. Consequently, the lamellae may buckle forward towards the NP. This splits the lamellae apart, causing tears in the AF (Adams et al., 2000; Holm et al., 2004).

The other possibility of inducing damage to the IVD is that the disc endures sudden extreme loading exceeding its physical limitation. Under this situation, the applied

compressive force required to cause prolapse is quite high, up to 5.4 kN on average (range 2.8-13.0 kN) (Adams and Hutton, 1982).

### **1.4.3.2 Compression and bending**

As the IVD has a higher compressive strength than the vertebral bodies on either side of it, direct physiological compressive loading cannot cause direct damage to the disc (Perey, 1957; Liu et al., 1983). The only proven method of inducing disc prolapse in response to mechanical loading is to bend the disc so much that the stretched and thinned posterior annulus becomes weaker than the vertebral endplate. At the same time, a compressive load is applied on the IVD, causing the herniation of the nucleus through the weakened annulus, or causing the annulus to collapse outwards (Adams and Hutton, 1982; Adams and Hutton, 1985).

### **1.4.3.3. Repetitive loading**

The combination of compression and bending has been found to induce disc prolapse at low levels during cyclic loading. When a cyclic load is applied, the water contained in the disc is expelled from the tissue. When the load cycle increases, the fluid continuously moves out of the disc, and there is not enough time for the NP to reabsorb the water, so there is a redistribution of water in the disc (Masuoka et al., 2007). At the same time, the cyclic loading repeatedly stretches the fibres of the annulus fibrosus, making it fragile and inducing the separation of the lamellae bundles. Therefore, the fluid and a small amount of material from the NP will collapse outwards, causing a decrease in nucleus pressure and disc height (Natarajan et al., 2004).

## **1.5 Biomechanics and biochemical changes of IVD**

When mechanical stimulation is applied to the IVD, there will be a dramatic alteration in IVD cell metabolism with ECM remodeling. Most of the knowledge about these changes is obtained from experiments performed *in vitro*. However, these results provide valuable clues as to what happens *in vivo* when the IVD endures mechanical stimulation.



### 1.5.1 Compression

Compressive stimuli associated with weight-bearing and loading of the intervertebral disc are believed to be important regulators of disc cell metabolism. As discussed above, hydrostatic pressure in the NP is variable according to the position of the body and its movement (Nachemson and Morris, 1964). Therefore, three different magnitudes of loading: 0.1MPa (low), 0.25-1.0 MPa (medium) and 2.0-10.0 MPa (high) were used in most of the experiments investigating the effect of static loading on the metabolism of the IVD. Most of the results show that medium compressive loads tend to increase type I collagen and aggrecan in the NP, but has no influence on MMP synthesis. In contrast, low and high levels of compression tend to inhibit anabolic protein expression but promote MMP synthesis in NP (Ishihara et al., 1996; Handa et al., 1997; Hutton et al., 1999; Hutton et al., 2001; Liu et al., 2001; Neidlinger-Wilke et al., 2006). These results suggest that physiological compressive stimulation is one of the essential factors for maintaining matrix turnover in the disc. Pressures that are too high or too low may cause an imbalance in matrix synthesis and promote disc degeneration.

Epidemiological studies suggest that whole body vibration is an important risk factor for low back pain (Bovenzi and Hulshof, 1999). Studies performed *in vivo* have shown that the frequency acting on the human spine during daily life is about 3-10Hz (Schulze and Polster, 1979). However, the human spinal system has a characteristic response to vibrational inputs in a seated posture. The first resonance occurs within a band of 4.5 to 5.5 Hz, and the second is identified in the range of 9.4 to 13.1 Hz (Pope et al., 1998). When 4.5-5.5Hz vibration passes through the human spine, a marked enhancement of vibration occurs and causes a high nucleus pressure (Kasra et al., 2006). 4.5-5.5Hz vibration can also disrupt normal intervertebral disc cell metabolism through inhibition of protein synthesis, promoting collagen and proteoglycan degradation (Kasra et al., 2006). In addition, another study using a rabbit model demonstrated that short-term application of high loading amplitudes and frequencies was beneficial in stimulating protein synthesis and reducing protein degradation (Kasra et al., 2003). Therefore, it is reasonable to assume that the key factor between vibration and disc degeneration is resonance (Pope et al., 1998).

## **1.5.2. Tensile forces**

Previous studies have shown that the NP is more responsive than annulus fibrosus to hydrostatic pressure, but it is mainly the annulus fibrosus cells that are subjected to stretch and shear stresses *in vivo* (Rannou et al., 2003). Therefore, most of the studies investigating the effect of cyclic stretch on IVD cells focus on the OAF. Cyclic stretch can inhibit proteoglycan synthesis, and thus may be involved in the pathogenesis of disc degeneration (Rannou et al., 2003; Benallaoua et al., 2006). In addition, nitric oxide (NO) may also be involved in inhibiting proteoglycan production in OAF cells subjected to cyclic stretch through a post-translational mechanism (Rannou et al., 2003; Benallaoua et al., 2006). Another study suggests that inflammatory agents such as prostaglandin-E<sub>2</sub> is highly increased in both NP and OAF cells after stimulation with cyclic mechanical stress (Miyamoto et al., 2006), and therefore may contribute to disc degeneration. Studies on the effect of cyclic mechanical stretch on NP cells is limited, but it has been shown to promote cell proliferation and collagen synthesis (Matsumoto et al., 1999).

## **1.6 Ageing and IVD degeneration**

### **1.6.1 Macroscopic Changes with Increasing Age**

Disc degeneration is an age-related disease, therefore degenerative changes to the IVD are often observed with age. Macroscopic changes to the disc include the appearance of horizontal splits and clefts midway between the centre of the disc and the cartilage endplates, which can eventually lead to fissures through the annulus. With age, there is a reduction disc depth due to the loss of water which is caused by the conversion of the NP tissue to a collagenous tissue. A gradual ossification of the endplate and protrusion of the disc tissue are also observed. Disc degeneration can also lead to potential weak points in the subchondral bone and in the posterior and posterolateral segments of the annulus, which are thinner and less firmly attached to the vertebra (Ferguson and Steffen, 2003).

## **1.6.2 Changes in Matrix Components with Age**

Age- and degeneration-related changes to disc tissue properties have been extensively evaluated. Iatridis et al concluded that changes to the mechanical properties suggest a shift from a “fluid like” behaviour to a more “solid like” behaviour with degeneration (Iatridis et al., 1997). At present, normal disc function is often envisaged in terms of the collagen fibrils of the AF and the aggrecan of the NP. The swelling of the NP due to the proteoglycans is resisted radially by the collagen fibrils of the annulus and axially by the vertebrae, and provides the ability to withstand the compressive loads due to weight and bending. The collagen fibrils of the AF also resist the tensile forces encountered during bending and twisting. However, the proteoglycan content in the NP decreases with age, leading to the inability of the NP to resist compression as the water retained by aggrecan declines (Sztrolovics et al., 1999). Enrichment in the aggrecan content of the IAF may be viewed as a mechanism to overcome the declining function of the NP with age. Some other proteoglycans in the disc also change with increasing age. For example, there is a decrease in fibromodulin in the adult NP with age (Sztrolovics et al., 1999). In addition, fibromodulin in the OAF exhibited a structural change with increasing age, as characterised by a shift toward the predominance of its glycoprotein form lacking keratan sulphate (Sztrolovics et al., 1999). An age-related redistribution of collagen types I and II is observed in disc, with more type I but less type II collagen in the NP (Hormel and Eyre, 1991). In addition, there is evidence showing an age-related increase in cross-linked collagen, which may play a pivotal role in disc function disorder (Duance et al., 1998). The elastic fibre content which is responsible for elasticity also changes with age (Barros et al., 2002), which is likely due to an increase in tissue density due to water loss.

## **1.6.3 Changes in Matrix Turnover and Catabolism with Age**

With increasing age, there are also dramatic changes in matrix turnover. It has been shown that types I and II collagen as well as aggrecan synthesis rates drop markedly with increasing age especially in the nucleus (Antoniou et al., 1996). The mechanism of the change is not clear to date, although some evidence has indicated that insulin-like

growth factor binding proteins may play a role in this age-related loss of aggrecan (Okuda et al., 2001). However, catabolic enzymes including the aggrecanases and MMPs play an increasing role during ageing of the disc. For example, there is an age-related increase in the abundance of aggrecan degradation products in the IVD, which are cleaved by both the aggrecanases and MMPs (Sztrolovics et al., 1997). Taken together, the decrease in matrix component synthesis as well as the increasing proteolytic activities in the ageing disc will eventually lead to an imbalance in ECM turnover favouring catabolism. The continual catabolism occurring in the disc matrix and the inability to replace degraded collagen and aggrecan with newly synthesised molecules throughout life ultimately results in a functionally impaired tissue, and onset of disc degeneration.

## 1.7 Pathology of low back pain

Low back pain is a worldwide endemic problem and a leading health concern. It is the second and fifth most frequently reported reason for visiting a doctor and hospitalisation respectively (Waddell, 1991). The prevalence of low back pain ranges from 12%-35%, with about 10% of sufferers becoming chronically disabled (Maniadakis and Gray, 2000). Despite the fact that 80% of the population will experience back pain at some point during their life (Waddell, 1991), up to 90% will recover spontaneously within four weeks, and only 5% remain disabled longer than three months (Papageorgiou and Rigby, 1991). Low back pain also imposes a huge economic burden. It cost approximately 1.7% of the gross national product in the U.K. and the direct business loss due to low back pain is around £5 billion per annum (Frymoyer and Cats-Baril, 1991; Wilkin, 2009).

The aetiologies of low back pain are many, but IVD degeneration appears to be the leading cause (Schwarzer et al., 1994). What is intervertebral disc degeneration, and what causes it? Disc degeneration is a very complex process with many biochemical, physical and mechanical factors including age, sex, nutrition, genetic inheritance and mechanical stimulation being involved. Therefore it is very difficult to give a precise definition of disc degeneration. Until recently, researchers proposed the following definition: “*the process of disc degeneration is an aberrant, cell mediated response to*

*progressive structural failure combined with accelerated or advanced signs of ageing. Early degenerative changes should refer to accelerated age-related changes in a structurally intact disc. Degenerative disc disease should be applied to a degenerate disc that is also painful” (Adams and Roughley, 2006).*

This definition contains at least 3 key points for disc degeneration. The first is that disc degeneration is a “cell-mediated process”, which would include all the abnormal alterations of cell metabolism in the disc, matrix remodelling such as altered enzyme activity, cell senescence and death as well as the changes in matrix macromolecules. All these alterations can cause the loss of tissue homeostasis and eventually lead to the second key point: “structure failure”, which usually includes disc tears, herniation and prolapsed discs.

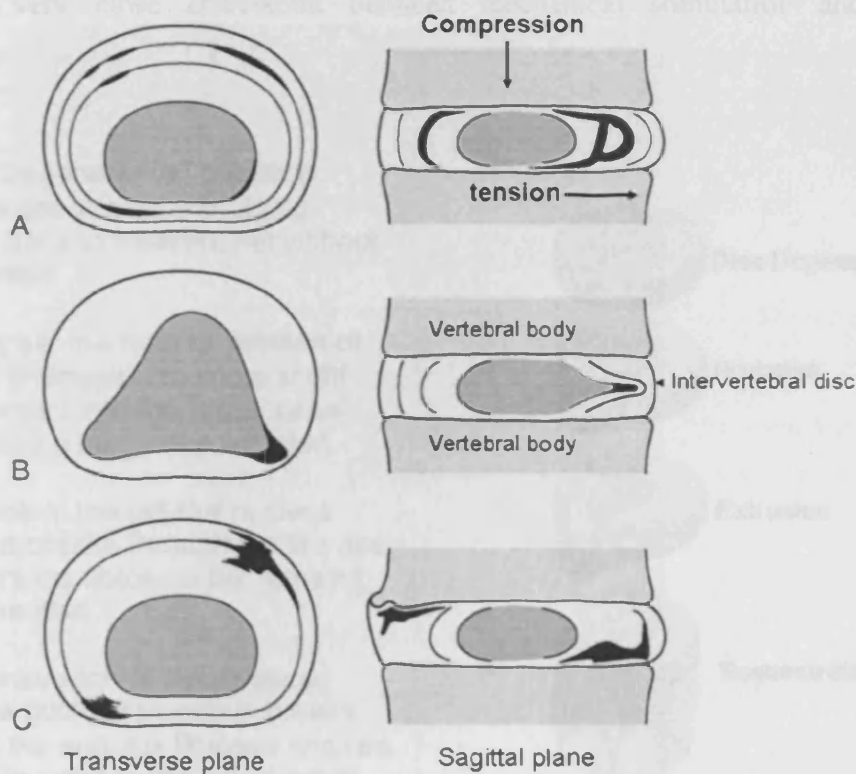


Figure 1-10. The three different types of annulus tears in the intervertebral disc. A: Circumferential clefts. B: Radial fissure. C: Peripheral rim lesion. Disrupted tissue is shown in black, and nucleus pulposus is shaded. *Adapted from Adams, M.A., and P.J. Roughley. 2006. Spine. 31:2151-61.*

There are three different kinds of tears in degenerative disc: circumferential tears, peripheral rim tears and radial fissures (Adams and Roughley, 2006) (Figure 1-10). Circumferential tears are a result of the effect of interlaminar shear stress, which are derived from compressive stress concentrations in older discs (Goel et al., 1995). Radial fissures can be stimulated by cyclic loading in bending and compression (Adams, 2004), whereas the peripheral rim tears may be associated with bony outgrowths (Hilton and Ball, 1984). When radial fissures allow the gross migration of the NP into the non-intact annulus under compressive load, the disc is herniated, or prolapsed. According to the extent of NP migration, disc herniation can be further divided into protrusion, extrusion or sequestration (Figure 1-11). Disc prolapse can result from the combination of bending and compression, with either one exceeding the physiological limits (Adams and Hutton, 1982). All of the above illustrate that there is a very close correlation between mechanical stimulation and disc degeneration.

1) **Disc Degeneration:** chemical changes associated with aging causes discs to weaken, but without a herniation.

2) **Prolapse:** the form or position of the disc changes with some slight impingement into the spinal canal. Also called a bulge or protrusion.

3) **Extrusion:** the gel-like nucleus pulposus breaks through the tire-like wall (annulus fibrosus) but remains within the disc.

4) **Sequestration or Sequestered Disc:** the nucleus pulposus breaks through the annulus fibrosus and lies outside the disc in the spinal canal (HNP).

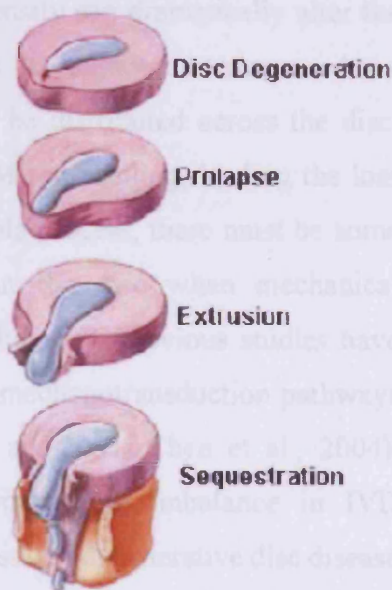


Figure 1-11. Different types of herniation in the intervertebral disc. Taken from <http://www.spineuniverse.com/displayarticle.php/article2681.html>

The third key point of disc degeneration is “ageing”. Low back pain is an age-related problem and most of the patients affected are above 45 years old (Deyo et al., 2006). Despite this, disc degeneration actually occurs far earlier than the appearance of low back pain. The first unequivocal findings of degeneration in the lumbar discs are seen in the age group 11-16 years, where about 20% of people experienced mild signs of disc degeneration (Boos et al., 2002), but most of them are asymptomatic. In human discs, there is an age-related alteration in cell population and ECM content including cell cluster formation (Hastreiter et al., 2001), increased cell apoptosis (Trout et al., 1982), loss of proteoglycan and alteration in the collagen type and distribution (Anderson and Tannoury, 2005). Ageing also leads to diminished metabolic output from the remaining disc cells (Antoniou et al., 1996), which will predominately weaken the disc structure. Therefore, ageing is a very important factor in disc degeneration, although there is some evidence that shows that ageing itself can not trigger the structural failure of the disc and the associated low back pain (Battie et al., 2004).

Age-related changes in matrix composition and cell density can dramatically alter the mechanical features of the whole disc as well as its adjacent structure. As a consequence, inappropriate stress concentrations will be distributed across the disc, which may induce abnormal cell metabolism and ECM remodelling, leading the loss of tissue homeostasis and disc degeneration. During this process, there must be some communication between the ECM and the cells in the disc when mechanical stimulation is applied. This is named “mechanotransduction”. Previous studies have shown that the cytoskeleton may be involved in these mechanotransduction pathways between the cell nucleus and the ECM (Hayes et al., 2001; Chen et al., 2004). Dysregulation of the cytoskeletal networks can promote an imbalance in IVD homeostasis favouring a catabolic phenotype characteristic of degenerative disc disease. However, the role of the cytoskeleton in the cells of different regions of discs and how the alterations in cytoskeletal elements develop with age and disease is not fully known, but it is very important for understanding the pathogenesis of IVD degradation. Therefore, the following hypotheses are proposed in this study:

## 1.8 Hypotheses

- An intact cytoskeleton is essential for transducing mechanical signals within cells of the intervertebral disc.
- There will be zonal variations and age-related differences in cytoskeletal element organisation and expression in IVD cells.
- An alteration in cytoskeletal element organisation and expression levels will be induced when IVD cells are subjected to mechanical stimulation.
- The alteration in ECM metabolism is associated with changes induced by mechanical stimulation.
- The response of IVD cells to compressive loading will be different to that of tensile loading.

## 1.9 Project Aims

- To characterise zonal variations in cytoskeletal element organisation and expression between NP and OAF disc tissue and cells.
- To characterise age-related differences in cytoskeletal element organisation and expression between young and mature disc tissue and cells.
- To characterise the response of cytoskeletal elements in IVD cells subjected to compression and/or tensile strain *in vitro*.
- To determine the metabolic response of IVD cells to compressive loading and/or tensile strain *in vitro*.



# CHAPTER 2.

Zonal and age-related differences in the  
organisation and expression of cytoskeletal  
elements within IVD cells in situ

## 2.1 Background

IVD is avascular and alymphatic, and comprises four morphologically distinct zones namely the NP), the annulus fibrosus (inner [IAF] and outer [OAF]) and the cartilaginous end plate. The IVD has important mechanical functions in maintaining flexibility and dissipating loads applied to the spine. IVD cells exposed to physiological mechanical loads experience complex physical stimuli including compressive, tensile and shear stresses and strains, fluid flow, hydrostatic pressure and osmotic pressure (Urban et al., 1993, Weidenbaum et al., 1992, Iatridis et al., 1996). These physical stimuli are believed to be important regulators of IVD cell metabolism contributing to matrix turnover – both synthesis and degradation, in normal and degenerative discs. However, it has been reported that the distinct cell populations of the IVD respond differently to compressive loads (Wang et al., 2007, Setton and Chen, 2006, Chen et al., 2004), suggesting that there may be intrinsic differences in the cell types. The IVD comprises a sparse population of heterogeneous cells; the NP cells resident at the centre of the disc closely resemble chondrocytes, whereas the OAF cells at the periphery of the disc are characteristic of fibroblasts (Errington et al., 1998). In bovine IVDs, the OAF cells have been shown to contain elongated processes containing filamentous F-actin (Errington et al., 1998, Bruehlmann et al., 2002) and vimentin (Bruehlmann et al., 2002). In the study by Errington et al. (Errington et al., 1998), specific cytoskeletal components in the cell processes were hypothesised to play a role in ‘sensing’ mechanical loads. More recently, it has been demonstrated that the cytoskeleton may play a crucial role in mechanotransduction between the IVD cells and their surrounding extracellular matrix (Hayes et al., 1999, Chen et al., 2004). The cytoskeleton, comprising actin microfilaments, tubulin microtubules and vimentin intermediate filaments in the IVD, is fundamental to the dynamic functions of the cell. Collectively, the three major cytoskeletal elements play important roles in cell division, motility, protein trafficking and secretion (Benjamin et al., 1994, Thyberg and Moskalewski, 1999). Furthermore, specific cytoskeletal features may reflect different mechanical influences on these cells, as it has been previously demonstrated that static load

## Chapter 2: Zonal and age-related differences in the organisation and expression of cytoskeletal elements within IVD cells *in situ*

---

increases vimentin polymerisation in IVD cells (Chen et al., 2004), and compressive load induces reorganisation of the vimentin architecture in articular chondrocytes (Durrant et al., 1999, Eggli et al., 1988, Blain et al. unpublished observations). Therefore, the activities of the NP and OAF cells of the IVD are likely to be dependent upon their morphology and hence cytoskeletal composition. With the exception of a few studies which have investigated F-actin and vimentin organisation in bovine IVD (Errington et al., 1998) and in normal versus pathological human discs (Johnson and Roberts, 2003) very little is known on the content and organisation of the 3 major cytoskeletal elements in the two distinct IVD cell populations, and whether there are differences with skeletal maturity.

The aim of the works described in this chapter was to fully characterise the abundance of the 3 major cytoskeletal elements; F-actin,  $\beta$ -tubulin and vimentin in the NP and OAF of immature (7 day old) and mature (18 month old) bovine IVDs using a combination of scanning laser confocal microscopy, quantitative PCR and Western blotting to examine, in detail, network organisation, mRNA and protein levels, respectively.

## **2.2 Materials and Methods**

All chemicals were obtained from Sigma (Poole, UK) unless otherwise stated and were of analytical grade or above.

### **2.2.1 Source of Bovine Intervertebral Discs**

Bovine tails from immature (7 day old) and skeletally mature (18 month old) steers were obtained from the abattoir within 6 hours of slaughter. The proximal coccygeal discs (CC1–CC5) were exposed, and cleaned of all surrounding ligaments and fascia. The discs were removed by dissection from the adjacent vertebrae. The NP and OAF were dissected out of the IVDs according to their morphology viewed by a dissecting microscope, snap frozen in liquid nitrogen and stored at -80°C until required. Accurate dissection of NP from OAF was verified by immunoblotting for types II and I collagen, respectively.

### **2.2.2 Analysis of cytoskeletal element organisation using confocal microscopy**

Bovine IVD samples were obtained from 7 day and 18 month old animal tails and placed in liquid nitrogen for rapid freezing prior to storage at -80°C. Frozen cryosections were taken at 10µm thickness as shown in Figure 2-1, placed on polylysine coated slides, and fixed in 4% paraformaldehyde at room temperature for 30 minutes. After repeated washes in modified Hank's balanced salt solution (mHBSS), tissue sections were permeabilised in 5% Triton X-100 for 30 minutes at room temperature. Sections were washed three times in mHBSS followed by blocking in 10% goat serum at room temperature for 60 minutes. Sections were then incubated with primary antibody or phosphate buffered saline (PBS)-Tween 20 (negative control) in the dark. Mouse anti-tubulin antibody (E7) (Developmental Studies Hybridoma Bank, University of Iowa, USA). 1:100 dilution was used at room temperature, whereas mouse anti-vimentin antibody (V9) 1:40 dilution (Sigma, Poole, UK) was used at 4°C overnight. Actin filaments were stained directly using

## Chapter 2: Zonal and age-related differences in the organisation and expression of cytoskeletal elements within IVD cells *in situ*

Alexa<sup>®</sup> 488 phalloidin (Invitrogen, Paisley, UK) 1:100 dilution at 4°C overnight. After extensive washes, goat anti-mouse immunoglobulin G (IgG) conjugated with Alexa<sup>®</sup> 488 secondary antibody (Invitrogen, Paisley, UK) was incubated with the sections at a 1:100 dilution (except the actin labelled sections, which were incubated in PBS-Tween) in the dark. Sections were washed extensively and mounted in Vectorshield™ containing propidium iodide (10µg/ml) (Vector Laboratories, Peterborough, UK) and stored at room temperature avoiding light before scanning. The staining of cytoskeletal elements was examined using a Leica DM6000B upright digital microscope (Leica, Wetzlar, Germany) and controlled by the Leica Control software, set up for dual-channel fluorescence recordings as described previously (Blain et al, 2006). Representative cells were continually scanned for 35-40 serial sections using a 63x oil immersion objective with appropriate excitation and emission settings for fluorescein isothiocyanate and propidium iodide. Leica confocal software (Leica, Wetzlar, Germany) was used to reconstruct the 3D organisation of the cytoskeletal elements according to the serial 2D images from the same sample. Negative controls, omitting the primary antibody, conducted in parallel were devoid of fluorescent signal.

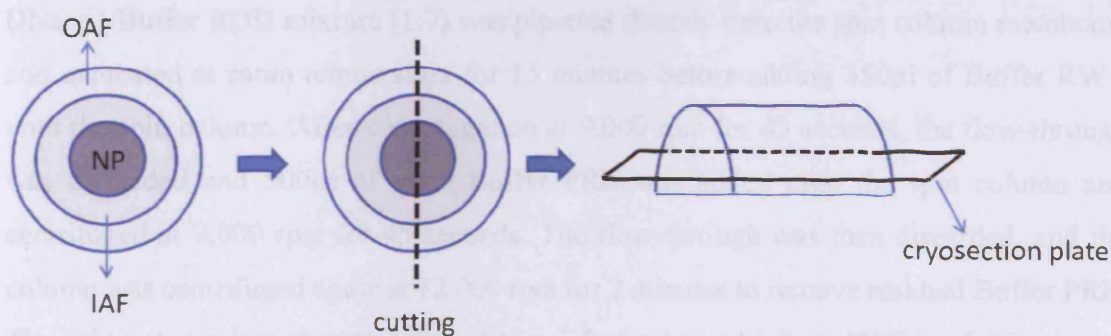


Figure 2-1 Schematic illustration of cryosection for confocal microscopy analysis.

## **2.2.3 Analysis of cytoskeletal element gene expression using quantitative polymerase chain reaction**

### **2.2.3.1 Total RNA extraction**

Total ribonucleic acid (RNA) was extracted from both NP and OAF of bovine IVDs. IVD tissue (50mg) was powdered at 2000rpm for 90 seconds in a liquid-nitrogen cooled Mikro-Dismembrator (Braun Biotech, Melsungen, Germany). 1ml Trizol™ reagent (Invitrogen, Paisley, UK) was added directly to the powdered tissue and warmed to room temperature. The samples were then transferred to 1.5ml tubes, mixed with 250µl chloroform, and stored at room temperature for 3-5 minutes. Samples were centrifuged at 14,000 rpm for 15 minutes at 4°C. The upper clear aqueous phase containing RNA was transferred to a sterile tube containing 375µl of 70% ethanol and mixed by inversion. Total RNA was then purified using Qiagen RNeasy mini kits (Qiagen, West Sussex, UK) according to the manufacturer's protocols. Briefly, the mixture described above was applied to a spin column from the Qiagen Kit and centrifuged at 9,000 rpm for 45 seconds. After discarding the flow-through, 350µl of Buffer RW I was added onto the spin column and centrifuged at 9,000 rpm for 15 seconds. After discarding the flow-through again, 80µl DNase I/Buffer RDD mixture (1:7) was pipetted directly onto the spin column membrane and incubated at room temperature for 15 minutes before adding 350µl of Buffer RW I onto the spin column. After centrifugation at 9,000 rpm for 45 seconds, the flow-through was discarded and 500µl of wash Buffer PRE was added onto the spin column and centrifuged at 9,000 rpm for 45 seconds. The flow-through was then discarded, and the column was centrifuged again at 12,000 rpm for 2 minutes to remove residual Buffer PRE. The spin column was then transferred to a 1.5ml tube and left at 37°C for 5-15 minutes before 30µl of nuclease-free water was added to dissolve the RNA which was collected by centrifugation at 9,000 rpm for 60 seconds.

### **2.2.3.2 cDNA synthesis**

First strand complementary deoxyribonucleic acid (cDNA) was synthesised (10µl RNA/20µl reaction volume) using Superscript™ III reverse transcriptase as previously described (Blain et al., 2006). Briefly, 1µg Oligo(dT)<sub>15</sub> (Promega, Southampton, UK) and 500µM dNTP (Promega, Southampton, UK) were added to 10 µl RNA, and incubated at 65°C for 5 minutes. After adding 4µl 5× first-strand buffer (250 mM Tris-HCl pH 8.3, 375 mM KCl, 15 mM MgCl<sub>2</sub>), 200mM dithiothreitol (DTT) and 10U RNase Inhibitor (Promega, Southampton, UK), the sample was incubated at 42°C for 2 minutes. 200U Superscript III reverse transcriptase (Invitrogen, Paisley, UK) was added to the sample and incubated for 50 minutes at 42°C. The reaction was stopped by heating the samples at 70°C for 15 minutes.

### **2.2.3.3 Generation of plasmid standards for real-time PCR**

#### **2.2.3.3.1 Amplification of target gene by PCR**

The target gene was amplified using GoTaq Flexi DNA polymerase kits (Sigma, Poole, UK) according to the manufacturer's protocol. Briefly, a 20µl PCR reaction was set up as detailed below (Table 2-1). After mixing thoroughly, the PCR reaction was performed according to the following conditions: Denaturation: 95°C 30 seconds; Annealing: varied according to the primers (see details below in Table 2-3) 30 seconds; Extension: 72°C 30 seconds. The reaction was stopped by heating to 72°C for 10 minutes after 40 cycles. PCR products were separated by electrophoresis on 2% agarose gels containing ethidium bromide (10µg/ml) and visualised under an ultraviolet transilluminator.

#### **2.2.3.3.2 PCR product clean up**

PCR products were purified using the QIAquick PCR purification kit (Qiagen, West Sussex, UK) according to the manufacturer's protocol. Briefly, 75µl of Buffer PBI was mixed with 15µl of the PCR sample. The mixture was then transferred to a QIAquick spin column in a collection tube followed by centrifugation for 60 seconds at 10,000rpm. After

discarding the flow-through, samples were washed once using 0.75ml of buffer PE followed by an additional centrifugation for 1 minute at 10,000rpm to remove residual buffer PE. At the end of the procedure, the PCR product was eluted with 50µl of dH<sub>2</sub>O.

### 2.2.3.3.3 pGEM<sup>®</sup>-T Easy Vector ligation

T4 DNA ligase was used to catalyse the joining of the target gene fragment to the pGEM<sup>®</sup>-T Easy Vector (Promega, Southampton, UK) according to the manufacturer's protocols. Briefly, a 5µl reaction was set up according to the Table below (Table 2-2). After mixing thoroughly, the ligation was performed overnight at 4°C.

**Table 2-1. PCR reaction mixture composition**

Reagent	Volume(µl)
dH <sub>2</sub> O	3
5mM dNTP	0.4
5x buffer	4
25mM MgCl	2
GoTaq (5U/µl)	0.22
10µM primers (F+R)	0.54
cDNA	10
Total	20.16

**Table 2-2. pGEM<sup>®</sup>-T Easy Vector ligation reaction components**

Reagent	Volume (µl)
2X Rapid Ligation Buffer, T4 DNA Ligase	2.5
pGEM <sup>®</sup> -T Vector (50ng)	0.5
PCR product	1.5
T4 DNA Ligase (3U/µl)	0.5
Total	5



#### **2.2.3.3.4 Transformation of competent *E. Coli* cells with the ligated pGEM<sup>®</sup>-T Easy Vector**

2µl of each ligation reaction sample was added to a sterile 1.5ml tube on ice, followed by adding 25µl of JM109 High Efficiency Competent Cells ( $>10^7$  cfu/µg; Promega, Southampton, UK). The tubes were then gently flicked to mix and placed on ice for 20 minutes. The mixture was heat-shocked for 45-50 seconds in a water bath at exactly 42°C, and then immediately returned to ice for 2 minutes. 475µl of SOC medium (Invitrogen, Paisley, UK) was added to the transformed cells, and incubated for 1.5 hours at 37°C with shaking at 220rpm. 100µl of transformation product was spread on LB/ampicillin/β-D-1-thiogalactopyranoside (IPTG) /X-Gal plates (LB agar solution containing 100µg/ml ampicillin, 80µg/ml X-gal and 0.5mM IPTG). The plates were incubated at 37°C overnight. Two white colonies from each plate were selected using a sterile tip and used to inoculate 10ml of LB broth solution containing 100µg/ml ampicillin. Cultures were incubated at 37°C with shaking at 180rpm overnight.

#### **2.2.3.3.5 Plasmid extraction and purification**

Plasmid was extracted from *E. Coli* cells and purified using Wizard<sup>®</sup> Plus SV Minipreps DNA Purification System (Promega, Southampton, UK) according to manufacturer's protocol. Briefly, cells were harvested by centrifugation for 10 minutes at 3300rpm. The cell pellet was resuspended using 250µl of cell resuspension solution. 250µl of cell lysis solution was added and samples were inverted several times to mix thoroughly. After no more than 5 minutes incubation, 10µl of alkaline protease solution was added and incubated for 5 minutes at room temperature. 350µl of neutralisation solution was then added and mixed immediately by hand followed by centrifugation at 14,000rpm for 10 minutes at room temperature. The supernatant was decanted into a spin column and centrifuged for 1 minute at maximum speed. After discarding the flow-through, the spin column was washed twice using column wash solution at room temperature. The plasmid DNA was then eluted by adding 100µl of dH<sub>2</sub>O and centrifuged at 14,000rpm for 1 minute at room temperature. PCR was performed as described above (Section 2.2.3.3.1) using the plasmid DNA as template to check the transformation product, and the concentration of

plasmid was determined using the NanoDrop™ 1000 Spectrophotometer (Thermo Fisher Scientific, Hemel Hempstead, UK).

## **2.2.3.4 Real-time PCR**

### **2.2.3.4.1 Real-time PCR background**

Real-time PCR is more sensitive and reproducible because it measures the fluorescence at each cycle as the amplification progresses, unlike endpoint PCR in which the fluorescence data is collected after the amplification reaction has been completed (usually after 30–40 cycles). This allows quantification of the template based on the fluorescent signal during the exponential phase of amplification, before limiting reagents, accumulation of inhibitors, or inactivation of the polymerase have started to have an effect on the efficiency of amplification. Fluorescence readings at these earlier cycles of the reaction will measure the amplified template quantity where the reaction is much more efficient and, hence, more reproducible than at the endpoint.

In this study, a double stranded DNA binding dye SYBR Green I was used to monitor the progress of the amplification reaction. When free in solution, SYBR Green I displays relatively low fluorescence, but when bound to double-stranded DNA its fluorescence increases by over 1000-fold. The more double-stranded DNA that is present, the more binding sites there are for the dye, so fluorescence increases proportionately to DNA concentration. This property of the dye provides the mechanism that allows it to be used to track the accumulation of PCR product. As the target is amplified, the increasing concentration of double stranded DNA in the solution can be directly measured by the increase in fluorescence signal.

### **2.2.3.4.2 Setting up a standard curve using plasmid DNA**

The initial amount of target RNA in an unknown sample was calculated using a standard curve prepared from the dilution series of plasmid of known concentration (Section 2.2.3.3.5). As shown in Figure 2-2, the cloned PCR product was diluted to 1 µg/ml as the

working stock of the standard curve. The stock sample was then serially diluted 10 fold using nuclease-free water and finally seven points for the standard curve including 1,  $1 \times 10^{-1}$ ,  $1 \times 10^{-2}$ ,  $1 \times 10^{-3}$ ,  $1 \times 10^{-4}$ ,  $1 \times 10^{-5}$  and  $1 \times 10^{-6}$  ng were prepared. The standard curve samples and the unknown samples as well as a negative control (without template) were transferred to a RNase DNase free 96-well microplate to perform real-time PCR.

#### 2.2.3.4.3 Real-time PCR

Quantitative real-time PCR was performed using SYBR<sup>®</sup> Green Jumpstart<sup>™</sup> Taq ReadyMix<sup>™</sup> kits on the Mx3000P<sup>®</sup> QPCR System (Stratagene, Edinburgh, UK). Briefly, 12.5  $\mu$ l of ReadyMix buffer was mixed with 10.5  $\mu$ l of dH<sub>2</sub>O, 1  $\mu$ l of primers (each primer was at a final concentration of 100nM) and 1  $\mu$ l of cDNA to make up a total 25  $\mu$ l reaction (Table 2-3).

**Table 2-3 Real-time PCR reaction components**

Reagent	Volume ( $\mu$ l)
Sybr <sup>®</sup> GreenReadyMix buffer	12.5
dH <sub>2</sub> O	10.5
5 $\mu$ M primer mixture	1
cDNA	1
Total	25

Chapter 2: Zonal and age-related differences in the organisation and expression of cytoskeletal elements within IVD cells *in situ*

---

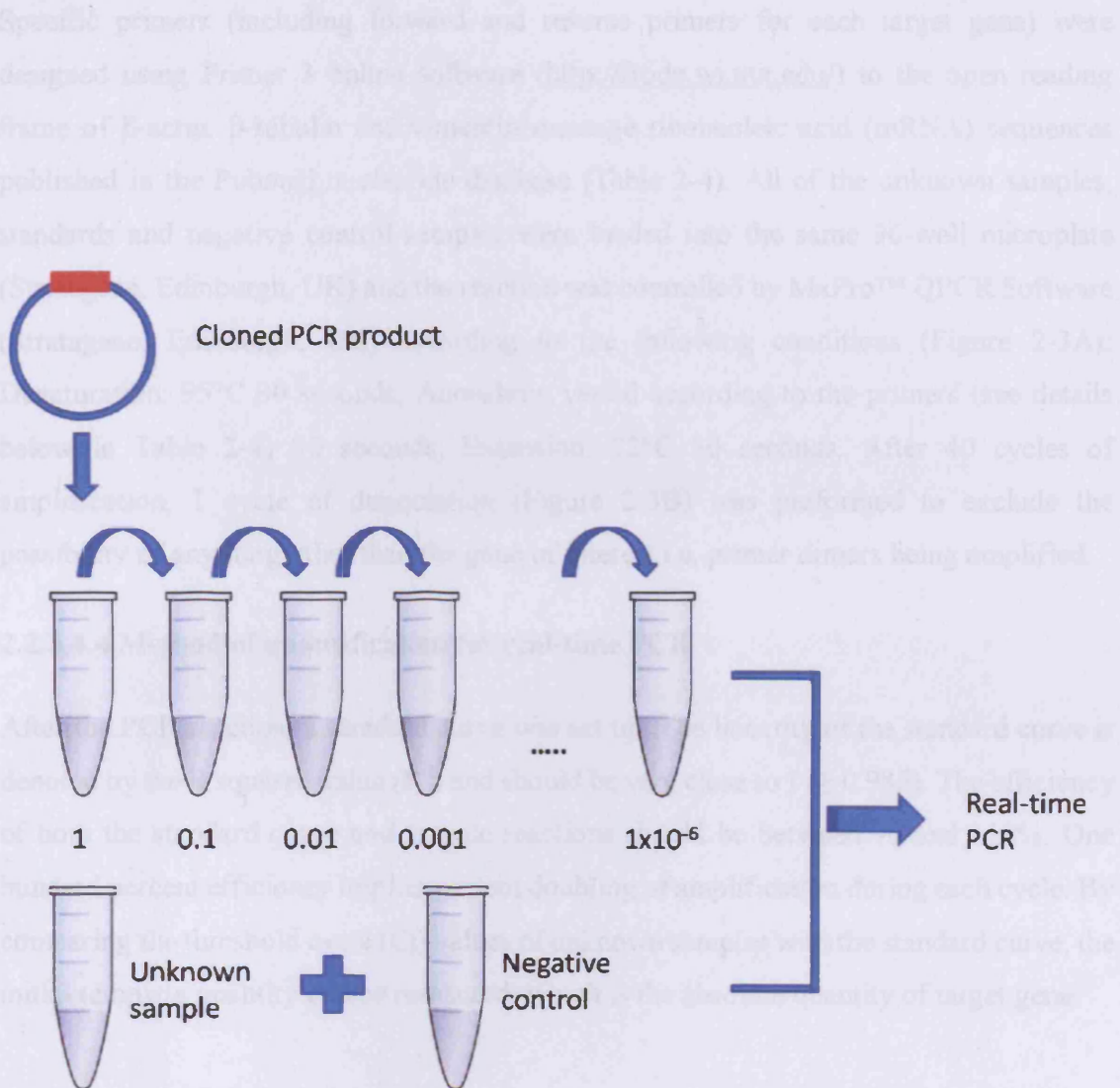


Figure 2-2. Experimental setup for producing a standard curve for real-time PCR. Using a known starting concentration of plasmid template, a dilution series is performed. These standards are run under the same conditions as the unknown samples and negative controls on the plate.

Specific primers (including forward and reverse primers for each target gene) were designed using Primer 3 online software (<http://frodo.wi.mit.edu/>) to the open reading frame of  $\beta$ -actin,  $\beta$ -tubulin and vimentin message ribonucleic acid (mRNA) sequences published in the Pubmed nucleotide database (Table 2-4). All of the unknown samples, standards and negative control samples were loaded into the same 96-well microplate (Stratagene, Edinburgh, UK) and the reaction was controlled by MxPro™ QPCR Software (Stratagene, Edinburgh, UK) according to the following conditions (Figure 2-3A): Denaturation: 95°C 30 seconds; Annealing: varied according to the primers (see details below in Table 2-4) 30 seconds; Extension: 72°C 30 seconds. After 40 cycles of amplification, 1 cycle of dissociation (Figure 2-3B) was performed to exclude the possibility of anything other than the gene of interest i.e. primer dimers being amplified.

#### **2.2.3.4.4 Method of quantification for real-time PCR**

After the PCR reaction, a standard curve was set up. The linearity of the standard curve is denoted by the R squared value ( $R^2$ ) and should be very close to 1 ( $\geq 0.985$ ). The efficiency of both the standard curve and sample reactions should be between 90 and 110%. One hundred percent efficiency implies perfect doubling of amplification during each cycle. By comparing the threshold cycle (Ct) values of unknown samples with the standard curve, the initial template quantity can be measured, which is the absolute quantity of target gene.

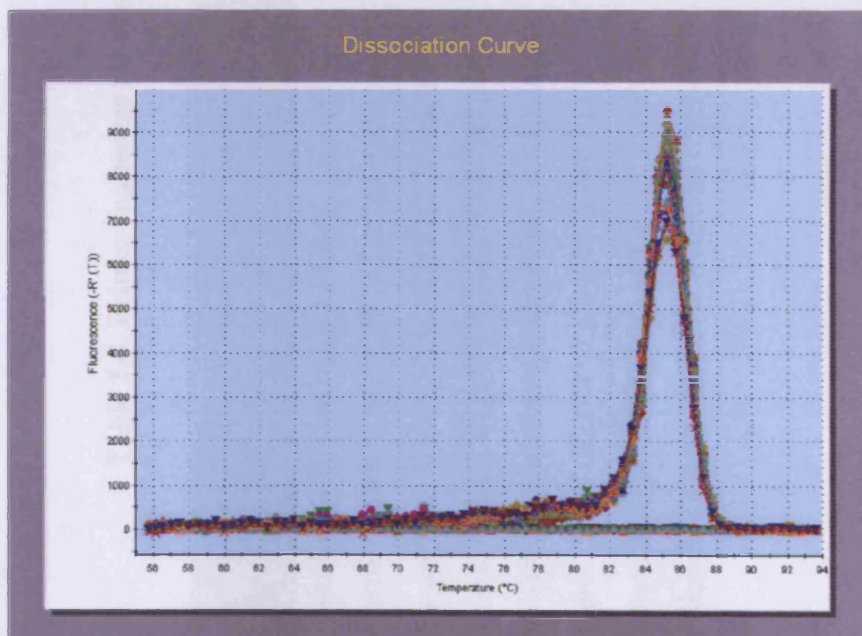
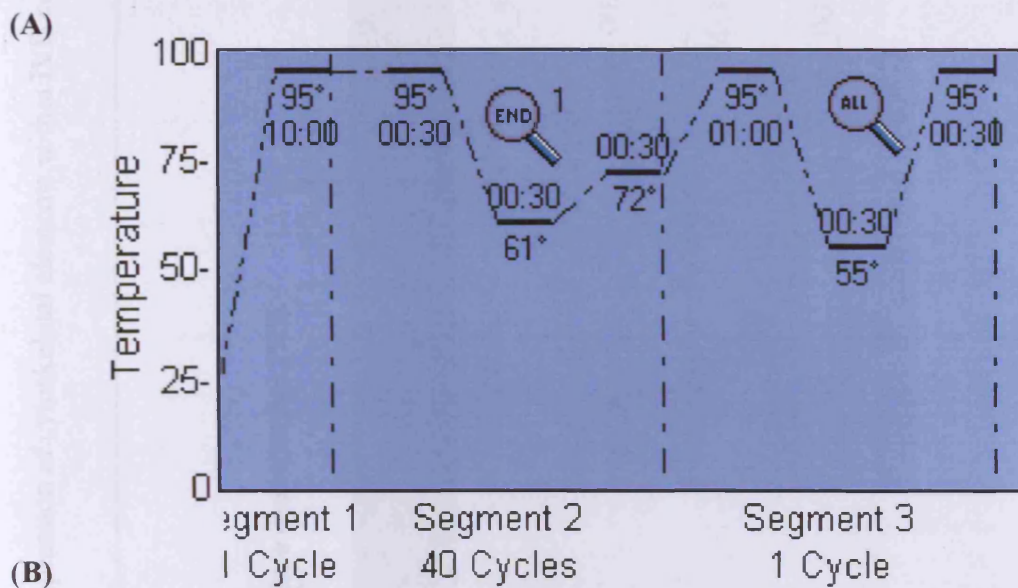


Figure 2-3 Representative reaction conditions and dissociation curve for real-time PCR. The unknown samples, standards and negative control samples were loaded onto the same microplate and the reaction was controlled by MxPro™ QPCR Software. **A:** a representative thermal profile for the PCR reaction; **B:** a representative dissociation curve, only one peak is observed.

To remove the potential errors induced by age-related variations in IVD cell metabolism and individual differences between animals, the unknown samples were normalised to the housekeeping gene GAPDH as described previously (Goossens et al., 2005; Blain et al., 2006). The relative concentration of the target gene was calculated according to the formula below. Where E corresponds to the efficiency of amplification of the target gene (a value from 0 to 1 that represents the number of amplification products generated during each cycle of the reaction per molecule of target sequence), Ct = threshold cycle (Ct), “normal” represents the internal control gene and target represents the target gene.

$$\text{Relative level of target gene} = \frac{(1 + E_{\text{target}})^{-\Delta C_{t\text{target}}}}{(1 + E_{\text{normal}})^{-\Delta C_{t\text{normal}}}}$$

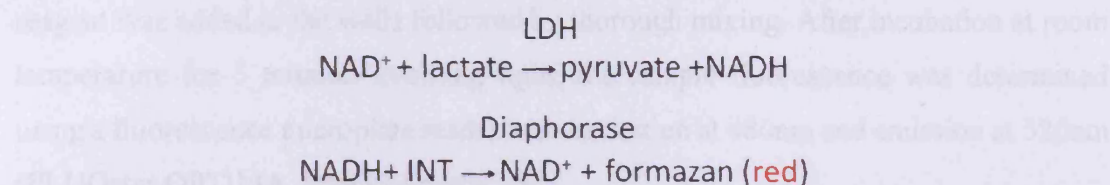
## 2.2.4 Determination of protein concentration using the BCA assay

Intervertebral disc tissue was divided into NP and OAF using a dissecting microscope and distilled water (200µl) was added, before samples were frozen in liquid nitrogen. The sample was then powdered at 2000rpm in a liquid-nitrogen cooled Mikro-Dismembrator (Braun Biotech, Melsungen, Germany). Soluble protein from the tissue (50mg tissue:1ml buffer) was extracted in 2x sample buffer (0.06M Tris pH 6.8, 2% (w/v) SDS, 10% (v/v) glycerol) plus protease inhibitors (a cocktail of protease inhibitors with broad specificity for the inhibition of serine, cysteine, aspartic and aminopeptidases) at 4°C overnight with agitation. Samples were pelleted by centrifugation at 14,000rpm at 4°C for 15 minutes, and the supernatant and pellet stored at -20°C for further treatment. The protein concentration of the supernatant was determined using the bicinchoninic acid (BCA) method according to the manufacturer's protocol (Perbio Science, Cramlington, UK). Briefly, a 2mg/ml stock of bovine serum albumin (BSA), provided by the BCA kit, was serially diluted using dH<sub>2</sub>O to set up a standard curve including 0, 25, 125, 250, 500, 750, 1000, 1500 and 2000µg/ml protein. 25µl of unknown samples or standards were pipetted into a microplate well in duplicate, and 200µl of the working reagent was added to each well and mixed thoroughly. After

incubation in the dark at 37°C for 30 minutes, the absorbance was measured at 575nm (FLUOstar OPTIMA, BMG Labtech, UK) and protein concentrations of unknown samples were related back to the standard curve.

## 2.2.5 Determination of cell viability using the lactate dehydrogenase assay

LDH is a stable cytosolic enzyme that is released upon cell lysis. After a chemical reaction as shown below, it can convert a tetrazolium salt (INT) into a red formazan product. The amount of color formed is proportional to the number of lysed cells.



The total number of cells within the tissue extracts was determined using the lactate dehydrogenase (LDH) assay according to the protocol from the non-radioactive cytotoxicity assay kit (Promega, Southampton, UK). Briefly, 50µl of the soluble protein samples extracted from tissue using 0.9% Triton X-100 was pipetted into a 96-well plate and mixed with 50µl of reconstituted substrate mix. After 10 minutes incubation at room temperature avoiding light, 50µl of stop solution was added to each well, and the absorbance values were determined at 492nm (FLUOstar OPTIMA, BMG Labtech, UK).

## 2.2.6 Determination of total cell number according to DNA concentration

Total cell number was also determined by measuring the DNA concentration of the cells. DNA was extracted from bovine IVD cells using a FlexiGene DNA kit (Qiagen, West Sussex, UK) according to the manufacturer's protocol. Briefly, the tissue powder described above (Section 2.2.4) was dissolved in 300µl of lysis buffer, and mixed by pipetting. After adding 300µl of denaturation buffer, samples were incubated at 65°C



for 10 minutes, before adding 600µl of isopropanol. After centrifugation at 10,000rpm for 3 minutes, the supernatant was discarded and the pellet was mixed with 600µl of 70% ethanol. After centrifugation as described above, the supernatant was discarded and the pellet was air dried at room temperature for 5 minutes. The DNA pellet was finally dissolved in 200µl of hydration buffer by incubation at 65°C for 30 minutes.

The DNA concentration was determined using Quant-iT™ PicoGreen® dsDNA reagents (Invitrogen, Paisley, UK) according to the manufacturer's protocol. Briefly, 100µl of DNA standards (0, 10, 100, 1000 and 10,000ng/ml of DNA) serially diluted from the stock DNA standard provided by the kit, or unknown samples were pipetted into a 96-well plate in duplicate, and 100µl of diluted Quant-iT™ PicoGreen® dsDNA reagent was added to the wells followed by thorough mixing. After incubation at room temperature for 5 minutes avoiding light, the sample fluorescence was determined using a fluorescence microplate reader with excitation at 480nm and emission at 520nm (FLUOstar OPTIMA, BMG Labtech, UK).

## **2.2.7 Analysis of proteins using Western Blotting**

Protein content was analysed using Western Blotting as described previously (Towbin et al., 1979).

### **2.2.7.1 Sample preparation**

Due to the inability to extract sufficient amounts of intracellular proteins direct from NP tissue, the NP and OAF tissues were subject to a short period of enzymatic digestion to release the cells prior to analysis. Separated NP or OAF tissue was minced into small pieces (about 3x3x3mm) and the cells extracted by rapid digestion, over 2 hours, using 2.5mg/ml type I collagenase for OAF tissue and 1mg/ml type II collagenase for NP tissue. After removing the tissue remnants by filtration through a 40µm cell strainer (BD Bioscience, Oxford, UK), cells were pelleted by centrifugation at 2000rpm for 10 minutes. Cells were resuspended in PBS and the cell number was determined using a haemocytometer under a light microscope. After centrifugation, cell pellets were subsequently lysed in 0.9% Triton X-100 to give a cell number of

$1 \times 10^6$  cells/100 $\mu$ l. The samples were then mixed with an equal volume of 2x loading buffer (0.06M Tris pH 6.8, 2% (w/v) sodium dodecyl sulphate (SDS), 10% (v/v) glycerol) and 0.01% (w/v) Bromophenol Blue) to give a final concentration of 1x sample buffer for analysis. If reduction of samples was required then 2.5% (v/v)  $\beta$ -mercaptoethanol was added to the sample. Samples were denatured by heating to 60°C for 30 minutes before loading onto polyacrylamide gels.

### **2.2.7.2 Sodium dodecyl sulphate-polyacrylamide gel electrophoresis**

Sodium dodecyl sulphate-polyacrylamide gel electrophoresis (SDS-PAGE) is a technique used for the separation and detection of proteins. 7.5% or 10% resolving gels were made up using the Biorad mini protean II system with the reagents listed in Table 2-5.

TEMED (tetramethylethylenediamine) was added to initiate co-polymerisation of the acrylamide. Gels were overlaid with dH<sub>2</sub>O and left to polymerise for 20 minutes; the dH<sub>2</sub>O was removed before the addition of a 4% stacking gel. Sample wells were created in the stack by insertion of combs prior to stacking gel polymerisation. After loading, the samples were run in 1x Laemmli buffer (0.025M Tris, 0.192 M Glycine and 0.1 % SDS) at 200V until the dye front was nearing the end of the gel. Rainbow protein molecular weight markers (Amersham, Bucks, UK) were loaded as a means of identifying the molecular weight. After electrophoresis, gels were stained using Coomassie blue staining buffer [0.25% (w/v) Coomassie brilliant blue R250, 45% (v/v) methanol, 10% (v/v) glacial acetic acid] for 60 minutes and destained in destaining solution (40% methanol, 7.5% acetic acid) until a clear background was achieved against the heavily stained protein bands.

### **2.2.7.3 Preparation of transfer membrane**

A polyvinylidene fluoride (PVDF) membrane used in Western Blotting is a microporous membrane for binding proteins > 10KDa. The membrane was soaked in

100% methanol for 30 seconds, and then equilibrated in transfer buffer [Laemmli running buffer containing 20% (v/v) methanol] for 5 minutes.

#### **2.2.7.4 Transfer of proteins from SDS-PAGE gel to PVDF membrane**

Protein, loaded on an equal cell number basis ( $5 \times 10^5$  cells), and separated on 10% polyacrylamide gels, were transferred to PVDF membrane (Millipore, Dundee, UK) at a voltage of 100V for 60 minutes at room temperature in transfer buffer. Miniprotein blotting apparatus (Bio-Rad, Herts, UK) was assembled according to the manufacturer's instructions. Briefly, sponges and filter papers were soaked in transfer buffer before a sandwich of sponge, filter paper, polyacrylamide gel, membrane, filter paper, sponge was assembled in a cassette (Figure 2-4). The cassette was placed into the blotting apparatus tank with the gel on the side of the negative electrode with respect to the filter. An ice pack was placed in the tank before it was filled with transfer buffer to cool down the potential increase in temperature during the transfer. On application of a current through the transfer buffer, negatively charged proteins from the gel were transferred onto the membrane.

#### **2.2.7.5 Immuno-probing of membrane**

After transfer, the membranes were incubated with Tris Buffered Saline (TBS) (0.05M Tris Base, 0.15M NaCl, pH 7.6) containing 3% (w/v) skimmed milk power for 30 minutes at room temperature to block non-specific protein binding. The membranes were then incubated with specific monoclonal antibodies that recognise  $\beta$ -actin (AC15, 1:100 dilution, Abcam, Cambridge, UK), vimentin (V9, 1:400 dilution),  $\beta$ -tubulin (E7, 1:500 dilution, Developmental Studies Hybridoma Bank, University of Iowa, USA), type I collagen (goat anti-bovine, 1:500 dilution, from Prof. Vic Duance, Cardiff University, UK) or type II collagen (mouse anti-human, clone AVT-6E3; 1:5 dilution, from Prof. Vic Duance, Cardiff University, UK) overnight at 4°C. Membranes were washed in TBS containing 0.05% Tween-20 to remove primary antibody and then incubated with either horseradish peroxidase (HRP)-conjugated sheep anti-mouse (1:10,000 dilution) or rabbit anti-goat (1:80,000 dilution) secondary antibodies for 60

minutes at room temperature. The membranes were then washed six times with a large volume of TBS containing 0.05% Tween-20 (200ml) for 20 minutes periods. The membrane for the negative control (no primary antibody) was washed separately from the other experimental membranes to avoid contamination.

**Table 2-5 Reagents used to make up resolving and stacking gels required for SDS-PAGE.**

Reagents	Resolving Gel			Stacking Gel
	7.5%	10%	12.5%	4%
40% acrylamide/bisacrylamide				
40:1	2.72ml	3.83ml	4.53ml	575µl
1M Tris/HCl pH8.8	3.63ml	3.63ml	3.63ml	-----
1M Tris/HCl pH6.8	-----	-----	-----	1.3ml
10%(w/v) SDS	100 µl	100 µl	100 µl	50µl
10%(w/v) APS	75 µl	75 µl	75 µl	37µl
dH <sub>2</sub> O	8.16ml	7.05ml	6.35ml	4.075ml
TEMED	15µl	15µl	15µl	7.5µl

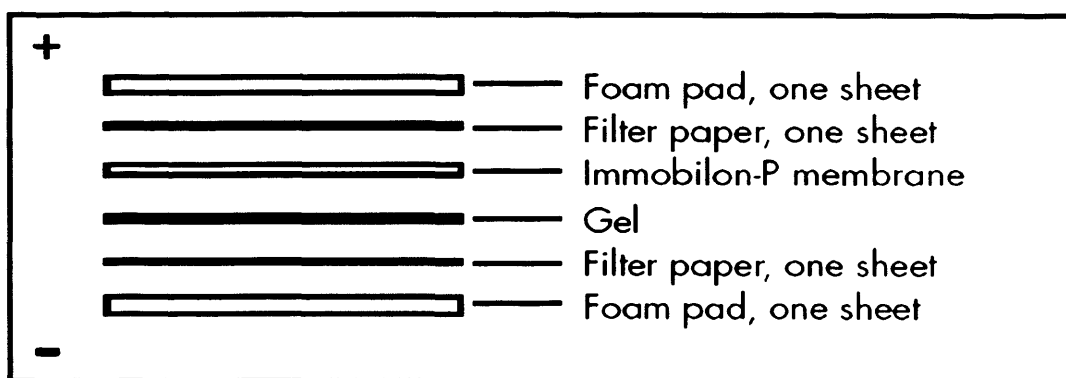


Figure 2-4 Schematic layout of transfer sandwich in Western Blotting. The gel should be on the negative cathode side of the membrane when placed in the tank. (Taken from Millipore PR02531)

### **2.2.7.6 Detection of immunoreactive bands**

Enhanced chemiluminescence (ECL) system is a light emitting non-radioactive method for the detection of immobilised specific antigens, conjugated directly or indirectly with HRP labelled antibodies. It consists of a lumigen PS-3 acridan substrate, which is converted to an acridinium ester intermediate when catalyzed by HRP. The ester intermediate reacts with peroxide in alkaline conditions and emits light, which can be detected by autoradiography film. After washing, the membranes were rinsed using ECL reagents (GE Healthcare, Bucks, UK) according to the manufacturer's instruction. Briefly, equal volumes of ECL reagents 1 and 2 were mixed and applied to the membrane for 1-2 minutes at room temperature. Excess ECL reagents were then removed by blotting the membrane onto tissue paper. The membrane was then sealed into a polythene bag and exposed to ECL hyperfilm (GE Healthcare, Bucks, UK) for variable times, from 5 minutes to overnight. Films were then developed using an automatic developer. All Western blots were then scanned and differences in the chemiluminescence intensity of digitised bands assessed using NIH Image software.

### **2.2.8 Statistical Analysis**

Data are presented as Mean  $\pm$  S.E.M, with tissue derived from between 4 and 6 individual animals. Samples were analysed in triplicate and all experiments were performed twice and representative data are presented. Data was tested for normality (Anderson-Darling test) and equal variance. Student's t test was carried out using GraphPad Prism 5.0 software unless otherwise stated. Differences were considered significant at P values of less than 0.05.

## 2.3 Results

### 2.3.1 Normalisation methods

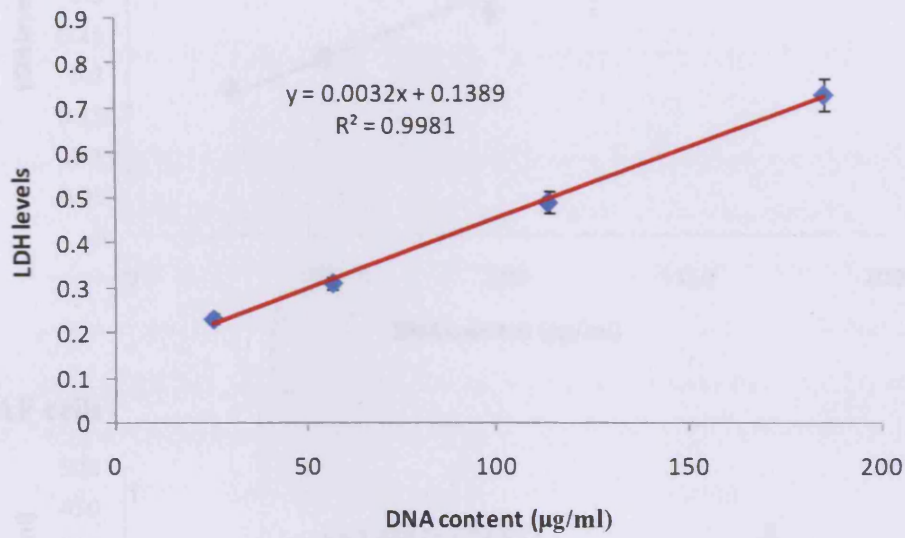
Due to the different phenotypes of the NP and OAF cells, a proper normalisation method was needed to compare cytoskeletal element expression levels in NP and OAF cells. Therefore, the LDH assay and BCA assay were investigated and the DNA concentration assay was used as a control for cell number. As shown in Figure 2-5, linear correlations between DNA concentration and LDH levels, as well as DNA concentration and protein content were observed in both NP and OAF cells, suggesting that either maximum LDH content or total protein levels can be used for cell number normalisation.

### 2.3.2 Confirmation of successful separation of nucleus pulposus from outer annulus fibrosus of the disc

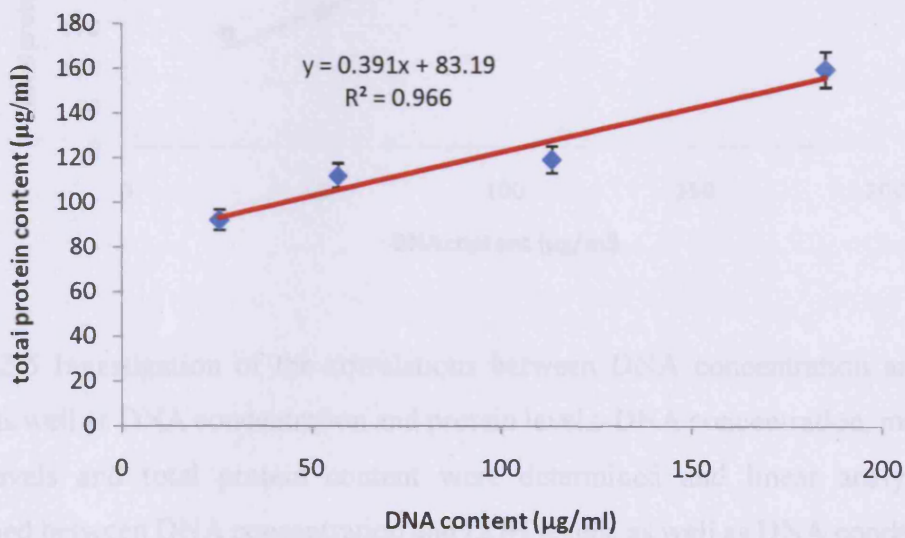
To confirm the successful separation of NP from the OAF of the intervertebral disc, Western blotting for types I and II collagen was performed (Figure 2-6). As expected, collagen types I and II were both expressed in the separated disc regions (Figure 2-6A). Type I collagen content was greatest in the OAF in both young and mature disc (Figure 2-6B,  $p=0.027$  and  $0.003$  respectively) and type II collagen levels greatest in the NP in both young and mature disc (Figure 2-6B,  $p=0.003$  and  $0.009$  respectively). These results are consistent with the features of collagen distribution (Eyre and Muir, 1976), suggesting the successful separation of NP and OAF.

The type I collagen Western blots show the  $\alpha 1$  and  $\alpha 2$  chains of type I collagen. In some samples the  $\alpha 2$  chain was absent in some samples as shown in Figure 2-6. This is caused by the anti-type I collagen polyclonal antibody mainly recognising the epitopes on the  $\alpha 1$  chain of type I collagen, e.g. on the young NP the amount of  $\alpha 2$  chain is below the sensitivity of the antibody.

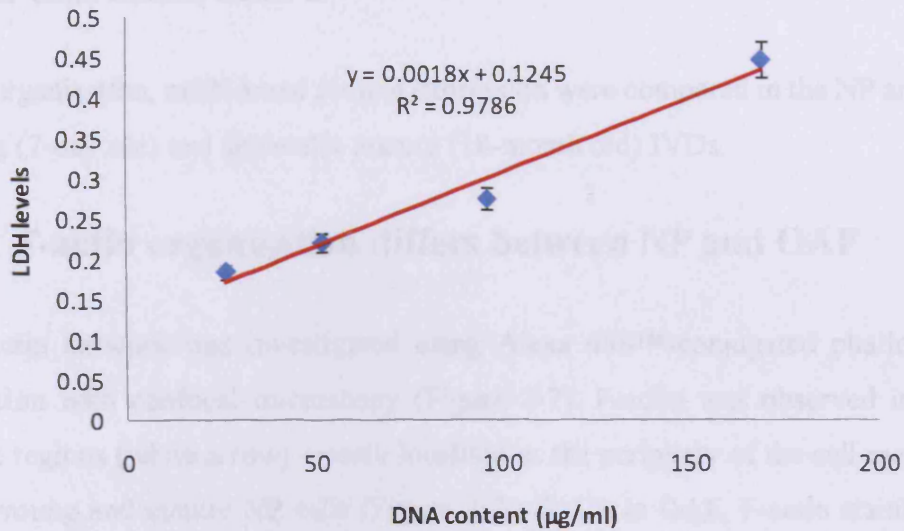
(A) NP cells



(B) NP cells



**(C) OAF cells**



**(D) OAF cells**

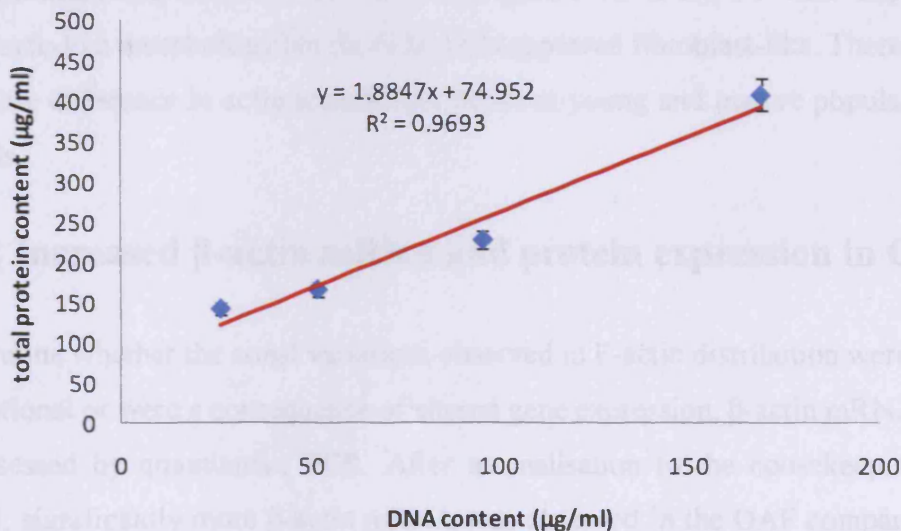


Figure 2-5 Investigation of the correlations between DNA concentration and LDH levels, as well as DNA concentration and protein levels. DNA concentration, maximum LDH levels and total protein content were determined and linear analysis was performed between DNA concentration and LDH levels, as well as DNA concentration and total protein content. A & B: linear analysis in nucleus pulposus cells; C & D: linear analysis in outer annulus fibrosus cells.



### **2.3.3 Differential F-actin organisation and $\beta$ -actin mRNA and protein expression in IVD**

F-actin organisation, mRNA and protein expression were compared in the NP and OAF of young (7-day old) and skeletally mature (18-month old) IVDs.

#### **2.3.3.1 F-actin organisation differs between NP and OAF**

The F-actin network was investigated using Alexa 488<sup>TM</sup>-conjugated phalloidin in conjunction with confocal microscopy (Figure 2-7). F-actin was observed in dense punctate regions (white arrow), evenly localised at the periphery of the cell membrane of both young and mature NP cells (Figure 2-7A & C). In OAF, F-actin staining was punctate, distributed throughout the cytoplasm extending into the cell processes of young and mature OAF cells (white arrow) (Figure 2-7B & D). NP cells displayed a chondrocyte-like morphology but the OAF cells appeared fibroblast-like. There was no discernable difference in actin architecture between young and mature populations of IVD cells.

#### **2.3.3.2 Increased $\beta$ -actin mRNA and protein expression in OAF**

To determine whether the zonal variations observed in F-actin distribution were purely organisational or were a consequence of altered gene expression,  $\beta$ -actin mRNA levels were assessed by quantitative PCR. After normalisation to the housekeeping gene GAPDH, significantly more  $\beta$ -actin mRNA was observed in the OAF compared with NP in both young (1.8-fold;  $p=0.008$ ) and mature disc (2.5-fold;  $p=0.025$ ) (Figure 2-8A). However, there was no age-related difference in  $\beta$ -actin mRNA levels between young and mature NP ( $p= 0.283$ ) or OAF ( $p= 0.304$ ).

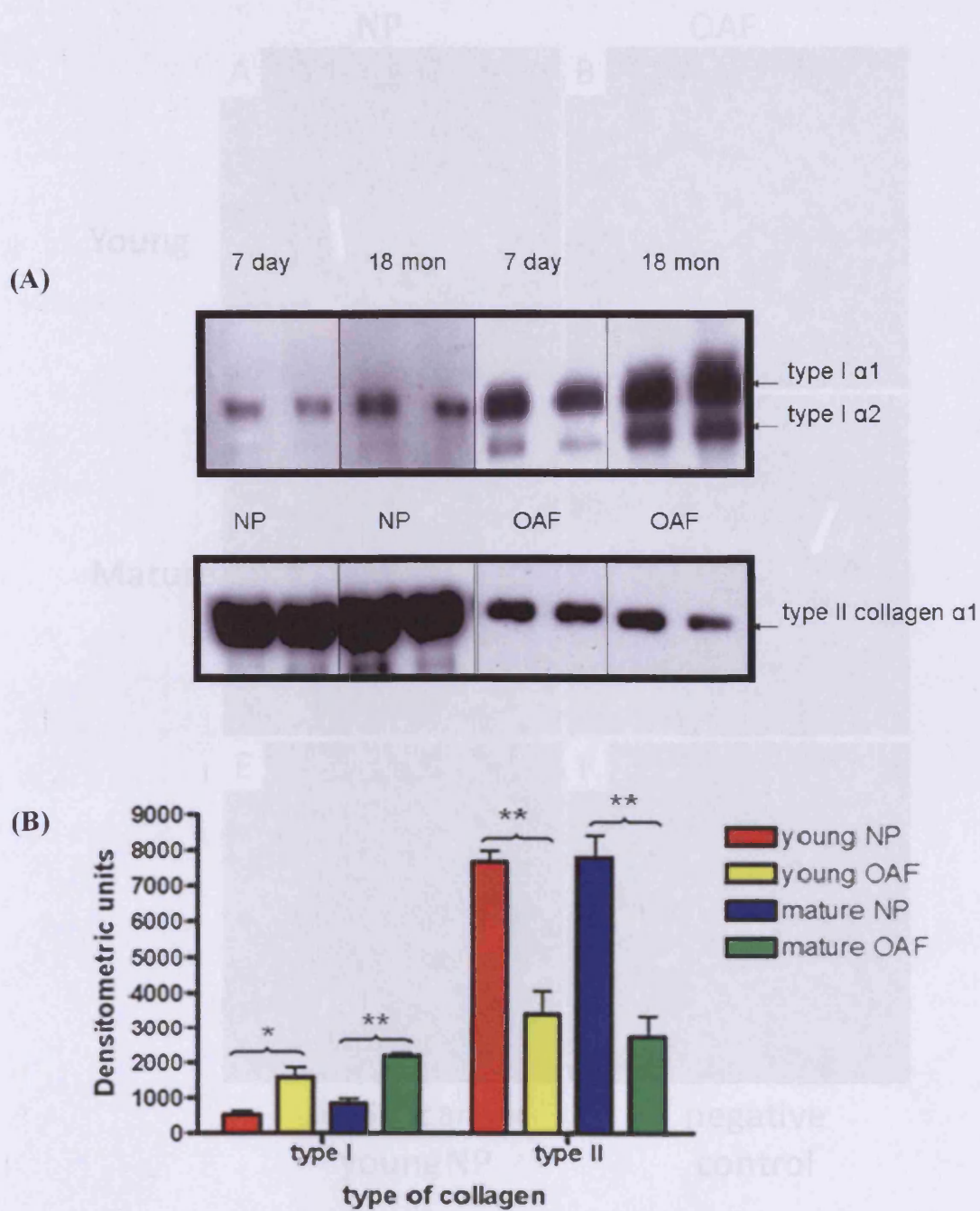


Figure 2-6 Intensity of cytoskeletal proteins in young and mature bovine IVD.

Figure 2-6 Western blot for types I and II collagen in protein extracted from young and mature bovine IVD. A: Types I and II collagen are found in both young and mature disc. B: There was more type II collagen in the NP and more type I collagen in the OAF. The samples were normalised to protein levels. \*\*  $p \leq 0.01$ , \* $p \leq 0.05$ , Student's t test (AVR $\pm$ SEM, n=5).

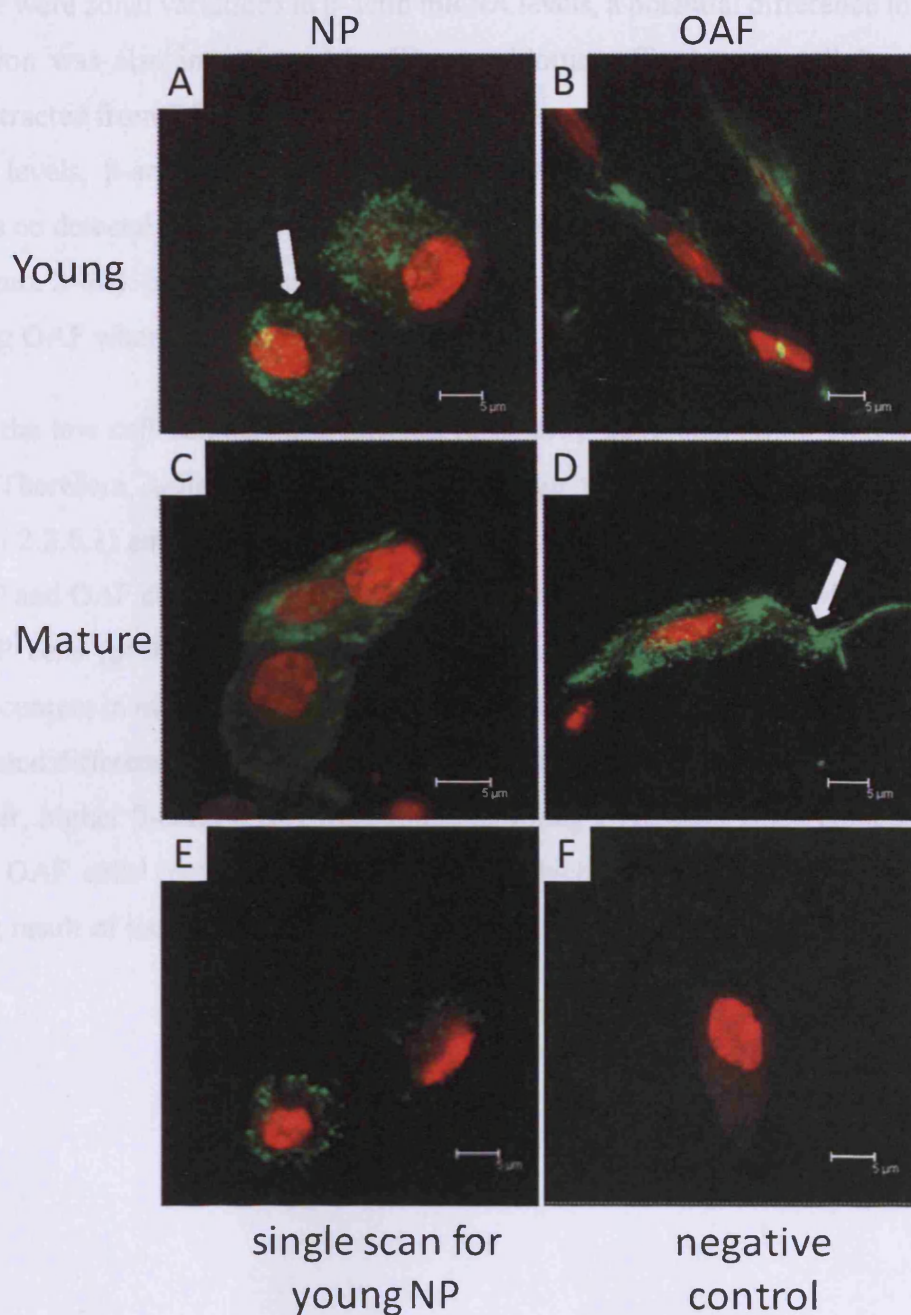
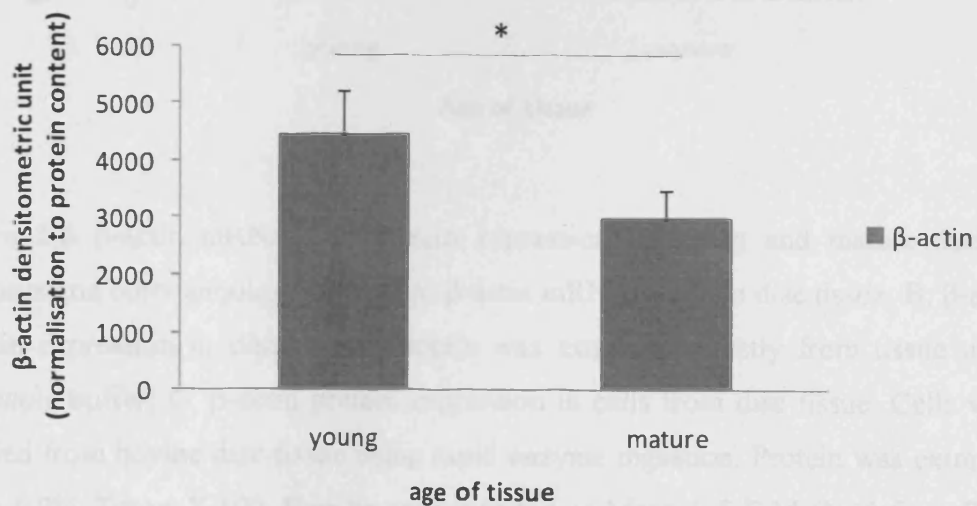
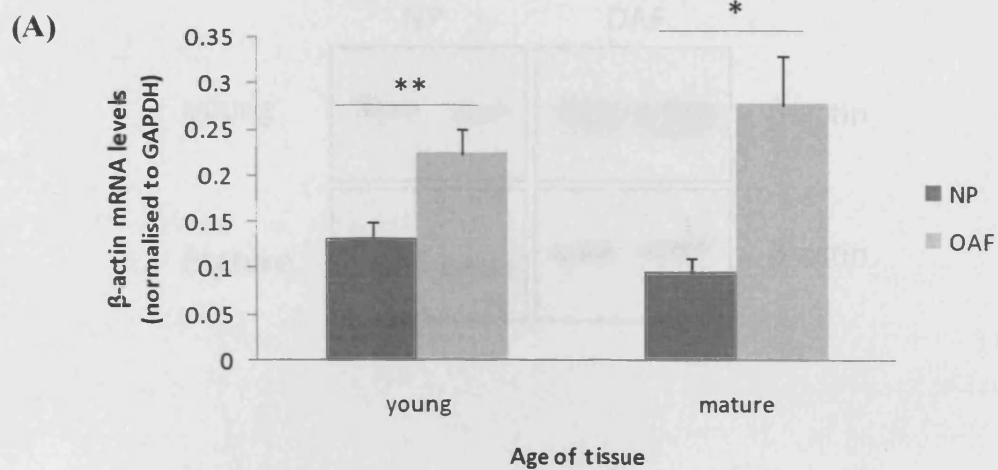


Figure 2-7 Immunofluorescent localisation of F-actin in young and mature bovine IVD. F-actin filaments were visualised using Alexa 488-conjugated phalloidin (Green) , with the nuclei counterstained using propidium iodide (Red). [A] young & [C] mature nucleus pulposus cells; [B] young & [D]: mature outer annulus fibrosus cells. A-D were 3D images which were reconstructed from serial sections. [E]: Single scan of actin in the middle layer of young NP cells; [F]: negative control. Scale bar 5µm. White arrow: punctate staining of F-actin in IVD cells.

As there were zonal variations in  $\beta$ -actin mRNA levels, a potential difference in protein expression was also investigated by Western blotting. Firstly, intracellular proteins were extracted from IVD tissue directly using  $2\times$  sample buffer. After normalisation to protein levels,  $\beta$ -actin bands were found in both young and mature OAF groups, whereas no detectable  $\beta$ -actin was found in the NP group due to the low cell number in NP (Figure 2-8B). Statistical analysis indicated that there was more  $\beta$ -actin expression in young OAF when compared with the mature OAF ( $p=0.041$ ) (Figure 2-8B).

Due to the low cell number, it is difficult to detect  $\beta$ -actin expression directly in NP tissue. Therefore, cells were isolated from tissue using a rapid enzyme digestion (Section 2.2.6.1) and Western blotting was performed.  $\beta$ -actin protein was detected in both NP and OAF cells. Greater  $\beta$ -actin was found in young OAF cells when compared with NP cells ( $p=0.0159$ ) (Figure 2-8C). However, there was no zonal variation in  $\beta$ -actin content in mature disc ( $p=1.00$ ). Consistent with gene expression, there were no age-related differences in the amount of  $\beta$ -actin protein detected in NP cells ( $p=0.6905$ ). However, higher  $\beta$ -actin levels were found in young OAF cells when compared with mature OAF cells ( $p=0.0247$ ) (Figure 2-8C), which is consistent with the Western blotting result of tissue extract (Figure 2-8B).



(C)

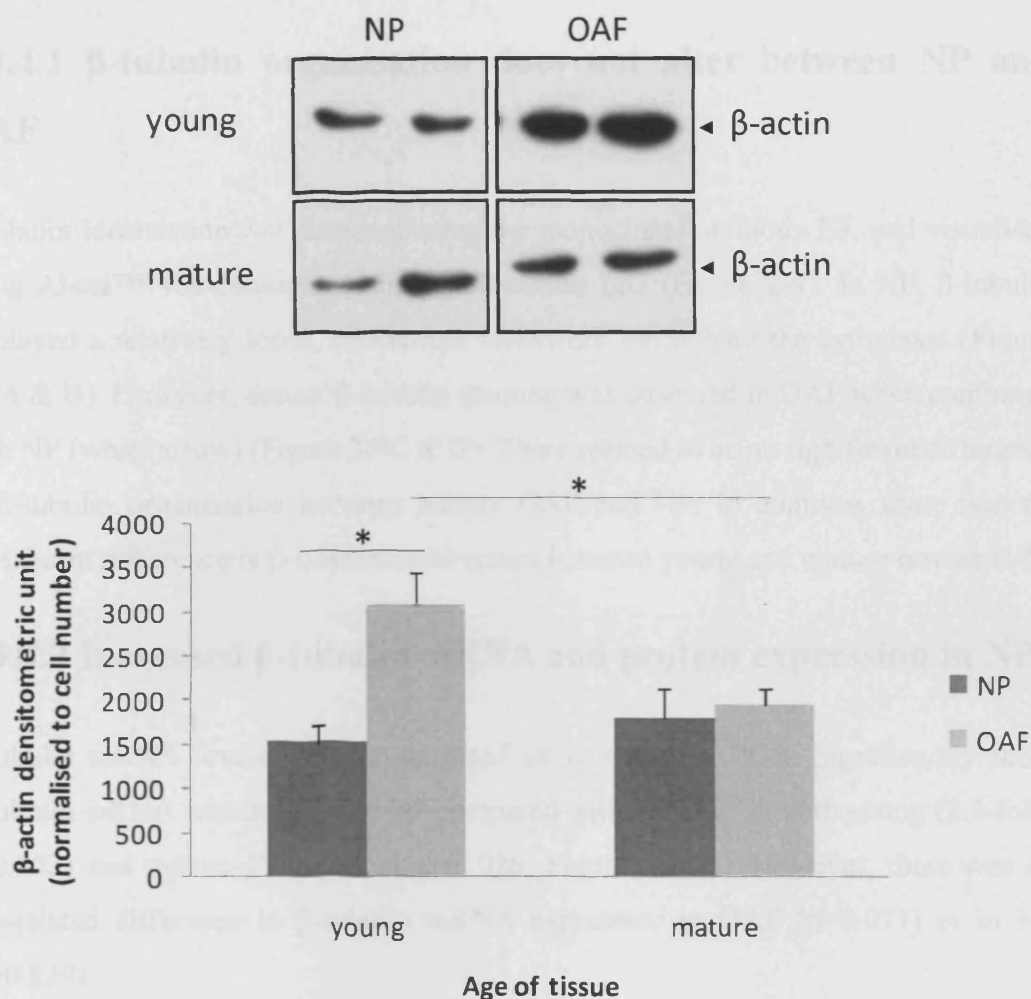


Figure 2-8  $\beta$ -actin mRNA and protein expression in young and mature nucleus pulposus and outer annulus fibrosus. A:  $\beta$ -actin mRNA levels in disc tissue; B:  $\beta$ -actin protein expression in disc tissue. Protein was extracted directly from tissue using 2 $\times$ sample buffer; C:  $\beta$ -actin protein expression in cells from disc tissue. Cells were isolated from bovine disc tissue using rapid enzyme digestion. Protein was extracted using 0.9% Triton X-100. Results are presented as Mean  $\pm$  S.E.M (N=6 for mRNA results and N=5 for protein results). \*\*  $p \leq 0.01$ , \*  $p \leq 0.05$ , Student's t test.

## **2.3.4 Differential $\beta$ -tubulin mRNA and protein expression in IVD**

### **2.3.4.1 $\beta$ -tubulin organisation does not alter between NP and OAF**

$\beta$ -tubulin localisation was detected using the monoclonal antibody E7, and visualised using Alexa™ 488-conjugated sheep anti-mouse IgG (Figure 2-9). In NP,  $\beta$ -tubulin displayed a relatively loose, basket-like meshwork throughout the cytoplasm (Figure 2-9A & B). However, denser  $\beta$ -tubulin staining was observed in OAF when compared with NP (white arrow) (Figure 2-9C & D). There seemed to be no significant difference in  $\beta$ -tubulin organisation between mature OAF and NP. In addition, there was no significant difference in  $\beta$ -tubulin architecture between young and mature bovine IVD.

### **2.3.4.2 Increased $\beta$ -tubulin mRNA and protein expression in NP**

$\beta$ -tubulin mRNA levels were investigated using real-time PCR. Significantly more  $\beta$ -tubulin mRNA was detected in NP compared with the OAF in both young (2.5-fold;  $p=0.023$ ) and mature IVD (2-fold;  $p=0.026$ ; Figure 2-10A). However, there was no age-related difference in  $\beta$ -tubulin mRNA expression in OAF ( $p=0.071$ ) or in NP ( $p=0.829$ ).

To confirm the changes observed at the mRNA level, Western blotting was performed using the protein samples extracted directly from tissue.  $\beta$ -tubulin was only detected in the OAF, where there was more  $\beta$ -tubulin protein in young OAF when compared with the mature group ( $p=0.041$ ) (Figure 2-10B).

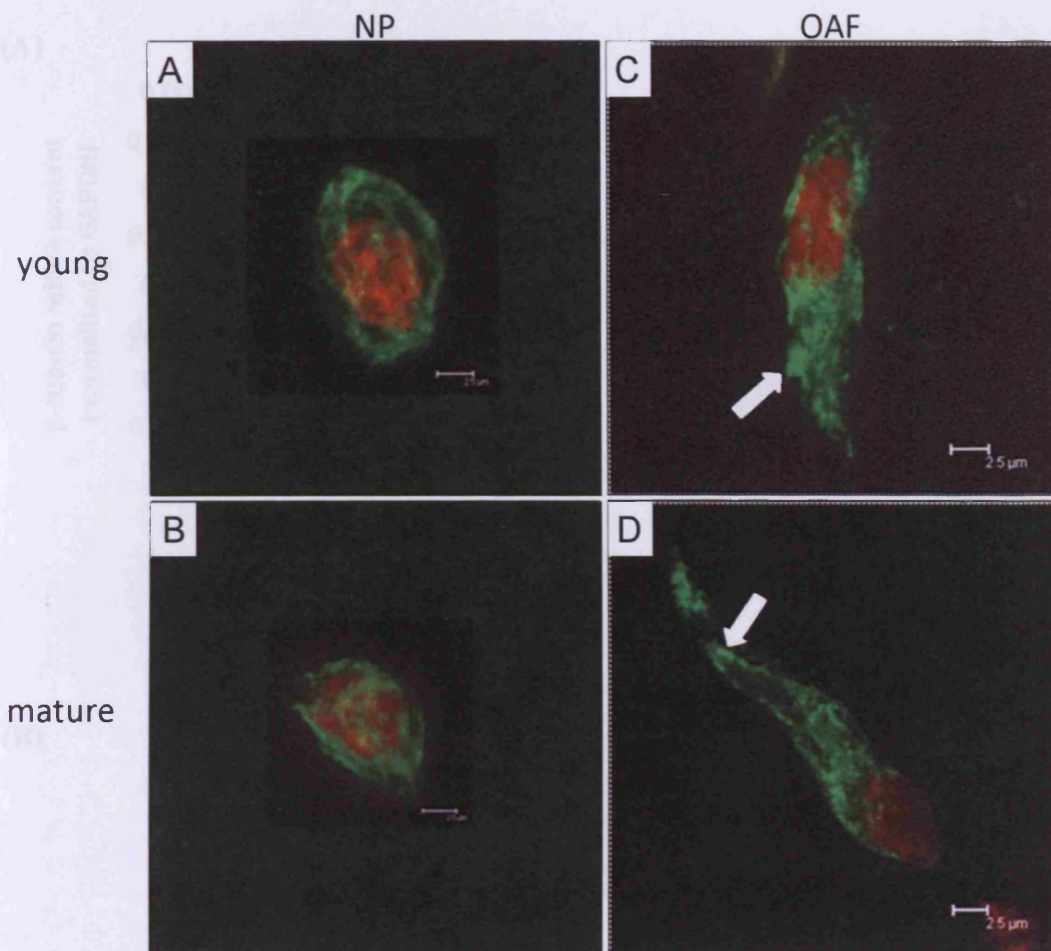
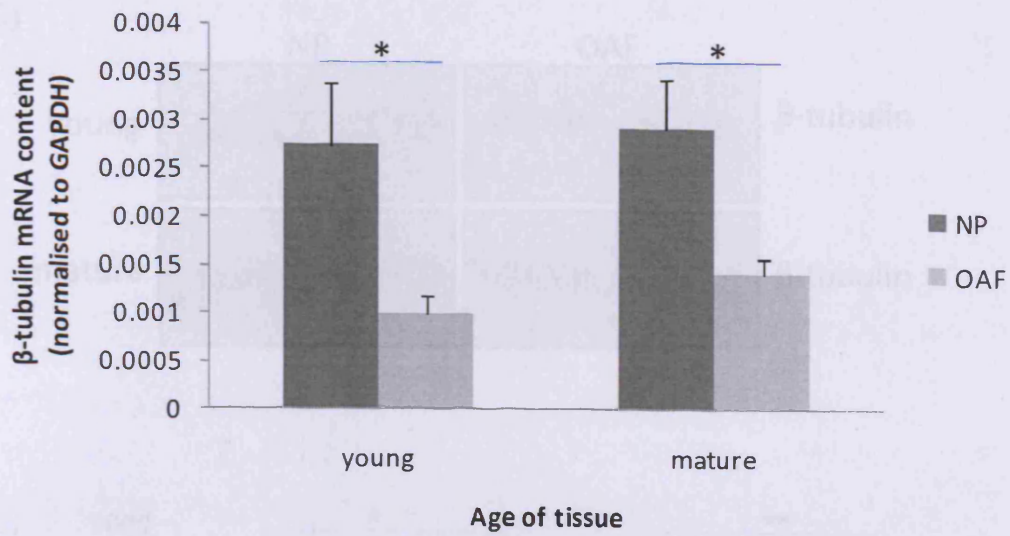


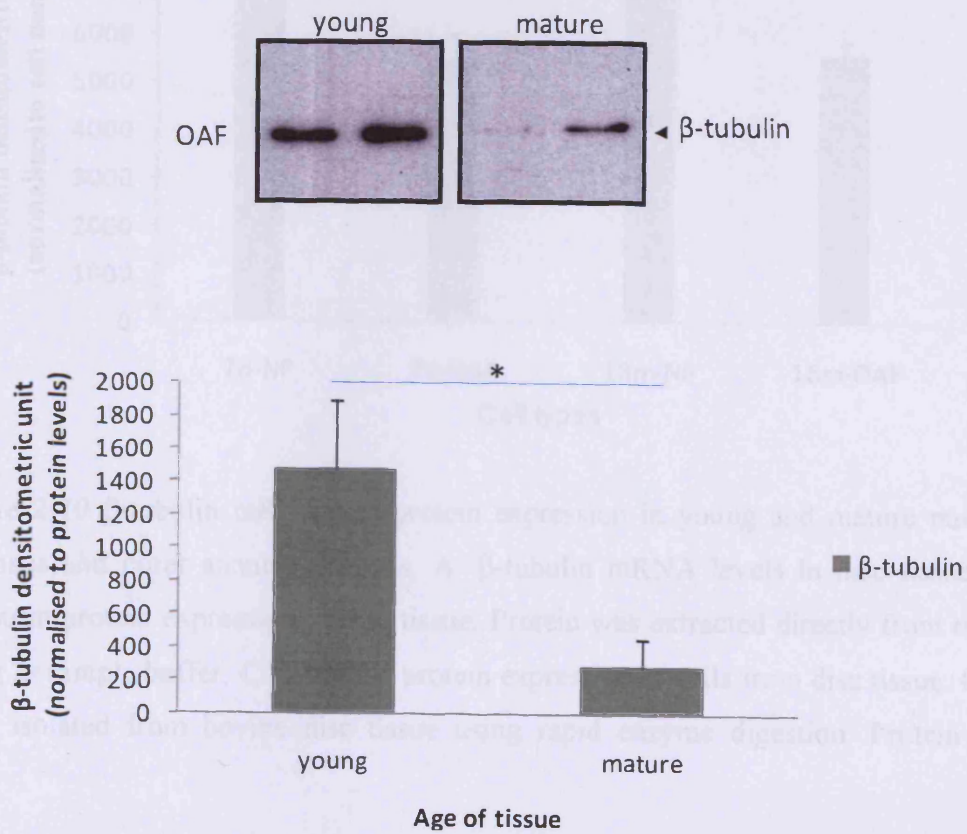
Figure 2-9. Immunofluorescent localisation of  $\beta$ -tubulin in young and mature bovine intervertebral disc.  $\beta$ -tubulin was detected using the monoclonal antibody E7, and visualised using Alexa 488-conjugated sheep anti-mouse IgG (green). Nuclei were counterstained using propidium iodide (red). [A] young & [B] mature nucleus pulposus cells; [C] young & [D] mature outer annulus fibrosus cells. The 3D images were reconstructed from serial sections. Scale bar 2.5 $\mu$ m. Arrow: intensive staining of  $\beta$ -tubulin in the cell processes in OAF cells.



(A)



(B)

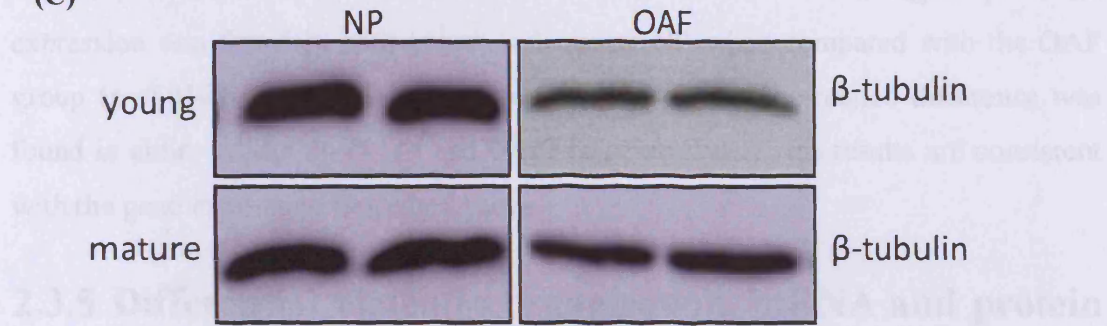


Chapter 2: Zonal and age-related differences in the organisation and expression of cytoskeletal elements within IVD cells *in situ*

extracted using 0.9% Triton X-100. Results are presented as Mean  $\pm$  S.E.M (N=6 for mRNA results and N=5 for protein results). \*\* p<0.01, \*p<0.05, Student's t test

$\beta$ -tubulin expression was also investigated using the protein samples from the cells which were isolated from tissue after rapid enzyme digestion. As shown in Figure

(C)



expression in IVD

2.3.3.1  $\beta$ -tubulin protein expression in young and mature NP and OAF cells

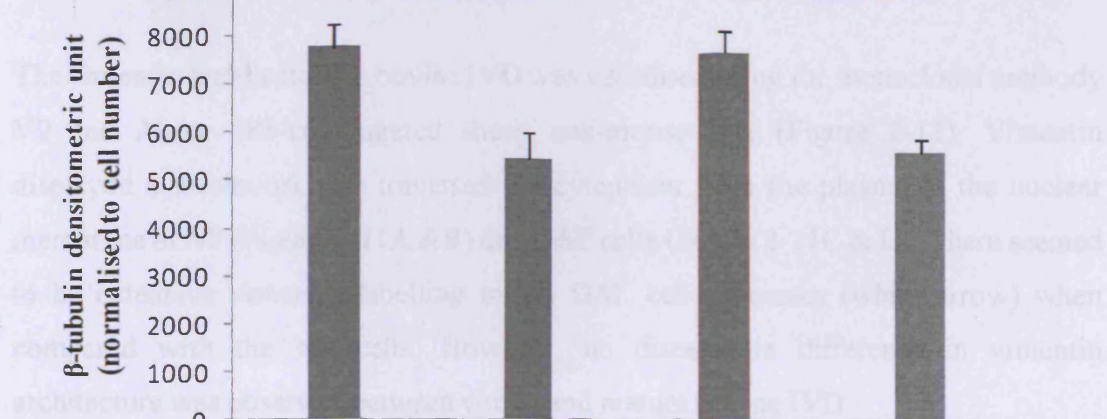


Figure 2-10  $\beta$ -tubulin mRNA and protein expression in young and mature nucleus pulposus and outer annulus fibrosus. **A:**  $\beta$ -tubulin mRNA levels in disc tissue; **B:**  $\beta$ -tubulin protein expression in disc tissue. Protein was extracted directly from tissue using 2 $\times$ sample buffer; **C:**  $\beta$ -tubulin protein expression in cells from disc tissue. Cells were isolated from bovine disc tissue using rapid enzyme digestion. Protein was

extracted using 0.9% Triton X-100. Results are presented as Mean  $\pm$  S.E.M (N=6 for mRNA results and N=5 for protein results). \*\*  $p \leq 0.01$ , \* $p \leq 0.05$ , Student's t test.

$\beta$ -tubulin expression was also investigated using the protein samples from the cells which were isolated from tissue after rapid enzyme digestion. As shown in Figure 2-10C,  $\beta$ -tubulin was detected in both NP and OAF cells, but higher  $\beta$ -tubulin expression was found in both young and mature NP when compared with the OAF group ( $p=0.0165$  and  $0.0084$  respectively). However, no age-related difference was found in either groups ( $p=0.114$  and  $0.677$  respectively). These results are consistent with the gene expression described above.

## **2.3.5 Differential vimentin organisation, mRNA and protein expression in IVD**

### **2.3.5.1 Vimentin organisation differs between NP and OAF**

The vimentin architecture in bovine IVD was visualised using the monoclonal antibody V9 and Alexa 488-conjugated sheep anti-mouse IgG (Figure 2-11). Vimentin displayed a meshwork that traversed the cytoplasm from the plasma to the nuclear membrane in NP (Figure 2-11A & B) and OAF cells (Figure 2-11C & D). There seemed to be extensive vimentin labelling in the OAF cell processes (white arrow) when compared with the NP cells. However, no discernable difference in vimentin architecture was observed between young and mature bovine IVD.

### 2.3.5.2 Differential vimentin mRNA and protein expression in NP and OAF

Quantitative mRNA analysis demonstrated appreciably more vimentin mRNA in both

young (2.1 ± 0.3) and mature (2.1 ± 0.3) OAF cells compared to NP cells (1.0 ± 0.1) in both

young (2.1 ± 0.3) and mature (2.1 ± 0.3) OAF cells compared to NP cells (1.0 ± 0.1) in both

young (2.1 ± 0.3) and mature (2.1 ± 0.3) OAF cells compared to NP cells (1.0 ± 0.1) in both

young (2.1 ± 0.3) and mature (2.1 ± 0.3) OAF cells compared to NP cells (1.0 ± 0.1) in both

young (2.1 ± 0.3) and mature (2.1 ± 0.3) OAF cells compared to NP cells (1.0 ± 0.1) in both

young (2.1 ± 0.3) and mature (2.1 ± 0.3) OAF cells compared to NP cells (1.0 ± 0.1) in both

young (2.1 ± 0.3) and mature (2.1 ± 0.3) OAF cells compared to NP cells (1.0 ± 0.1) in both

young (2.1 ± 0.3) and mature (2.1 ± 0.3) OAF cells compared to NP cells (1.0 ± 0.1) in both

young (2.1 ± 0.3) and mature (2.1 ± 0.3) OAF cells compared to NP cells (1.0 ± 0.1) in both

young (2.1 ± 0.3) and mature (2.1 ± 0.3) OAF cells compared to NP cells (1.0 ± 0.1) in both

young (2.1 ± 0.3) and mature (2.1 ± 0.3) OAF cells compared to NP cells (1.0 ± 0.1) in both

young (2.1 ± 0.3) and mature (2.1 ± 0.3) OAF cells compared to NP cells (1.0 ± 0.1) in both

young (2.1 ± 0.3) and mature (2.1 ± 0.3) OAF cells compared to NP cells (1.0 ± 0.1) in both

young (2.1 ± 0.3) and mature (2.1 ± 0.3) OAF cells compared to NP cells (1.0 ± 0.1) in both

young (2.1 ± 0.3) and mature (2.1 ± 0.3) OAF cells compared to NP cells (1.0 ± 0.1) in both

young (2.1 ± 0.3) and mature (2.1 ± 0.3) OAF cells compared to NP cells (1.0 ± 0.1) in both

young (2.1 ± 0.3) and mature (2.1 ± 0.3) OAF cells compared to NP cells (1.0 ± 0.1) in both

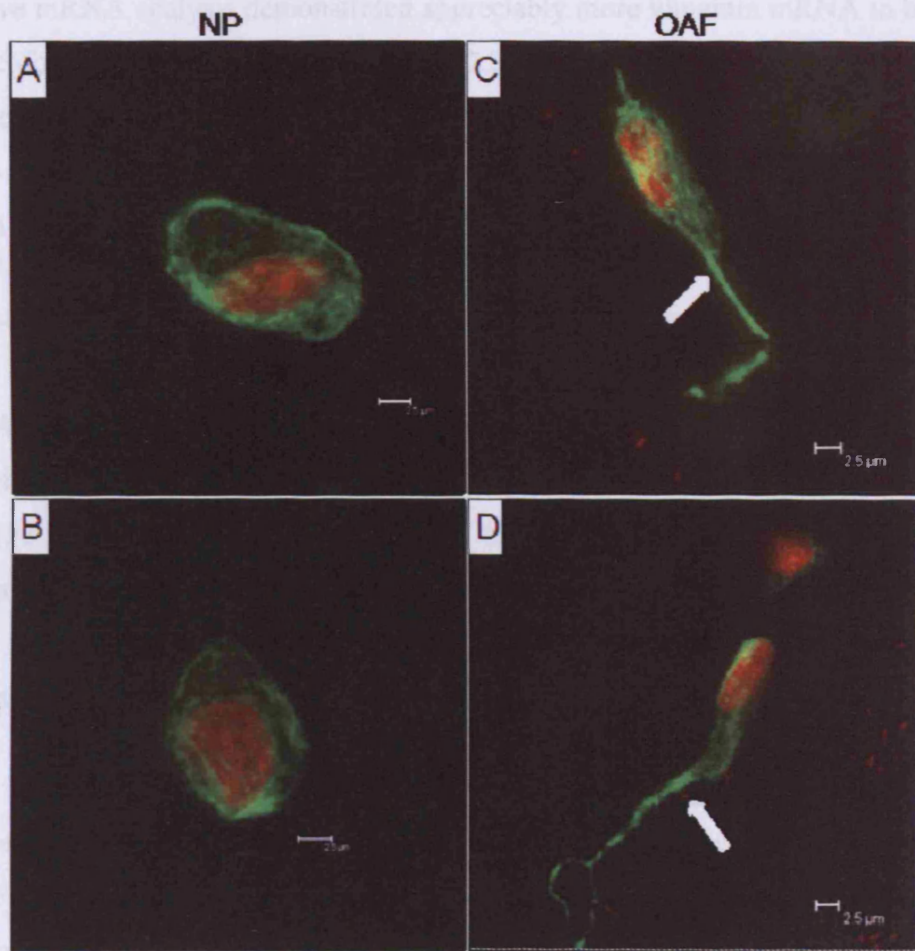


Figure 2-11 Immunofluorescent localisation of vimentin in young and mature bovine intervertebral disc. Vimentin was detected using the monoclonal antibody V9, and visualised using Alexa 488-conjugated sheep anti-mouse IgG (green). Nuclei were counterstained using propidium iodide (red). [A] young & [B] mature nucleus pulposus cells; [C] young & [D] mature outer annulus fibrosus cells. The 3D images were reconstructed from serial sections. Scale bar 2.5 $\mu$ m. Arrow: intensive staining of vimentin in the cell processes in OAF cells.

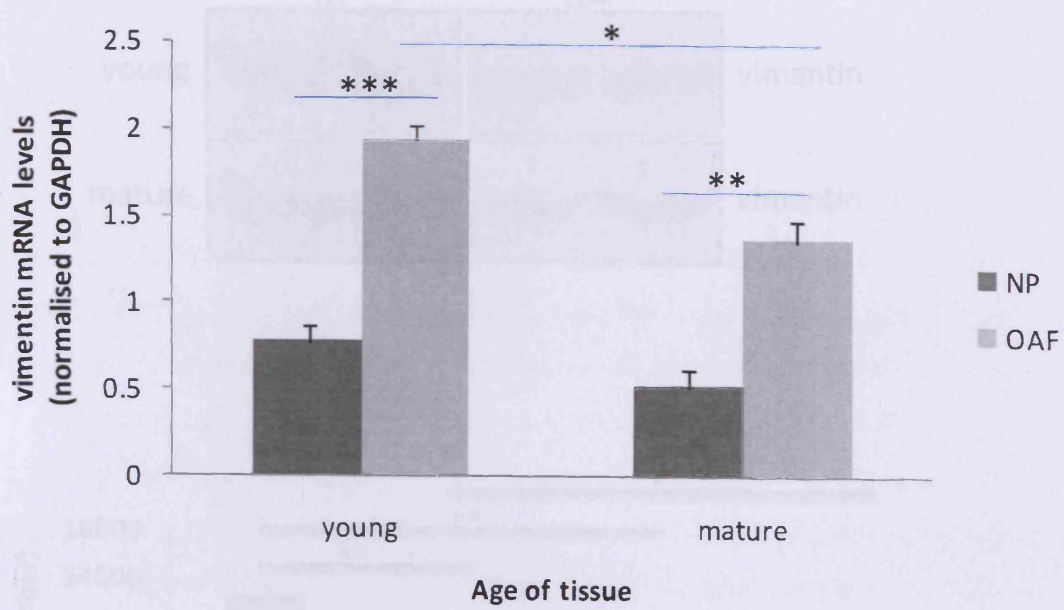
### **2.3.5.2 Differential vimentin mRNA and protein expression in NP and OAF**

Quantitative mRNA analysis demonstrated appreciably more vimentin mRNA in both young (2.5-fold;  $p < 0.001$ ) and mature OAF (2.3-fold;  $p = 0.002$ ), although vimentin gene expression in the OAF decreased with skeletal maturity (1.4-fold;  $p = 0.018$ ) (Figure 2-12A). However, there were no age-related differences in vimentin gene expression between young and mature NP tissue ( $p = 0.154$ ).

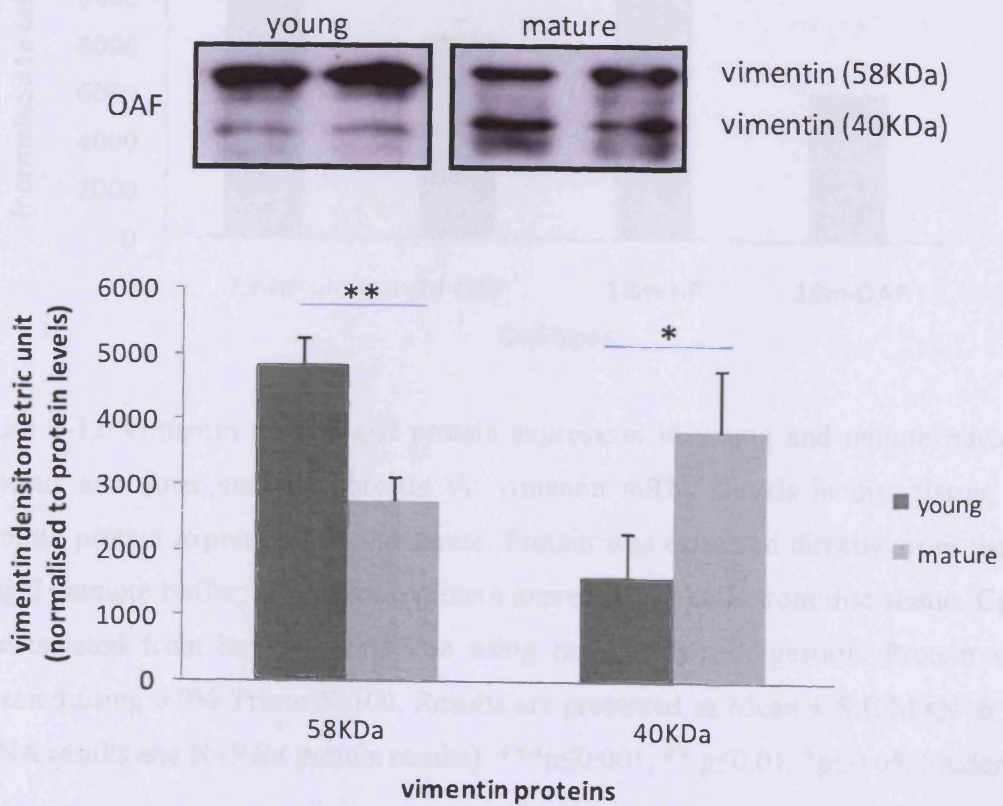
Using protein samples extracted from tissue directly, two vimentin bands with a molecular mass of approximately 40 kDa and 58 kDa were detected in young and mature OAF. The 58 kDa band has been identified as intact vimentin, and the 40 kDa band is believed to be a vimentin degradation product (Lambrecht et al., 2008). More vimentin (58 kDa) was detected in young OAF than in the mature ( $p = 0.004$ ), whereas more degraded vimentin product (40kDa) was observed in mature OAF when compared with young OAF ( $p = 0.04$ ) (Figure 2-12B). Vimentin expression was not detected in NP tissue due to the low cell number.

To further investigate vimentin expression in NP, rapid enzyme digestion samples were used as described previously. Only the 58kDa vimentin band was found in these samples (Figure 2-12C), and there was less vimentin protein in the OAF than in the NP in both young ( $p = 0.0015$ ) and mature IVD ( $p = 0.001$ ). An age-related reduction in vimentin protein expression was also evident in both the NP ( $p = 0.007$ ) and the OAF cells ( $p = 0.04$ ).

(A)



(B)



2.4 Discussion

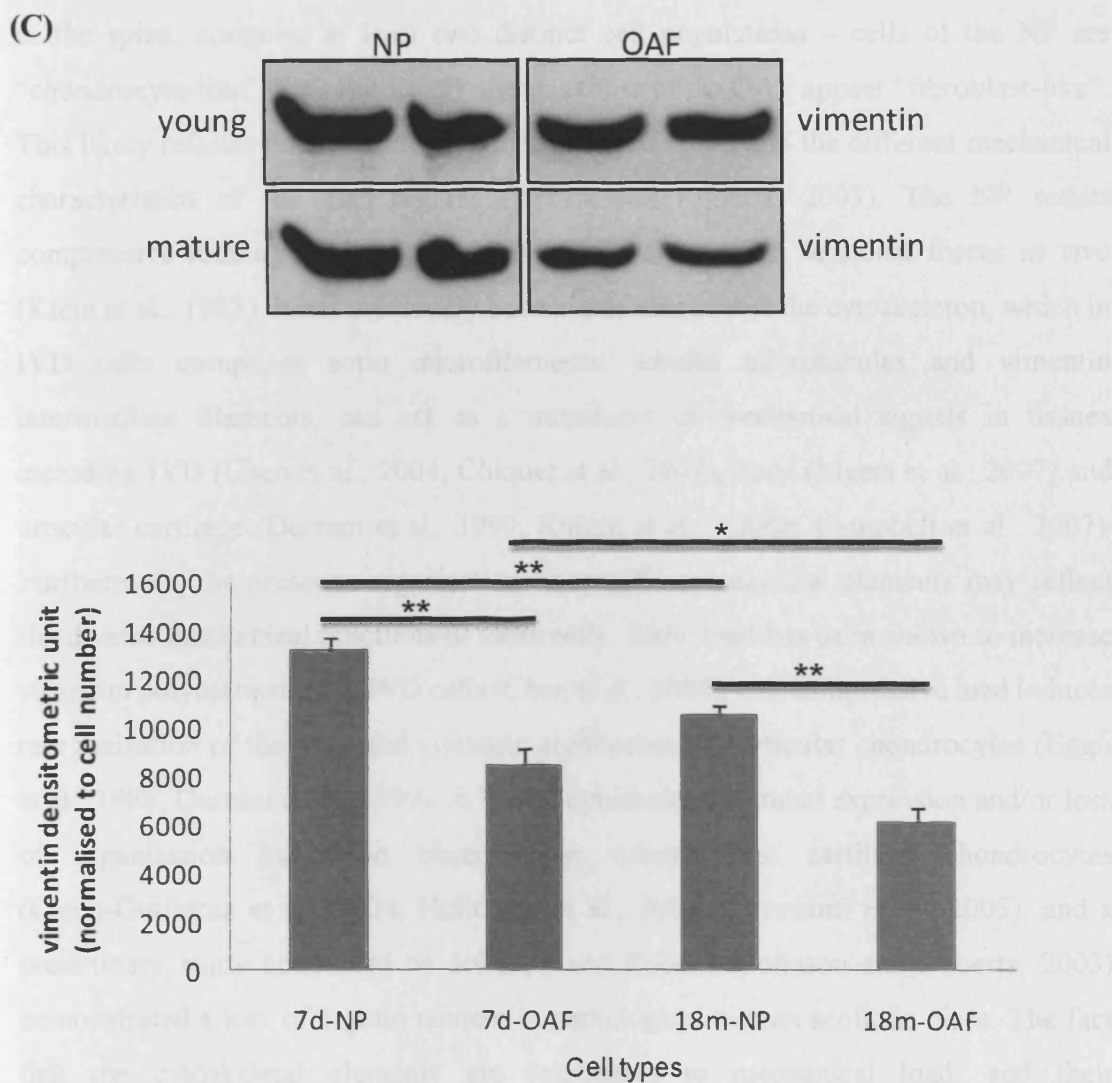


Figure 2-12 Vimentin mRNA and protein expression in young and mature nucleus pulposus and outer annulus fibrosus. A: vimentin mRNA levels in disc tissue; B: vimentin protein expression in disc tissue. Protein was extracted directly from tissue using 2×sample buffer; C: vimentin protein expression in cells from disc tissue. Cells were isolated from bovine disc tissue using rapid enzyme digestion. Protein was extracted using 0.9% Triton X-100. Results are presented as Mean ± S.E.M (N=6 for mRNA results and N=5 for protein results). \*\*\*p<0.001, \*\* p<0.01, \*p<0.05, Student's t test.

## 2.4 Discussion

Intervertebral discs, which are important for dissipating loads and providing flexibility to the spine, comprise at least two distinct cell populations – cells of the NP are “chondrocyte-like” in morphology, whereas those of the OAF appear “fibroblast-like”. This likely reflects both the different matrix organisation and the different mechanical characteristics of the disc regions (Urban and Roberts, 2003). The NP resists compressive loading whereas the OAF mainly counteracts tensional forces *in vivo* (Klein et al., 1983). It has previously been hypothesised that the cytoskeleton, which in IVD cells comprises actin microfilaments, tubulin microtubules and vimentin intermediate filaments, can act as a transducer of mechanical signals in tissues including IVD (Chen et al., 2004; Chiquet et al., 2007), bone (Myers et al., 2007) and articular cartilage (Durrant et al., 1999; Knight et al., 2006b; Campbell et al., 2007). Furthermore, the presence/organisation of specific cytoskeletal elements may reflect the diverse mechanical functions of these cells. Static load has been shown to increase vimentin polymerisation in IVD cells (Chen et al., 2004), and compressive load induces reorganisation of the actin and vimentin architectures in articular chondrocytes (Egglie et al., 1988; Durrant et al., 1999). A loss of cytoskeletal element expression and/or loss of organisation has been observed in osteoarthritic cartilage chondrocytes (Capin-Gutierrez et al., 2004; Holloway et al., 2004; Fioravanti et al., 2005), and a preliminary study conducted by Johnson and Roberts (Johnson and Roberts, 2003) demonstrated a loss of F-actin content in pathological human scoliotic discs. The fact that the cytoskeletal elements are responsive to mechanical load, and their distribution/content is altered in pathological conditions suggests a pivotal role in mechanotransduction and cell sensing.

To date, there has been little characterisation of the composition of the three major cytoskeletal elements in the IVD (Errington et al., 1998; Guilak et al., 1999; Bruehlmann et al., 2002; Johnson and Roberts, 2003; Li et al., 2007b), and none directly comparing the cytoskeletal composition of NP versus OAF. Therefore, a combination of scanning laser confocal microscopy, quantitative PCR and Western blotting was utilised to analyse the organisation and expression levels of F-actin,



$\beta$ -tubulin and vimentin of NP and OAF cells in IVDs *in situ*. Interestingly, the data demonstrates that the organisation, mRNA and protein content of the cytoskeletal elements alter across the IVD, coincident with the two distinct cell populations. Of the three major cytoskeletal elements, the composition of the actin cytoskeleton is most altered between the NP and OAF of bovine IVDs. F-actin is punctate and localised to the periphery of NP cells, a staining pattern that correlates with that observed in chondrocytes (Guilak, 1995; Holloway et al., 2004; Blain et al., 2006). In the OAF, stress fibres are apparent and actin filaments extend out to the cell processes reflecting the fibroblast-like morphology (Dunlevy and Couchman, 1993; Baschong et al., 1997; Pritchard and Guilak, 2004). The distinct localisation of F-actin in the NP and OAF is evident in both young and mature IVD. As scanning laser confocal microscopy can only indicate cell morphology and is not quantitative, both mRNA and protein levels were also analysed to determine whether there were inherent differences in expression levels. Interestingly,  $\beta$ -actin mRNA levels were significantly higher in OAF compared to NP cells, irrespective of age. This trend was also reflected in enhanced  $\beta$ -actin protein amounts in the OAF cells; however this was only true for young IVD and not mature. It has been suggested that the formation of prominent actin stress fibres in the cell processes of OAF disc cells may play a role in “sensing” mechanical loads (Errington et al., 1998). Previous studies in the OAF (Guilak et al., 1999; Pritchard et al., 2002; Pritchard and Guilak, 2004) demonstrated reorganisation of the actin cytoskeleton in response to osmotic stress. It is widely reported that tensile strains induce reorganisation of the actin filaments in many tissues that comprise fibroblast-like cells (Farsi and Aubin, 1984; Pender and McCulloch, 1991; Yoshigi et al., 2005; Langevin et al., 2006) whereas fibroblasts subjected to compressive loads do not show appreciable differences in F-actin distribution (Mizutani et al., 2004). Therefore, the observation of increased  $\beta$ -actin expression in cells of the OAF likely reflects the tensional forces exerted on this tissue.

To date, the microtubular networks have not been characterised in IVD cells. This study demonstrates that  $\beta$ -tubulin is expressed in cells of the NP and OAF. In both cell populations,  $\beta$ -tubulin forms a loose, basket-like meshwork throughout the cytoplasm correlating with its organisation in chondrocytes (Blain et al., 2006). In contrast to

$\beta$ -actin, there is significantly more  $\beta$ -tubulin mRNA in NP than OAF cells, irrespective of age; these higher trends of  $\beta$ -tubulin mRNA are also reflected in higher protein expression. Previous studies have shown that microtubules may be involved in modulating mechanical signals, in particular compressive loading of chondrocytes (Jortikka et al., 2000; Fioravanti et al., 2005) and the suprapatellar ligament (Ralphs et al., 1991). For example, the application of an increasing compressive load has been shown to promote denser  $\beta$ -tubulin architecture in cardiomyocytes (Schroder et al., 2002). It is currently unclear whether  $\beta$ -tubulin fulfils such a function in the intervertebral disc, although the data presented in this chapter demonstrates the presence of a more organised  $\beta$ -tubulin meshwork in cells of the NP, which are subject to compressive loads *in vivo*. Enhanced  $\beta$ -tubulin mRNA and protein expression levels in response to compressive loads have been previously observed in other cell types including osteoblasts (Ingber, 1991; Ingber, 1993; Searby et al., 2005).

Vimentin is a highly expressed cytoskeletal protein providing the cell with rigidity; the dense meshwork of filaments supports the cell shape (Brown et al., 2001) and acts to absorb mechanical loads (Kreplak et al., 2005). The vimentin intermediate filaments of the NP were displayed as a dense meshwork that traversed the cytoplasm from the plasma to the nuclear membrane. The organisation of vimentin in cells of the NP is characteristic of articular chondrocytes (Postacchini et al., 1982; Durrant et al., 1999; Langelier et al., 2000; Blain et al., 2006) and cells of the meniscus (Hellio Le Graverand et al., 2001). In the OAF, vimentin filaments were observed throughout the cytoplasm as well as extending into the cell processes. This organisation has previously been reported in cells of the OAF, with cell processes parallel to the collagen fibre direction (Bruehlmann et al., 2002). The arrangement of the vimentin filaments may be a mechanism for transduction of mechanical deformation from cell membrane to nucleus; a phenomenon that has been observed in chondrocytes (Guilak, 1995; Lee et al., 2000a).

Significantly higher vimentin mRNA levels were observed in the OAF compared to NP cells, although there was an age-related decrease in the OAF. This age-related reduction in vimentin expression was also evident at the protein level in both NP and OAF cells, suggestive of a transcriptional shutdown in expression of this cytoskeletal

element with age. Meanwhile, the increase in the degraded vimentin products (40KDa) and decrease in intact vimentin protein (58KDa) expression in the mature OAF tissue suggests accelerated vimentin degradation in disc tissue with age. Taken together, vimentin expression significantly declined with age due to the decrease in synthesis and increase in degradation, which may alter the mechanical features of the cells, and disrupt the mechanotransduction pathways between the cell nucleus and the ECM. This may lead to an imbalance between anabolic and catabolic metabolism in the disc.

However, we consistently observed more vimentin protein in the NP tissue, although mRNA levels were shown to decrease. It may be that there are sufficient amounts of vimentin protein in the NP and that turnover is much slower than in OAF, thus transcription is decreased accordingly to maintain a steady state balance in vimentin filament amounts. Previous studies have shown that there is an inter-relationship between mechanical stimulation and vimentin content. For example, Wang and Stamenovic found that vimentin contributes to cell stiffness with increasing cell deformation (Wang and Stamenovic, 2000). Vimentin has been found to accumulate in fibrocartilage (Benjamin et al., 1994) and endothelial cells (Schnittler et al., 1993) with increased mechanical load. Significantly increased vimentin levels were observed in chondrocytes derived from regions of articular cartilage that were subject to the most weight-bearing (Eggli et al., 1988). The evidence suggests that vimentin may play a crucial role in mechano-sensing, in particular, in response to compressive loads, as supported by this data demonstrating increased vimentin protein levels in NP cells. This may offer an explanation as to why the vimentin architecture and expression levels are different in cells of the OAF which are subject to tensional forces *in vivo*.

## 2.5 Conclusions

- Both maximum LDH content and total protein levels are suitable for cell number normalisation between NP and OAF in this study.
- F-actin filaments are punctate and distributed beneath the cell membrane. There is higher  $\beta$ -actin expression in OAF.

Chapter 2: Zonal and age-related differences in the organisation and expression of cytoskeletal elements within IVD cells *in situ*

---

- $\beta$ -tubulin filaments form a meshwork distributed throughout the cytoplasm and there is more  $\beta$ -tubulin gene and protein expression in NP.
- Vimentin filaments form a meshwork distributed throughout the cytoplasm, and there is decreased vimentin protein content in OAF. An age-related decline of vimentin protein expression is also observed in both NP and OAF.

# CHAPTER 3.

The effects of cyclic stretching on  
cytoskeletal elements and extracellular  
matrix metabolism of bovine intervertebral  
disc cells *in vitro*

### 3.1 Background

IVD degeneration is regarded as one of the major causes of low back pain (Schwarzer et al., 1994). Although many morphological and biochemical changes have been observed during the process of IVD degeneration, the actual aetiology and pathogenesis are not clear to date. It is thought that mechanical stimulation can induce disc degeneration (Court et al., 2001; Rannou et al., 2003; Walsh and Lotz, 2004).

The main functions of the IVD are to support large loads and permit multi-axial motions of the spine. As a primary loading-bearing structure of the spine, compressive load is mainly experienced by the NP, which is a highly hydrated component containing a large number of proteoglycans and is localised in the centre of the IVD. Due to the special structure of the IVD, axial compression is radially transmitted to stretch and shear forces transversally distributed across the OAF (Leone et al., 2007). The OAF is regarded as the outer shell of the IVD and is composed of a dense network of collagen fibres. Therefore, at least three different types of mechanical stimulation can be observed in IVD: compressive mainly in the NP, and tensional and shear forces mainly in the OAF.

Although tensional force is mainly experienced in the OAF of IVD, there are site-variations in the tensile features of annulus fibrosus lamellae *in vivo*. The anterior annulus fibrosus has larger values for tensile moduli and failure stresses than the posterolateral annulus in human discs, suggesting a different tensional force distribution within the OAF during daily life (Skaggs et al., 1994; Ebara et al., 1996). Further studies have determined the tensile properties of single lamellae *in vitro* and the results indicate that the annulus is much stronger in the plane of individual lamellae, especially when stretched along the collagen fibres, with failure occurring at a stress of 1-3MPa and a strain of 10-25% (Ebara et al., 1996). When many lamellae were stacked together, the failure occurred at a stress of 4-9MPa and a strain of 30-70% (Green and Adams, 1993).

Further studies have investigated the relationship between mechanical strain and metabolic alterations of IVD cells but the results are inconsistent. Using the Flexcell

system where cells were cultured as a monolayer and subjected to a controllable strain, it was found that tensile force (5% elongation, 1Hz) significantly inhibited the production of proteoglycan in human OAF cells through post-translational regulation involving nitric oxide (Rannou et al., 2003; Benallaoua et al., 2006). However, a very recent study indicated that 6% elongation at 0.05Hz exerted a protective effect on rat OAF cells by inhibiting the expression of catabolic genes such as MMP-13 induced by the inflammatory agent IL-1 $\beta$ ; there were no significant changes in production of type I collagen and aggrecan (Sowa and Agarwal, 2008). The difference between these two results may come from the different cell types (human and rat respectively) and frequencies (1Hz and 0.05Hz) used in the experiments. Furthermore, using a 3D culture system such as a collagen gel, it was found that 1, 2, 4, and 8% strain at 1 Hz increased collagen type II and aggrecan expression but decreased MMP-3 gene expression in OAF cells (Neidlinger-Wilke et al., 2005), suggesting a protective effect of physiological strain on OAF cells. Compared with OAF, limited information has been acquired about the effects of tensional strain on NP cells. Matsumoto et al found that a high magnitude of tensional strain (20% elongation, 0.05Hz) promoted collagen synthesis, cell proliferation and production of the inflammatory agent prostaglandin-E2 in NP cells cultured as a monolayer (Matsumoto et al., 1999; Neidlinger-Wilke et al., 2005; Miyamoto et al., 2006), which was very similar to the response observed in articular chondrocytes (Huang et al., 2007).

When mechanical stimulation is applied to IVD tissue, cells respond by synthesising many proteolytic enzymes including aggrecanases (ADAMTSs), matrix metalloproteinases (MMPs) and tissue inhibitor of metalloproteinases (TIMPs) to remodel the ECM (Maclean et al., 2004; MacLean et al., 2005; Omlor et al., 2006). Therefore, pathways must exist in the disc, through which the cells can communicate with the ECM and respond to physiologic/pathogenic alterations in the ECM.

Recent studies have implicated the cytoskeleton in transducing extracellular mechanical signals to the nucleus (Chen et al., 2004; Li et al., 2007b). Mechanical stimulation can promote expression of specific cytoskeletal components and can change their organisation such as F-actin and vimentin in articular chondrocytes (Connelly et al., 2004; Campbell et al., 2007) and IVD cells (Errington et al., 1998),

These studies suggest that the cytoskeleton may be involved in mechanotransduction pathways and might play a role in 'sensing' mechanical strain. However, specific cytoskeletal features may reflect different mechanical influences on the cells. It has been confirmed that there is an alteration in the architecture of vimentin intermediate filaments within rat articular cartilage chondrocytes in explant cultures when subjected to static compressive force (1,2 or 4MPa for 1 hour) (Durrant et al., 1999), whereas increased vimentin content is observed *in vivo* in the greater rather than the lesser weight-bearing regions of cartilage (Eggli et al., 1988).

Specifically for tensile force, cytoskeletal elements including actin, tubulin and vimentin filaments were also found to be involved in mechanotransduction induced by tension. For example, cellular responses to tensile forces applied through integrins require an intact actin network (D'Addario et al., 2001; Wang et al., 2005). Locally applied tensile force was found to promote growth of microtubules (Kaverina et al., 2002). Further studies have shown that tensile force regulated the actin network through filamin A in a microtubule-dependent way in gingival fibroblast cells (D'Addario et al., 2003). Therefore, the microtubules are likely to be involved in tensile force-induced mechanotransduction. In the vimentin knockout mouse, the cellular response of arteries to flow-induced tensile and shear force was decreased, suggesting that vimentin also plays a role in mechanotransduction (Henrion et al., 1997).

Disc degeneration is an age-related disease. Cell metabolism and in particular synthesis of ECM components will dramatically change with age and may subsequently induce the redistribution of mechanical force throughout the IVD. Also, cytoskeletal elements alter with age in IVD cells (Chapter 2). Therefore, abnormal mechanical stimulation such as tensile force or a dysregulated cytoskeletal network may contribute to the loss of homeostasis in IVD, eventually inducing disc degeneration. However, the relationship between tensile force and cytoskeletal elements in intervertebral disc is largely unknown.

In this chapter, the organisation and expression of cytoskeletal elements including  $\beta$ -actin,  $\beta$ -tubulin and vimentin as well as key markers of matrix metabolism were



Chapter 3: The effects of cyclic stretching on cytoskeletal elements and extracellular matrix metabolism of bovine intervertebral disc cells *in vitro*

---

investigated in intervertebral disc cells cultured as a monolayer and subjected to a tensile force for various periods of time.

## 3.2 Materials and Methods

All chemicals were obtained from Sigma (Poole, UK) unless otherwise stated and were of analytical grade or above.

### 3.2.1 Cell isolation and cell culture

Bovine tails were obtained from 7 day old calves as described previously (Section 2.2.1). The proximal coccygeal discs (CC1–CC5) were exposed, and cleaned of all surrounding ligaments and fascia. The discs were removed by sharp dissection from the adjacent vertebrae. The NP and OAF were separated under an anatomical microscope with scalpel and blunt forceps, and the transient region between NP and OAF was discarded. The NP and OAF tissue were then washed in Hank's balanced-salt solution (Invitrogen, Paisley, UK) supplemented with 400 IU/mL penicillin and 400 µg/mL streptomycin for 3 × 20 minutes. The tissue was then cut into medium sized pieces (about 1 cm<sup>3</sup>), and digested with 0.8mg/ml type II collagenase (for NP) or 1.5mg/ml type I collagenase (for OAF) combined with 0.3mg/ml pronase (Invitrogen, Paisley, UK) at 37°C overnight with agitation. Tissue remnants were removed by filtering through a 45µm strainer, and the cells were collected by centrifugation at 3000rpm for 10 minutes. The cells were then washed twice to remove the collagenase and pronase using Dulbecco's Modified Eagle Medium/F12 (DMEM/F-12) (1:1) with GlutaMAX™ I (Invitrogen, Paisley, UK). After the final centrifugation, cells were resuspended using DMEM/F12 (1:1) cell culture medium supplemented with 10% fetal bovine serum (FBS) (Invitrogen, Paisley, UK) plus 100µg/ml penicillin-streptomycin and 1% fungizone (Invitrogen, Paisley, UK). Cell number and viability were determined using the trypan blue assay. Preparations were only used when the cell viability was higher than 95%.

Cells were seeded as primary cultures in flasks ( $0.5 \times 10^6/\text{cm}^2$ ) and cultured in DMEM/F12 (1:1) containing 10% FBS plus 100µg/ml penicillin-streptomycin and 1% fungizone at 37 °C in a humidified atmosphere of 5% CO<sub>2</sub> for 4 days without changing the media. After 4 days, the healthy cells adhered to the bottom of the culture flask,

whereas the dead cells floated in the media. Changing the culture media removed most of the dead cells. The cell cultures were maintained by changing the culture media every two days until confluent. The cells were then removed from the bottom of the flask by incubation with 0.25% trypsin-EDTA solution (Invitrogen, Paisley, UK) for 10-15 minutes at 37°C, pelleted by centrifugation and washed twice as described above. Cell number and viability were determined using the trypan blue assay and preparations were only used when the cell viability was higher than 95%. Cells were then subcultured in 6-well flexible-bottomed culture plates coated with type I collagen (Flex I culture plates; Flexcell International, USA) at a density of  $1.0 \times 10^6$ /per well (for protein and mRNA) or  $0.25 \times 10^6$ /per well (for confocal microscopy). Cells were cultured in DMEM/F12 (1:1) containing insulin-transferrin-sodium selenite (ITS) plus 100µg/ml penicillin-streptomycin and 1% fungizone at 37 °C in a humidified atmosphere of 5% CO<sub>2</sub> for 24 hours prior to the stretching experiments.

### 3.2.2 Application of cyclic tensile strain

Bovine IVD cells cultured as a monolayer on the Flex I culture plates were divided into three groups for gene expression, scanning confocal microscopy and protein expression analysis.

Cells for gene expression and scanning confocal microscopy were subjected to cyclic tensile strain (CTS) using the Flexcell FX-3000 system (Flexcell International Corp, Hillsborough, NC) with 10% elongation at 1Hz for 10, 30 or 60 minutes respectively. As a control, cells were cultured equivalently in all steps, except that no CTS was applied. After stretching, samples for RNA extraction were lysed immediately using Trizol reagent (Invitrogen, Paisley, UK) and stored at -80°C. Samples for confocal microscopy were fixed with 4% paraformaldehyde at room temperature followed by immunofluorescent staining as described below (Section 3.2.4).

Cells for protein expression were subjected to CTS using the Flexcell FX-3000 system with 10% elongation at 1Hz for 60 minutes, followed by incubation at 37°C in a humidified atmosphere of 5% CO<sub>2</sub> for a further 0, 3, 8 or 24 hours. Cells were then



lysed using 0.9% Triton X-100 solution containing protease inhibitors and stored at -20°C. Culture media was also collected and stored at -20°C.

### 3.2.3 Determination of cell viability using the LDH assay

To investigate whether CTS induces cell death, cell viability after stretching was determined using the LDH assay. Briefly, IVD cells cultured as a monolayer on type I collagen were lysed using 0.9% Triton X-100. Total LDH levels were then determined using the LDH assay as described previously (Section 2.2.5). LDH levels in the culture media were also determined. Cell viability was calculated according to the formula below:

$$\text{Cell viability} = \left( 1 - \frac{\text{LDH levels in culture media}}{\text{Total LDH levels}} \right) \times 100\%$$

### 3.2.4 Analysis of cytoskeletal element organisation using confocal microscopy

Bovine IVD cells cultured on type I collagen as a monolayer, and subjected to tensile strain, were fixed with 4% paraformaldehyde and the organisation of cytoskeletal elements were localised as described previously (Section 2.2.2) with minor modifications. Specifically, F-actin filaments within cells were stained directly using Alexa 488™ -conjugated phalloidin 1:200 dilution (Invitrogen, Paisley, UK). After incubation with primary antibodies,  $\beta$ -tubulin and vimentin filaments were labelled using Alexa® 633 conjugated goat anti-mouse secondary antibody 1:100 dilution (Invitrogen, Paisley, UK) for 60 minutes at room temperature avoiding light. Cells were washed extensively and mounted using Vectorshield™ (Vector Laboratories, Peterborough, UK) and stored at room temperature avoiding light before scanning. The scanning procedures were similar to that described previously (Section 2.2.2).

### **3.2.5 Analysis of cytoskeletal element gene expression using quantitative PCR**

RNA was extracted from IVD cells subjected to CTS and cDNA was synthesised according to the methods described previously (Section 2.2.3.1-2). To quantify target gene expression, real-time PCR with custom-designed primers was performed using the Mx3000P<sup>®</sup> QPCR System as described previously (Section 2.2.3.4). The sequences of primers used for target gene amplification are shown in Table 3-1. Calculation of starting concentration was based on standard curves for each target DNA run in parallel, and all the data are presented as fold-change in gene expression after initially being normalised to the housekeeping gene GAPDH and then normalised to an endogenous control in the experiment i.e. to unstretched young NP cells which were assigned a value of 1 (Figure 3-1). Therefore, fold changes in gene expression above 1 suggest an increase in transcription whereas values below 1 indicate a decrease relative to the baseline control i.e. unstretched NP cells.

**Table 3-1. Primer sequences for real-time quantitative PCR**

Gene	Primer sequence	T <sub>m</sub> (°C)	Product size (bp)	Accession No.
<b>β-actin</b>	Forward: 5'-TTCGAGACCTTCAACACCCC-3'	60	68	NM_173979
	Reverse: 5'-GGCCAGAGGCATACAGGGA-3'			
<b>tubulin</b>	Forward: 5'-GAGGAGGAGGTGGCCTAGAG-3'	60	175	NM_001034663
	Reverse: 5'-GCTTTAATGGTGGTGGCTGT-3'			
<b>vimentin</b>	Forward: 5'-AAGGAAGAGATGGCTCGTCA-3'	53.7	164	NM_173969
	Reverse: 5'-TTGGTTTCCCTCAGGTTTCAG-3'			
<b>aggrecan</b>	Forward 5'-GCTACCCTGACCCTTCATC-3'	60	76	NM_173981
	Reverse 5'-AAGCTTTCTGGGATGTCCAC-3'			
<b>type I collagen</b>	Forward 5'-ACATGCCGAGACTTGAGACTCA-3'	61	86	NM_174520
	Reverse: 5'-GCATCCATAGTACATCCTTGGTTAGG-3'			
<b>type II collagen</b>	Forward: 5'- AACGGTGGCTTCCACTTC-3'	60	69	NM_001113224
	Reverse: 5'-GCAGGAAGGTCATCTGGA-3'			

Chapter 3: The effects of cyclic stretching on cytoskeletal elements and extracellular matrix metabolism of bovine intervertebral disc cells  
*in vitro*

---

Gene	Primer sequence	T <sub>m</sub> (°C)	Product size (bp)	Accession No.
<b>MMP-1</b>	Forward 5'-CAAATGCTGGAGGTATGATGA-3'	60	82	NM_174112
	Reverse: 5'-AATTCCGGGAAAGTCTTCTG-3'			
<b>MMP-2</b>	Forward 5'-TCTGCCCCCATGAAGCCCTGTT-3'	65	347	NM_174745
	Reverse 5'-GCCCCACTTGCGGTCATCATCGTA-3'			
<b>MMP-3</b>	Forward: 5'-TGGAGATGCTCACTTTGATGATG-3'	60	221	XM_586521
	Reverse: 5'-GAGACCCGTACAGGAACTGAATG-3'			
<b>MMP-9</b>	Forward: 5'-ATGTGGGCTACGTGACCTTC-3'	59	162	NM_174744
	Reverse: 5'-CCTCCTCGTCCTTCAGAACA-3'			
<b>MMP-13</b>	Forward 5'-TGGTGATGAAACCTGGACAA-3'	55	237	NM_174389
	Reverse: 5'-GGCGTTTTGGGATGTTTAGA-3'			
<b>TIMP-1</b>	Forward: 5'-CTGCGGATACTTCCACAGGT-3'	60	75	NM_174471
	Reverse: 5'-ATGGATGAGCAGGGAAACAC-3'			
<b>TIMP-2</b>	Forward: 5'-ATAGTGATCAGGGCCAAAGCAGTC-3'	63	277	NM_174472
	Reverse: 5'-TGTCCCAGGGCACGATGAAGTC-3'			

Chapter 3: The effects of cyclic stretching on cytoskeletal elements and extracellular matrix metabolism of bovine intervertebral disc cells  
*in vitro*

---

Gene	Primer sequence	T <sub>m</sub> (°C)	Product size (bp)	Accession No.
<b>TIMP-3</b>	Forward: 5'-GATGTACCGAGGATTCACCAAGAT-3' Reverse: 5'-GCCGGATGCAAGCGTAGT-3'	60	356	NM_174473
<b>vinculin</b>	Forward: 5'-GCACGATTGAGAGCATTCTG-3' Reverse: 5'-GCACGATTGAGAGCATTCTG-3'	57	212	NM_001078093
<b>talin2</b>	Forward: 5'-CCTTCCTGCCTGTCACTAGC-3' Reverse: 5'-TATTACAGCCCCTGCTCACC-3'	60	214	XM_606666
<b>destrin</b>	Forward: 5'-GTGCCACAGGAAAAACATC-3' Reverse: 5'-ACGCCAGAGGAAATCAAGAA-3'	58	243	NM_001015586
<b>cofilin</b>	Forward: 5'-TTGTCTGGCAGCATCTTGAC-3' Reverse: 5'-TGGGGTCATCAAAGTGTTCA-3'	58	207	NM_001015655
<b>filamin A</b>	Forward: 5'-GGCTTTTGGGAATAGCATCA-3' Reverse: 5'-TTAGCAAACCCACCCACTTC-3'	58	213	XM_614269
<b>α-actinin</b>	Forward: 5'-CCGGAACATTCATCTGCT-3' Reverse: 5'-TCTTCGACAACAAGCACACC-3'	58	158	NM_001035351



Chapter 3: The effects of cyclic stretching on cytoskeletal elements and extracellular matrix metabolism of bovine intervertebral disc cells  
*in vitro*

---

Gene	Primer sequence	T <sub>m</sub> (°C)	Product size (bp)	Accession No.
<b>paxillin</b>	Forward: 5'-CCTGCAGTCTGACCTGAACA-3' Reverse: 5'-AGTAGTAGCAGCGCGGAGAG-3'	60	239	XM_595626
<b>gelsolin</b>	Forward: 5'-GAAGCTCTCCCAGGACACAG-3' Reverse: 5'-TGCAGCTGGATGACTACCTG-3'	60	233	NM_001113284
<b>thymosin β4</b>	Forward: 5'-GGTTTTAAACTTTTTATTTG-3' Reverse: 5'-TGGGACGACAGTGAAA-3'	60	156	BC133478
<b>GAPDH</b>	Forward 5'-GGCATCGTGGAGGGACTTATGA-3' Reverse 5'-GGGCCATCCACAGTCTTCTG -3'	60	68	XM_001252511

### **3.2.6 Analysis of protein expression within cells using Western Blotting**

Protein within bovine IVD cells cultured on type I collagen as a monolayer and subjected to tensile strain, was extracted using 0.9% Triton X-100 plus protease inhibitors. Cytoskeletal protein levels were investigated using Western Blotting as described previously (Section 2.2.6). The samples were normalised to total protein levels according to the BCA Assay results (Section 2.2.4). Samples were denatured at 60°C for 30 minutes and reduced by adding 2.5% (v/v)  $\beta$ -mercaptoethanol.

### **3.2.7 Analysis of MMPs using gelatin zymography**

MMP-2 and MMP-9 levels in culture media from the bovine IVD cells subjected to tensile strain were investigated using gelatin zymography.

#### **3.2.7.1 Sample preparation**

Samples were normalised to total cell number according to the LDH assay as previously described (Section 2.2.5), mixed with an equal volume of 2x loading buffer and heated at 60°C for 30 minutes without reduction.

Chapter 3: The effects of cyclic stretching on cytoskeletal elements and extracellular matrix metabolism of bovine intervertebral disc cells *in vitro*

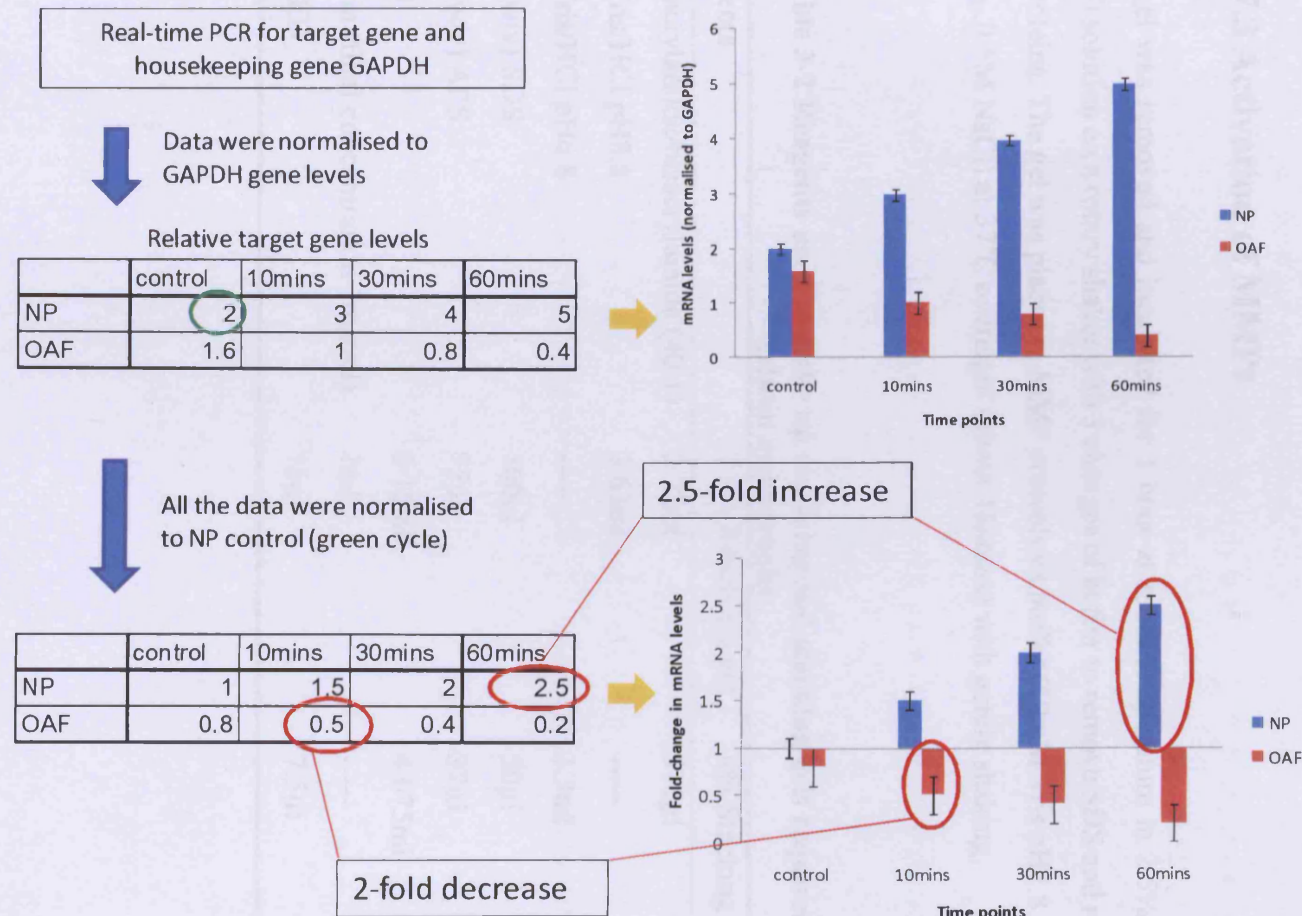


Figure 3-1 Explanatory diagram of the calculation of the fold-change in mRNA levels. After real-time PCR, all the data are presented as fold-change in gene expression after initially being normalised to the housekeeping gene GAPDH and then normalised to an endogenous control (green circle) in the experiment. X-axis crosses the value at 1.0, and the increased mRNA lies above the X-axis but the decreased gene expression lies below the X-axis.

### 3.2.7.2 Gelatin zymography analysis

A 7.5% resolving gel incorporating 1mg/ml gelatin, and a 4% stacking gel was made up according to Table 3-2. The samples were loaded into the wells, and electrophoresis was carried out at 120V for 1 to 1.5 hours, at which time the bromophenol blue dye had reached the bottom of the gel.

### 3.2.7.3 Activation of MMPs

The gel was removed and incubated for 1 hour at room temperature in 2.5% Triton X-100 solution on a rotary shaker with 3 changes of buffer to remove SDS and renature the proteins. The gel was placed in MMP proteolysis buffer (50mM Tris pH7.8, 50mM CaCl<sub>2</sub>, 0.5M NaCl) at 37°C overnight (about 18hours) with gentle shaking.

**Table 3-2 Reagents used to make up resolving and stacking gels required for gelatin zymography**

Reagents	7.5% Resolving gel	4% Stacking Gel
40% acrylamide/bisacrylamide (40:1)	2.72ml	575µl
1M Tris/HCl pH8.8	3.63ml	-----
1M Tris/HCl pH6.8	-----	1.3ml
10%(w/v) SDS	100µl	50µl
10%(w/v) APS	75µl	37µl
dH <sub>2</sub> O	6.16ml	4.075ml
Gelatin (final concentration 1mg/ml)	1ml	-----
TEMED	15µl	7.5µl

### **3.2.7.4 Staining and destaining of the gel**

After activation, the gel was stained using Coomassie staining buffer [10% (v/v) glacial acetic acid, 45% (v/v) methanol, 0.25% (w/v) Coomassie brilliant blue R250] for 60 minutes at room temperature on a rotary shaker. After discarding the staining buffer, the gel was destained in destaining buffer [7.5% (v/v) acetic acid glacial, 10% (v/v) methanol] at room temperature on a rotary shaker until white bands appeared on a blue background. The gels were scanned and differences in staining intensity of the digitised bands were assessed using NIH Image software. To compare the samples across different gels, MMP-2 and 9 standards were loaded onto each gel. After scanning and digitisation, all the unknown samples were normalised to the mean value of the standards.

### **3.2.8 Analysis of TIMPs using reverse gelatin zymography**

TIMP-1, TIMP-2 and TIMP-3 levels in culture media from the bovine IVD cells subjected to tensile strain were investigated using reverse gelatin zymography.

#### **3.2.8.1 Sample preparation**

The samples were prepared using the same method described in gelatin zymography (Section 3.2.7.1).

#### **3.2.8.2 SDS-PAGE gel electrophoresis**

A 12% resolving gel containing 2.08mg/ml gelatin and 1ml of conditioned media containing a source of MMPs (from Dr. Emma Blain), and a 4% stacking gel were made up according to Table 3-3. The samples were loaded into the wells and electrophoresis was carried out as described above (Section 3.2.7.2).

### 3.2.8.3 Activation of MMPs

MMP activation was performed using the same protocols as described above (Section 3.2.7.3).

**Table 3-3 Reagents used to make up resolving and stacking gels required for reverse gelatin zymography**

Reagents	12.5% Resolving gel	4% Stacking Gel
40% acrylamide/bisacrylamide(40:1)	4.53ml	575 $\mu$ l
1M Tris/HCl pH8.8	3.63ml	-----
1M Tris/HCl pH6.8	-----	1.3ml
10%(w/v) SDS	100 $\mu$ l	50 $\mu$ l
10%(w/v) APS	75 $\mu$ l	37 $\mu$ l
dH <sub>2</sub> O	4.35ml	4.075ml
Gelatin (final concentration 2mg/ml)	1ml	-----
Conditional media	1ml	-----
TEMED	15 $\mu$ l	7.5 $\mu$ l

### 3.2.8.4 Staining and destaining of the gel

Staining and destaining were performed using the same protocols as described above (Section 3.2.7.4). The presence of TIMPs was seen as blue bands on a clear background which was quantified as described (Section 3.2.7.4).

### 3.2.9 Statistical Analysis

Data are presented as mean  $\pm$  S.E.M, with tissue derived from between 4 and 6 individual animals. Samples were analysed in triplicate and all experiments were performed twice and representative data are presented. One-way ANOVA plus Dunnett's (Gaussian distribution) or Dunn's (not Gaussian distribution) post hoc test was carried out using GraphPad Prism 5.0 software unless otherwise stated. Differences were considered significant at P values of less than 0.05.

## **3.3 Results**

### **3.3.1 Effect of stretching on cell viability**

To determine whether stretching can induce cell death, cell viability was investigated at different time points (control, 0, 3, 8, and 24 hours) after tensile strain (10% elongation, 1Hz, 60 minutes). No decline in cell viability was observed after tensile stretching at any of the time points when compared with the control unstretched group ( $P>0.05$ ), suggesting that tensile force did not affect cell viability (Figure 3-2).

### **3.3.2 Characterisation of the phenotype of IVD cells in monolayer culture**

In this study, IVD cells were cultured as a monolayer which can greatly change the cell morphology especially of NP cells. In order to make sure both NP and OAF cells retained their initial phenotype, types I and II collagen and aggrecan gene expression in the control samples were investigated.

There was 1.3-fold higher type I collagen gene expression (Student's t test,  $p=0.0289$ ), 30-fold lower type II collagen (Student's t test,  $p<0.0001$ ) and 10-fold lower aggrecan gene expression (Student's t test,  $p=0.0001$ ) in OAF cells compared with NP cells (Figure 3-3).

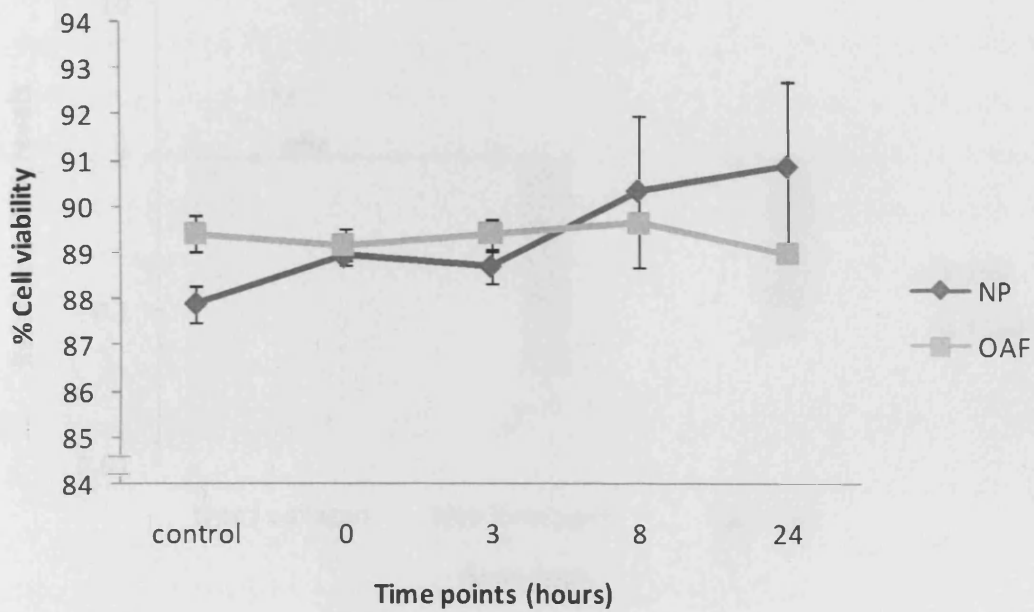


Figure 3-2 Effect of stretch on cell viability. Bovine IVD cells cultured as a monolayer on type I collagen were subjected to cyclic tensile force (10% elongation, 1Hz) for 60 minutes. Cell viability was determined using the LDH assay at different time points after stretching (0, 3, 8 and 24 hours). Data is presented as Mean  $\pm$  S.E.M. (n=6). No decline in cell viability of NP or OAF cells was observed after stretching.



### 3.3.3 The effect of tensile force on $\beta$ -actin filaments

#### 3.3.3.1 Tensile force alters the organization of F-actin in IVD cells

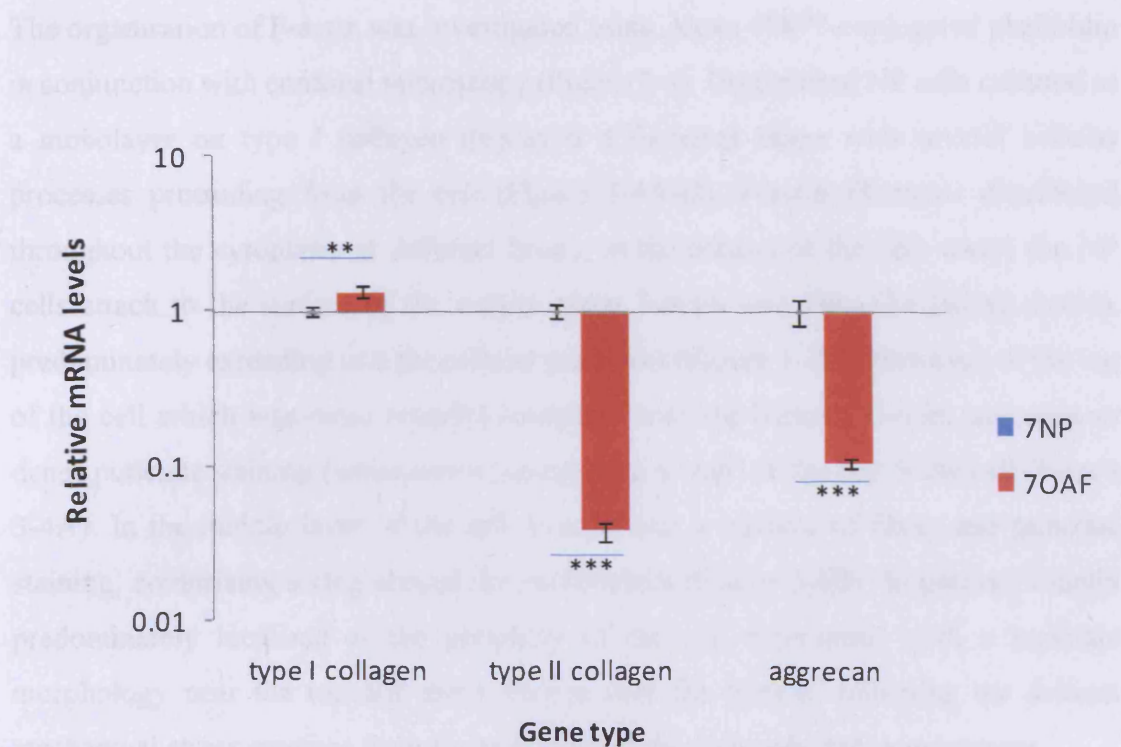


Figure 3-3 Zonal differences in ECM component gene expression in unstretched IVD cells. Cells were cultured on type I collagen as a monolayer and total RNA was extracted. Types I and II collagen and aggrecan mRNA levels were determined using real-time PCR. Data were normalised to the house-keeping gene GAPDH and were relative to NP cells. Data are shown as Mean  $\pm$  S.E.M. (n=5). \*\*\*:  $p \leq 0.001$ , \*\*:  $p \leq 0.01$ , Student's t test.

### 3.3.3 The effect of tensile force on $\beta$ -actin filaments

#### 3.3.3.1 Tensile force alters the organisation of F-actin in IVD cells

The organisation of F-actin was investigated using Alexa 488<sup>TM</sup>-conjugated phalloidin in conjunction with confocal microscopy (Figure 3-4). Unstretched NP cells cultured as a monolayer on type I collagen displayed a flattened shape with several cellular processes protruding from the cell (Figure 3-4A-D). F-actin filaments distributed throughout the cytoplasm at different layers; in the bottom of the cell, where the NP cells attach to the surface of the culture plate, F-actin was fibre-like (white arrow), predominately extending into the cellular processes (Figure 3-4C). However, at the top of the cell which was more rounded compared with the bottom, F-actin was seen as dense punctate staining (white arrow) comprising a 'cap' on the top of the cell (Figure 3-4A). In the middle layer of the cell, F-actin was a mixture of fibres and punctate staining, comprising a ring around the cell nucleus (Figure 3-4B). In general, F-actin predominately localised at the periphery of the cell membrane, with a punctate morphology near the top and more fibrous near the bottom, reflecting the distinct mechanical stress gradient from top to bottom of the cells cultured in monolayer.

After cells were subjected to 10% elongation at 1Hz for 60 minutes, NP cells became flatter, and more elongated. F-actin filaments, actually stress fibres (white arrow), were distributed beneath the cell membrane, extending towards the cell processes (Figure 3-4P). In the bottom of the cells, F-actin filaments were distributed along the membrane which attached to the surface of the culture plate, especially in the cell processes, suggesting a close relationship between F-actin and strain (Figure 3-4O). In the middle layer of the cell, most of the fibres localised in the cellular protrusions, and the region where the nucleus localised to was absent of F-actin staining (Figure 3-4N). In the top of the cell, F-actin staining displayed thin fibres, protruding towards the direction of the cell processes (white arrow) (Figure 3-4M). In general, 60 minutes of tensile force significantly flattened and elongated NP cells, and F-actin staining consequently changed from a mainly punctate to a predominately fibre-like morphology, distributing along the direction of strain, especially in the top layer of cells.

After stretching for 10 (Figure 3-4 E-H) and 30 minutes (Figure 3-4I-L), the organisation of F-actin in NP cells was similar with that of the control group with cell processes protruding in random directions. However, it seemed that there are more stress fibres and less punctate-like staining in the cells.

The organisation of F-actin within OAF cells, in the absence or presence of stretching, was similar to that in the NP as described above (data not shown).

### **3.3.3.2 CTS promoted $\beta$ -actin gene and protein expression in IVD cells**

To determine whether the observed differences in cytoskeletal element architecture in NP and OAF cells were purely organisational or due to altered gene/protein amounts, expression levels of  $\beta$ -actin mRNA and protein were quantified.

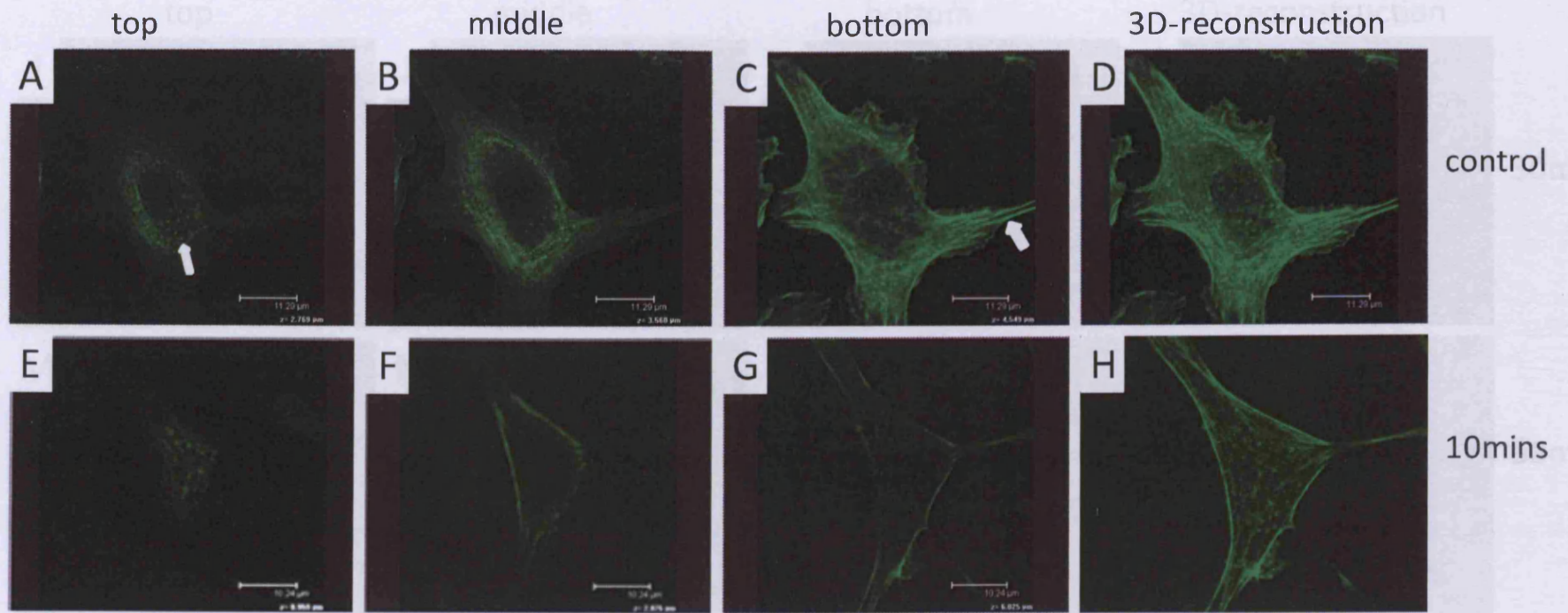
#### **3.3.3.2.1 Tensile strain promotes $\beta$ -actin gene expression in NP and OAF cells**

There was a significant increase in  $\beta$ -actin gene expression within OAF cells after being subjected to CTS for 10 (1.5-fold,  $p < 0.01$ ), 30 (2.1-fold,  $p < 0.001$ ) or 60 minutes (2-fold,  $p < 0.001$ ) (Figure 3-5). In contrast to OAF cells, there was no significant alteration in  $\beta$ -actin gene levels in NP cells after CTS for 10 ( $p > 0.05$ ) and 30 minutes ( $p > 0.05$ ). However, a 1.5-fold increase in  $\beta$ -actin mRNA in NP cells was observed after 60 minutes of stretching ( $p < 0.05$ ) (Figure 3-5)

Figure 3-4 Localisation of F-actin filaments in nucleus pulposus cells cultured on type I collagen as a monolayer. Cells were subjected to cyclic tensile strain (10% elongation, 1Hz) for 10, 30 or 60 minutes, and un-stretched cells were used as a control. F-actin was stained with Alexa-488™ conjugated phalloidin. Images are presented at different layers of the cell from top to bottom. 3D reconstructions are reconstructed images of serial sections through the depth of one cell. [A-D] unstretched NP cells; [E-H] 10 minutes; [I-L] 30 minutes; [M-P] 60 minutes. Arrow: the fibre-like staining of F-actin filaments after strain.

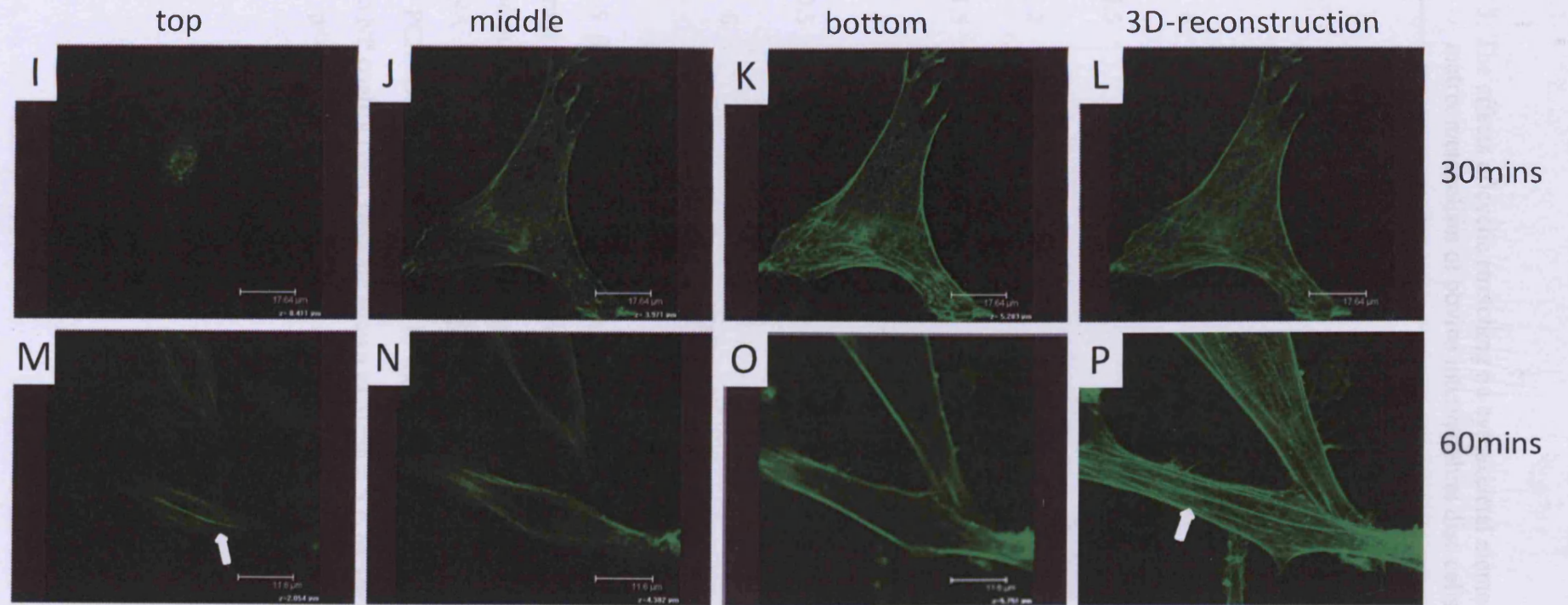
Chapter 3: The effects of cyclic stretching on cytoskeletal elements and extracellular matrix metabolism of bovine intervertebral disc cells *in vitro*

---



Chapter 3: The effects of cyclic stretching on cytoskeletal elements and extracellular matrix metabolism of bovine intervertebral disc cells *in vitro*

---



Chapter 3: The effects of cyclic stretching on cytoskeletal elements and extracellular matrix metabolism of bovine intervertebral disc cells *in vitro*

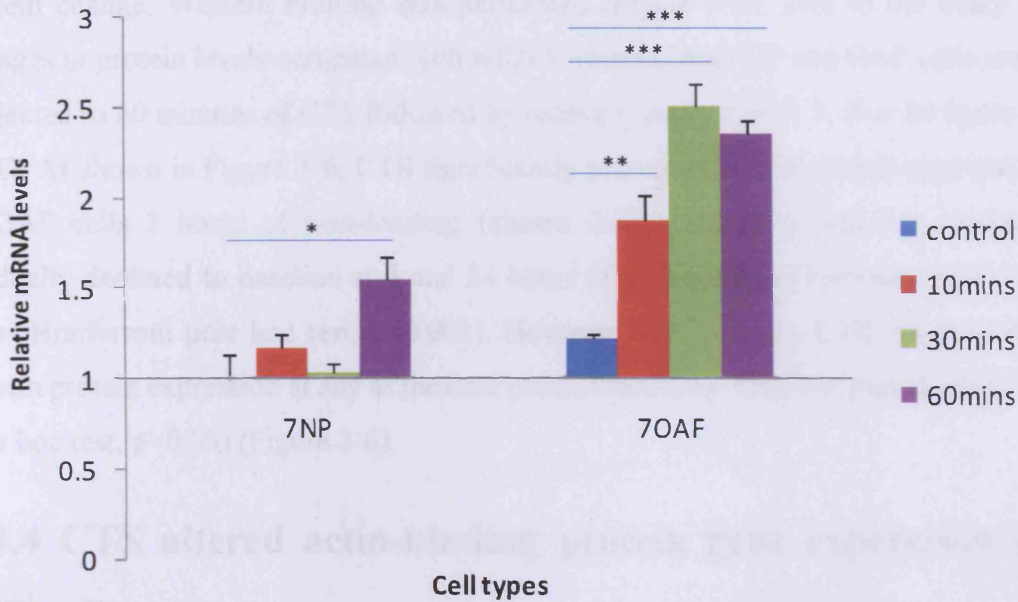


Figure 3-5  $\beta$ -actin gene expression in bovine intervertebral disc cells subjected to tensile strain. Cells were cultured on type I collagen as a monolayer and subjected to 10% elongation at 1Hz for 10, 30 or 60 minutes. Unstretched cells were used as a control. Total RNA was then extracted and  $\beta$ -actin mRNA levels were determined using real-time PCR. Data were normalised to the house-keeping gene GAPDH and were relative to NP control cells. Data are shown as Mean  $\pm$  S.E.M. (n=5). \*\*\*:  $p \leq 0.001$ , \*\*:  $p \leq 0.01$ , \*:  $p < 0.05$  when compared with control group.

### 3.3.3.2.2 Tensile strain promotes $\beta$ -actin protein expression in both NP and OAF cells

To further investigate whether the alteration in  $\beta$ -actin gene expression induces a protein change, Western blotting was performed (Figure 3-6). Due to the delay in changes in protein levels compared with mRNA content, both NP and OAF cells were subjected to 60 minutes of CTS followed by recovery periods of 0, 3, 8 or 24 hours at 37°C. As shown in Figure 3-6, CTS significantly promoted  $\beta$ -actin protein expression in OAF cells 3 hours of post-loading (almost 2-fold increase), and this increase gradually declined to baseline at 8 and 24 hours of post-loading (Two-way ANOVA plus Bonferroni post hoc test,  $p < 0.001$ ). However, for NP cells, CTS did not alter  $\beta$ -actin protein expression at any of the time points (Two-way ANOVA plus Bonferroni post hoc test,  $p > 0.05$ ) (Figure 3-6).

### 3.3.4 CTS altered actin-binding protein gene expression in IVD cells

To further address whether the actin binding proteins were involved in the tensile-induced F-actin reorganisation and expression alterations,  $\alpha$ -actinin, cofilin, filamin A and thymosin  $\beta 4$  mRNA levels were investigated using real-time PCR.

**NP cells:** a small but significant increase in cofilin gene expression was observed after 10 ( $p < 0.001$ ), 30 ( $p < 0.05$ ) and 60 minutes ( $p < 0.05$ ) of strain (Figure 3-7A). However, there were no alterations in  $\alpha$ -actinin, filamin A, and thymosin  $\beta 4$  mRNA levels in response to CTS.

**OAF cells:** a small but significant increase in cofilin gene expression was observed after 10 ( $p < 0.01$ ), 30 ( $p < 0.001$ ) and 60 minutes ( $p < 0.001$ ) of strain (Figure 3-7B). In contrast, 10, 30 and 60 minutes of strain decreased  $\alpha$ -actinin ( $p < 0.001$ , 0.001 and 0.01 respectively), filamin A ( $p < 0.01$ , 0.01 and 0.05 respectively) and thymosin  $\beta 4$  ( $p < 0.01$ , 0.01 and 0.001 respectively) gene expression (Figure 3-7B).



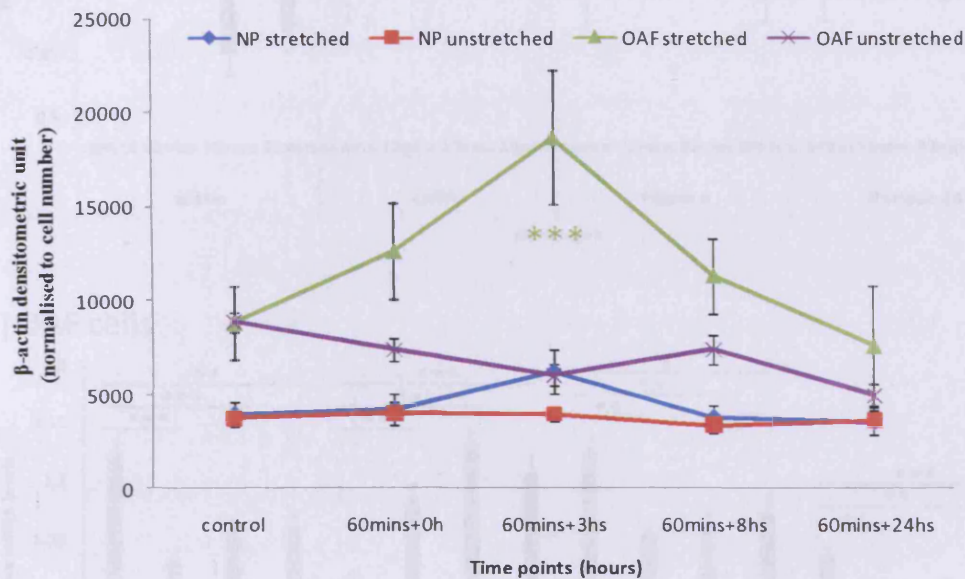
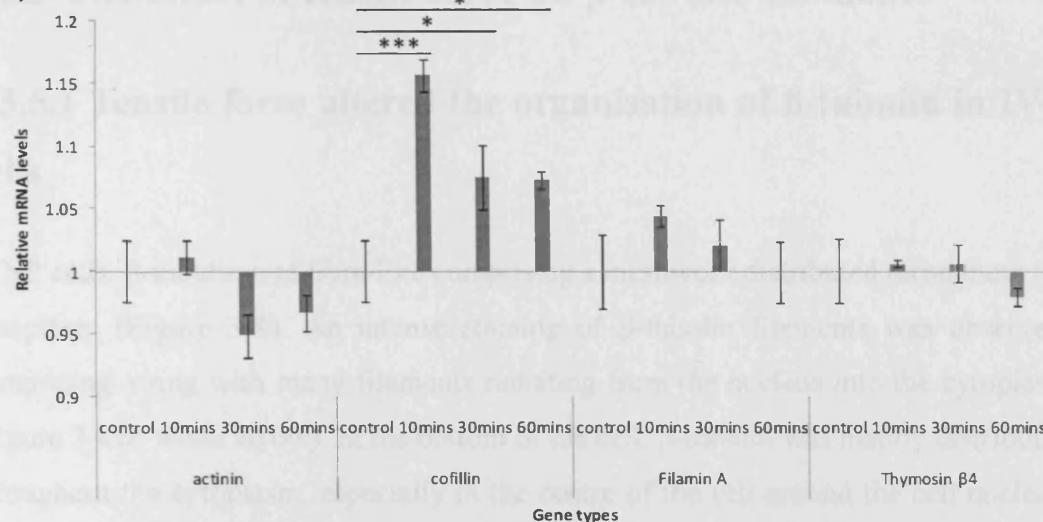


Figure 3-6 β-actin protein expression in NP and OAF cells subjected to cyclic tensile strain. Bovine NP and OAF cells were cultured on type I collagen and subjected to cyclic tensile strain for 60 minutes followed by culture for a further 0, 3, 8 or 24 hours. Samples were normalised to cell number. Unstretched cells were cultured under the same conditions as the stretched samples and used as controls for the different time points. To remove the error induced by differences in film exposure, a control sample was used as a standard to normalise the other samples. Data are presented as Mean ± S.E.M. (n=5). \*\*\*:  $p \leq 0.001$ , when compared with control samples.

Chapter 3: The effects of cyclic stretching on cytoskeletal elements and extracellular matrix metabolism of bovine intervertebral disc cells *in vitro*

(A) NP cells



(B) OAF cells

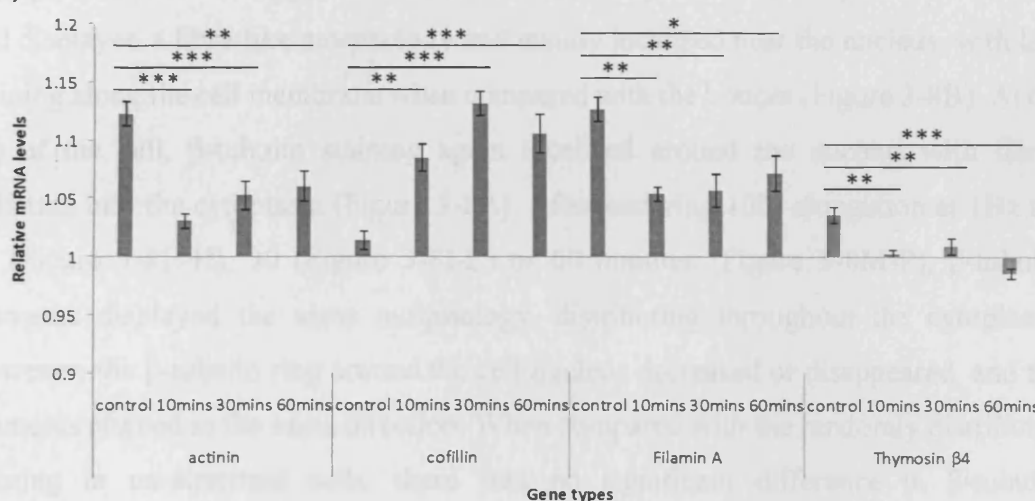


Figure 3-7 Actin-binding protein gene expression in bovine intervertebral disc cells subjected to tensile strain. Cells were cultured on type I collagen as a monolayer and subjected to 10% elongation at 1Hz for 10, 30 or 60 minutes. Unstretched cells were used as a control. Total RNA was then extracted and target gene mRNA levels were determined using real-time PCR. Data were normalised to the house-keeping gene GAPDH and were relative to NP control cells. Data are shown as Mean  $\pm$  S.E.M. (n=5). \*\*\*:  $p \leq 0.001$ , \*\*:  $p \leq 0.01$ , \*:  $p < 0.05$  when compared with control group. A: NP cells; B: OAF cells.

### **3.3.5 The effect of tensile force on $\beta$ -tubulin filaments**

#### **3.3.5.1 Tensile force altered the organisation of $\beta$ -tubulin in IVD cells**

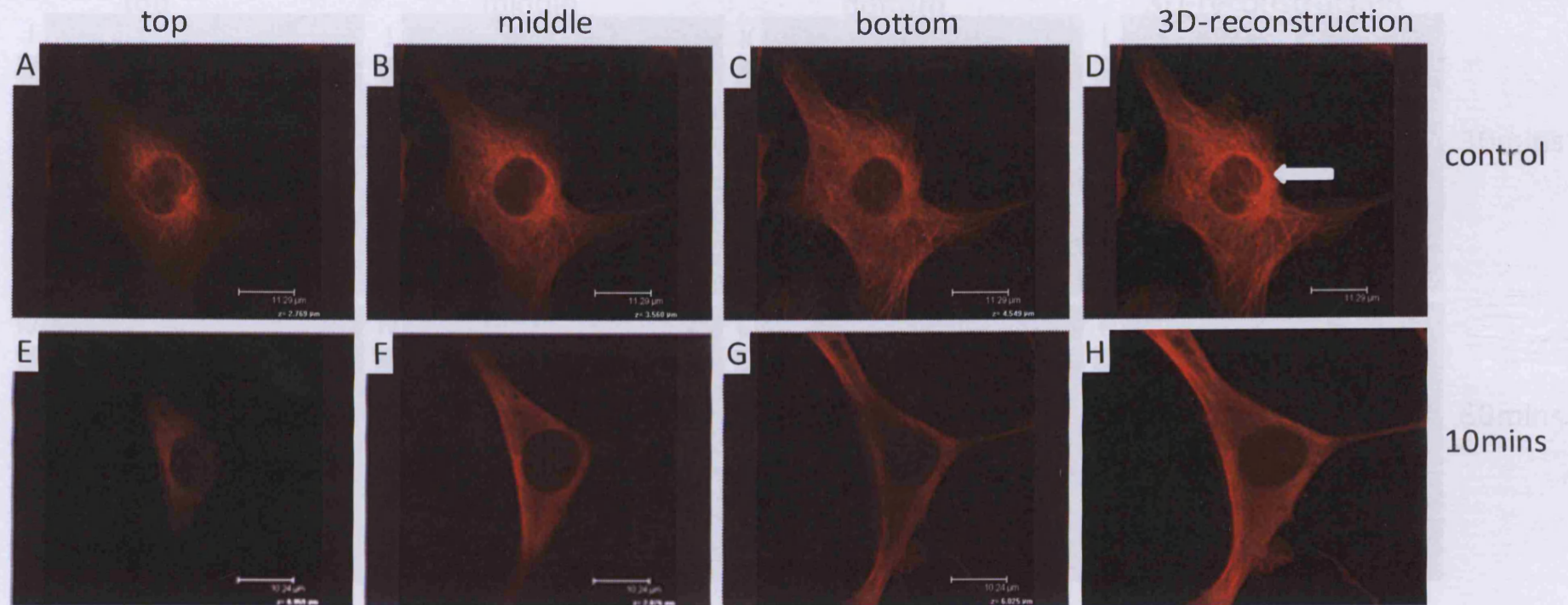
In NP cells,  $\beta$ -tubulin was fibre-like comprising a meshwork distributed throughout the cytoplasm (Figure 3-8). An intense staining of  $\beta$ -tubulin filaments was observed, comprising a ring with many filaments radiating from the nucleus into the cytoplasm (Figure 3-8D, white arrow). In the bottom of the cell,  $\beta$ -tubulin was mainly distributed throughout the cytoplasm, especially in the centre of the cell around the cell nucleus. The filaments protruding towards the cell processes were distributed randomly without any specific direction (Figure 3-8C). In the middle layer of the cell,  $\beta$ -tubulin staining still displayed a fibre-like morphology and mainly localised near the nucleus, with less staining along the cell membrane when compared with the bottom (Figure 3-8B). At the top of the cell,  $\beta$ -tubulin staining again localised around the nucleus with fibres radiating into the cytoplasm (Figure 3-8A). After enduring 10% elongation at 1Hz for 10 (Figure 3-8E-H), 30 (Figure 3-8I-L) or 60 minutes (Figure 3-8M-P),  $\beta$ -tubulin filaments displayed the same morphology, distributing throughout the cytoplasm. However, the  $\beta$ -tubulin ring around the cell nucleus decreased or disappeared, and the filaments aligned in the same direction. When compared with the randomly distributed staining in un-stretched cells, there was no significant difference in  $\beta$ -tubulin architecture in different layers of the cells subjected to 60 minutes of stretching.

The organisation of  $\beta$ -tubulin in cells of the young OAF in the absence or presence of stretching was similar to that in the NP cells as described above (Data not shown).

Figure 3-8. Localisation of  $\beta$ -tubulin in nucleus pulposus cells cultured on type I collagen as a monolayer. Cells were subjected to cyclic tensile strain (10% elongation, 1Hz) for 10, 30 or 60 minutes; unstretched cells were used as a control.  $\beta$ -tubulin was detected using mouse anti-tubulin monoclonal antibody E7 and visualised by incubation with Alexa-633™ conjugated goat anti-mouse secondary antibody. Images are presented at different layers of the cell from top to bottom. 3D reconstructions are the reconstructed images of serial sections through the depth of one cell. [A-D] unstretched NP cells; [E-H] 10 minutes; [I-L] 30 minutes; [M-P] 60 minutes. Arrow: the intensive staining of  $\beta$ -tubulin filaments around cell nucleus.

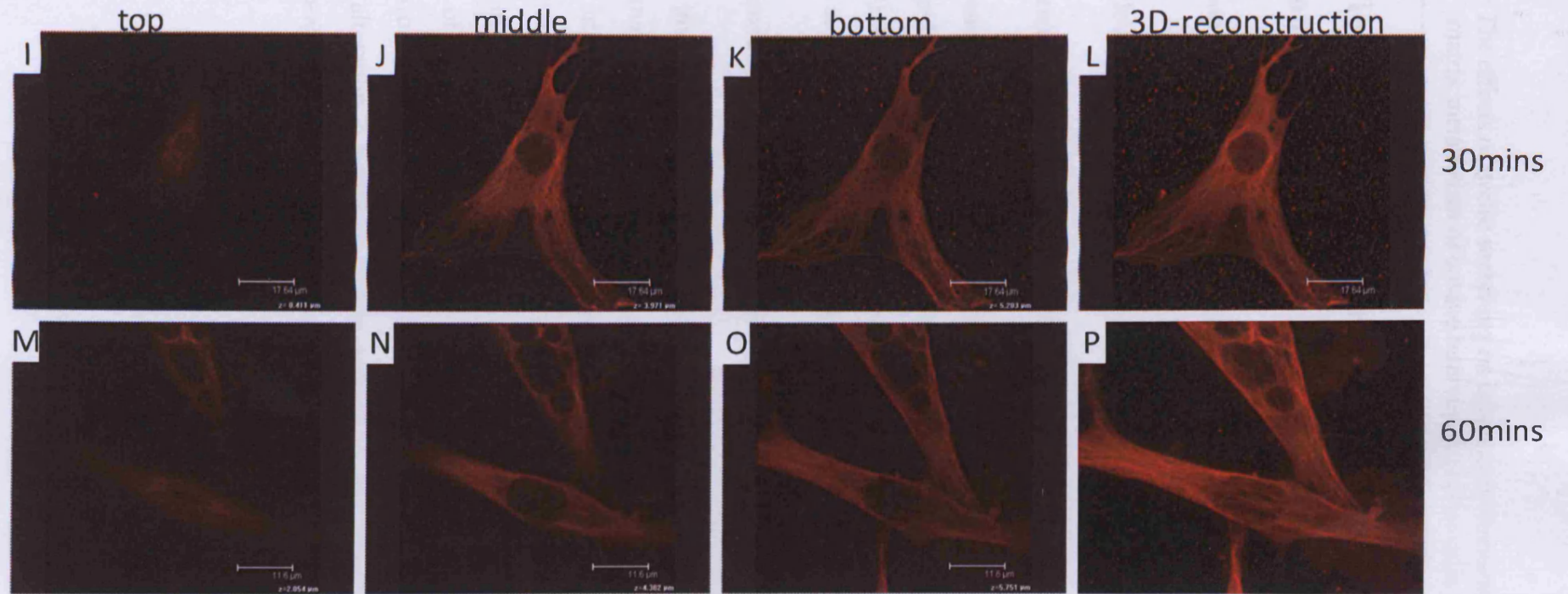
Chapter 3: The effects of cyclic stretching on cytoskeletal elements and extracellular matrix metabolism of bovine intervertebral disc cells *in vitro*

---



Chapter 3: The effects of cyclic stretching on cytoskeletal elements and extracellular matrix metabolism of bovine intervertebral disc cells  
*in vitro*

---



### **3.3.5.2 Tensile strain promoted $\beta$ -tubulin gene and protein expression in OAF cells**

To determine whether the observed differences in  $\beta$ -tubulin architecture in NP and OAF cells were purely organisational or due to altered gene/protein amounts, expression levels of  $\beta$ -tubulin mRNA and protein were quantified.

#### **3.3.5.2.1 Tensile strain promoted $\beta$ -tubulin gene expression in OAF cells**

$\beta$ -tubulin gene expression significantly increased in OAF cells subjected to CTS for 10 (3.8-fold;  $p < 0.0001$ ), 30 (3.8-fold;  $p < 0.0001$ ) or 60 (3.4-fold;  $p < 0.0001$ ) minutes (Figure 3-9). However, there was no significant alteration of  $\beta$ -tubulin gene expression in NP cells subjected to CTS at any of the time points ( $p > 0.05$ ) (Figure 3-9).

#### **3.3.5.2.2 Tensile strain promoted $\beta$ -tubulin protein expression in OAF cells**

To further investigate whether the alteration in  $\beta$ -tubulin gene expression induces a protein change, Western blotting was performed. To remove the error induced by differences in exposure of individual films, unstretched samples at time 0 hour were used as a standard., CTS induced a significant 1.5-fold increase in  $\beta$ -tubulin protein expression in OAF cells (Figure 3-10), and this increase lasted up to 3 hours after application of the strain, and then gradually declined to baseline (Two-way ANOVA plus Bonferroni post test,  $p = 0.0002$ ). Consistent with the gene expression analysis, no significant alteration in  $\beta$ -tubulin protein expression was observed in NP cells after strain (Two-way ANOVA plus Bonferroni post test,  $p = 0.8044$ ).

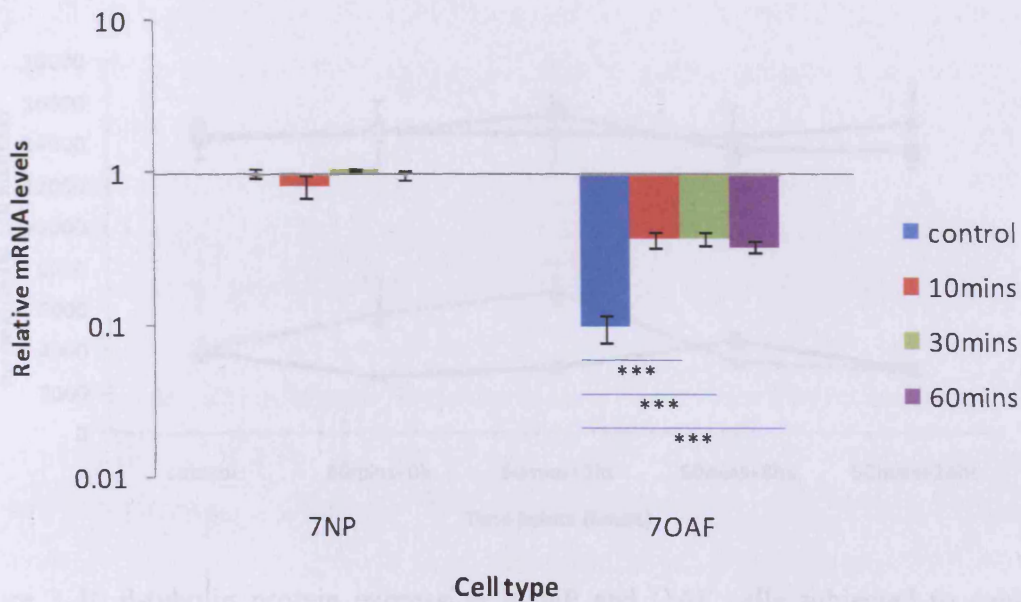


Figure 3-9  $\beta$ -tubulin gene expression in bovine intervertebral disc cells subjected to tensile strain. Cells were cultured on type I collagen as a monolayer and stretched (10% elongation at 1Hz) for 10, 30 or 60 minutes. Unstretched cells were used as a control. Total RNA was then extracted and  $\beta$ -tubulin mRNA levels were determined using real-time PCR. Data were normalised to the house-keeping gene GAPDH and were relative to young NP controls. Data are shown as Mean  $\pm$  S.E.M. (n=5). \*\*\*:  $p \leq 0.001$ .



3.3.6 The effect of tensile force on vimentin filaments

3.3.6.1 Tensile force did not alter the organization of vimentin in IVD cells

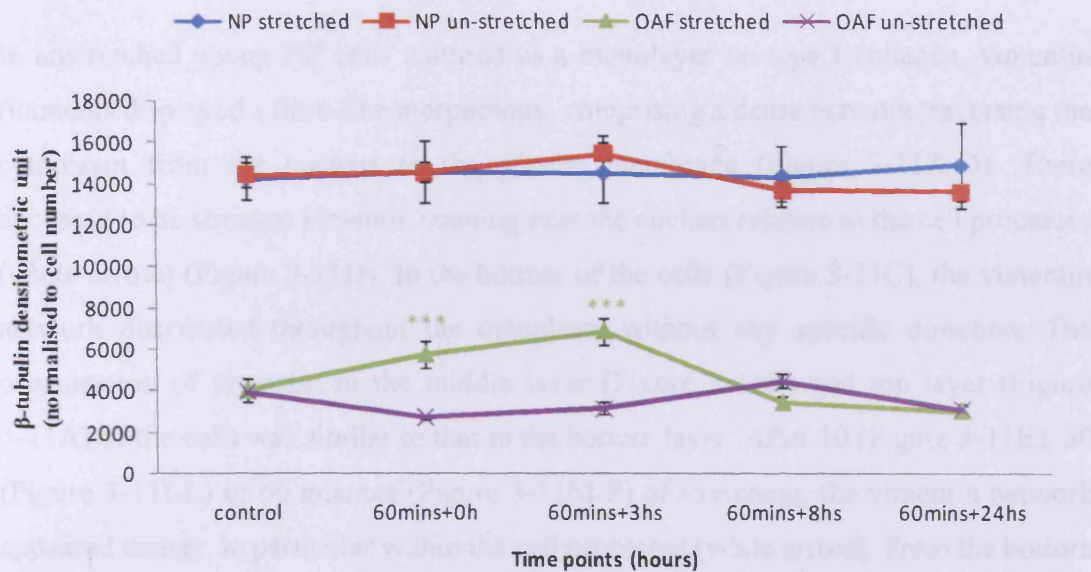


Figure 3-10  $\beta$ -tubulin protein expression in NP and OAF cells subjected to cyclic tensile strain. Bovine NP and OAF cells were cultured on type I collagen and subjected to cyclic tensile strain for 60 minutes followed by culture for a further 0, 3, 8 or 24 hours.  $\beta$ -tubulin protein expression was determined by Western blotting. Samples were normalised to cell number. Unstretched cells were cultured under the same conditions as the stretched samples and used as a control for different time points. To remove the error induced by differences in film exposure, a control sample was used as a standard to normalise the other samples. Data are presented as Mean  $\pm$  S.E.M. (n=5). \*\*\*:  $p \leq 0.001$ .

### **3.3.6 The effect of tensile force on vimentin filaments**

#### **3.3.6.1 Tensile force did not alter the organisation of vimentin in IVD cells**

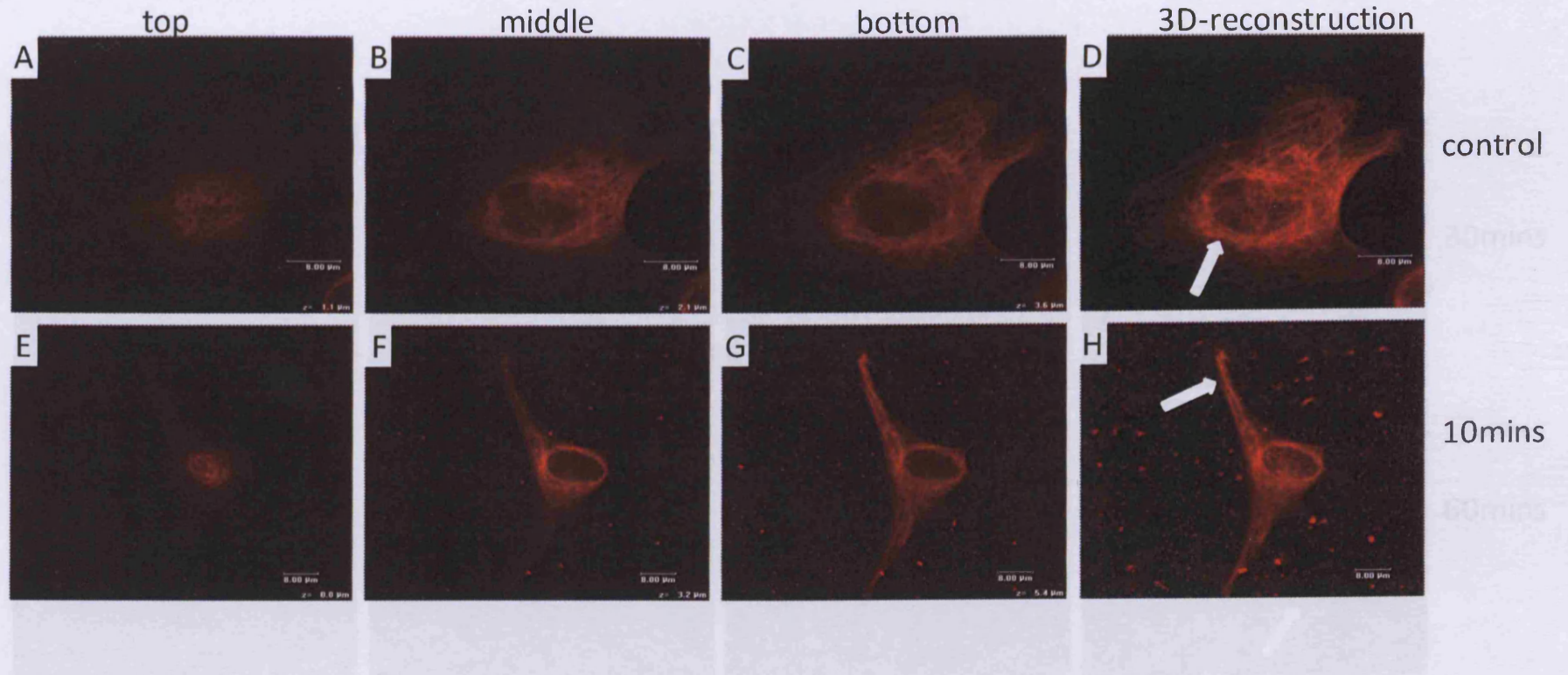
In unstretched young NP cells cultured as a monolayer on type I collagen, vimentin filaments displayed a fibre-like morphology, comprising a dense network traversing the cytoplasm from the nucleus to the plasma membrane (Figure 3-11A-D). There appeared to be stronger vimentin staining near the nucleus relative to the cell processes (white arrow) (Figure 3-11D). In the bottom of the cells (Figure 3-11C), the vimentin network distributed throughout the cytoplasm without any specific direction. The organisation of vimentin in the middle layer (Figure 3-11B) and top layer (Figure 3-11A) of the cells was similar to that in the bottom layer. After 10 (Figure 3-11E), 30 (Figure 3-11I-L) or 60 minutes (Figure 3-11M-P) of stretching, the vimentin network appeared denser, in particular within the cell processes (white arrow). From the bottom to the top of the cell, the organisation of vimentin filaments was similar, without any significant alteration when compared to that of the control cells.

The organisation of vimentin in cells of the young OAF in the absence or presence of stretching is similar to that in the NP as described above (Data not shown).

Figure 3-11. Localisation of vimentin in nucleus pulposus cells cultured on type I collagen as a monolayer. Cells were subjected to cyclic tensile strain (10% elongation, 1Hz) for 10, 30 or 60 minutes; unstretched cells were used as a control. Vimentin was detected using mouse anti-vimentin monoclonal antibody V9 and visualised by incubation with Alexa-633™ conjugated goat anti-mouse secondary antibody. Images are presented at different layers of the cell from top to bottom. 3D reconstructions are the reconstructed images of serial sections through the depth of one cell. [A-D] unstretched NP cells; [E-H] 10 minutes; [I-L] 30 minutes; [M-P] 60 minutes. Arrow: relatively intensive staining of vimentin filaments in cell processes.

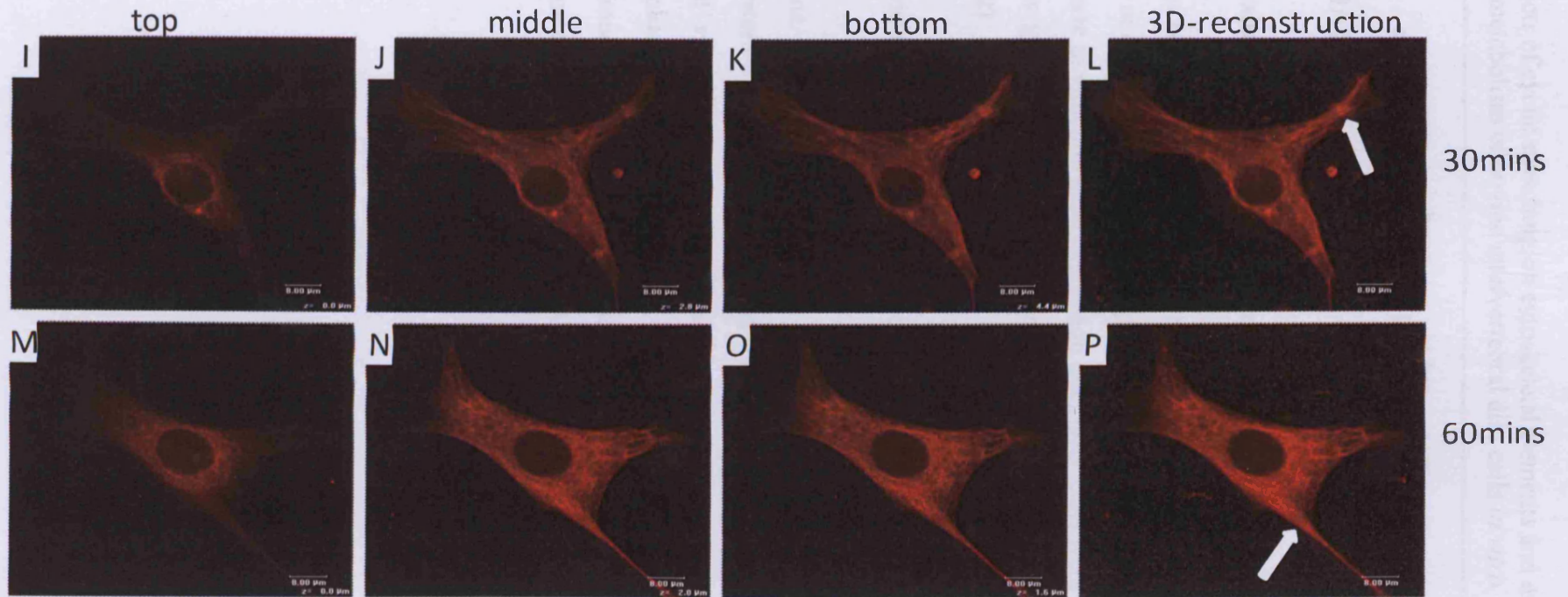
Chapter 3: The effects of cyclic stretching on cytoskeletal elements and extracellular matrix metabolism of bovine intervertebral disc cells  
*in vitro*

---



Chapter 3: The effects of cyclic stretching on cytoskeletal elements and extracellular matrix metabolism of bovine intervertebral disc cells  
*in vitro*

---



### **3.3.6.2 Tensile strain inhibited vimentin gene and protein expression in OAF cells**

#### **3.3.6.2.1 Tensile strain decreased vimentin gene expression in OAF cells**

In contrast to  $\beta$ -actin and  $\beta$ -tubulin, CTS did not change vimentin gene expression in NP cells after 10, 30 or 60 minutes of stretching ( $p>0.05$ ) (Figure 3-12). However, there was a 1.9-fold decrease in vimentin gene expression after OAF cells were subjected to CTS for 60 minutes ( $p<0.01$ ), but no alteration was observed at other time points ( $p>0.05$ ; Figure 3-12).

#### **3.3.6.2.2 Tensile strain inhibited vimentin protein expression in OAF cells**

To further investigate whether the alteration in vimentin gene expression induces a protein change, Western blotting was performed (Figure 3-13). 60 minutes of strain transiently inhibited vimentin protein expression in OAF cells (2-fold decrease; Two-way ANOVA plus Bonferroni post test,  $p=0.0118$ ). After a further 3 hours culture, vimentin levels returned to baseline. CTS did not alter vimentin protein content in NP cells at any of the time points (Two-way ANOVA plus Bonferroni post test,  $p=0.2683$ ).

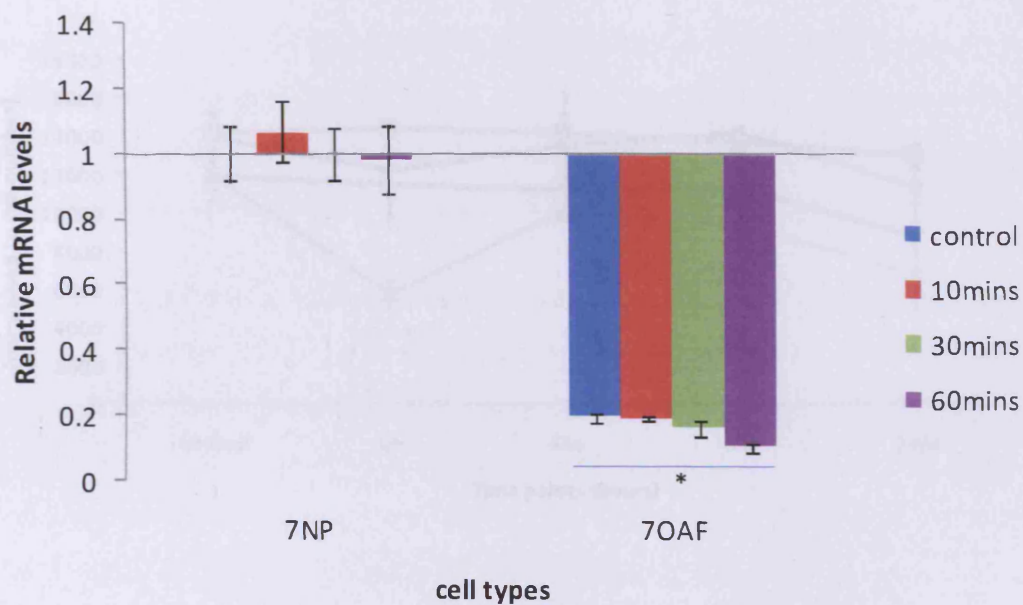


Figure 3-12 Vimentin protein expression in NP and OAF cells subjected to cyclic

Figure 3-12 Vimentin gene expression in bovine intervertebral disc cells subjected to tensile strain. Cells were cultured on type I collagen as a monolayer and stretched with 10% elongation at 1Hz for 10, 30 or 60 minutes. Unstretched cells were used as a control. Total RNA was then extracted and vimentin mRNA levels were determined using real-time PCR. Data were normalised to the house-keeping gene GAPDH and were relative to young NP controls. Data are shown as Mean  $\pm$  S.E.M. (n=5). \*: p<0.05.

### 3.3.7 Effect of CTS on the metabolism of ECM components

To address the metabolic response of (VD) cells to the application of CTS, gene expression levels of types I and II collagen and aggrecan were investigated using real-time PCR.

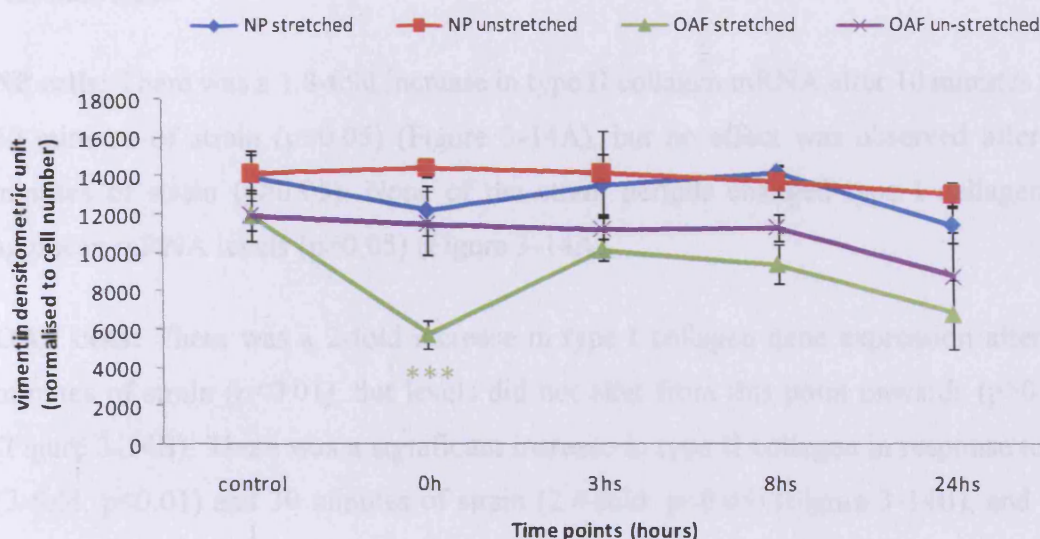


Figure 3-13 Vimentin protein expression in NP and OAF cells subjected to cyclic tensile strain. Bovine NP and OAF cells cultured on type I collagen were subjected to cyclic tensile strain for 60 minutes followed by culture for further 0, 3, 8 or 24 hours. Vimentin protein expression within cells was determined by Western blotting. Samples were normalised to cell number. Unstretched cells were cultured under the same conditions as the stretched samples and used as a control for different time points. To remove the error induced by differences in film exposure, a control sample was used as a standard to normalise the other samples. Data are presented as Mean  $\pm$  S.E.M. (n=4). \*\*\*:  $p \leq 0.001$ .



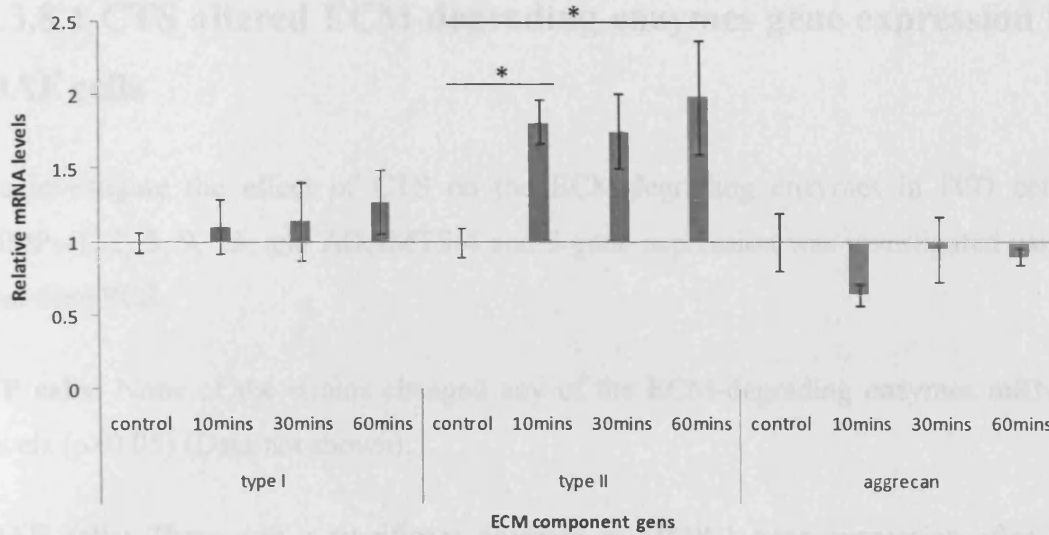
### 3.3.7 Effect of CTS on the metabolism of ECM components

To address the metabolic response of IVD cells to the application of CTS, gene expression levels of types I and II collagen and aggrecan were investigated using real-time PCR.

**NP cells:** There was a 1.8-fold increase in type II collagen mRNA after 10 minutes and 60 minutes of strain ( $p < 0.05$ ) (Figure 3-14A), but no effect was observed after 30 minutes of strain ( $p > 0.05$ ). None of the strain periods changed type I collagen or aggrecan mRNA levels ( $p > 0.05$ ) (Figure 3-14A).

**OAF cells:** There was a 2-fold increase in type I collagen gene expression after 10 minutes of strain ( $p < 0.01$ ), but levels did not alter from this point onwards ( $p > 0.05$ ) (Figure 3-14B). There was a significant increase in type II collagen in response to 10 (3-fold;  $p < 0.01$ ) and 30 minutes of strain (2.4-fold;  $p < 0.05$ ) (Figure 3-14B), and this increase returned to baseline after 60 minutes of strain ( $p > 0.05$ ). None of the strains changed aggrecan mRNA expression ( $p > 0.05$ ) (Figure 3-14B).

(A) NP cells



(B) OAF cells

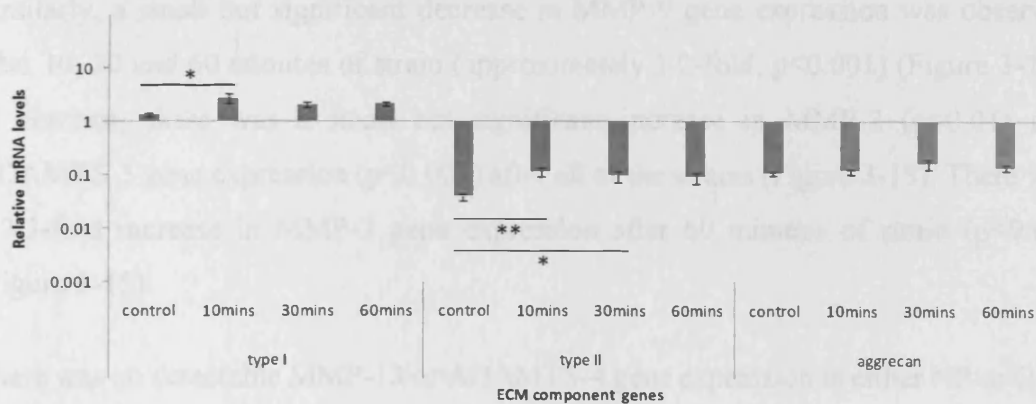


Figure 3-14. ECM component mRNA levels in NP and OAF cells subjected to cyclic tensile strain. Cells were cultured on type I collagen and stretched with 10% elongation at 1Hz for 10, 30 or 60 minutes, and unstretched samples were used as controls. Total RNA was extracted and types I and II collagen and aggrecan mRNA levels were determined using real-time PCR. **A:** NP cells **B:** OAF cells. Data were normalised to the house-keeping gene GAPDH and were relative to NP control cells. Data are shown as Mean  $\pm$  S.E.M. (n=5). \*\*:  $p < 0.01$ , \*:  $p < 0.05$ .

### **3.3.8 Effect of CTS on the metabolism of ECM-degrading enzymes**

#### **3.3.8.1 CTS altered ECM-degrading enzymes gene expression in OAF cells**

To investigate the effect of CTS on the ECM-degrading enzymes in IVD cells, MMPs-1, 2, 3, 9, 13, and ADAMTS-4 and 5 gene expression was investigated using real-time PCR.

**NP cells:** None of the strains changed any of the ECM-degrading enzymes mRNA levels ( $p > 0.05$ ) (Data not shown).

**OAF cells:** There was a significant decrease in MMP-1 gene expression after 10 (3.7-fold), 30 (5.8-fold) and 60 (3.9-fold) minutes of strain ( $p < 0.001$ ) (Figure 3-15). Similarly, a small but significant decrease in MMP-9 gene expression was observed after 10, 30 and 60 minutes of strain (approximately 1.2-fold;  $p < 0.001$ ) (Figure 3-15). In contrast, there was a small but significant increase in MMP-2 ( $p < 0.01$ ) and ADAMTS-5 gene expression ( $p < 0.001$ ) after all of the strains (Figure 3-15). There was a 3.3-fold increase in MMP-3 gene expression after 60 minutes of strain ( $p < 0.05$ ) (Figure 3-15).

There was no detectable MMP-13 or ADAMTS-4 gene expression in either NP or OAF cells.

Chapter 3: The effects of cyclic stretching on cytoskeletal elements and extracellular matrix metabolism of bovine intervertebral disc cells  
*in vitro*

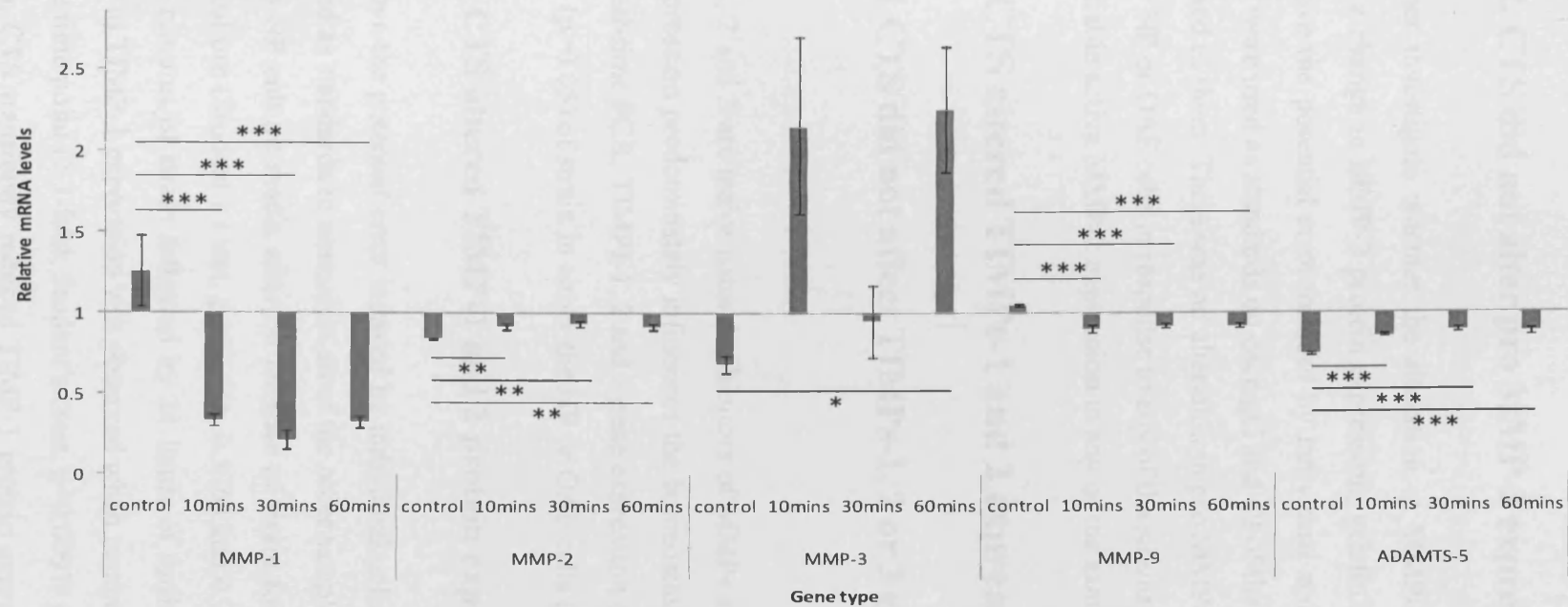


Figure 3-15. ECM-degrading enzymes mRNA levels in NP and OAF cells subjected to cyclic tensile strain. Cells were cultured on type I collagen and stretched with 10% elongation at 1Hz for 10, 30 or 60 minutes, and unstretched samples were used as controls. Total RNA was extracted and MMP-1, 2, 3, 9 and ADAMTS-5 mRNA levels were determined using real-time PCR. Data were normalised to the house-keeping gene GAPDH and were relative to NP control cells. Data are shown as Mean  $\pm$  S.E.M. (n=5). \*\*\*:  $p \leq 0.001$ , \*\*:  $p \leq 0.01$ , \*:  $p \leq 0.05$  when compared with control samples.

### **3.3.8.2. CTS did not alter pro MMP-2 expression in culture media**

To further investigate whether the alteration in MMP-2 gene levels in OAF cells induces a change in MMP-2 protein expression, gelatin zymography was performed. To remove the potential error induced by individual staining of different gels, some samples were used as standards on each gel and all of the unknown samples were then normalised to them. There was no alteration in pro MMP-2 levels in the culture media of either NP or OAF cells in response to any of the strains (Data not shown). There was no detectable active MMP-2 expression in any of the samples.

### **3.3.9 CTS altered TIMPs-1 and 2 expression in IVD cells**

#### **3.3.9.1 CTS did not affect TIMPs-1, 2 or 3 gene expression in IVD cells**

TIMP-1, 2 and 3 are major natural inhibitors of MMPs and aggrecanases *in vivo*, and their expression predominately influences the homeostasis of the ECM in IVD tissue. Using real-time PCR, TIMPs-1, 2 and 3 gene expression did not alter after 10, 30 or 60 minutes ( $p > 0.05$ ) of strain in either the NP or OAF cells (Data not shown).

#### **3.3.9.2 CTS altered TIMP-1 and 2 protein expression in IVD cells**

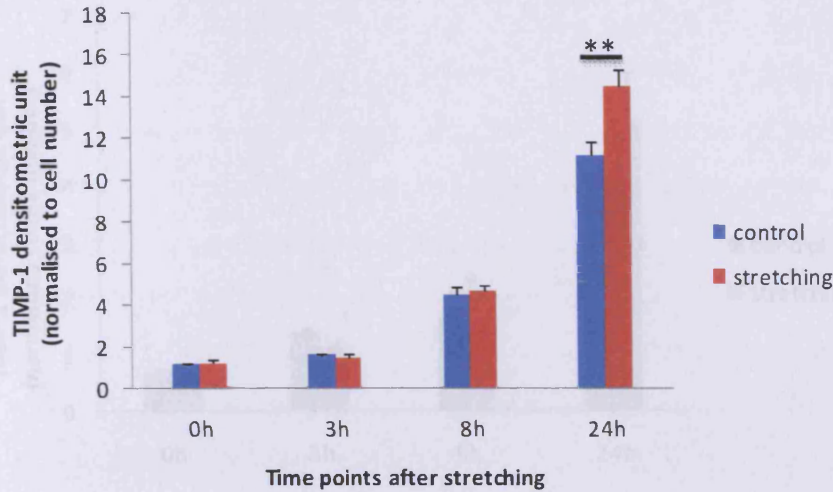
To remove the potential error induced by individual gel staining, unstretched samples were used as standards to normalise all of the other samples. CTS did not alter TIMP-1 levels in NP culture media after 60 minutes of strain followed by 0, 3 or 8 hours of further culture (Student's t test,  $p = 0.7441$ ,  $0.5765$  and  $0.7846$  respectively). However, after 60 minutes of strain followed by 24 hours of further culture, a stretch-induced increase in TIMP-1 expression was observed when compared with the control group at the same time point (1.3-fold; Student's t test,  $p = 0.0097$ ) (Figure 3-16A). In contrast to NP cells, CTS transiently reduced TIMP-1 protein expression in culture media from OAF cells subjected to 60 minutes of strain followed by 3 (1.8-fold; Student t test,  $p = 0.0040$ ) and 8 hours (1.6-fold; Student t test,  $p = 0.0002$ ) of further culture when compared with the control group at the same time points. However, after 24 hours of

further culture, there was no significant difference in TIMP-1 content between the control and strain group (Student's t test,  $p=0.7443$ ) (Figure 3-16B).

### **3.3.9.3 CTS inhibited TIMP-2 protein expression in IVD cells**

CTS did not alter TIMP-2 expression in culture media of either NP (Student's t test,  $p=0.5795$  and  $0.0910$  respectively) or OAF cells (Student's t test,  $p=0.4199$ ,  $0.2302$  respectively) subjected to 60 minutes of strain followed by 0 or 3 hours of further culture. However, after 8 hours of further culture, a decrease in TIMP-2 expression was observed in NP (1.3-fold; Student's t test,  $p=0.0328$ ) and OAF cells (1.8-fold; Student's t test,  $p=0.001$ ) when compared with the control group at the same time point (Figure 3-17). After 24 hours of recovery, the transient decrease in TIMP-2 recovered to the same level as that in the control group in both NP and OAF cells (Student t test,  $p=0.2932$  and  $0.1511$  respectively) (Figure 3-17). There was no detectable TIMP-3 in culture media from either NP or OAF cells.

(A) NP cells



(B) OAF cells

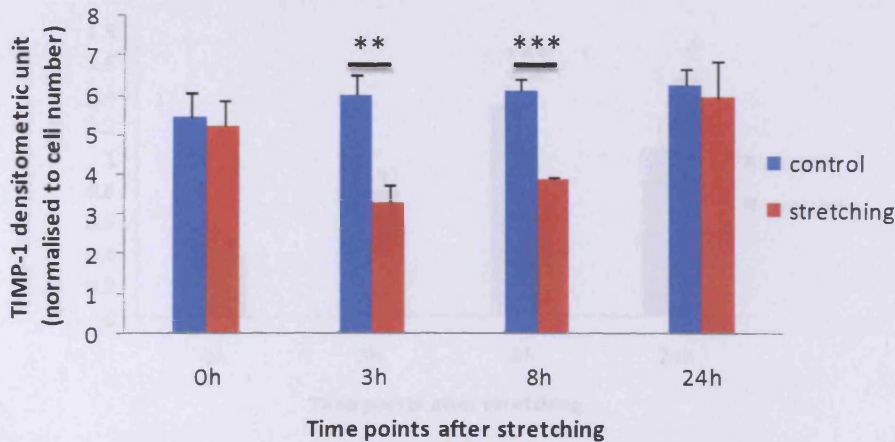
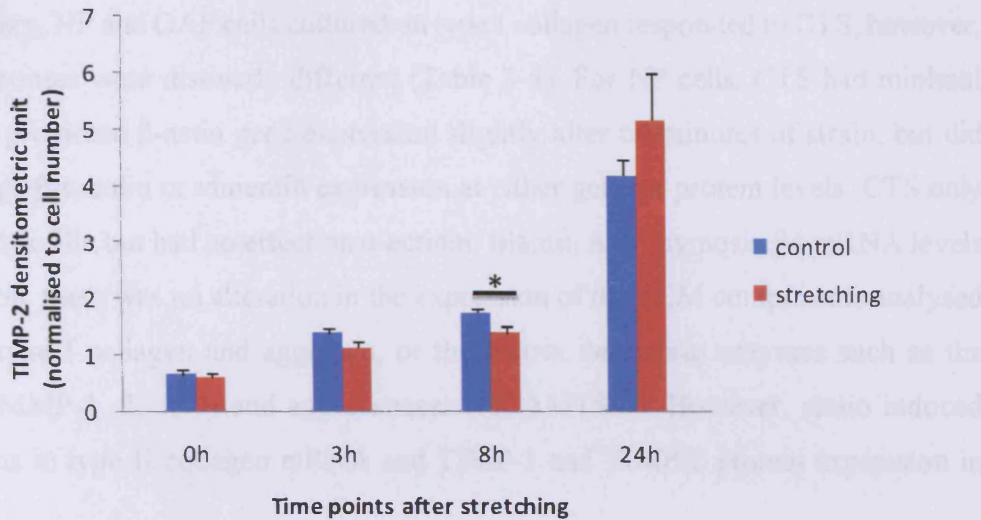


Figure 3-16. TIMP-1 levels in NP and OAF cells. Bovine (A) NP and (B) OAF cells cultured on type I collagen were subjected to cyclic tensile strain for 60 minutes followed by culture for a further 0, 3, 8 or 24 hours. TIMP-1 levels in culture media were determined using reverse gelatin zymography. Samples were normalised to cell number. To remove the potential error induced by the various staining on different gels, unstretched samples on individual gels were used as standards to normalise all of the other samples. Data are presented as Mean  $\pm$  S.E.M. (n=5). \*\*\*:  $p \leq 0.001$ , \*\*:  $p \leq 0.01$  when compared with control group under the same time point.

(A) NP cells



(B) OAF cells

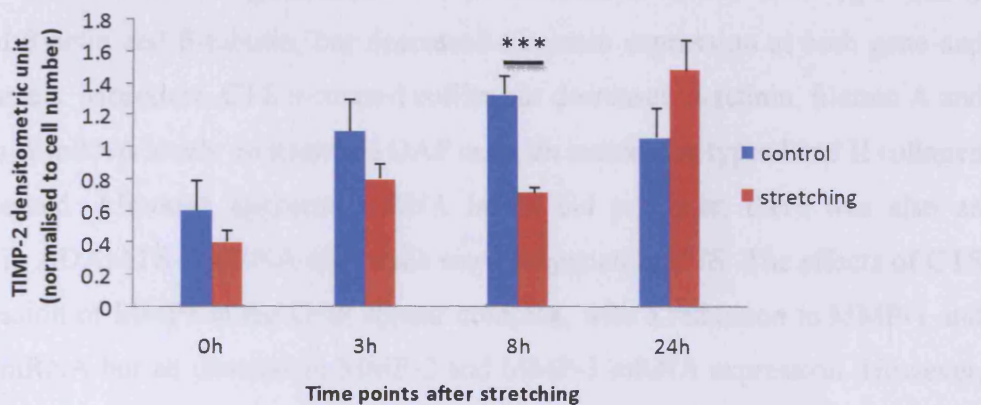


Figure 3-17 TIMP-2 levels in NP and OAF cells. Bovine (A) NP and (B) OAF cells cultured on type I collagen were subjected to cyclic tensile strain for 60 minutes followed by culture for a further 0, 3, 8 or 24 hours. TIMP-2 levels in culture media were determined using reverse gelatin zymography. Samples were normalised to cell number. To remove the potential error induced by the various staining on different gels, unstretched samples on individual gels were used as standards to normalise all of the other samples. Data are presented as Mean  $\pm$  S.E.M. (n=5). \*\*\*:  $p \leq 0.001$ , \*:  $p \leq 0.05$  when compared with control group under the same time point.



### 3.3.10 Summary

In summary, NP and OAF cells cultured on type I collagen responded to CTS, however, their responses were distinctly different (Table 3-4). For NP cells, CTS had minimal effect; it promoted  $\beta$ -actin gene expression slightly after 60 minutes of strain, but did not change  $\beta$ -tubulin or vimentin expression at either gene or protein levels. CTS only increased cofilin but had no effect on  $\alpha$ -actinin, filamin A or thymosin  $\beta$ 4 mRNA levels. In addition, there was no alteration in the expression of the ECM components analysed such as type I collagen and aggrecan, or the matrix degrading enzymes such as the MMPs (MMP-1, 2, 3, 9) and aggrecanases (ADAMTS-5). However, strain induced alterations in type II collagen mRNA and TIMP-1 and TIMP-2 protein expression in NP cells.

In contrast to NP cells, OAF cells responded to CTS more actively (Table 3-4). Besides the alteration in F-actin organisation after 60 minutes of strain, CTS significantly increased  $\beta$ -actin and  $\beta$ -tubulin, but decreased vimentin expression at both gene and protein levels. Moreover, CTS increased cofilin but decreased  $\alpha$ -actinin, filamin A and thymosin A mRNA levels. In stretched OAF cells, an increase in types I and II collagen was observed. Although aggrecan mRNA levels did not alter, there was also an increase in ADAMTS-5 mRNA after cells were subjected to CTS. The effects of CTS on expression of MMPs in the OAF appear complex, with a reduction in MMP-1 and MMP-9 mRNA but an increase in MMP-2 and MMP-3 mRNA expression. However, there was no alteration in pro MMP-2 protein levels after stretching. In addition, TIMP-1 and TIMP-2 released into the culture media were inhibited when compared with the control groups although neither TIMP-1 nor TIMP-2 mRNA expression was altered by CTS.

**Table 3-4. The effects of CTS (10% elongation, 1Hz) on bovine IVD cells.**

		NP	OAF
<b>β-actin</b>	mRNA	↑	↑
	protein	↔	↑
<b>α-actinin</b>	mRNA	↔	↓
<b>cofilin</b>	mRNA	↑	↑
<b>filamin A</b>	mRNA	↔	↓
<b>Thymosin β4</b>	mRNA	↔	↓
<b>β-tubulin</b>	mRNA	↔	↑
	protein	↔	↑
<b>vimentin</b>	mRNA	↔	↓
	protein	↔	↓
<b>type I collagen</b>	mRNA	↔	↑
<b>type II collagen</b>	mRNA	↑	↑
<b>aggrecan</b>	mRNA	↔	↔
<b>ADAMTS-4</b>	mRNA	N.D.	N.D.
<b>ADAMTS-5</b>	mRNA	↔	↑
<b>MMP-1</b>	mRNA	↔	↓
<b>MMP-2</b>	mRNA	↔	↑
	protein	↔	↔
<b>MMP-3</b>	mRNA	↔	↑
<b>MMP-9</b>	mRNA	↔	↓
	protein	N.D.	N.D.
<b>MMP-13</b>	mRNA	N.D.	N.D.
<b>TIMP-1</b>	mRNA	↔	↔
	protein	↑	↓
<b>TIMP-2</b>	mRNA	↔	↔
	protein	↓	↓
<b>TIMP-3</b>	mRNA	↔	↔
	protein	N.D.	N.D.

(N.D.= not detected)

## 3.4 Discussion

The cell morphology and phenotypes of NP and OAF cells *in vivo* are quite different. NP cells are chondrocyte-like, displaying a round or elliptical morphology and mainly synthesise type II collagen and aggrecan. In contrast, OAF cells are elongated with cell processes, and predominately produce type I collagen (Colombini et al., 2008). In this study, both NP and OAF cells were cultured as a monolayer on type I collagen, which significantly changes the cellular morphology when compared with that *in vivo*. To assess the cell phenotypes, especially for NP cells, mRNA levels of types I and II collagen as well as aggrecan were investigated using real-time PCR. Greater levels of type II collagen and aggrecan mRNA were observed in NP cells when compared with OAF cells. In contrast, more type I collagen gene expression was observed in OAF cells. These results illustrate that both NP and OAF cells maintained their basic cell phenotypes, although there are some alterations in cellular morphologies during the monolayer culture.

### 3.4.1 Effect of CTS on the cytoskeletal elements in NP and OAF cells

In the mechanical stimulation experiments, 10% elongation was applied at a frequency of 1Hz (0.5 second elongation, followed by 0.5 second relaxation), as it has previously been shown that the intervertebral discs are subjected to a strain of between 1 and 13% (Broberg, 1983; Klein et al., 1983; Ebara et al., 1996; Rannou et al., 2003), and 1Hz corresponds to a walking frequency (Rannou et al., 2003).

In chondrocytes, the F-actin network lies primarily at the cell cortex, and is regarded as a structural link from the cell surface to the nucleus (Durrant et al., 1999). Recent studies performed in cartilage suggested that the actin filament is implicated in transducing signals between the ECM and cell nucleus *in vivo* - “mechanotransduction” (Guilak, 1995; Blain et al., 2003). In addition, it was found that dynamic tensile force significantly altered actin filament organisation in chondrocytes (Iscru et al., 2008),

suggesting CTS plays an important role in chondrocyte mechanotransduction. Due to the similar mechanical environment and ECM composition of articular cartilage and intervertebral disc, especially in the NP region, it is reasonable to hypothesise that CTS regulates the organisation and expression of actin filaments in intervertebral disc cells, and the results presented in this chapter confirm this hypothesis.

The confocal results indicate that stretching can significantly change the architecture of F-actin in both NP and OAF cells cultured on type I collagen. The distribution of F-actin filaments on the top of the cell, in the absence of stretch, is punctate, with some thin fibres distributed between the dots. There are two possibilities for the staining. The first is that the F-actin is indeed punctate, just like the staining from the intervertebral disc cells *in situ* (Chapter 2). Another possibility is that the F-actin is still fibre-like, but being viewed end-on. However, using 3D reconstruction technology, we found that the F-actin staining in the top of the cytoplasm of monolayer intervertebral disc cells cultured on type I collagen is indeed punctate. Further actin-binding protein real-time results indicated that there was a tensile-induced increase in cofilin mRNA, but a decrease in  $\alpha$ -actinin, filamin A and thymosin  $\beta$ 4 gene expression. Cofilin can sever actin filaments to provide free barbed ends for actin polymerisation and nucleation (Ichetovkin et al., 2002). In contrast, thymosin  $\beta$ 4 holds ATP-bound G-actin in a form that is unable to polymerise, therefore the decreased thymosin  $\beta$ 4 gene expression generates more ATP-bound G-actin for polymerisation (Atkinson et al., 2004).  $\alpha$ -actinin and filament can also inhibit actin assembly. Taken together, tensile force will promote the rate of actin turnover and form more stress fibres to increase cell contractility to adapt the tensile strain applied.

In the bottom and middle layer of unstretched cells, F-actin filaments are fibre-like, localising close to the cell membrane. This may be induced by contractile forces generated when cells spread along the surface of the substratum, suggesting a close relationship between F-actin organisation and tensile force. After stretching, especially 60 minutes of strain, a large amount of stress fibre formation was observed, and the F-actin staining in the top of the cells changed from a punctate to primarily a fibre-like morphology. These results are similar to a study performed on chondrocytes (Iscru et al., 2008), suggesting that CTS can remodel F-actin organisation in both NP and OAF

cells and may thereby be involved in mechanotransduction. Moreover, this stretch-induced F-actin reorganisation is time-dependent, as there was more stress fibre formation after 60 minutes of strain when compared to that after 10 or 30 minutes of strain.

In order to address whether the alteration in F-actin architecture is induced by gene or protein expression,  $\beta$ -actin mRNA and protein levels in NP and OAF cells subjected to CTS were investigated. As expected, increased  $\beta$ -actin gene and protein expression were found in OAF cells, whereas only a slight increase in  $\beta$ -actin mRNA in NP cells was observed. Previous studies have shown that there are different mechanical features in the different regions of the intervertebral disc; the main function of the NP is to resist compressive loading whereas the OAF mainly resist tensional force *in vivo* (Klein et al., 1983). Therefore, it is not surprising that even 10 minutes of stretching promoted  $\beta$ -actin gene expression in OAF cells. However, there was no alteration in  $\beta$ -actin mRNA levels in NP cells until 60 minutes of strain, suggesting that OAF cells respond more actively than NP cells. Considering the different mechanical environment *in vivo*, this difference may illustrate the close relationship between actin filaments and tensile force. However, another possible explanation that should not be ignored is the potential alteration of cell phenotype. To use the Flexcell system, both NP and OAF cells were cultured as a monolayer on type I collagen. Although expression levels of types I and II collagen as well as aggrecan mRNA indicated that the NP cells have a similar phenotype as *in vivo*, there were some changes in cell morphology. Real-time PCR results indicated that there was more type I collagen gene expression in NP cells when compared with the type II collagen and aggrecan gene expression, indicating that the NP cells were undergoing differentiation. Therefore, an *in vivo* loading study or stretching cells in a 3D-culture system would be a more favourable model (See Chapter 5).

In contrast to F-actin which was mainly distributed beneath the cell periphery,  $\beta$ -tubulin filaments were predominately localised near the cell nucleus, and radiated throughout the whole cytoplasm, thereby appearing as a 'ring' around the cell nucleus. This result is similar to a prior study, in which microtubules have been shown to radiate from the centrosome with their plus-ends directed towards the plasma membrane

(Etienne-Manneville, 2004). The distinct distributions between actin filaments and microtubules within cells illustrates that they have different biomechanical functions. It is well known that the microtubule network mainly provides a transport system for organelle and protein movement within the cytoplasm (Musch, 2004), and contributes to cell migration in a cell type-dependent manner (Etienne-Manneville, 2004), consistent with the peri-nuclear localisation of  $\beta$ -tubulin filaments in this study.

After stretching, there was a significant decrease or disappearance of the '  $\beta$ -tubulin ring' around the cell nucleus when compared with the unstretched cells, suggesting that cyclic tensile force may induce a redistribution or inhibition of  $\beta$ -tubulin filament organisation. It was also found that  $\beta$ -tubulin filaments were arranged in parallel, with extensions towards the leading edges of the cell. This alteration is likely caused by the changes in cell shape, from a rounded cell body with random cellular processes to spindle-like with bipolar protrusions and a flattened cell body. All of these changes suggest that CTS indeed regulates the architecture of  $\beta$ -tubulin filaments in disc cells, therefore  $\beta$ -tubulin is likely to be involved in mechanotransduction, as has been reported in studies performed on fibroblasts (Putnam et al., 2001; D'Addario et al., 2003; Zeiger and Layton, 2008). To further investigate the relationship between  $\beta$ -tubulin and CTS, gene and protein expression were investigated, and it was found that CTS significantly promoted  $\beta$ -tubulin mRNA and protein expression in OAF cells. This indicated that the decreased staining of  $\beta$ -tubulin filaments around the cell nucleus was caused by a redistribution and not the inhibition of  $\beta$ -tubulin synthesis. A previous study performed on fibroblasts suggests that tensile force-induced expression of filamin A is dependent on the microtubule network (D'Addario et al., 2003). Filamin A is an actin-binding protein and contributes to the remodelling of actin filaments induced by tensile force (D'Addario et al., 2002). Therefore, the redistribution and increased synthesis of  $\beta$ -tubulin in response to CTS may aid the remodelling of the actin filaments during mechanotransduction.

Unlike the architecture of F-actin and  $\beta$ -tubulin in IVD cells, vimentin filaments are distributed throughout the cytoplasm as a dense network from the cell processes to the nucleus. More importantly, the architecture of vimentin through the whole depth of the cell is similar. There was no alteration in the organisation of vimentin after strain,

illustrating that vimentin filaments are not sensitive to tensile force in the IVD. This deduction has been confirmed by a previous study performed in vimentin knockout mice. In both *in vivo* and *in vitro* experiments, it was found that lack of vimentin significantly inhibited the response of mesenteric resistance arteries to shear stress, but not tensile force, suggesting vimentin is not sensitive to tensile stimulation (Henrion et al., 1997). To further confirm this deduction, vimentin gene and protein expression were investigated, and there was only a transient decline in both after strain. Previous studies have shown that the main function of vimentin in cells is to act as a cell filler by cross-linking with actin and tubulin, to give the cell its shape and elastic properties to resist mechanical forces (Galou et al., 1997; Pekny and Lane, 2007). Therefore, vimentin should alter when the cell volume changes. This may explain the transient decline in vimentin gene and protein expression after 60 minutes of strain.

Compared with OAF cells, cytoskeletal elements within NP cells seldom responded to CTS, except for  $\beta$ -actin gene expression. The main mechanical stimulus NP cells experience *in vivo* is compressive loading, therefore, it is reasonable for NP cells to respond slowly when CTS is applied. In addition, the fact that only  $\beta$ -actin responds to CTS in NP cells further indicates that actin filaments are the main cytoskeletal element that endures tensile force within cells.

### 3.4.2 Effect of CTS on ECM synthesis

The effects of CTS on cell metabolism was also investigated, and CTS increased types I and II collagen gene expression, especially in OAF cells, which is consistent with previous studies (Matsumoto et al., 1999; Rannou et al., 2003; Benallaoua et al., 2006), suggesting that CTS promotes collagen synthesis in disc cells. However, the observation of unaltered aggrecan mRNA levels after strain differs to prior studies (Matsumoto et al., 1999; Rannou et al., 2003; Benallaoua et al., 2006), in which tensile force was shown to inhibit aggrecan expression. The differences between these studies are the animal model, the magnitude and frequency of the strain, and the length of time the cells were exposed to the tensile force. For example, a very recent study performed on rat OAF cells indicated that tensile force alone (6% stress at 0.05 Hz ) did not change

the metabolism of ECM components (Sowa and Agarwal, 2008), which is consistent with the aggrecan result in this study.

### **3.4.3 Effect of CTS on ECM remodelling proteases and inhibitors**

Aggrecanases (ADAMTS-4 and 5), MMPs (MMP-1, MMP-2, MMP-3, MMP-9, MMP-13) and their natural inhibitors TIMPs (TIMP-1, 2 and 3) were also investigated. There was little alteration in these ECM-related enzymes when NP cells were subjected to CTS, whereas OAF cells responded to tensile strain more actively. However, there was no uniform trend for the changes of these enzymes in OAF cells, with some of them increasing (such as MMP-2, MMP-3 and ADAMTS-5) and some of them decreasing (MMP-1, MMP-9, TIMP-1 and TIMP-2).

MMP-1 is a collagenase, and its main function is to degrade fibrillar collagen such as type I collagen which is most abundant in the OAF of IVD *in vivo*. However, the precise role of MMP-1 during the process of mechanically-induced ECM remodelling is largely unknown. Previous studies have shown that CTS (6% elongation at 0.05Hz) abrogated IL-1 induced MMP-1 expression in fibrochondrocytes, suggesting physiological CTS may have an “anti-catabolic” effect (Agarwal et al., 2001). When OAF cells are subjected to physiological tensile strain, type I collagen is the main component in the ECM to resist this mechanical stimulation. A decline in MMP-1 could result in decreased degradation of type I collagen and strengthen the integrity of the ECM, which is valuable for IVD functions. The decreased MMP-1 expression in OAF cells subjected to CTS observed in this study is consistent with a previous study (Agarwal et al., 2001).

MMP-3 is highly expressed in intervertebral disc. It can cleave many ECM molecules such as basement membrane components, fibronectin, laminin, and proteoglycan core protein (Suzuki et al., 1990). It is believed to be involved in the activation of other MMPs such as MMP-1 (Murphy et al., 1987), and plays an important role in disc degeneration (Haro et al., 2000). However, the requirement of MMP-3 in cartilage



formation (Pelttari et al., 2008) and the fact that the absence of MMP-3 in cells could neither prevent nor reduce cartilage destruction (Mudgett et al., 1998) illustrates that MMP-3 is not only responsible for ECM degradation, but also contributes to the turnover of the ECM and tissue homeostasis. Therefore, the increased MMP-3 mRNA expression in response to CTS demonstrates that mechanical stimulation can induce a significant ECM remodelling process. Due to the multiple functions of MMP-3 in the turnover of the ECM, this would be expected to increase overall MMP activity, as well as activate other MMP proteins, thereby promoting ECM remodelling.

MMP-2 and MMP-9 are members of the gelatinase family, and their main function is to degrade type IV collagen and gelatin, the product of collagen degradation after proteolysis by collagenases (Raffetto and Khalil, 2008). Previous studies have indicated an increase in MMP-2 and MMP-9 in degenerative disc tissue (Crean et al., 1997; Weiler et al., 2002), suggesting their gelatinolytic activity in disc degradation. Due to the main functions of the spine, it is assumed that mechanical stimulation regulates the expression of these enzymes, and this assumption is supported by the studies performed in muscle and periodontal ligament (Brown and Hudlicka, 2003; Cantarella et al., 2006). In OAF cells the tensile force promoted MMP-2 but suppressed MMP-9 expression, but there was no alteration in these two enzymes in NP cells subjected to CTS.

It is well known that there are two different MMP-2 isoforms *in vivo*, an inactive pro-enzyme pro-MMP-2 (72KDa) and an active MMP-2 (68/66KDa) (Shelton and Rada, 2007). After secretion, proMMP-2 is assumed to be bound to its specific inhibitor, TIMP-2, to complete the whole activation process. However, TIMP-2 is also the natural inhibitor of active MMP-2. Therefore, the ratio between MMP-2 and TIMP-2 may influence MMP-2 activation, and regulate the activity of MMP-2. In this study, there was a decline in TIMP-2 expression after OAF cells were subjected to strain. Considering the increased MMP-2 expression at the same time, there are two possibilities one can speculate on. The first is that the amount of TIMP-2 is enough to activate MMP-2, therefore the decline in TIMP-2 would decrease its inhibitory effect for all MMPs. Alternatively, the amount of TIMP-2 may be at a level insufficient to activate MMP-2, therefore the decline in TIMP-2 would abrogate MMP-2 activation,

thereby inducing “anti-catabolism” in cells. Considering the consistent expression of TIMP-2 in many cells including IVD (Chakrabarti and Patel, 2005), it is unusual for very low TIMP-2 expression in cells, therefore the first assumption is preferred, although active MMP-2 was not detected in culture media due to the short cell culture time before the analysis.

In contrast to MMP-2, CTS suppressed the expression of MMP-9 in OAF cells, suggesting that physiological CTS has a distinct effect on the metabolism of these two gelatinases. Due to the differences in the promoter regions of their respective genes, distinct expression profiles exist between MMP-2 and MMP-9. MMP-2 is produced constitutively and by a wide range of cell types, whereas constitutive MMP-9 is restricted to neutrophils (Devarajan et al., 1992) and eosinophils (Schwingshackl et al., 1999). However, an inflammatory stimulus can lead to increased MMP-9 expression in many cell types including IVD cells (Nagase and Woessner, 1999), suggesting that MMP-9 can be regarded as a ‘pathological gelatinase’. Therefore, the decline in MMP-9 in this study suggests that physiological CTS promoted ECM anabolism in the OAF cells. Interestingly, there was a corresponding suppression of TIMP-1 in OAF cells after strain. TIMP-1 has a similar structure but a different physiological substrate to TIMP-2. TIMP-1 preferentially inhibits MMP-9, whereas TIMP-2 inhibits MMP-2 (Chakrabarti and Patel, 2005).

In summary, the results in this chapter indicate that physiological CTS inhibits the expression of degradative enzymes such as MMP-1 and MMP-9, whilst it simultaneously increases the expression of other enzymes such as MMP-2 and MMP-3. Overall, it appears that there is enhanced ECM remodelling in OAF cells subjected to physiological CTS with less catabolism but unchanged or increased anabolism.

### 3.5 Conclusion

- NP and OAF cells retain their respective phenotype in monolayer culture.
- Intervertebral disc cells cultured as a monolayer on type I collagen can respond to physiological tensile strain.
- OAF cells are more responsive to tensile strain than NP cells, which corresponds to their distinct mechanical environment *in vivo*.
- Physiological cyclic tensile strain induces an alteration in F-actin and  $\beta$ -tubulin filament organisation, and regulates mRNA and protein expression of cytoskeletal components including  $\beta$ -actin,  $\beta$ -tubulin and vimentin, suggesting that the cytoskeleton is involved in OAF cell mechanotransduction.
- CTS promotes cofilin but inhibit  $\alpha$ -actinin, filamin A and thymosin  $\beta$ 4 gene expression in OAF cells, suggesting a tensile-induced actin polymerisation.
- Physiological cyclic tensile strain changes the expression of some ECM-related enzymes, illustrating enhanced ECM remodelling in OAF cells.

# CHAPTER 4.

The effect of different cyclic tensile strain  
on cytoskeletal elements and extracellular  
matrix metabolism in bovine intervertebral  
disc cells *in vitro*

## 4.1 Background

Different mechanical stimuli including compressive loading, tensile force, shear force and osmotic pressure are found in the intervertebral disc *in vivo* (Meir et al., 2008). Due to the distinct composition and localisation of the nucleus pulposus (NP) and outer annulus fibrosus (OAF) *in vivo*, it is believed that the NP mainly resists compressive loading whereas the OAF primarily endures tensile force (Leone et al., 2007). However, the distribution of tensile force within IVD is uneven. From the outer shell to the centre of the IVD, there is a linear decline in tensile force between the OAF and NP (Zhu et al., 2006). Due to the higher magnitude of tensile moduli, there is a higher tensile force applied on the anterior annulus when compared with the posterolateral annulus (Skaggs et al., 1994; Ebara et al., 1996; O'Connell et al., 2007; Meir et al., 2008).

Further studies found that single OAF lamellae can endure up to 1-3MPa stress or 10-25% strain (Ebara et al., 1996). Very recently, O'Connell et al determined the internal deformations and strains in human spine motion sections using MRI and found that the peak radial strain applied on the OAF was 1-19% when the sections were subjected to a compressive load of 1000 N (O'Connell et al., 2007). However, some evidence indicates that the ultimate tensile force is generated by a combination of axial rotation with lateral bending and axial rotation with flexion, which would induce 10-25% strain on the annulus fibres (Schmidt H et al., 2007). Therefore, it seems that the highest magnitude of tensile strain applied on the OAF *in situ* is 25%. However, the distribution of the strain on different parts of the IVD *in vivo* is variable, and different magnitudes of strain may play distinct roles in ECM remodelling and tissue homeostasis.

Disc degeneration is an age-related disease. Cell metabolism and ECM components of the IVD change with age. As a consequence, the mechanical modulus of collagen fibres and the distribution of stress will also alter. For example, Horst and Brinckmann reported that axial stresses on the endplate are non-uniform and asymmetric during eccentric loading of the motion segment and appeared to increase with age-related degradation (Horst and Brinckmann, 1981). Degenerative discs have a weaker radial tensile modulus, with a 20-30% decrease in the magnitude of stress and strain in grade

II annulus fibrosus (Fujita et al., 1997). The tensile modulus along the circumferential direction of the annulus fibrosus was also found to decrease with age and degeneration (Acaroglu et al., 1995). All of these alterations in the tensile modulus in the annulus fibrosus will dramatically change the distribution of tensile forces applied on the disc *in vivo*, subsequently inducing disc degeneration. However, the difference in response of young and mature IVD cells to tensile stimulation (including physiological and pathological strain) is still largely unknown.

This chapter describes experiments to investigate the effects of different magnitudes of cyclic tensile strain (CTS) on cytoskeletal element composition and ECM metabolism in young and mature IVD disc cells (NP and OAF), in an attempt to understand the role of tensile force during age-related disc degeneration.

## **4.2 Materials and Methods**

All chemicals were obtained from Sigma (Poole, UK) unless otherwise stated and were of analytical grade or above.

### **4.2.1 Cell isolation and cell culture**

Bovine tails were obtained from 7 day and 18 month old steers (Section 2.2.1), and cell isolation and culture procedures were conducted as described previously (Section 3.2.1).

### **4.2.2 Application of cyclic tensile strain**

Cells were cultured in DMEM/F12 (1:1) containing insulin-transferrin-sodium selenite (ITS) plus 1% penicillin-streptomycin and fungizone at 37°C in a humidified atmosphere of 5% CO<sub>2</sub> for approximately 4 days before cells reached confluence. NP and OAF cells were subjected to 5%, 10% and 15% cyclic tensile strain (CTS) for 60 minutes at 1Hz on the Flexcell FX-3000 system (Flexcell International Corp, Hillsborough, NC). As a control, cells were cultured equivalently in all steps, except that no CTS was applied.

After mechanical stimulation, cells were lysed immediately in Trizol reagent (Invitrogen, Paisley, UK) and stored at -80°C for RNA extraction, or were fixed immediately with 4% paraformaldehyde at room temperature followed by immunofluorescent staining and scanning confocal microscopy. Cells were also lysed in 0.9% Triton X-100 solution containing protease inhibitors and stored at -20°C along with the culture media until analysed by Western blotting and gelatin zymography respectively.

### **4.2.3 Analysis of cytoskeletal element organisation using confocal microscopy**

The reagents and procedures for immunostaining and scanning confocal microscopy were as described previously (Section 3.2.4).

### **4.2.4 Analysis of cytoskeletal element gene expression using quantitative PCR**

RNA was extracted from IVD cells subjected to CTS and cDNA was synthesised according to the methods described previously (Section 2.2.3.1 & 2.2.3.2). To quantitatively determine target gene expression, real-time PCR using custom-designed primers was performed using the Mx3000P® QPCR System as described previously (Section 2.2.3.4.3). The sequences of primers used for target gene amplification are shown in Table 3-1. Calculation of starting concentration was based on standard curves for each target DNA run in parallel, and the relative amount of target gene was calculated as previously described (Section 2.2.3.4.4). For some target genes which lacked a standard curve, the relative amount of RNA was calculated by normalising the Ct value of the target gene with the Ct value of GAPDH. All the data are presented as fold-change in gene expression after initially being normalised to the housekeeping gene GAPDH and then normalised to an endogenous control in the experiment i.e. to young unstretched NP cells which were assigned a value of 1. Therefore, fold changes in gene expression above 1 suggest an increase in transcription whereas values below 1 indicate a decrease relative to the baseline control i.e. unstretched young NP cells.

### **4.2.5 Determination of total cell number using the lactate dehydrogenase assay**

Total cell number was determined using the same reagents and methods described previously (Section 2.2.5).



## **4.2.6 Analysis of protein expression within cells using Western Blotting**

Protein from bovine IVD cells cultured as a monolayer on type I collagen and subjected to tensile strain was extracted using 0.9% Triton X-100 plus protease inhibitors. Cytoskeletal protein levels were investigated using Western blotting as described previously (Section 2.2.7). The samples were normalised to total cell number according to the LDH assay results (Section 2.2.5). Samples were mixed with 2x sample buffer and denatured at 60°C for 30 minutes with reduction by adding 2.5% (v/v)  $\beta$ -mercaptoethanol.

## **4.2.7 Determination of MMP expression and activation using gelatin zymography**

Levels of MMP-2 and MMP-9 in culture media from the bovine IVD cells subjected to tensile strain were investigated using gelatin zymography as described previously (Section 3.2.7). In contrast to Chapter 3, the culture media samples were collected straight after the stretching experiments. Media samples were normalised to total cell number according to the LDH assay as previously described (Section 2.2.5). Samples were mixed with 2x sample buffer and denatured at 60°C for 30 minutes without reduction.

## **4.2.8 Determination of TIMP expression using reverse gelatin zymography**

TIMP-1, TIMP-2 and TIMP-3 levels in culture media from the bovine IVD cells subjected to tensile strain were investigated using reverse gelatin zymography as described previously (Section 3.2.8). In contrast to Chapter 3, the culture media samples were collected straight after the stretching experiments. Media samples were normalised to total cell number according to the LDH assay (Section 2.2.5). Samples were mixed with 2x sample buffer and denatured at 60°C for 30 minutes without reduction.

### **4.2.9 Statistical Analysis**

Data are presented as Mean  $\pm$  S.E.M, with tissue derived from between 4 and 6 individual animals. Samples were analysed in triplicate and all experiments were performed twice and representative data are presented. One-way ANOVA plus Dunnett's (Gaussian distribution) or Dunn's (not Gaussian distribution) post hoc test was carried out using GraphPad Prism 5.0 software unless otherwise stated. Differences were considered significant at P values of less than 0.05.

## 4.3 Results

### 4.3.1 Characterisation of the phenotype of IVD cells in monolayer culture

The Flexcell system applies a uniform strain to cells seeded in monolayer, therefore the IVD cells were cultured as a monolayer on type I collagen coated plates. However, this may change the cell phenotype especially for the NP cells, and therefore may significantly influence cell metabolism and their response to mechanical stimulation. In order to make sure both NP and OAF cells retained their initial phenotype, levels of types I and II collagen and aggrecan mRNA were investigated in the unstretched samples (Figure 4-1).

As shown in Figure 4-1, more type I collagen gene expression was observed in both young (1.9-fold) and mature OAF cells (2.4-fold) when compared with young and mature NP cells (Student's t test,  $p=0.0004$  and  $0.0005$  respectively). Higher type I collagen mRNA levels were also found in mature NP (1.9-fold) and OAF cells (2.3-fold) when compared with young NP and OAF cells (Student's t test,  $p=0.0050$  and  $0.0004$  respectively), mirroring trends observed in NP and OAF *in situ*.

Significant zonal differences in type II collagen mRNA expression were observed in IVD cells cultured as a monolayer. There were higher type II collagen mRNA levels in young (74-fold) and mature NP cells (70-fold) when compared with young and mature OAF cells (Student's t test,  $p<0.0001$ ), indicating retention of both the NP and OAF phenotypes (Figure 4-1). No age-related differences were observed between young NP and OAF cells when compared with mature NP and OAF cells (Student's t test,  $p>0.05$ ).

Chapter 4: The effect of different cyclic tensile strain on cytoskeletal elements and extracellular matrix metabolism of bovine intervertebral disc cells *in vitro*

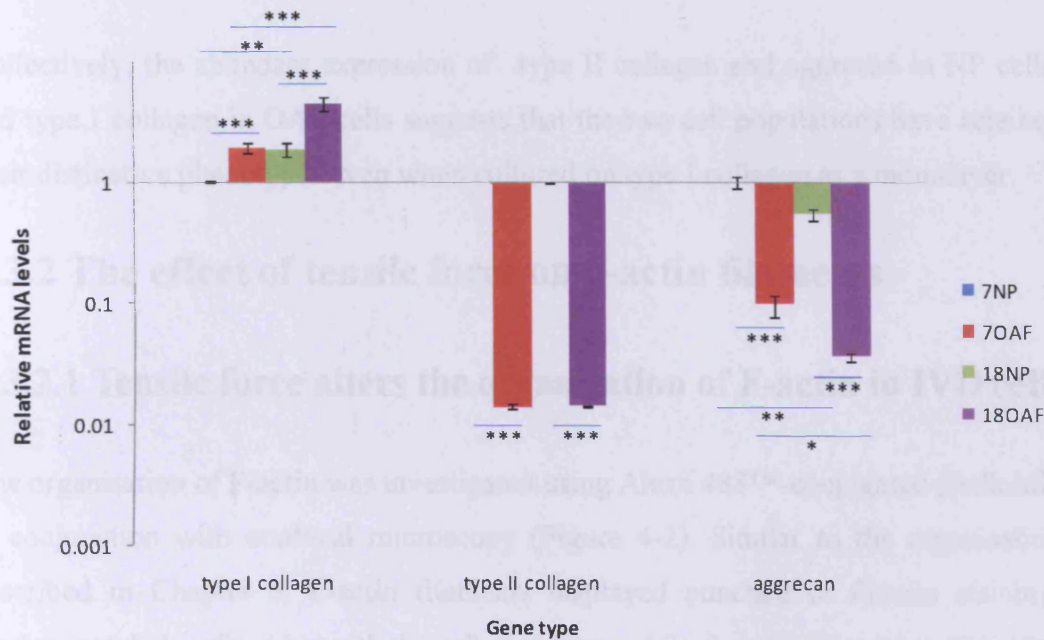


Figure 4-1 Zonal and age-related differences in types I and II collagen and aggrecan mRNA levels in bovine IVD cells indicated that the cells retained their phenotype when cultured on type I collagen as a monolayer. Total RNA was extracted and types I and II collagen and aggrecan mRNA levels were determined using real-time PCR. Data are shown as Mean  $\pm$  S.E.M. (n=6). Data were normalised to the house-keeping gene GAPDH and was relative to young NP cells. Student's t test, \*\*\*:  $p \leq 0.001$ , \*\*:  $p \leq 0.01$ , \*:  $p < 0.05$ .

Zonal and age-related differences in aggrecan mRNA levels in cells cultured as a monolayer were also observed. There were much higher levels of aggrecan mRNA in young (10-fold) and mature NP cells (15-fold) when compared with young and mature OAF cells (Student's t test,  $p < 0.0001$ ). In addition, higher aggrecan gene expression was found in young NP (1.9-fold) and OAF cells (2.7-fold) when compared with mature NP and OAF cells (Student's t test,  $p = 0.0039$  and  $0.0115$  respectively) (Figure 4-1).

Collectively, the abundant expression of type II collagen and aggrecan in NP cells, and type I collagen in OAF cells suggests that the two cell populations have retained their distinctive phenotypes even when cultured on type I collagen as a monolayer.

### **4.3.2 The effect of tensile force on $\beta$ -actin filaments**

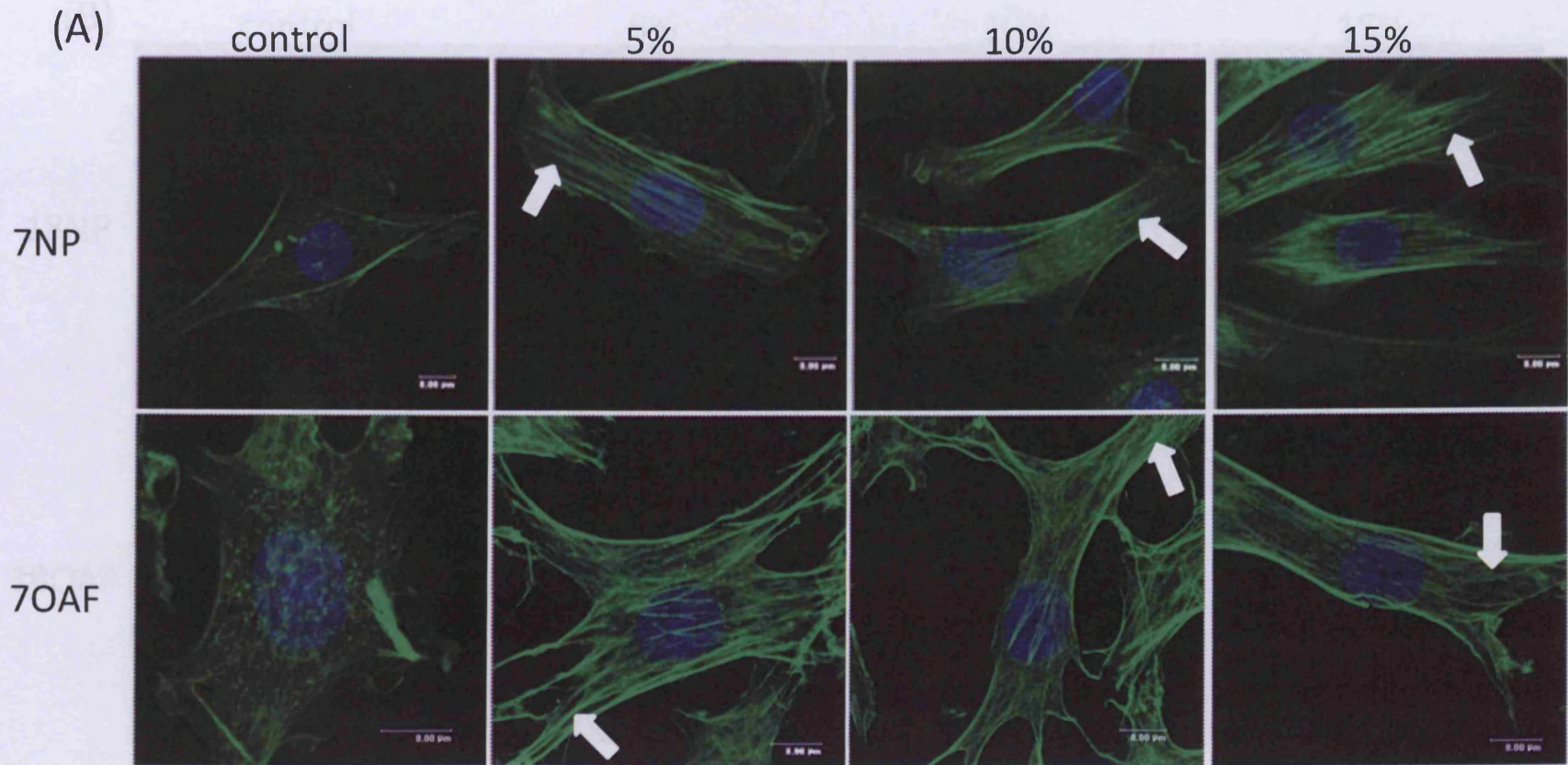
#### **4.3.2.1 Tensile force alters the organisation of F-actin in IVD cells**

The organisation of F-actin was investigated using Alexa 488<sup>TM</sup>-conjugated phalloidin in conjunction with confocal microscopy (Figure 4-2). Similar to the organisation described in Chapter 3, F-actin filaments displayed punctate or fibrous staining, predominately localised beneath the cell membrane. After being subjected to 5%, 10% or 15% CTS for 60 minutes, the cells became elongated and flattened. A large amount of stress fibre formation was observed, which was distributed throughout the cytoplasm, extending towards the cellular protrusions in young NP and OAF cells (white arrow) (Figure 4-2A). There was no significant difference in F-actin organisation within cells subjected to different magnitudes of CTS. We also investigated the organisation of F-actin within mature NP and OAF cells cultured on type I collagen and similarly subjected to variable CTS, and there was no apparent difference in organisation between the young and mature IVD cells (Figure 4-2B)

Figure 4-2. Localisation of F-actin filaments in nucleus pulposus and outer annulus fibrosus cells cultured on type I collagen as a monolayer. Cells were subjected to cyclic tensile strain (5%, 10% or 15% elongation) at 1Hz for 60 minutes; unstretched cells served as a control. F-actin was stained with Alexa-488™ conjugated phalloidin and the cell nucleus was counterstained with DAPI. Images are presented as 3D reconstructions. **A:** 7 day old intervertebral disc cells; **B:** 18 month old intervertebral disc cells. Arrow: fibre-like F-actin filaments after strain.

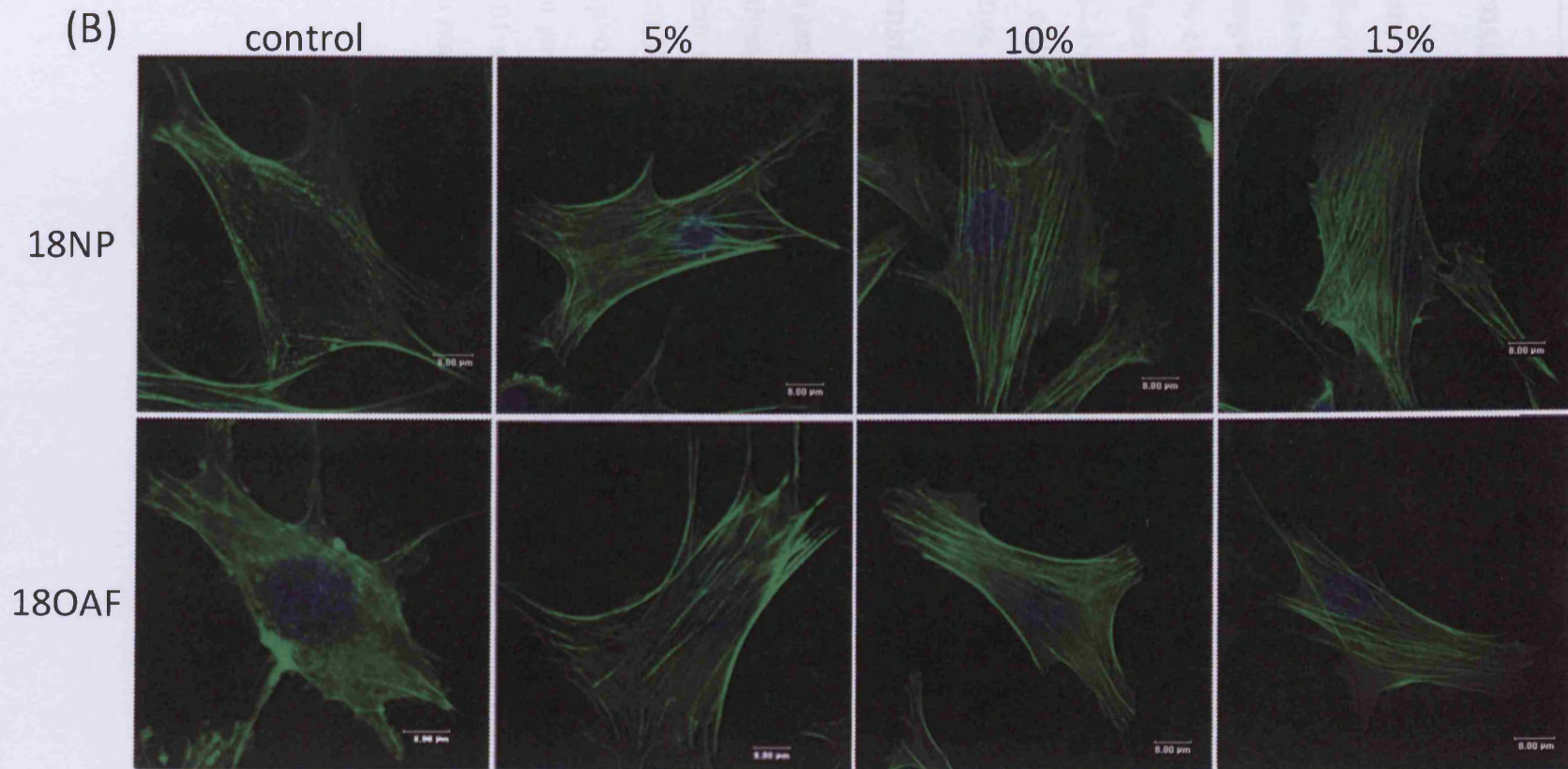
Chapter 4: The effect of different cyclic tensile strain on cytoskeletal elements and extracellular matrix metabolism of bovine intervertebral disc cells *in vitro*

---



Chapter 4: The effect of different cyclic tensile strain on cytoskeletal elements and extracellular matrix metabolism of bovine intervertebral disc cells *in vitro*

---





#### **4.3.2.2 Tensile force alters $\beta$ -actin mRNA levels in IVD cells**

To investigate whether the changes in F-actin organisation is strain magnitude dependent,  $\beta$ -actin mRNA levels were determined by real-time PCR. Both young NP and OAF cells responded similarly to CTS; 5% (2.3-fold;  $p < 0.01$ ) and 15% (3.1-fold;  $p < 0.001$ ) elongation significantly increased  $\beta$ -actin gene expression in young NP cells, whereas 10% elongation did not change  $\beta$ -actin gene expression in young NP cells ( $p > 0.05$ ) (Figure 4-3). 5% (1.9-fold;  $p < 0.01$ ), 10% (1.7-fold;  $p < 0.05$ ) and 15% elongation (2.1-fold;  $p < 0.001$ ) significantly promoted  $\beta$ -actin mRNA expression in young OAF cells (Figure 4-3). However, strain did not alter  $\beta$ -actin gene expression levels in mature NP or OAF cells ( $p > 0.05$ ) (Figure 4-3).

#### **4.3.2.3 Tensile force alters $\beta$ -actin protein expression in IVD cells**

As  $\beta$ -actin organisation and mRNA levels were responsive to strain, protein expression was also analysed by Western blotting (Figure 4-4). 15% strain significantly increased  $\beta$ -actin protein expression in both young (1.4-fold;  $p < 0.05$ ) and mature NP cells (2.1-fold;  $p < 0.001$ ), whereas there was no effect on cells subjected to 5% and 10% elongation ( $p > 0.05$ ). A 1.7-fold, 1.5-fold and 1.4-fold increase in  $\beta$ -actin protein expression in young OAF cells was observed in response to 5%, 10% and 15% strain ( $p < 0.001$ , 0.01 and 0.05 respectively), but only 15% strain increased  $\beta$ -actin protein expression in mature OAF cells (1.9-fold;  $p < 0.001$ ).

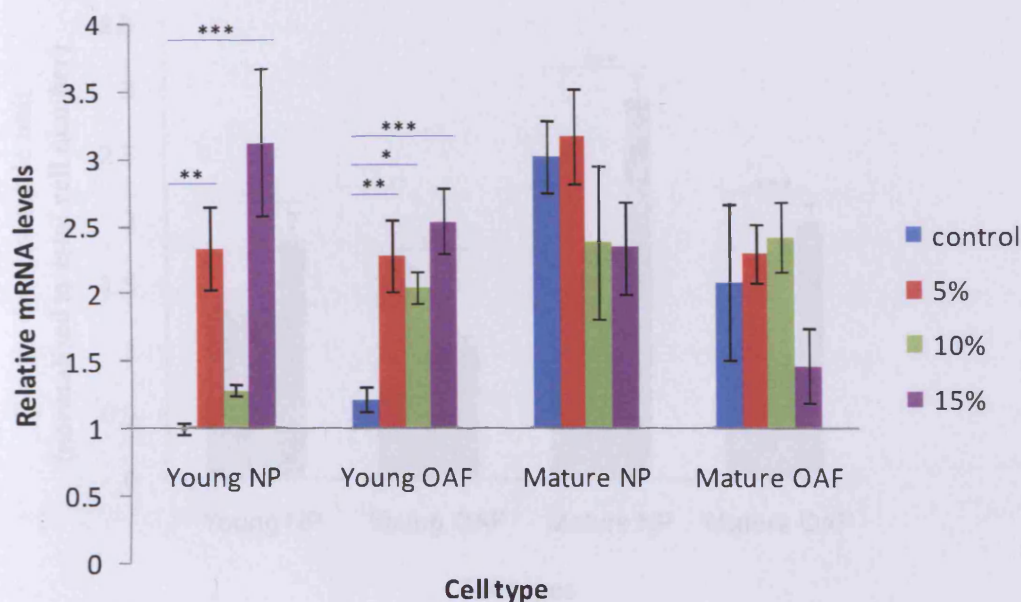


Figure 4-3.  $\beta$ -actin mRNA expression in IVD cells subjected to different magnitudes of cyclic tensile force. Cells were cultured on type I collagen as a monolayer and stretched with 5%, 10% or 15% elongation at 1Hz for 60 minutes. Unstretched cells were used as a control. Total RNA was extracted and  $\beta$ -actin mRNA levels were determined using real-time PCR. Data are shown as Mean  $\pm$  S.E.M. (n=5). Data were normalised to the house-keeping gene GAPDH and were relative to unstretched young NP cells. \*\*\*:  $p \leq 0.001$ , \*\*:  $p \leq 0.01$ , \*:  $p \leq 0.05$  when compared with control group.

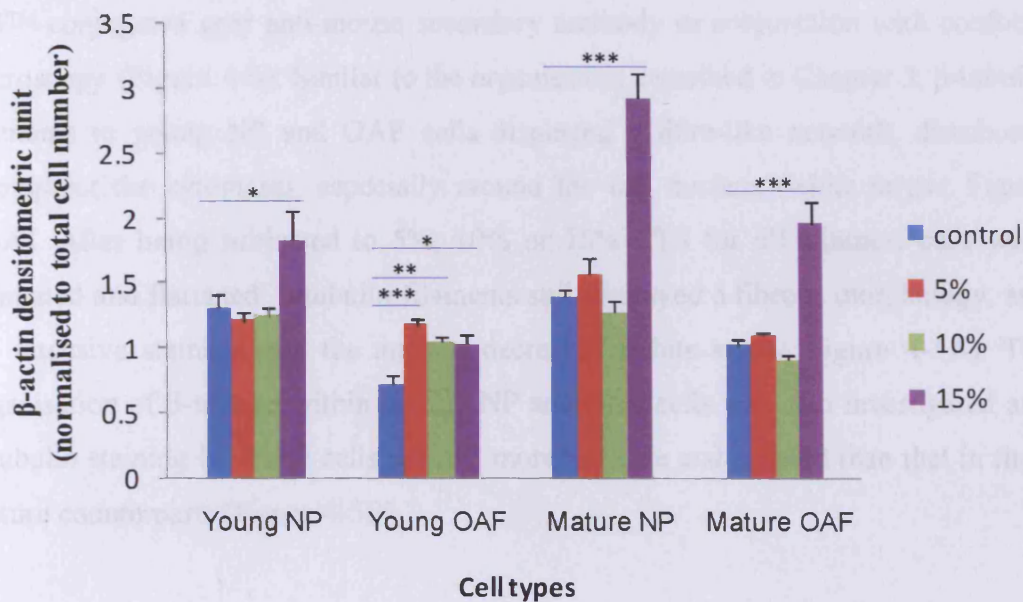


Figure 4-4.  $\beta$ -actin protein expression in IVD cells after being subjected to different magnitudes of cyclic tensile force. Cells were cultured on type I collagen as a monolayer and stretched with 5%, 10% or 15% elongation at 1Hz for 60 minutes. Total protein was extracted and  $\beta$ -actin protein levels were determined using Western-blotting. Unstretched cells were used as a control. Samples were normalised to total cell number according to the LDH assay. Data are shown as Mean  $\pm$  S.E.M. (n=4). \*\*\*:  $p \leq 0.001$ , \*\*:  $p \leq 0.01$ , \*:  $p \leq 0.05$  when compared with control group.

### **4.3.3 The effect of tensile force on $\beta$ -tubulin filaments**

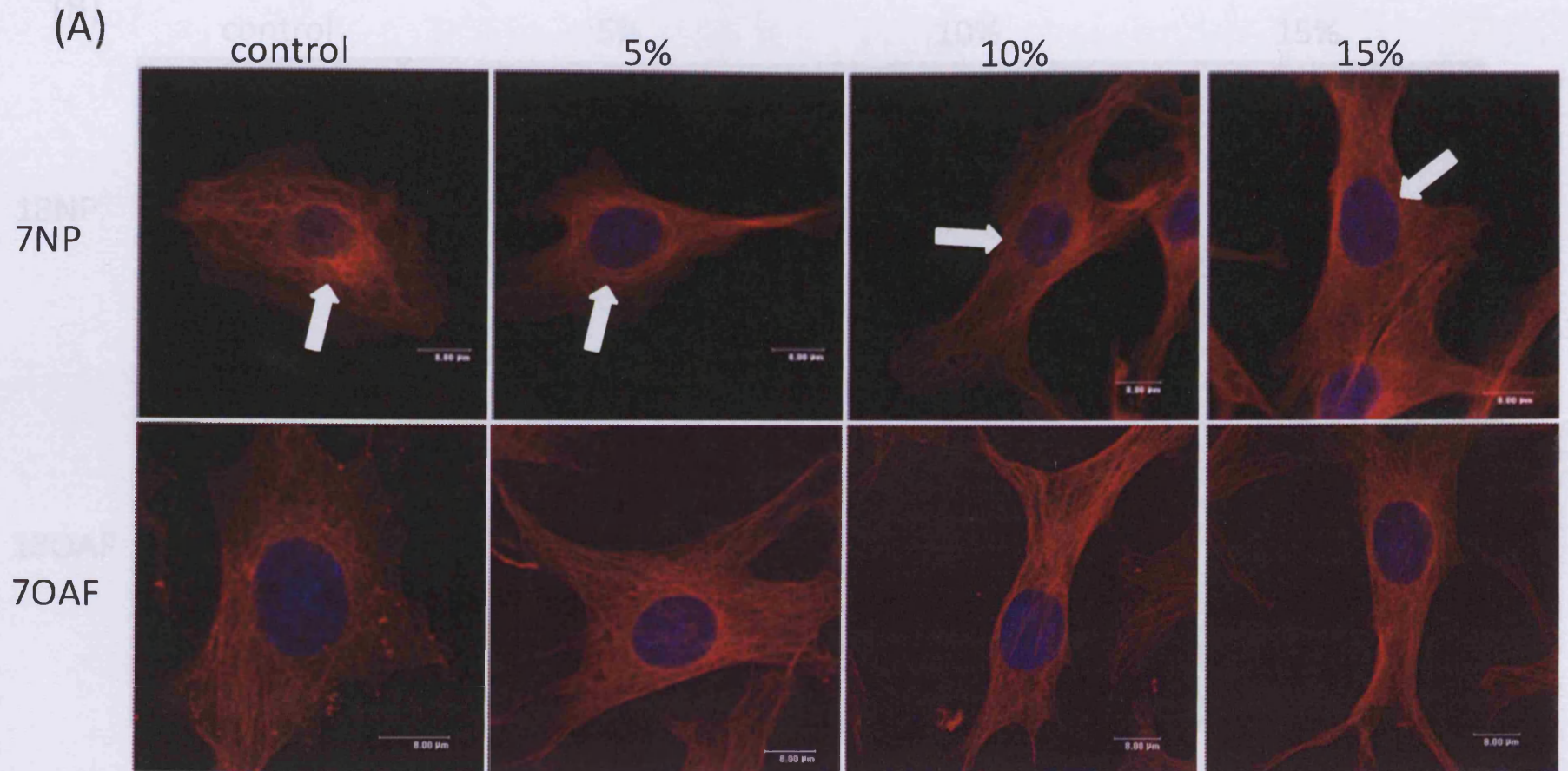
#### **4.3.3.1 Tensile force altered the organisation of $\beta$ -tubulin in IVD cells**

The organisation of  $\beta$ -tubulin was visualised using E7 primary antibody with Alexa 633<sup>TM</sup>-conjugated goat anti-mouse secondary antibody in conjunction with confocal microscopy (Figure 4-5). Similar to the organisation described in Chapter 3,  $\beta$ -tubulin filaments in young NP and OAF cells displayed a fibre-like network, distributed throughout the cytoplasm, especially around the cell nucleus (white arrow; Figure 4-5A). After being subjected to 5%, 10% or 15% CTS for 60 minutes, cells were elongated and flattened;  $\beta$ -tubulin filaments still displayed a fibrous morphology, and the intensive staining near the nucleus decreased (white arrow; Figure 4-5A). The organisation of  $\beta$ -tubulin within mature NP and OAF cells was also investigated and  $\beta$ -tubulin staining in young cells seemed more intricate and ordered than that in their mature counterparts (Figure 4-5B).

Figure 4-5. Localisation of  $\beta$ -tubulin filaments in nucleus pulposus and outer annulus fibrosus cells in monolayer cultured on type I collagen. Cells were subjected to cyclic tensile strain at 1Hz (5%, 10% or 15% elongation) for 60 minutes.  $\beta$ -tubulin was stained with E7 primary antibody and Alexa-633™ conjugated goat anti-mouse antibody. Cell nuclei were counterstained with DAPI. Images are presented as 3D reconstructions. **A**: 7 day old intervertebral disc cells; **B**: 18 month old intervertebral disc cells. Arrow: the intensive staining of  $\beta$ -tubulin around cell nucleus disappeared after strain.

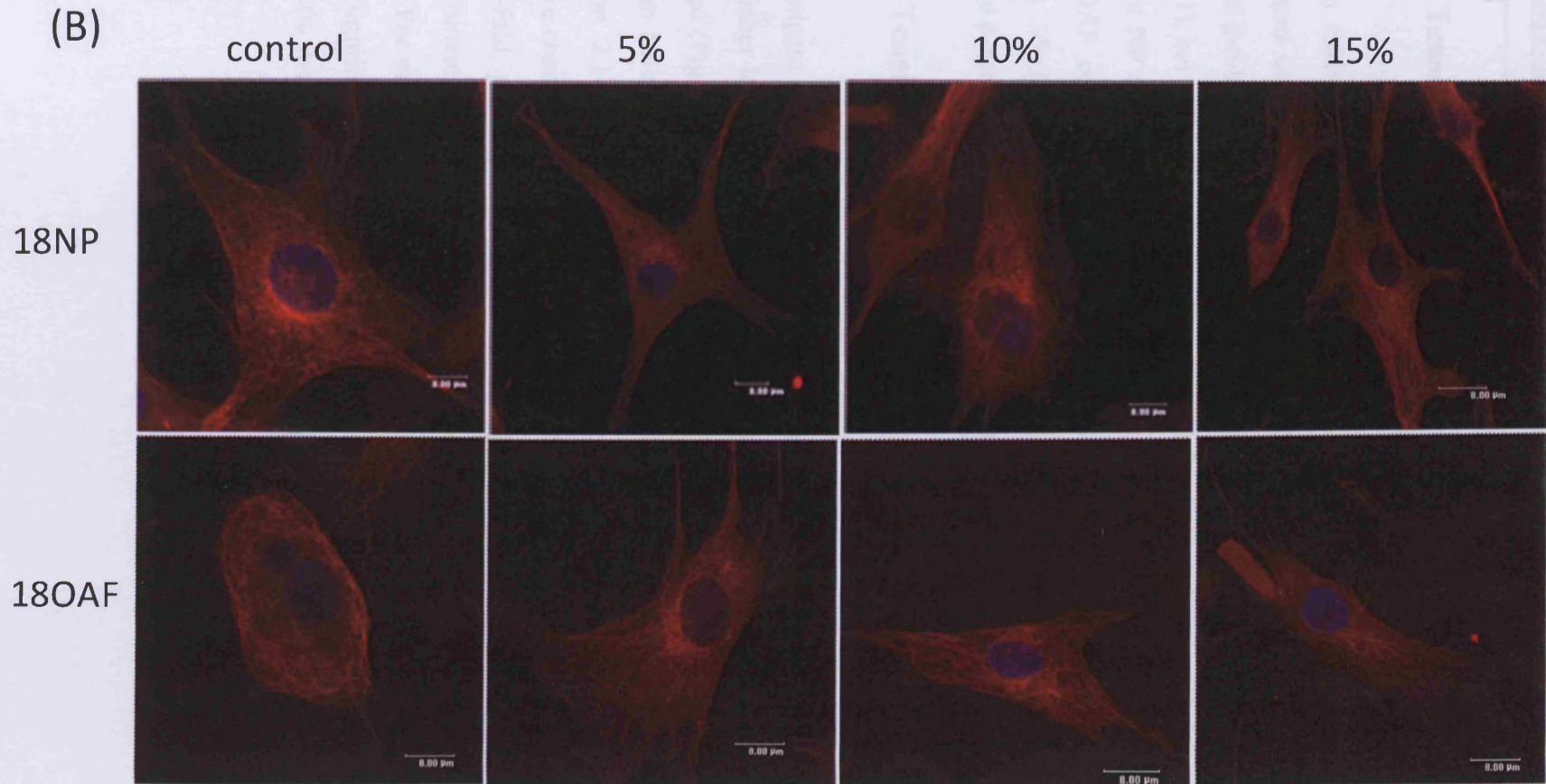
Chapter 4: The effect of different cyclic tensile strain on cytoskeletal elements and extracellular matrix metabolism of bovine intervertebral disc cells *in vitro*

---



Chapter 4: The effect of different cyclic tensile strain on cytoskeletal elements and extracellular matrix metabolism of bovine intervertebral disc cells *in vitro*

---



#### 4.3.3.2 Tensile force decreased $\beta$ -tubulin mRNA levels in IVD cells

$\beta$ -tubulin mRNA levels in IVD cells subjected to 5%, 10% or 15% strain were investigated using real-time PCR (Figure 4-6). 5% and 15% strain significantly decreased  $\beta$ -tubulin mRNA levels in young and mature NP cells (approximately 2-fold;  $p < 0.0001$ ), but 10% elongation had no effect on  $\beta$ -tubulin mRNA levels in either young or mature NP cells ( $p > 0.05$ ). 10% elongation increased  $\beta$ -tubulin gene expression in young OAF cells (2.9-fold;  $p < 0.001$ ), but 5% and 15% elongation had no effect ( $p > 0.05$ ). 5% (2.3-fold), 10% (1.5-fold) and 15% elongation (2.7-fold) significantly decreased  $\beta$ -tubulin mRNA levels in mature OAF cells ( $p < 0.0001$ ).

#### 4.3.3.3 Tensile force alters $\beta$ -tubulin protein expression in IVD cells

To investigate whether the alterations in  $\beta$ -tubulin mRNA levels induced by strain could further lead to changes in  $\beta$ -tubulin protein expression, Western blotting was performed (Figure 4-7). 5% and 15% strain significantly decreased  $\beta$ -tubulin protein content in both young (approximately 2.1-fold;  $p < 0.001$ ) and mature NP cells (5% elongation: 2.1-fold;  $p < 0.01$ . 15% elongation: 1.5-fold;  $p < 0.05$ ). 10% elongation did not induce changes in either young or mature NP cells ( $p > 0.05$ ). For young OAF cells, 5% (6.5-fold;  $p < 0.01$ ) and 15% elongation (9.7-fold;  $p < 0.001$ ) decreased  $\beta$ -tubulin protein content whereas 10% elongation increased  $\beta$ -tubulin protein levels (1.4-fold;  $p < 0.05$ ). For mature OAF cells, 5% (3.1-fold;  $p < 0.05$ ) and 15% elongation (6.3-fold;  $p < 0.01$ ) significantly decreased  $\beta$ -tubulin protein expression, but there was no effect after a 10% strain ( $p > 0.05$ ).



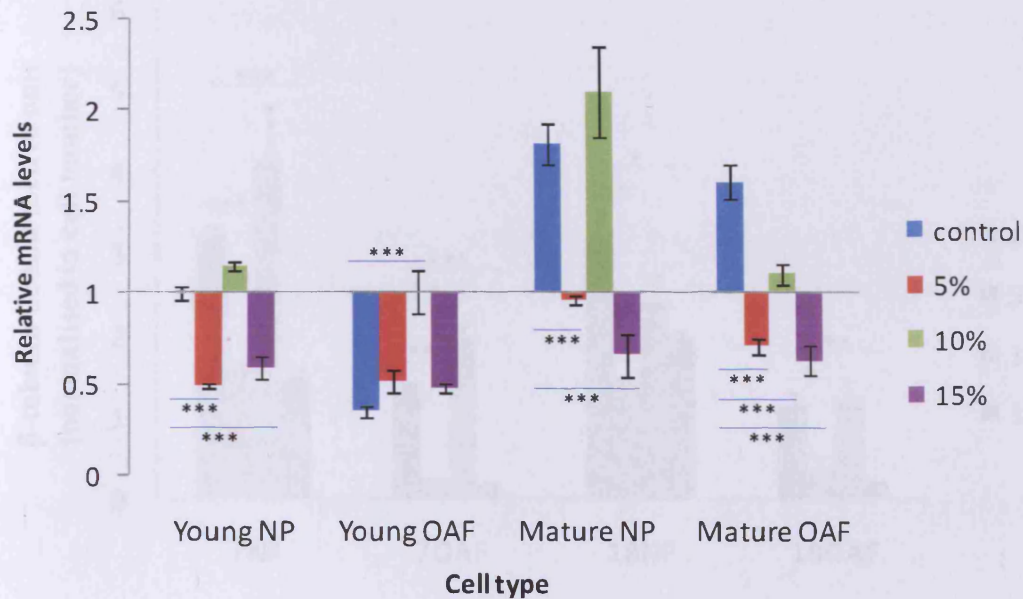


Figure 4-6.  $\beta$ -tubulin mRNA expression in IVD cells subjected to different magnitudes of cyclic tensile force. Cells were cultured on type I collagen as a monolayer and stretched with 5%, 10% or 15% elongation at 1Hz for 60 minutes. Unstretched cells were used as a control. Total RNA was extracted and  $\beta$ -tubulin mRNA levels were determined using real-time PCR. Data are shown as Mean  $\pm$  S.E.M. (n=6). Data were normalised to the house-keeping gene GAPDH and were relative to unstretched young NP cells. \*\*\*:  $p \leq 0.001$  when compared with control group.

#### 4.3.4 The effect of tensile force on vimentin filaments

##### 4.3.4.1 Tensile force did not alter the organisation of vimentin in IVD cells

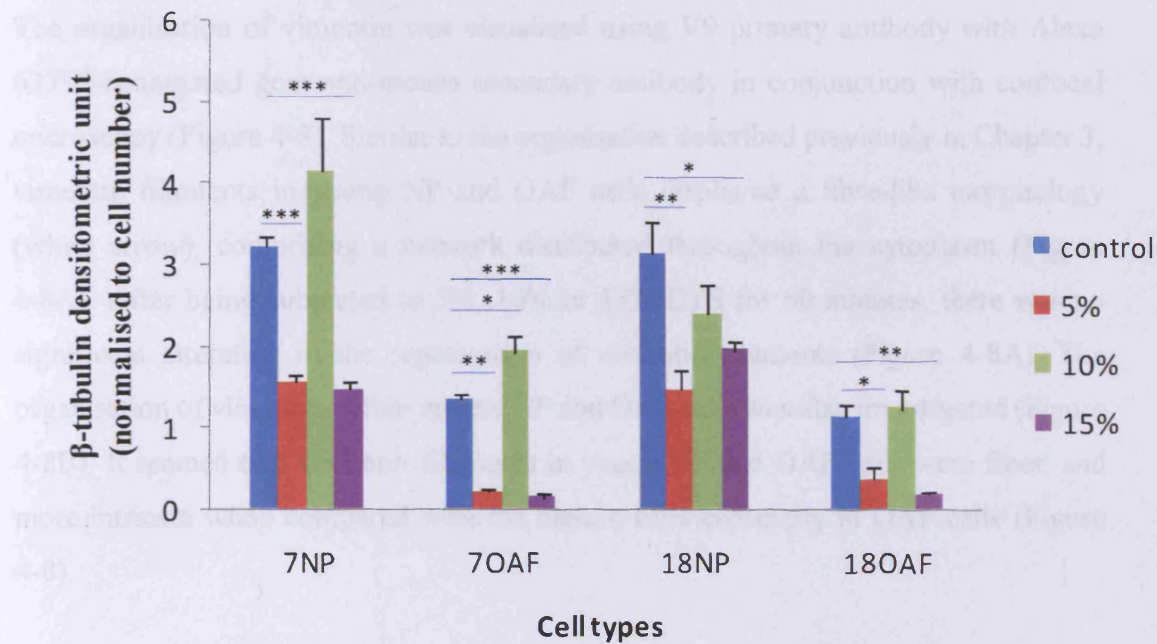


Figure 4-7.  $\beta$ -tubulin protein expression in IVD cells after being subjected to different magnitudes of cyclic tensile force. Cells were cultured on type I collagen as a monolayer and stretched with 5%, 10% or 15% elongation at 1Hz for 60 minutes. Total protein was extracted and  $\beta$ -tubulin protein levels were determined using Western-blotting. Unstretched cells were used as a control. Samples were normalised to total cell number according to the LDH assay. Data are shown as Mean  $\pm$  S.E.M. (n=4). \*\*\*:  $p \leq 0.001$ , \*\*:  $p \leq 0.01$ , \*:  $p \leq 0.05$  when compared with control group.

### **4.3.4 The effect of tensile force on vimentin filaments**

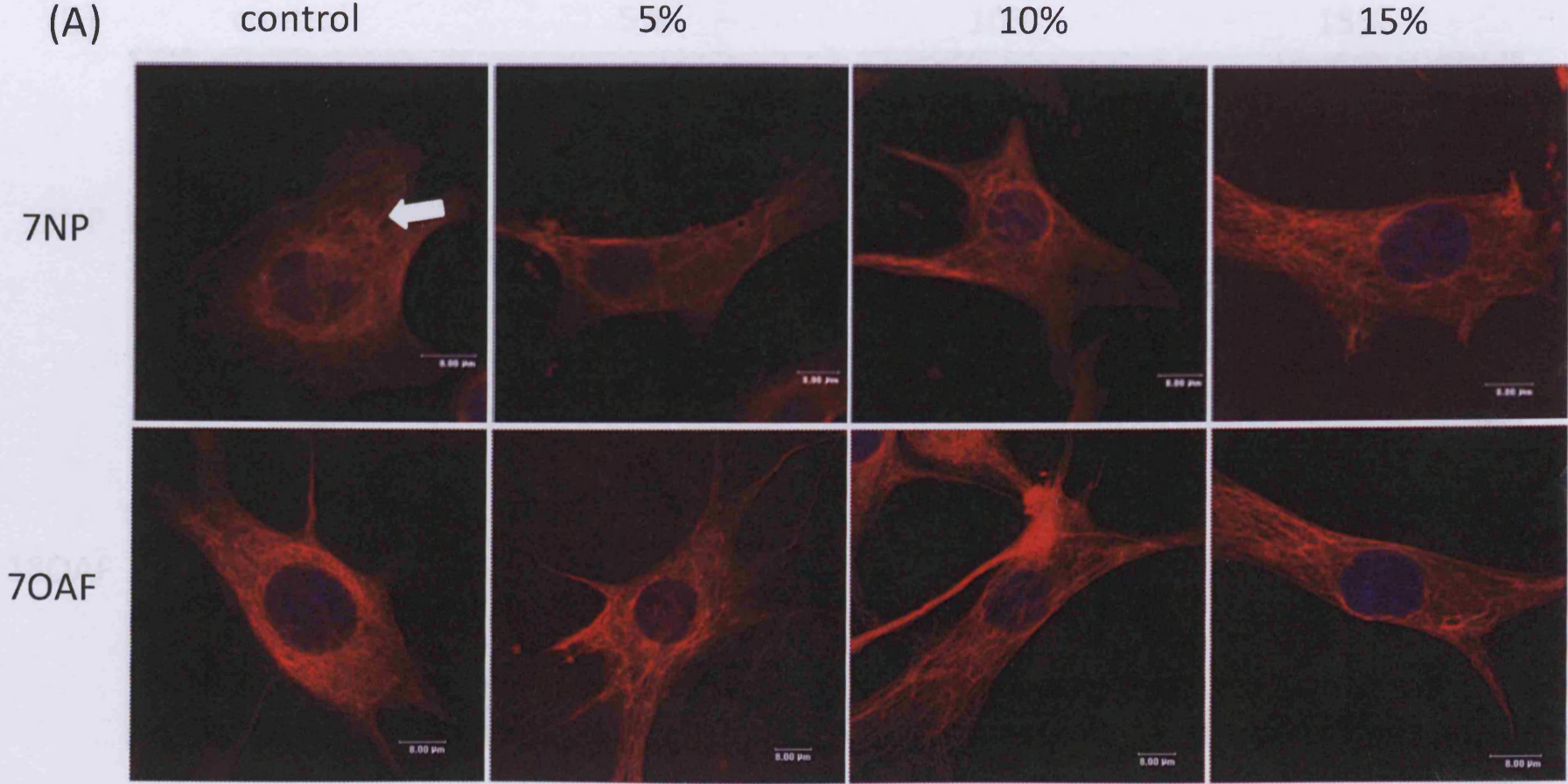
#### **4.3.4.1 Tensile force did not alter the organisation of vimentin in IVD cells**

The organisation of vimentin was visualised using V9 primary antibody with Alexa 633™-conjugated goat anti-mouse secondary antibody in conjunction with confocal microscopy (Figure 4-8). Similar to the organisation described previously in Chapter 3, vimentin filaments in young NP and OAF cells displayed a fibre-like morphology (white arrow), comprising a network distributed throughout the cytoplasm (Figure 4-8A). After being subjected to 5%, 10% or 15% CTS for 60 minutes, there was no significant alteration in the organisation of vimentin filaments (Figure 4-8A). The organisation of vimentin within mature NP and OAF cells was also investigated (Figure 4-8B). It seemed that vimentin filaments in young NP and OAF cells were finer, and more intricate when compared with the mature cells especially in OAF cells (Figure 4-8).

Figure 4-8. Localisation of vimentin filaments in nucleus pulposus and outer annulus fibrosus cells cultured on type I collagen as a monolayer. Cells were subjected to cyclic tensile strain (5%, 10% or 15% elongation respectively) at 1Hz for 60 minutes. Vimentin was stained with V9 primary antibody and Alexa-633™ conjugated goat anti-mouse secondary antibody. Cell nuclei were counterstained with DAPI. Images are presented as 3D reconstructions. **A:** 7 day old intervertebral disc cells; **B:** 18 month old intervertebral disc cells. Arrow: fibre-like vimentin filaments in disc cells.

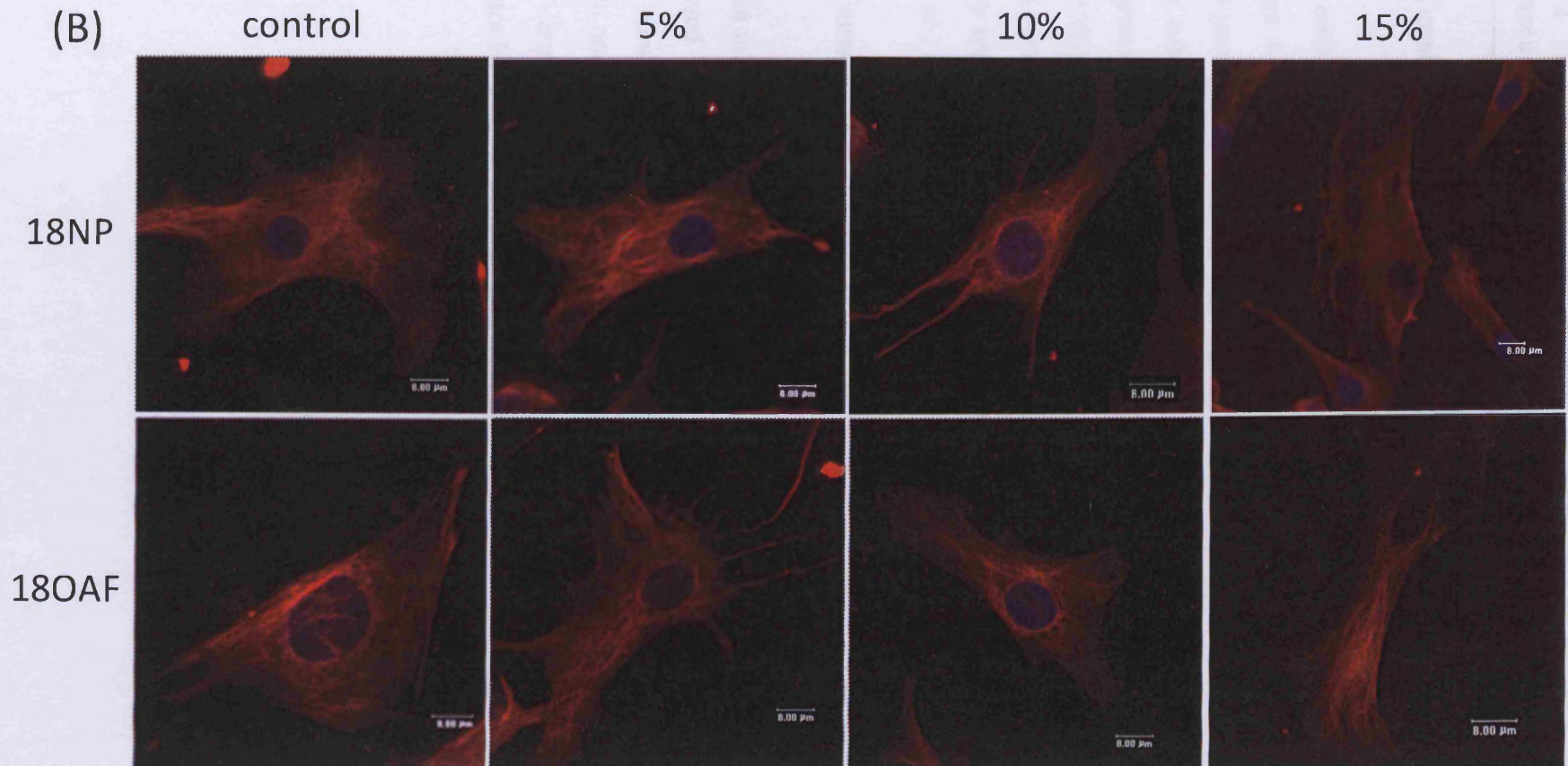
Chapter 4: The effect of different cyclic tensile strain on cytoskeletal elements and extracellular matrix metabolism of bovine intervertebral disc cells *in vitro*

---



Chapter 4: The effect of different cyclic tensile strain on cytoskeletal elements and extracellular matrix metabolism of bovine intervertebral disc cells *in vitro*

---



#### **4.3.4.2 Tensile force decreased vimentin gene expression in IVD cells**

Vimentin mRNA levels in cells subjected to CTS were investigated using real-time PCR (Figure 4-9). 15% elongation significantly decreased vimentin gene expression by 3.3-fold in young NP cells ( $p < 0.01$ ), whereas no alteration was found after young NP cells were subjected to 5% or 10% strain ( $p > 0.05$ ). None of the strains affected vimentin gene expression in mature NP cells ( $p > 0.05$ ). In contrast, all of the strains (5%, 10% and 15%) decreased vimentin mRNA levels by approximately 2-fold in young OAF cells ( $p < 0.001$ , 0.01 and 0.001 respectively). Vimentin mRNA expression was inhibited by approximately 2-fold in mature OAF cells subjected to 5% ( $p < 0.001$ ), 10% ( $p < 0.001$ ) or 15% strain ( $p < 0.01$ ) (Figure 4-9).

#### **4.3.4.3 Tensile force altered vimentin protein expression in IVD cells**

As vimentin mRNA levels were responsive to strain, vimentin protein expression was also analysed by Western blotting (Figure 4-10). Only 15% strain significantly decreased vimentin protein expression in young NP and OAF cells (approximately 2-fold,  $p < 0.0001$ ) (Figure 4-10), whereas 5% and 10% elongation had no effect ( $p > 0.05$ ). Vimentin protein levels were not sensitive to increasing strains applied to either mature NP or OAF cells ( $p > 0.05$ ) (Figure 4-10).

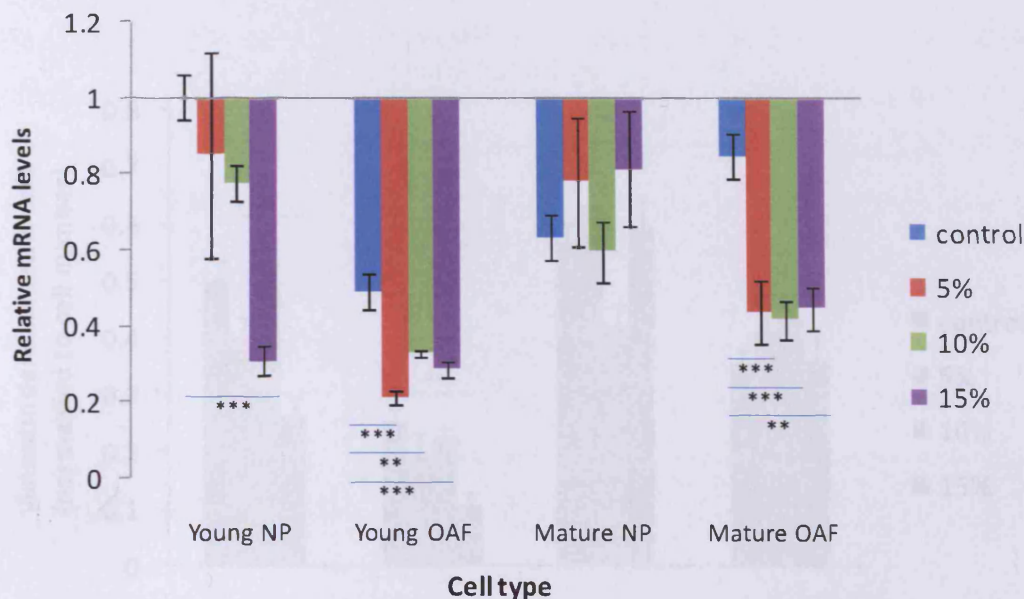


Figure 4-9. Vimentin mRNA expression in IVD cells after being subjected to different magnitudes of cyclic tensile force. Cells were cultured on type I collagen as a monolayer and subjected to 5%, 10% or 15% elongation at 1Hz for 60 minutes. Total RNA was extracted and vimentin mRNA levels were determined using real-time PCR. Unstretched cells were used as a control. Data are shown as Mean  $\pm$  S.E.M. (n=5). Data were normalised to the house-keeping gene GAPDH and were relative to unstretched young NP cells. \*\*\*:  $p \leq 0.001$ , \*\*:  $p \leq 0.01$  when compared with control group.



#### 4.3.5 The effect of CTS on markers of ECM metabolism

To further investigate the effects of different magnitudes of strain on cell metabolism, gene expression levels of ECM markers were determined using real-time PCR (Figure 4-9).

Young NP cells at all strains (5%, 10% and 15% elongation) significantly increased type I collagen expression by approximately 1.5-fold ( $p < 0.05$ ) (Figure 4-11A). In contrast, 15% strain significantly decreased aggrecan gene expression by 2 and

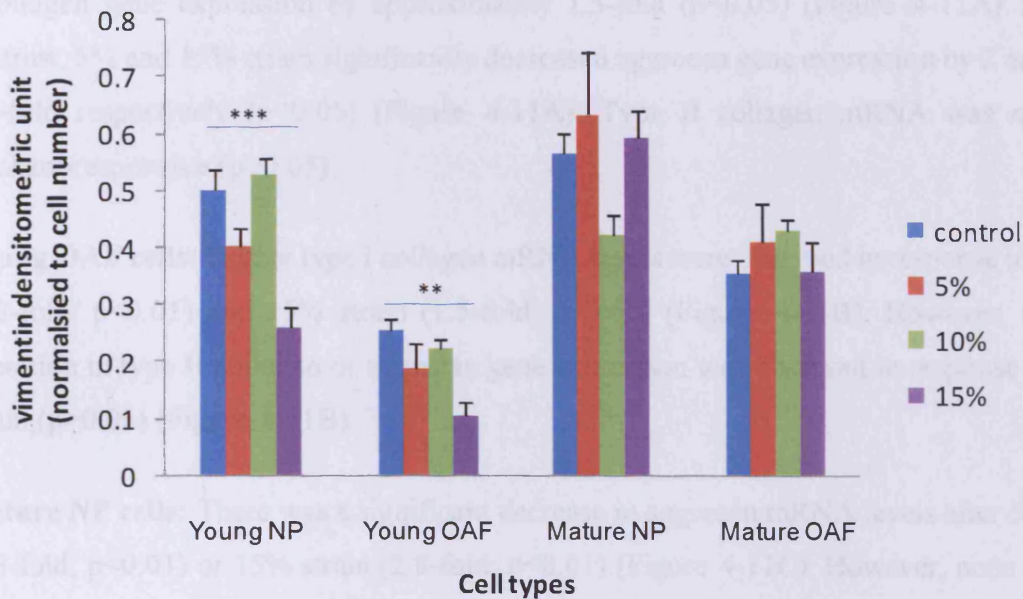


Figure 4-10 Vimentin protein expression in IVD cells after being subjected to different magnitudes of cyclic tensile force. Cells were cultured on type I collagen as a monolayer and stretched with 5%, 10% or 15% elongation at 1Hz for 60 minutes. Total protein was extracted and vimentin protein levels were determined using Western blotting. Unstretched cells were used as a control. Samples were normalised to total cell number according to the LDH assay. Data are shown as Mean  $\pm$  S.E.M. (n=4). \*\*\*:  $p \leq 0.001$ , \*\*:  $p \leq 0.01$  when compared with control group.

### 4.3.5 The effect of CTS on markers of ECM metabolism

To further investigate the effects of different magnitudes of strain on cell metabolism, gene expression levels of ECM-markers were determined using real-time PCR (Figure 4-11).

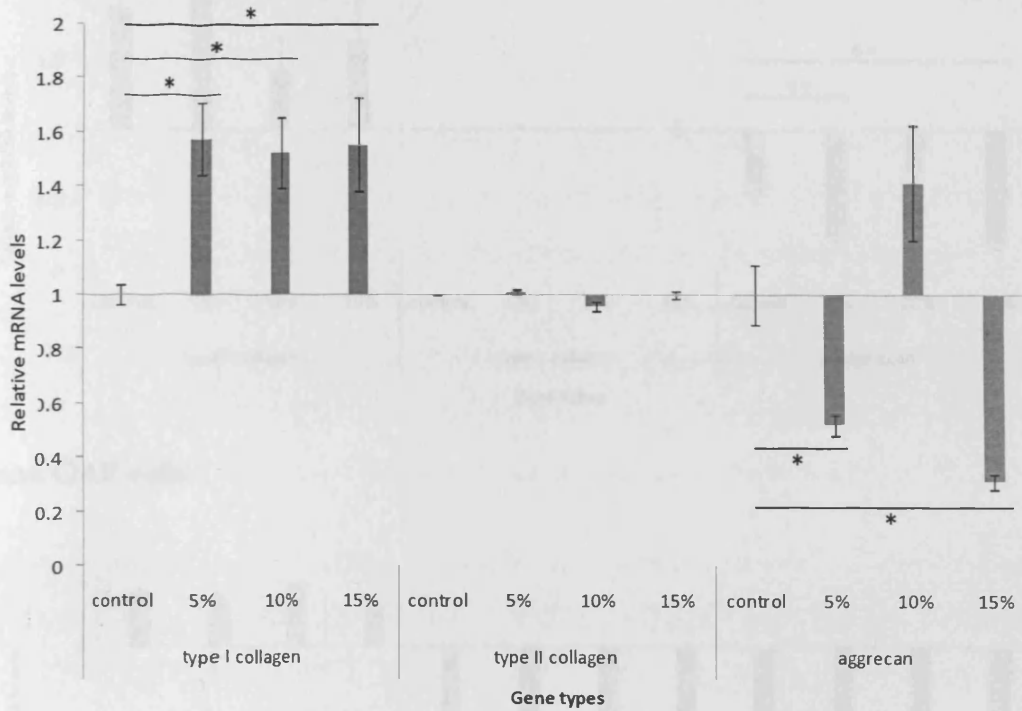
**Young NP cells:** all strains (5%, 10% and 15% elongation) significantly increased type I collagen gene expression by approximately 1.5-fold ( $p < 0.05$ ) (Figure 4-11A). In contrast, 5% and 15% strain significantly decreased aggrecan gene expression by 2 and 3.3-fold respectively ( $p < 0.05$ ) (Figure 4-11A). Type II collagen mRNA was not mechanoresponsive ( $p > 0.05$ ).

**Young OAF cells:** Higher type I collagen mRNA levels were observed in response to 5% (1.8-fold;  $p < 0.01$ ) and 15% strain (1.5-fold;  $p < 0.05$ ) (Figure 4-11B). However, no alteration in type II collagen or aggrecan gene expression was observed in response to strain ( $p > 0.05$ ) (Figure 4-11B).

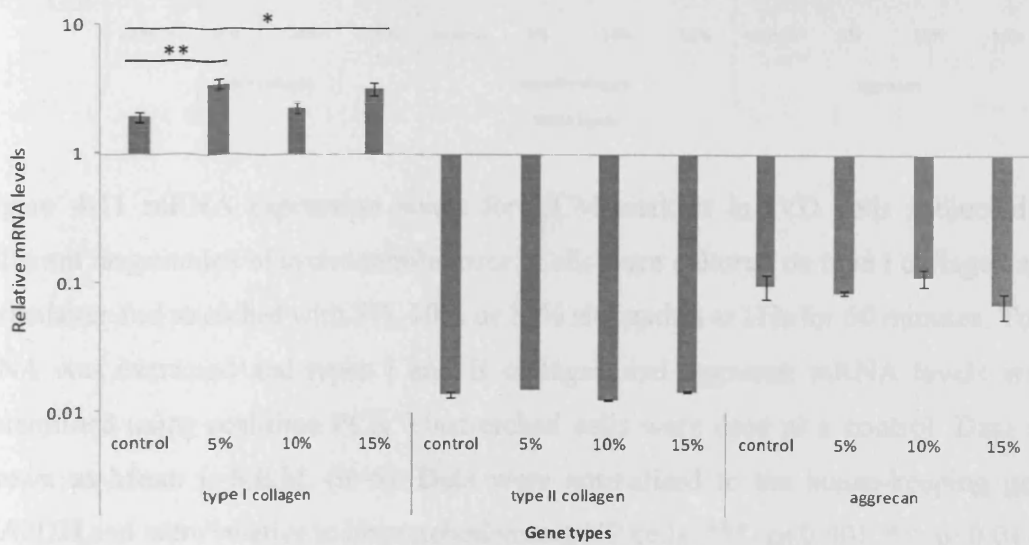
**Mature NP cells:** There was a significant decrease in aggrecan mRNA levels after 5% (2.3-fold;  $p < 0.01$ ) or 15% strain (2.8-fold;  $p < 0.01$ ) (Figure 4-11C). However, none of the strains affected types I or II collagen gene expression ( $p > 0.05$ ) (Figure 4-11C).

**Mature OAF cells:** 10% strain induced a small but significant reduction ( $p < 0.001$ ) in type II mRNA levels (Figure 4-11D). Similarly, there was a significant decrease in aggrecan mRNA levels after 5% (1.5-fold;  $p < 0.05$ ), 10% (2.3-fold;  $p < 0.001$ ) and 15% strain (1.8 fold;  $p < 0.01$ ) (Figure 4-11D). In contrast to the trends observed for young OAF cells, there was no alteration in type I collagen mRNA in response to any of the strains ( $p > 0.05$ ).

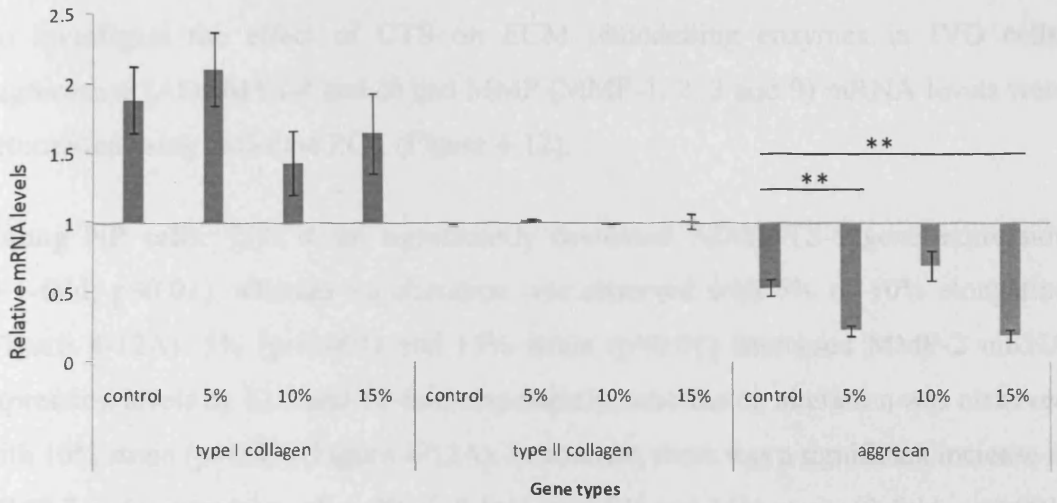
**(A) Young NP cells**



**(B) Young OAF cells**



(C) Mature NP cells



(D) Mature OAF cells

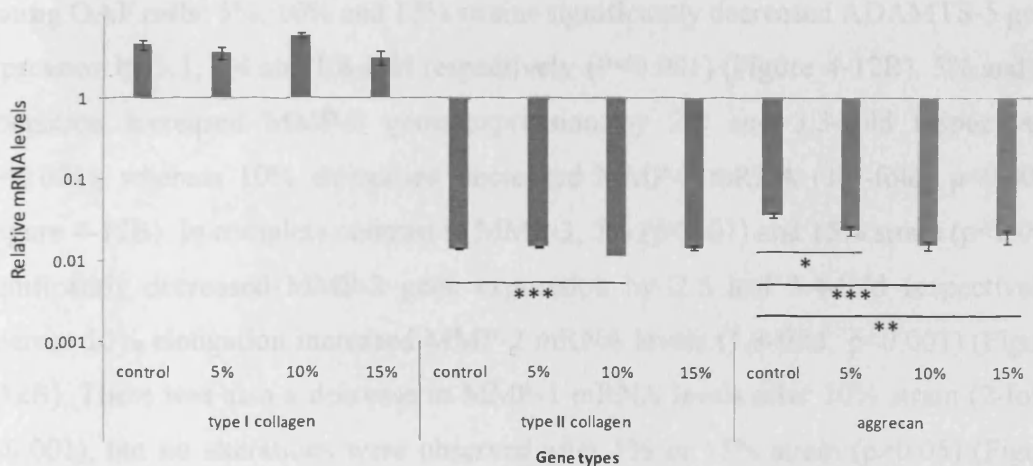


Figure 4-11 mRNA expression levels for ECM-markers in IVD cells subjected to different magnitudes of cyclic tensile force. Cells were cultured on type I collagen as a monolayer and stretched with 5%, 10% or 15% elongation at 1Hz for 60 minutes. Total RNA was extracted and types I and II collagen and aggrecan mRNA levels were determined using real-time PCR. Unstretched cells were used as a control. Data are shown as Mean  $\pm$  S.E.M. (n=5). Data were normalised to the house-keeping gene GAPDH and were relative to unstretched young NP cells. \*\*\*:  $p \leq 0.001$ , \*\*:  $p \leq 0.01$ , \*:  $p \leq 0.05$  when compared with control group. [A]: young NP, [B]: young OAF, [C]: mature NP, [D]: mature OAF.

### 4.3.6 The effect of CTS on ECM remodelling enzymes

To investigate the effect of CTS on ECM remodelling enzymes in IVD cells, aggrecanase (ADAMTS-4 and 5) and MMP (MMP-1, 2, 3 and 9) mRNA levels were determined using real-time PCR (Figure 4-12).

**Young NP cells:** 15% strain significantly decreased ADAMTS-5 gene expression (3.1-fold;  $p < 0.01$ ), whereas no alteration was observed with 5% or 10% elongation (Figure 4-12A). 5% ( $p < 0.001$ ) and 15% strain ( $p < 0.01$ ) decreased MMP-2 mRNA expression levels by 12.5 and 10-fold respectively, whereas no alteration was observed with 10% strain ( $p > 0.05$ ) (Figure 4-12A). In contrast, there was a significant increase in MMP-3 gene expression after 5% (1.8-fold,  $p < 0.01$ ) and 15% strain (2-fold,  $p < 0.001$ ) (Figure 4-12A). MMP-1 transcription was not sensitive to tensile strain.

**Young OAF cells:** 5%, 10% and 15% strains significantly decreased ADAMTS-5 gene expression by 3.1, 1.4 and 1.8-fold respectively ( $P < 0.001$ ) (Figure 4-12B). 5% and 15% elongation increased MMP-3 gene expression by 2.2 and 3.3-fold respectively ( $p < 0.001$ ), whereas 10% elongation decreased MMP-3 mRNA (1.9-fold;  $p < 0.001$ ) (Figure 4-12B). In complete contrast to MMP-3, 5% ( $p < 0.01$ ) and 15% strain ( $p < 0.001$ ) significantly decreased MMP-2 gene expression by 2.6 and 3.4-fold respectively, whereas 10% elongation increased MMP-2 mRNA levels (1.8-fold;  $p < 0.001$ ) (Figure 4-12B). There was also a decrease in MMP-1 mRNA levels after 10% strain (2-fold;  $p < 0.001$ ), but no alterations were observed after 5% or 15% strain ( $p > 0.05$ ) (Figure 4-12B).

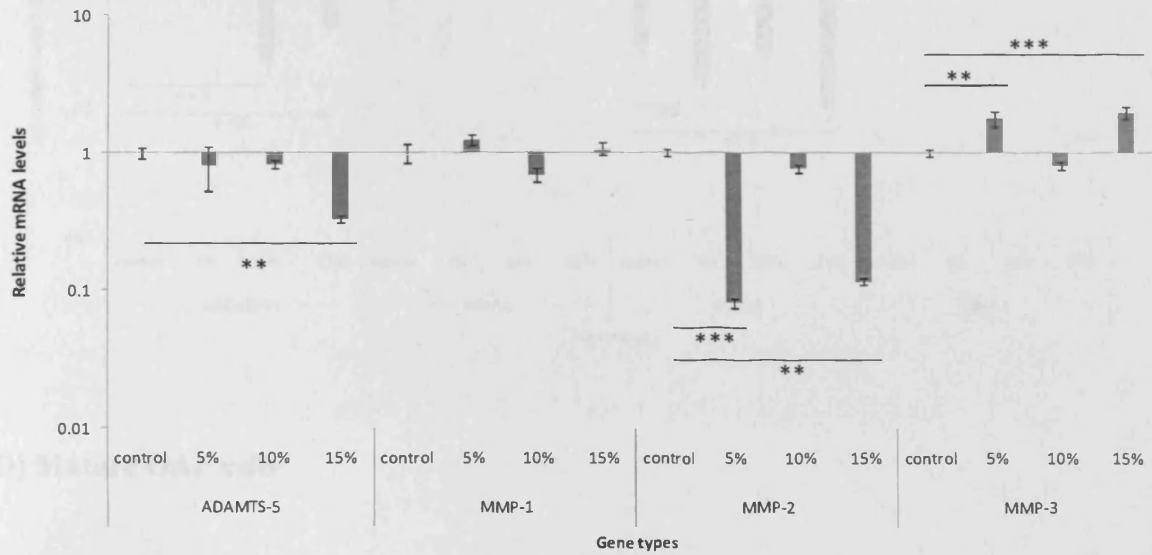
**Mature NP cells:** 10% and 15% strain significantly inhibited ADAMTS-5 gene expression (1.3 and 2.3-fold;  $p < 0.0001$ ) and MMP-2 mRNA levels (1.9-fold;  $p < 0.01$  and 3.2 fold;  $p < 0.001$  respectively) (Figure 4-12C). In contrast, 10% (3.6-fold;  $p < 0.01$ ) and 15% elongation (2.9-fold,  $p < 0.05$ ) significantly increased MMP-1 mRNA levels (Figure 4-12C). Similarly, 5% and 15% strain increased MMP-3 mRNA levels by 3.8 ( $p < 0.01$ ) and 3.5-fold ( $p < 0.001$ ) respectively (Figure 4-12C).

**Mature OAF cells:** 5% elongation increased MMP-1 (1.4-fold;  $p < 0.01$ ) but in contrast, 10% elongation reduced its expression (1.9-fold;  $p < 0.01$ ). MMP-2 was reduced at 5% (3-fold;  $p < 0.01$ ), 10% (1.4-fold;  $p < 0.05$ ) and 15% (3-fold,  $p < 0.001$ ). 15% elongation increased ADAMTS-5 (2-fold;  $p < 0.01$ ) (Figure 4-12D). MMP-3 transcription was not mechano-responsive.

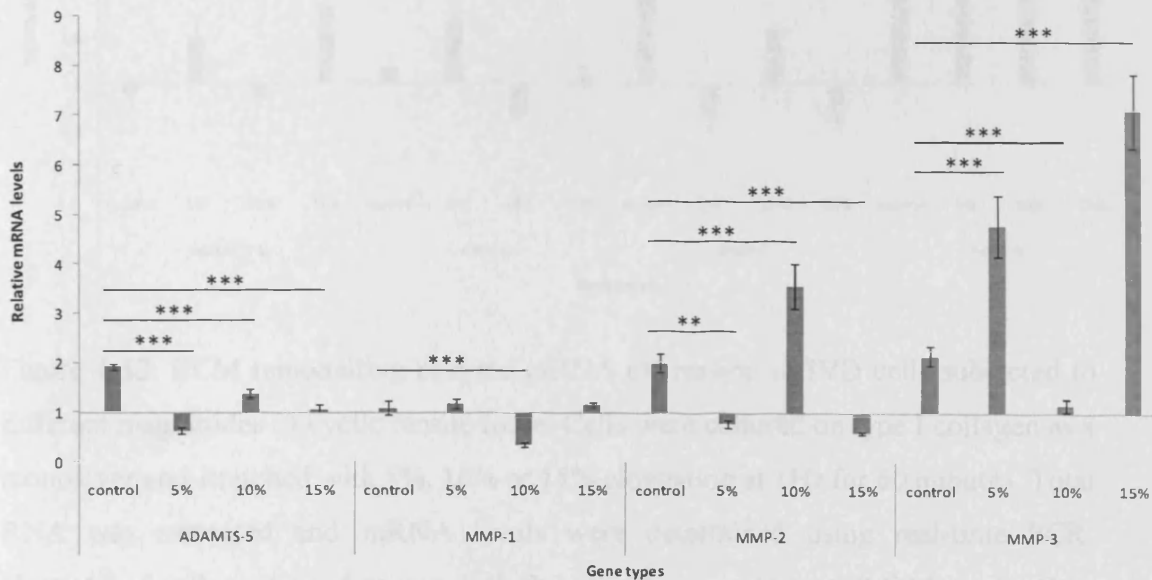
ADAMTS-4 and MMP-9 gene expression were also investigated using real-time PCR. Due to the huge variability in the expression of ADAMTS-4 and MMP-9 between individual samples; i.e. either present or absent, statistical analysis was unable to be performed (data not shown).

Chapter 4: The effect of different cyclic tensile strain on cytoskeletal elements and extracellular matrix metabolism of bovine intervertebral disc cells *in vitro*

(A) Young NP cells

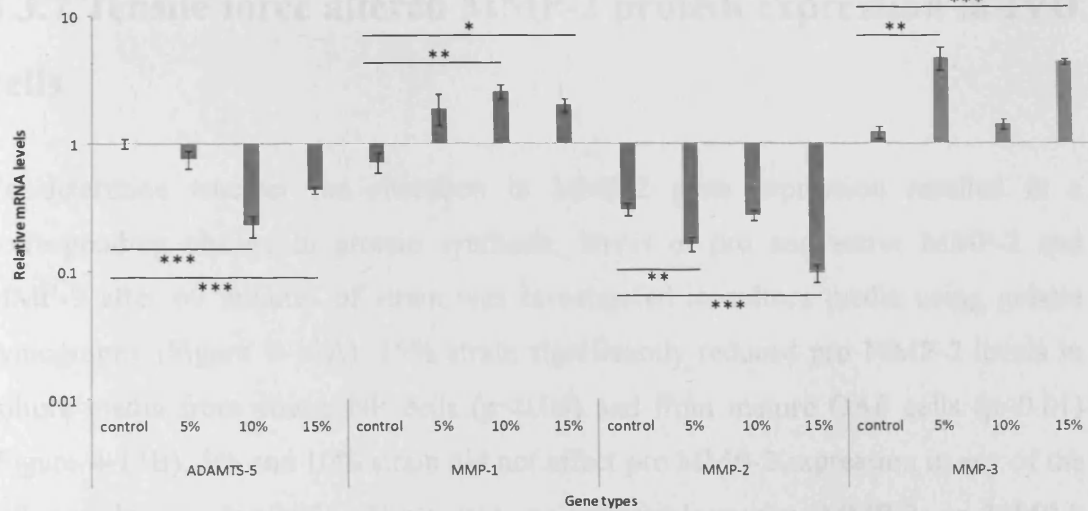


(B) Young OAF cells



Chapter 4: The effect of different cyclic tensile strain on cytoskeletal elements and extracellular matrix metabolism of bovine intervertebral disc cells *in vitro*

(C) Mature NP cells



(D) Mature OAF cells

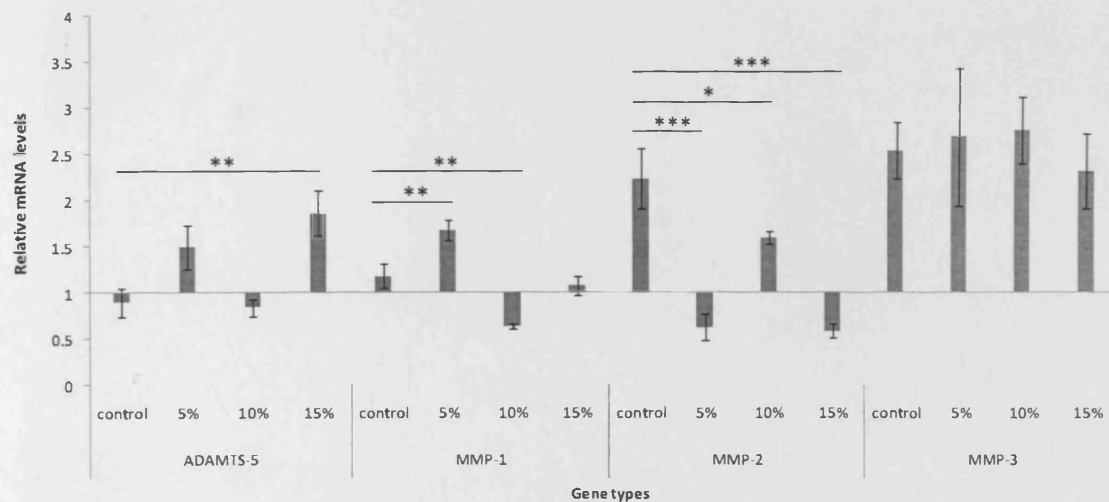


Figure 4-12. ECM remodelling enzyme mRNA expression in IVD cells subjected to different magnitudes of cyclic tensile force. Cells were cultured on type I collagen as a monolayer and stretched with 5%, 10% or 15% elongation at 1Hz for 60 minutes. Total RNA was extracted and mRNA levels were determined using real-time PCR. Unstretched cells were used as a control. Data are shown as Mean  $\pm$  S.E.M. (n=5). Data were normalised to the house-keeping gene GAPDH and were relative to unstretched young NP cells. \*\*\*:  $p \leq 0.001$ , \*\*:  $p \leq 0.01$ , \*:  $p \leq 0.05$  when compared with control group. [A]: young NP, [B]: young OAF, [C]: mature NP, [D]: mature OAF.



### **4.3.7 Tensile force altered MMP-2 protein expression in IVD cells**

To determine whether the alteration in MMP-2 gene expression resulted in a corresponding change in protein synthesis, levels of pro and active MMP-2 and MMP-9 after 60 minutes of strain was investigated in culture media using gelatin zymography (Figure 4-13A). 15% strain significantly reduced pro MMP-2 levels in culture media from young NP cells ( $p < 0.05$ ) and from mature OAF cells ( $p < 0.01$ ) (Figure 4-13B). 5% and 10% strain did not affect pro MMP-2 expression in any of the cell populations ( $p > 0.05$ ). There was no detectable active MMP-2 or MMP-9 expression in the culture media from any of these experimental conditions.

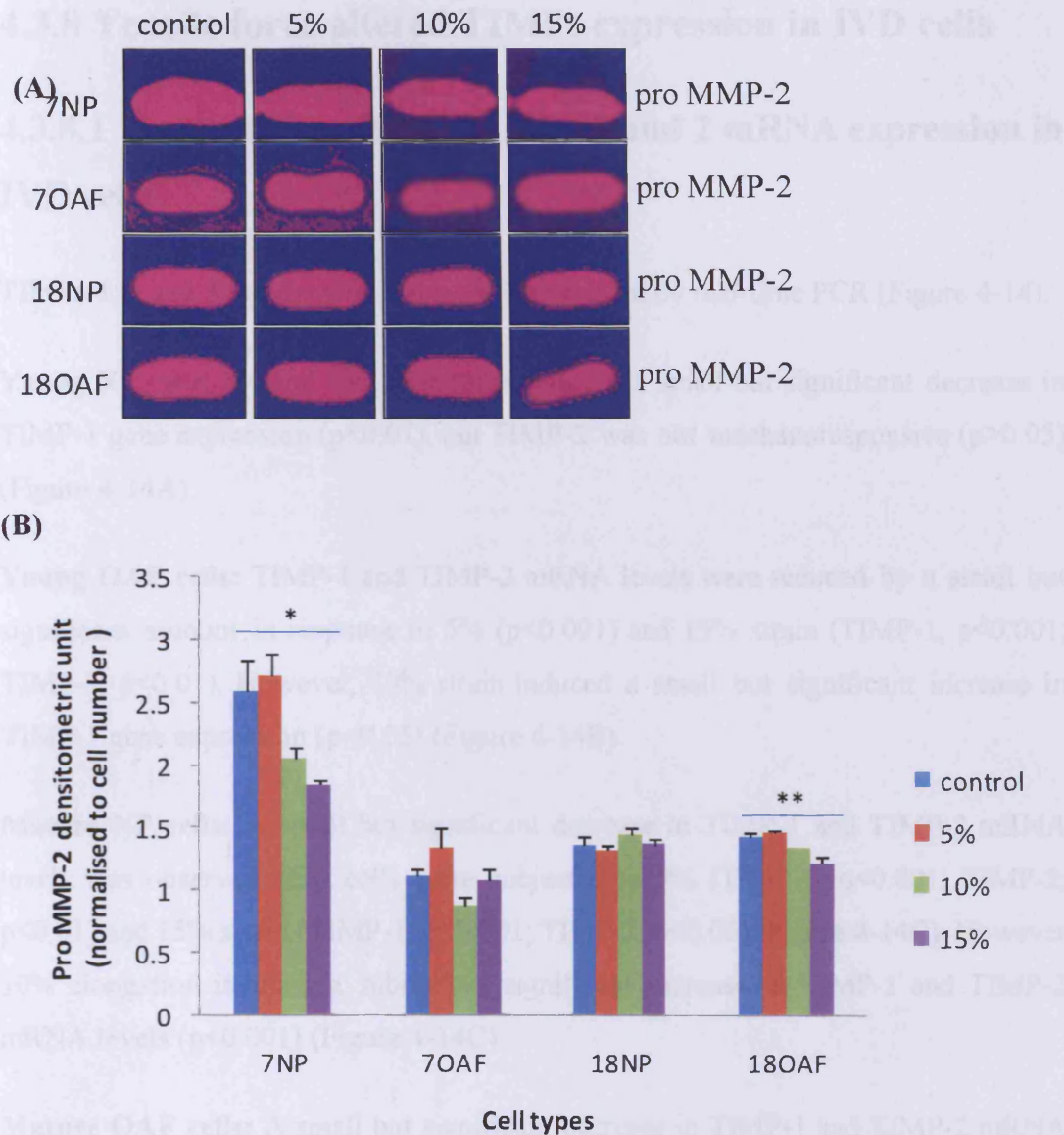


Figure 4-13 Pro MMP-2 in culture media from bovine NP and OAF cells subjected to tensile strain as detected by [A] gelatin zymography. Cells were cultured on type I collagen as a monolayer and stretched with 5%, 10% or 15% elongation at 1Hz for 60 minutes. Unstretched cells were used as a control. Cellular protein was extracted using 0.9% Triton X-100 plus protease inhibitors. [B] Media samples were normalised to cell number and denatured without reduction. To remove the potential error induced by individual gel staining, data were normalised to a standard. Data are shown as Mean  $\pm$  S.E.M. (n=5). \*\*:  $p \leq 0.01$ , \*:  $p \leq 0.05$  when compared with control group.

### 4.3.8 Tensile force altered TIMPs expression in IVD cells

#### 4.3.8.1 Tensile force altered TIMPs-1 and 2 mRNA expression in IVD cells

TIMPs-1, 2 and 3 gene expression were investigated by real-time PCR (Figure 4-14).

**Young NP cells:** 5% and 15% elongation induced a small but significant decrease in TIMP-1 gene expression ( $p < 0.01$ ), but TIMP-2 was not mechanoresponsive ( $p > 0.05$ ) (Figure 4-14A).

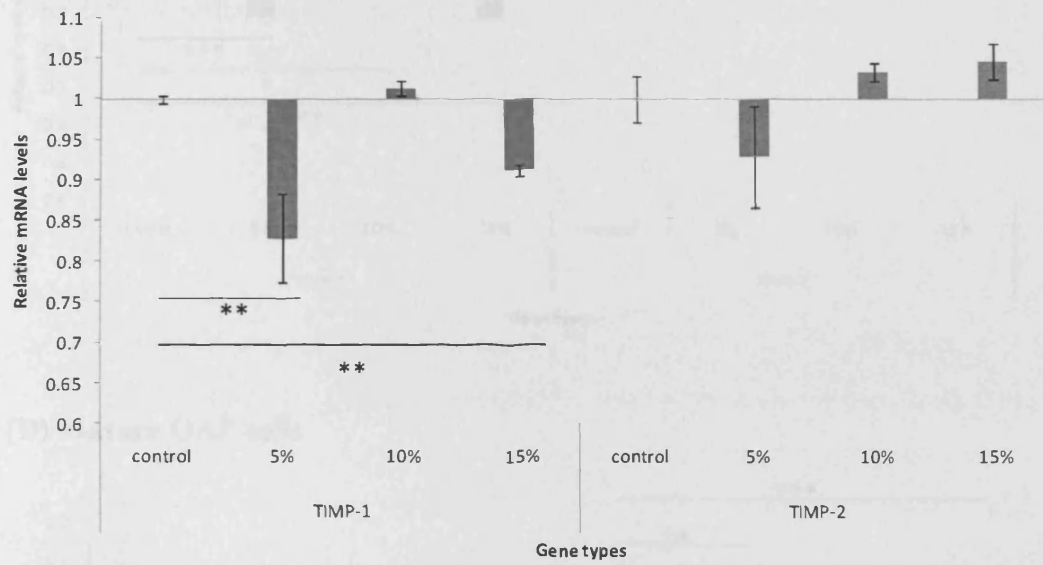
**Young OAF cells:** TIMP-1 and TIMP-2 mRNA levels were reduced by a small but significant amount in response to 5% ( $p < 0.001$ ) and 15% strain (TIMP-1,  $p < 0.001$ ; TIMP-2,  $p < 0.01$ ). However, 10% strain induced a small but significant increase in TIMP-1 gene expression ( $p < 0.05$ ) (Figure 4-14B).

**Mature NP cells:** A small but significant decrease in TIMP-1 and TIMP-2 mRNA levels was observed after cells were subjected to 5% (TIMP-1,  $p < 0.001$ ; TIMP-2,  $p < 0.01$ ) and 15% strain (TIMP-1,  $p < 0.001$ ; TIMP-2,  $p < 0.05$ ) (Figure 4-14C). However, 10% elongation induced a subtle but significant increase in TIMP-1 and TIMP-2 mRNA levels ( $p < 0.001$ ) (Figure 4-14C).

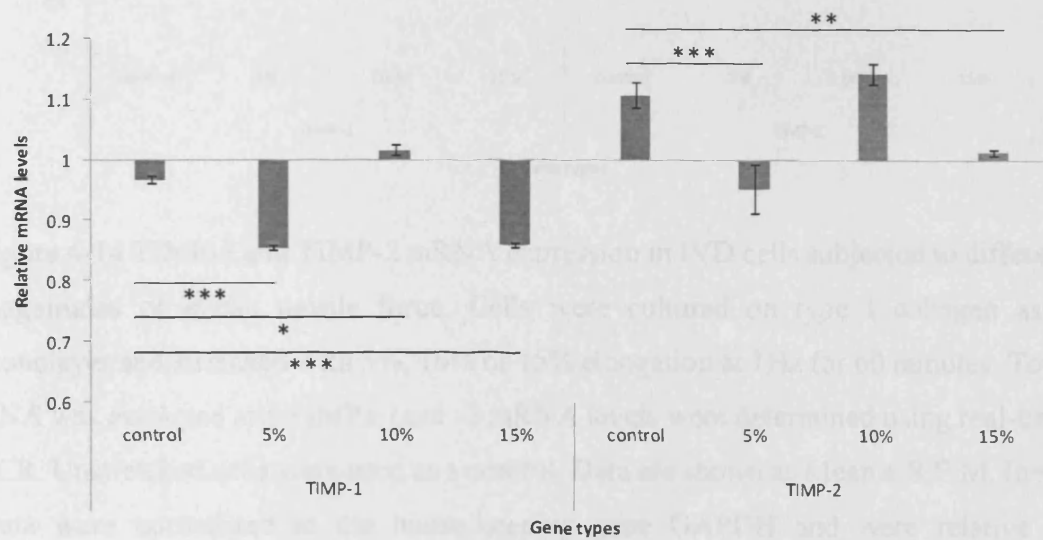
**Mature OAF cells:** A small but significant decrease in TIMP-1 and TIMP-2 mRNA levels was observed after 5% ( $p < 0.001$  and  $0.01$  respectively) and 15% strain ( $p < 0.001$ ) (Figure 4-14D). 10% elongation had no effect on TIMP-1 and 2 transcription.

There was no detectable TIMP-3 gene expression in IVD cells in response to CTS (Data not shown).

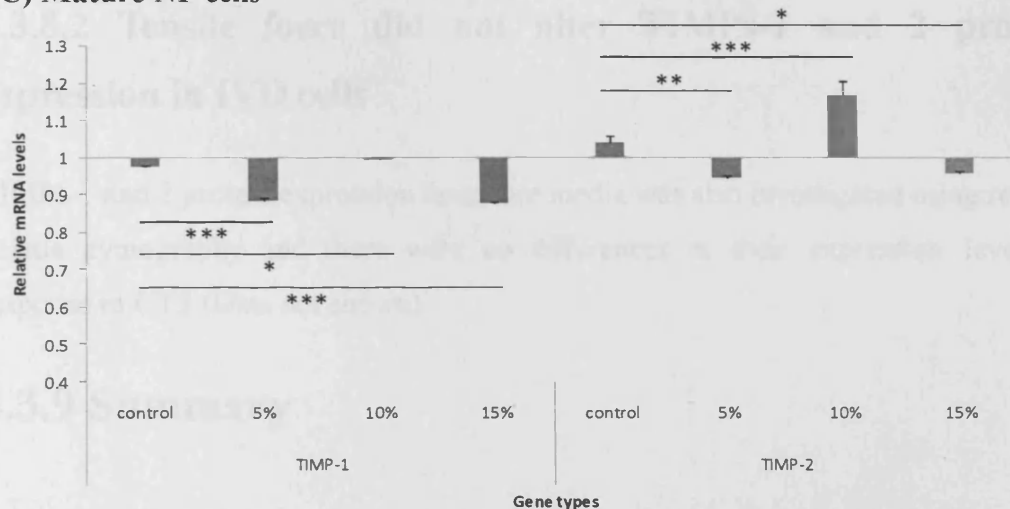
(A) Young NP cells



(B) Young OAF cells



(C) Mature NP cells



(D) Mature OAF cells

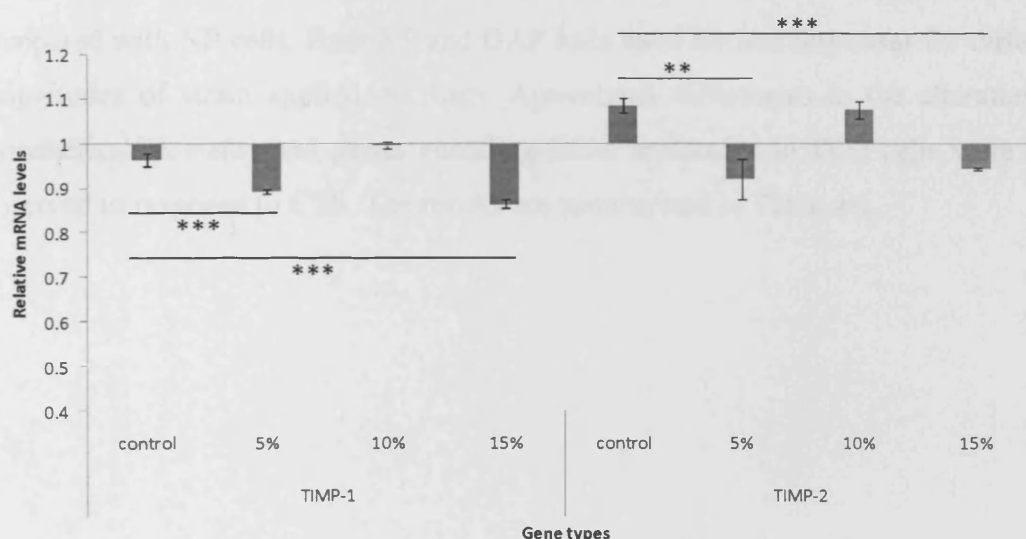


Figure 4-14 TIMP-1 and TIMP-2 mRNA expression in IVD cells subjected to different magnitudes of cyclic tensile force. Cells were cultured on type I collagen as a monolayer and stretched with 5%, 10% or 15% elongation at 1Hz for 60 minutes. Total RNA was extracted and TIMPs-1 and -2 mRNA levels were determined using real-time PCR. Unstretched cells were used as a control. Data are shown as Mean  $\pm$  S.E.M. (n=5). Data were normalised to the house-keeping gene GAPDH and were relative to unstretched young NP cells. \*\*\*:  $p \leq 0.001$ , \*\*:  $p \leq 0.01$ , \*:  $p \leq 0.05$  when compared with control group. [A]: young NP, [B]: young OAF, [C]: mature NP, [D]: mature OAF.

#### **4.3.8.2 Tensile force did not alter TIMPs-1 and 2 protein expression in IVD cells**

TIMPs-1 and 2 protein expression in culture media was also investigated using reverse gelatin zymography and there were no differences in their expression levels in response to CTS (Data not shown).

#### **4.3.9 Summary**

Reflecting the results described in Chapter 3 (effect of 10% strain for different periods), both NP and OAF cells cultured on type I collagen as a monolayer responded to mechanical stimulation i.e. CTS. OAF cells appeared to be more responsive to CTS compared with NP cells. Both NP and OAF cells have distinct responses for different magnitudes of strain applied on them. Age-related differences in the alteration of cytoskeletal elements and genes encoding ECM molecules in IVD cells were also observed in response to CTS. The results are summarised in Table 4-1.

Chapter 4: The effect of different cyclic tensile strain on cytoskeletal elements and extracellular matrix metabolism of bovine intervertebral disc cells *in vitro*

Table 4-1 Summary for the effects of cyclic tensile force on bovine intervertebral disc cells

		young NP			mature NP			young OAF			mature OAF		
		5%	10%	15%	5%	10%	15%	5%	10%	15%	5%	10%	15%
<b>β-actin</b>	mRNA	↑	↔	↑	↔	↔	↔	↑	↑	↑	↔	↔	↔
	protein	↔	↔	↑	↔	↔	↑	↑	↑	↑	↔	↔	↑
<b>β-tubulin</b>	mRNA	↓	↔	↓	↓	↔	↓	↔	↑	↔	↓	↓	↓
	protein	↓	↔	↓	↓	↔	↓	↓	↑	↓	↓	↔	↓
<b>vimentin</b>	mRNA	↔	↔	↓	↔	↔	↔	↓	↓	↓	↓	↓	↓
	protein	↔	↔	↓	↔	↔	↔	↔	↔	↓	↔	↔	↔
<b>type I collagen</b>	mRNA	↑	↑	↑	↔	↔	↔	↑	↔	↑	↔	↔	↔
<b>type II collagen</b>	mRNA	↔	↔	↔	↔	↔	↔	↔	↔	↔	↔	↓	↔
<b>aggrecan</b>	mRNA	↓	↔	↓	↓	↔	↓	↔	↔	↔	↓	↓	↓
<b>ADAMTS-5</b>	mRNA	↔	↔	↓	↔	↓	↓	↓	↓	↓	↔	↔	↑
<b>MMP-1</b>	mRNA	↔	↔	↔	↔	↑	↑	↔	↓	↔	↑	↓	↔
<b>MMP-2</b>	mRNA	↓	↔	↓	↓	↔	↓	↓	↑	↓	↔	↑	↔
	protein	↔	↔	↓	↔	↔	↔	↔	↔	↔	↔	↔	↓
<b>MMP-3</b>	mRNA	↑	↔	↑	↑	↔	↑	↑	↔	↑	↔	↔	↔
<b>TIMP-1</b>	mRNA	↓	↔	↓	↓	↑	↓	↓	↑	↓	↓	↔	↓
	protein	↔	↔	↔	↔	↔	↔	↔	↔	↔	↔	↔	↔
<b>TIMP-2</b>	mRNA	↔	↔	↔	↓	↑	↓	↓	↔	↓	↓	↔	↓
	protein	↔	↔	↔	↔	↔	↔	↔	↔	↔	↔	↔	↔

## 4.4 Discussion

The magnitude of strain is an important influencing factor involved in load-induced disc degeneration. Therefore, in this study, three different strains were investigated: 5%, 10% and 15%, which represent the low, medium and high intensities respectively of strain *in vivo*. In order to address whether age affects the response of cells to CTS, 7 day and 18 month old bovine disc cells were used. To exclude the influence of other factors such as loading frequency, 1Hz was applied for the strains, which is equal to the physiological frequency generated by walking during daily life *in vivo* (Skaggs et al., 1994).

### 4.4.1 Effect of CTS on the cytoskeletal elements in NP and OAF cells

As observed in Chapter 3, each strain generally induced similar alterations in the organisation of the cytoskeletal elements, although some variations were observed. For actin filaments, all strains significantly induced an increase in the formation of F-actin stress fibres. Consistent with the reorganisation of the actin cytoskeleton, there was an increase in  $\beta$ -actin mRNA and protein expression, suggesting a pivotal role for actin filaments during mechanotransduction induced by CTS within cells.

There were some zonal and aged-related differences in  $\beta$ -actin expression between NP and OAF cells subjected to CTS. Young OAF cells were more reactive to CTS compared with young NP cells, with increased  $\beta$ -actin gene and protein expression in response to all three magnitudes of strain. Considering the distinct mechanical environments between NP and OAF *in vivo*, these different responses may reflect the different mechanical features between NP and OAF cells. 5% and 10% elongation did not induce any alteration in  $\beta$ -actin protein expression in mature OAF cells when compared with young OAF. It may be that mature OAF cells react more slowly or have a higher threshold to CTS, limiting the mechanotransduction response in mature OAF cells, which over time could induce a loss of tissue homeostasis.



Previous studies have shown that one of the main functions of  $\beta$ -tubulin filaments within cells is intra-cytoplasmic transport (Vale, 1987), which coincides with the intense staining of  $\beta$ -tubulin filaments around the cell nucleus. After strain, the decrease or disappearance of the  $\beta$ -tubulin staining around the nucleus reflects the reorganisation of microtubule filaments within IVD cells as regulated by CTS.  $\beta$ -tubulin gene and protein expression were also altered by different magnitudes of strain, and significant zonal and age-related differences were observed. For young NP cells, 10% elongation did not change  $\beta$ -tubulin gene and protein expression, however, 10% strain increased  $\beta$ -tubulin mRNA and protein levels in young OAF cells. This suggests that NP and OAF cells have distinct reactivities to CTS, reflecting their different cellular phenotype and morphology. A significant age-related difference was also observed when subjected to 10% elongation, with increased  $\beta$ -tubulin mRNA synthesis in young OAF cells but decreased levels in mature OAF cells. This difference illustrates that ageing may influence the turnover of  $\beta$ -tubulin in OAF cells in response to a physiological strain, which may play an important role in mechanotransduction. However, the mechanism of this age-related difference in  $\beta$ -tubulin is not clear, although very limited studies have shown that microtubule assembly and its regulation may be involved (Wagner, 1989; Putnam et al., 2001).

As observed in Chapter 3, OAF cells showed greater changes in vimentin organisation and expression in response to CTS when compared with the NP cells, irrespective of age. Only 15% strain significantly decreased vimentin gene and protein expression in young NP cells and none of the strains affected vimentin expression in mature NP cells. Although OAF cells were more responsive to strain-induced changes in vimentin gene expression, only 15% strain in young cells translated to a detectable inhibition of protein expression. Clearly vimentin is less responsive than actin, and to a lesser extent tubulin, to low physiological strain but is sensitive to the higher physiological strains that would be experienced *in vivo*. As with actin and tubulin, there is an age-related decrease in vimentin synthesis, suggesting that the cells lose some of their ability to respond to physiological loads with age, which may affect the ability to maintain tissue homeostasis.

#### 4.4.2 Effect of CTS on ECM synthesis

Types I and II collagen are major ECM components in the IVD, and due to their distinct distribution within the tissue it is reasonable to assume that type I collagen mainly endures tensile force whereas type II collagen mainly resists compressive loading *in vivo*. Therefore, when cells are subjected to CTS, it is anticipated that more type I collagen will be synthesised to adapt to the mechanical stimulation applied to the cells. Our results are consistent with this hypothesis, with increased type I collagen mRNA content in young NP and OAF cells but no alteration in type II collagen gene expression, in agreement with previous studies (Matsumoto et al., 1999). There was however no alteration in type I collagen mRNA levels within mature NP and OAF cells, suggesting a lower reactivity to CTS in cells from mature tissue. Despite no alteration in type II collagen in young and mature NP and young OAF cells, 10% elongation significantly decreased type II gene expression in mature OAF cells, further illustrating that CTS is an important factor contributing to fibroblast maintenance of the cell phenotype.

Aggrecan is another important ECM component in IVD tissue and its main function is to resist compressive loading. Therefore, aggrecan synthesis should be decreased or unchanged when cells are subjected to tensile force. Such a response was indeed found, which is consistent with previous studies (Rannou et al., 2003; Benallaoua et al., 2006). Interestingly, a significant age-related difference was observed: aggrecan and type II collagen appear to be co-ordinately regulated, with CTS also significantly decreasing aggrecan gene expression in mature OAF cells, whereas no alteration in aggrecan mRNA levels was found in young OAF cells. Considering these age-related differences in types I and II collagen and aggrecan expression induced by CTS, it is interesting to find that the increased expression of type I collagen, the major ECM component that resists stretching, was less responsive in mature OAF cells, whereas the inhibitory expression of type II collagen and aggrecan, which are the ECM components that resist compressive loading, were more actively regulated in ageing cells. These abnormal syntheses of ECM molecules in the distinct cell populations in response to CTS could cause a loss of homeostasis, which may subsequently result in disc degeneration.

### 4.4.3 Effect of CTS on ECM remodelling proteases and inhibitors

ECM remodelling enzymes play important roles in modulating ECM turnover. The alteration in expression of the aggrecanases, MMPs and TIMPs within IVD cells in response to CTS was therefore investigated. ADAMTS-5 gene expression was significantly inhibited within young NP and OAF as well as mature NP cells in response to CTS. ADAMTS-5 is one of the major enzymes that degrade proteoglycans *in vivo*, which predominantly affects the function of aggrecan in IVD. When subjected to CTS, there was a decline in aggrecan synthesis in cells. The expression of aggrecanases, as expected, was also decreased. Interestingly, a different reactivity between NP and OAF cells in response to different magnitudes of strain were observed. There was generally an inhibition or no effect on ADAMTS-5 expression except for an increase in ADAMTS-5 gene levels in mature OAF cells when subjected to 15% elongation. This is further evidence that ageing may contribute to abnormal ECM remodelling in IVD, especially in OAF cells in response to high physiological strain. ADAMTS-4 gene expression was also investigated in this study. However, because ADAMTS-4 mRNA was either absent or at a low level in these samples, statistical analysis could not be performed.

MMP-1 is a collagenase, and its main function is to degrade type I collagen which is most abundant in the OAF of IVD. To address the role of MMP-1 in the ECM remodelling process induced by CTS, the alteration of MMP-1 in combination with type I collagen expression needs to be considered. In young NP and OAF cells, type I collagen gene expression was generally elevated but MMP-1 gene expression was unchanged or decreased. Young NP and OAF cells therefore appear to react positively to CTS. However, type I collagen mRNA levels were unchanged whereas there was an increase in MMP-1 gene expression in mature NP cells subjected to all magnitudes of strain. This suggests that strain may induce catabolism in mature NP cells, which would significantly affect tissue homeostasis.

MMP-3 has the ability to cleave many ECM components and is believed to be involved in the activation of other MMPs such as MMP-1 (Murphy et al., 1987; Suzuki et al., 1990), suggesting that MMP-3 takes part in ECM degradation. Previous studies have also shown that MMP-3 expression is necessary for wound repair (Armstrong and Jude, 2002), and more importantly, a requirement in cartilage formation (Pelttari et al., 2008). The absence of MMP-3 in cells neither prevented nor reduced cartilage destruction (Mudgett et al., 1998) illustrating that MMP-3 is a requisite for the turnover of the ECM and cartilage homeostasis. Therefore, the increased MMP-3 gene expression within cells induced by CTS may suggest that strain significantly accelerates ECM turnover. None of the strains used induced any alterations in MMP-3 gene expression in mature OAF cells, suggesting that ageing could slow down the response of OAF cells to tensile stimulation, and may affect matrix remodelling.

TIMP-1 is the major inhibitor of MMP-1 and MMP-3 *in vivo*, forming 1:1 stoichiometric complexes with these proteases (Raif, 2008). CTS inhibited TIMP-1 gene expression but did not apparently change its protein expression. There are two explanations for this, firstly the lag of protein synthesis behind changes in gene expression is longer than anticipated, therefore these time points were too early. Secondly and perhaps more likely is that 60 minutes of CTS induced only a transient transcriptional response that had relatively little effect on overall protein synthesis, which could not be detected by reverse gelatin zymography.

MMP-2 is a gelatinase, and its main function is to degrade type IV collagen and degraded fibrillar collagen. The alteration of MMP-2 gene expression in IVD cells is inconsistent, suggesting that different magnitudes of strain may have different regulatory effects on ECM metabolism. It was noticed that NP and OAF cells displayed distinctly different responses in MMP-2 gene expression, especially in mature cells. Previous studies investigating the effects of tensile force on MMP-2 expression in different cell types indicated cell/tissue specific responses. For example, MMP-2 gene and protein expression were not altered by tensile force in chondrocytes (Honda et al., 2000), whereas stretching significantly increased MMP-2 gene and protein expression in arteries (Grabellus et al., 2007) and fibroblasts (Berry et al., 2003). Therefore, this

difference in MMP-2 gene expression between NP and OAF cells may reflect their distinct phenotypes.

TIMP-2 is the major inhibitor for MMP-2 *in vivo*, and also plays an important role during the pro MMP-2 activation process in the matrix. The alteration in TIMP-2 expression in response to different magnitudes of strain is distinct, especially between 5% and 10% elongation, suggesting that magnitudes of strain may have different effects on MMP-2 activity. However, due to the complex function of TIMP-2 in pro MMP-2 activation as described previously (Section 3.4), it is difficult to conclude that 10% elongation has an opposing effect on MMP-2 activity in IVD cells when compared with 5% and 15% elongation.

Comparing the data presented here with the results in Chapter 3, there are some inconsistencies in gene /protein expression in young NP and OAF cells in response to 10% elongation such as  $\beta$ -tubulin, vimentin and type I collagen. Many influencing factors including individual animal differences, cell passage and cell density can induce these variations (personal communication with Dr. Jane Millward-Sadler, Manchester University). Although a standard procedure was set up for different experiments, it was still difficult to ensure all of the conditions remained constant. For example, confluency can greatly change the mechanical and metabolic behaviour of the cell (Gal et al., 1981; Jaasma et al., 2006), but it is very difficult to control the exact time of detaching cells from the culture flask when cells reach confluency. In addition, although the cells were reseeded on Bioflex culture plates for stretching experiments at the same cell density, it was difficult to ensure the cell density still remained the same after 24 hours of proliferation. All of these variations may alter cell behaviour, thereby inducing some of the differences observed in response to similar CTS regimes.

In summary, CTS significantly altered the organisation of F-actin and  $\beta$ -tubulin filaments, but not the vimentin architecture. CTS increased  $\beta$ -actin gene and protein expression but decreased vimentin content. All of these results indicate that the actin filaments are the major cytoskeletal components that respond to tensile force in IVD cells. ECM remodelling, including alterations in molecules involved in catabolism and anabolism, was observed with CTS promoting type I collagen synthesis and inhibiting

aggrecan expression, thereby promoting a fibroblast rather than a chondrogenic phenotype. Another interesting finding is that the cellular response is magnitude-dependent. 5% and 15% strains induced similar alterations in cells but 10% elongation is quite distinct. The mechanism of this difference is not clear, although it is thought that MAPK (ERK) signalling may be involved in mechanotransduction (Lee et al., 1999; Honda et al., 2000). More importantly, it was found that ageing is an important influencing factor for ECM remodelling induced by CTS. It appears that there is some delay or a slower response in reorganisation/synthesis of the cytoskeletal and ECM components after CTS in mature cells when compared with younger cells. These differences would greatly influence the ECM remodelling process in adapting to tensile force.

#### **4.4.4 Conclusion**

- CTS induces significant alterations in the organisation and synthesis of cytoskeletal elements and ECM molecules (anabolic and catabolic).
- Magnitude of strain is an important factor for the alterations induced by CTS.
- F-actin is the major cytoskeletal element that responds to CTS in IVD cells.
- Type I collagen is increased but aggrecan decreased in response to CTS in NP and OAF cells.
- Development appears to be an important influencing factor for mechanotransduction.

# CHAPTER 5.

The effects of cyclic compressive loading on  
cytoskeletal elements and extracellular  
matrix metabolism in bovine intervertebral  
disc cells cultured in agarose

## 5.1 Background

One of the main functions of the spine is to resist the upper body weight. Therefore, compressive loading is the major mechanical stimulus applied to IVDs. Using an intradiscal compression sensor, the physiological compressive loads *in vivo* have been determined. Compressive forces on the lumbar spine are 700-1000N when sitting erect, 150-250N when lying, 500-800N when standing erect, and 1900N when stooping to lift a 10kg weight (Nachemson and Morris, 1964; Sato et al., 1999). Recent studies performed by Wilke confirmed these results, and suggested that the absolute pressure values in disc were 0.5MPa when standing, 0.1-0.25MPa when lying, 0.55MPa when sitting erect and 1.1-1.8MPa when holding a 20kg weight (Wilke et al., 1999; Wilke et al., 2001). The difference between these studies is the pressure in the IVD when sitting, which was also observed by Rohlmann when determining the resultant force acting on the vertebral body replacement implant (Rohlmann et al., 2008), suggesting that there may be two different groups due to the patients' condition: in one group the spinal loading is higher for sitting than for standing and in the other group it is the opposite.

Due to the different biological functions of the OAF when compared to the NP, the compressive pressure applied on the OAF should be much smaller. This was confirmed by a recent study using discogram technology, in which the peak compressive load in NP was 199psi but only 45psi was observed in OAF. However, torn lamellae can induce a lower distribution of compressive loading in NP and a rapid increase in pressure in OAF (Lee et al., 2004), suggesting that the main function of the OAF may be to maintain the compressive stress in the NP to resist the loading applied to the disc.

When compressive loading is applied to the disc, deformation of the ECM and cells occurs, resulting in alterations in cell metabolism to maintain ECM turnover. Many *in vitro* studies have addressed these biological responses, but the results are inconsistent. Using disc tissue and disc cells cultured in alginate, dynamic compressive loading (1MPa, 1Hz) significantly increased types I and II collagen and aggrecan synthesis in both NP and OAF cells, suggesting anabolic changes after loading (Wenger et al., 2005; Wang et al., 2007; Korecki et al., 2008). Dynamic compressive loading also increased



the oxygen concentration, reduced lactate accumulation, and promoted oxygen consumption and lactate production in IVD, illustrating an accelerated transport of nutrients when the IVD was subjected to dynamic compressive loads (Huang and Gu, 2008). However, studies performed *in vivo* suggested that similar levels of dynamic compressive loading stimulated catabolic gene expression such as MMP-3 and MMP-13 but did not influence (Maclean et al., 2004) or down-regulated (MacLean et al., 2003) types I and II collagen and aggrecan gene expression in both NP and OAF cells. The effect of static compressive loading on the ECM remodelling process was also investigated and again, the results were confusing. Chen et al found that 25% compressive strain promoted transcription of types I and II collagen, aggrecan, biglycan, decorin and lumican in OAF cells but did not induce any alteration in NP cells (Chen et al., 2004). However, Wang et al suggested that 1MPa static compressive loading decreased types I and II collagen and aggrecan gene expression in IVD cells (Wang et al., 2007). The differences between these studies may be caused by different species and culture systems used, as well as the magnitude and duration of the loads applied, suggesting that the remodelling of the ECM in adapting to compressive loading in IVD cells is regulated by multiple factors. Further studies are needed to determine the precise mechanism.

Recent studies have shown that the linkage provided by the cytoskeleton may be involved in mechanotransduction between the cells and their surrounding extracellular matrix (Errington et al., 1998; Hayes et al., 1999; Bruehlmann et al., 2002; Chen et al., 2004; Li et al., 2007b). Therefore, the alteration in ECM metabolism of the NP and OAF cells of the IVD in response to compressive loading is likely to be dependent upon their cytoskeletal composition. With age, there is a redistribution of mechanical stress in the disc (Adams et al., 1996) and an alteration of the cytoskeleton was also observed (Ronot et al., 1988; Li et al., 2007b). This may significantly change the metabolism of the IVD cells, subsequently inducing a loss of tissue homeostasis, and onset of disc degeneration. With the exception of a few studies which have investigated vimentin changes in bovine cells under static loading (Chen et al., 2004), very little is known about the content and organisation of the three major cytoskeletal elements in the two distinct IVD cell populations when subjected to compressive loading. It is also unclear

Chapter 5: The effects of cyclic compressive loading on cytoskeletal elements and extracellular matrix metabolism in bovine intervertebral disc cells cultured in agarose

---

whether there are differences in cytoskeletal elements in the disc cells in response to compressive loading with skeletal maturity.

The aim of the work described in this chapter was to: (1) Fully characterise the organisation and expression of the three major cytoskeletal elements: F-actin,  $\beta$ -tubulin and vimentin in the NP and OAF of young (7-day-old) and mature (18-month-old) bovine IVD cells in response to dynamic compressive loading, and (2) Investigate the effect of dynamic compressive loading on ECM remodelling processes in young and mature NP and OAF cells.

## **5.2 Materials and methods**

All chemicals were obtained from Sigma (Poole, UK) unless otherwise stated and were of analytical grade or above.

### **5.2.1 Cell isolation**

Bovine tails were obtained from 7 day and 18 month old steers (Section 2.2.1) and cell isolation and monolayer culture procedures are as described previously (Section 3.2.1).

### **5.2.2 Cell culture in agarose gel**

Cells were diluted to  $4 \times 10^6$ /ml using DMEM/F12 (1:1) containing 1% penicillin-streptomycin and fungizone, followed by incubation at 37°C. 0.39g of type VII low temperature gelling agarose was weighed in a small glass bottle and 6.5ml of Earle's Balanced Salt Solution (EBSS) was pipetted into the bottle to make a 6% agarose solution. The agarose was autoclaved then cooled down to 37°C on a roller apparatus to prevent gel formation. 6.5ml of cells at 37°C was then added to 6.5ml of agarose solution carefully and quickly to make a 3% agarose gel containing cells and mixed thoroughly. The mixture was then poured into a 60mm diameter sterile petri-dish carefully to make sure there was no air bubble formation. The covered petri-dish was stored at room temperature until the gel had set. A 10mm diameter biopsy punch was then used to cut the agarose plugs to a depth of 15mm, which were carefully transferred to a 24-well culture plate. Agarose plugs were cultured in DMEM/F12 (containing 10% FBS, 1% penicillin-streptomycin, 1% fungizone) for 24 hours at 37°C, after which the culture media was discarded and replaced with 2ml of fresh DMEM/F12 culture media (containing ITS, 1% penicillin-streptomycin, fungizone). The agarose plugs were cultured for 48 hours before the compressive loading experiment was performed.

### 5.2.3 Application of cyclic compressive loading

To prevent the 3% agarose plugs slipping sideways under cyclic compressive loading, an autoclaved 1% agarose solution was made up using PBS buffer. 3ml of this 1% agarose solution was then pipetted into each well of a 6-well plate (Invitrogen, Paisley, UK), and stored at room temperature until the gel had set. A sterile 12mm diameter biopsy punch was used to cut a hole in the centre of the 1% agarose gel in each well, which was a little bit larger than the diameter of the 3% agarose plug. Agarose plugs were carefully transferred into the 6-well plate, and 2ml of pre-warmed DMEM/F12 culture media (containing ITS and 1% penicillin-streptomycin, 1% fungizone) was added to each well. After the 6-well plate was placed in the loading rig, each loading platen was screwed down carefully to make contact with the surface of the central 3% agarose gel containing the cells but without compressing it.

The agarose plugs were then subjected to 10% compressive loading at 1Hz (compressive loading applied for 0.5 seconds followed by release for 0.5 second for 10, 30 or 60 minutes using a custom-built loading apparatus (Avocet Engineering, UK) (Figure 5-1). As a control, cells were cultured equivalently in all steps, except that no compressive loading was applied. After loading, parts of the agarose-cell plugs were snap frozen in liquid nitrogen and stored at -80°C for RNA extraction and confocal microscopy, and the remainder of the agarose plugs were immediately used for investigating cell viability. The culture media was collected and stored at -20°C for further analysis.

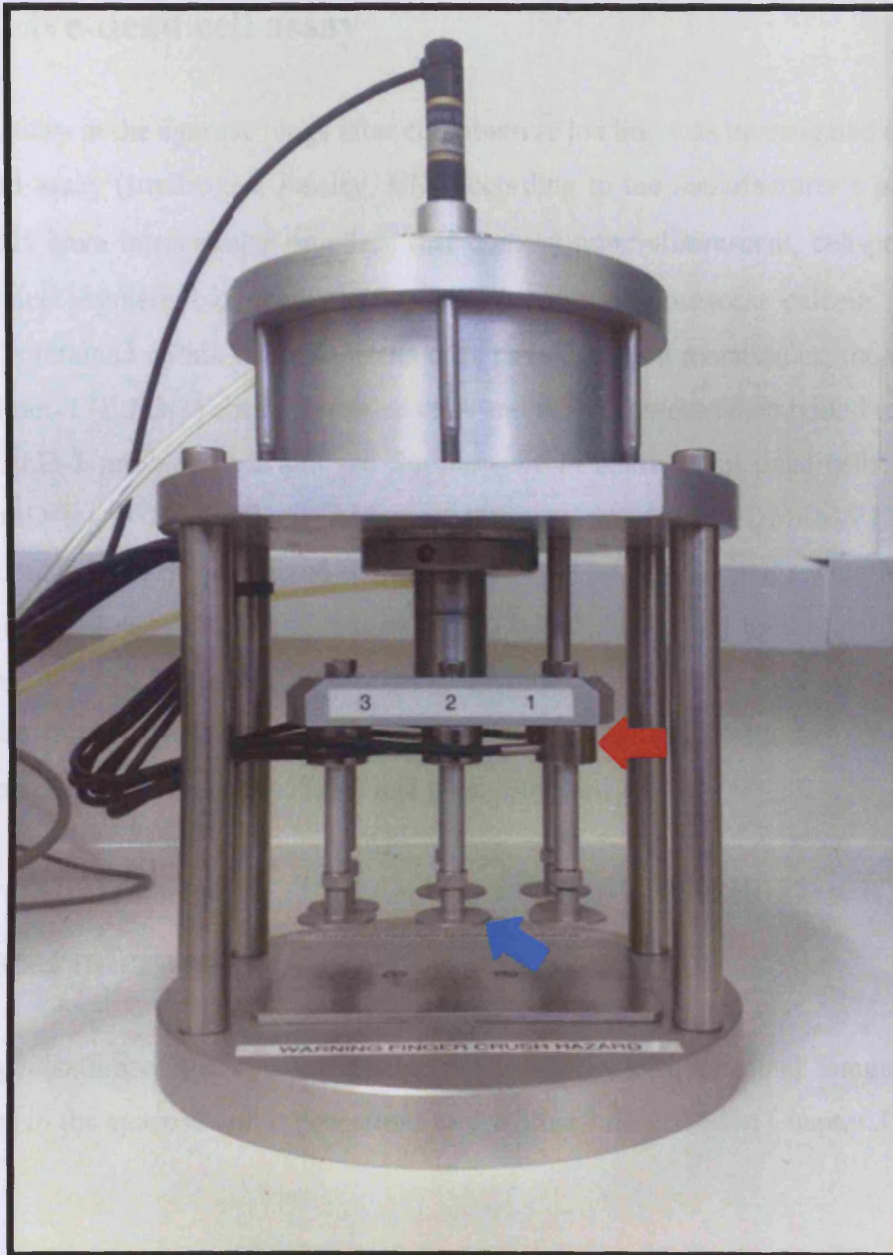


Figure 5-1. Custom-built compressive loading apparatus (Avocet Engineering, UK). A 6-well plate was placed in the rig and the load platens (blue arrow) were screwed down until they made contact with the surface of the agarose plugs. The movement of load platens was driven by compressed air and the displacement was monitored by the sensors (red arrow) on the top of the load platen.

### **5.2.4 Live-dead cell assay**

Cell viability in the agarose plugs after compressive loading was investigated using the live-dead assay (Invitrogen, Paisley, UK) according to the manufacturer's protocols. Live cells have intracellular esterases that convert non-fluorescent, cell-permeable calcein acetoxymethyl (calcein AM) to the intensely fluorescent calcein. Cleaved calcein is retained within the cells. Dead cells have damaged membranes; the ethidium homodimer-1 (EthD-1) enters damaged cells and is fluorescent when bound to nucleic acids. EthD-1 produces a bright red fluorescence in damaged or dead cells. Briefly, 4 $\mu$ M EthD-1 and 2 $\mu$ M Calcein AM solutions were prepared in DMEM/F12 culture media containing ITS and mixed thoroughly (1:1). The agarose plugs were incubated with this solution at room temperature for 30 minutes avoiding light. Agarose plugs were then washed 3 $\times$ 10 minutes at room temperature using sterile PBS avoiding light. After the final wash, cell viability was investigated using fluorescence microscopy (Olympus, Japan) with red (633nm) and green (488nm) filters.

### **5.2.5 Analysis of cytoskeletal element organisation using confocal microscopy**

The organisation of the cytoskeletal elements F-actin,  $\beta$ -tubulin and vimentin were analysed in the agarose-cell cryosections as previously described in Chapter 3 (Section 3.2.4).

### **5.2.6 RNA extraction from agarose-cell plugs**

Total RNA was extracted from the agarose-cell plugs using Qiagen RNeasy mini kits (Qiagen, West Sussex, UK). Briefly, the volume of agarose-cell plug was calculated according to the formula  $v = \pi\gamma^2h$  ( $v$  : volume;  $\gamma$ : radius;  $h$ : height). The frozen agarose-cell plug was placed in 4 volumes of RLT buffer, and stored at room temperature for 15 minutes. The agarose-cell plugs were pipetted up and down carefully to disrupt the cells within the gel. 2M sodium acetate solution was added to the agarose solution to adjust the pH (5.05 $\mu$ l of sodium acetate per 1 volume of agarose

plug plus RLT buffer). 100% ethanol was pipetted into the solution and mixed thoroughly by hand (0.71 volume of ethanol per 1 volume of RLT buffer). The mixture was then transferred into a spin column provided by the kit and centrifuged for 45 seconds at 10,000rpm. 700µl of RWI buffer was added to the column followed by centrifugation for 45 seconds at 10,000rpm. After discarding the flow-through, 350µl of Buffer RW I was added to the spin column and centrifuged at 10,000 rpm for 15 seconds. 80µl of DNase I was pipetted directly onto the spin column membrane and incubated at room temperature for 15 minutes before adding 350µl of Buffer RW I to the spin column. After centrifugation at 9,000 rpm for 45 seconds, the flow-through was discarded and 500µl of wash Buffer PRE was added to the spin column and centrifuged at 9,000 rpm for 45 seconds. The flow-through was discarded, and the column was centrifuged again at 12,000 rpm for 2 minutes. The spin column was transferred to a 1.5ml tube from the Qiagen Kit and left at 37°C (in a tissue culture incubator) for 15 minutes. At the end of the procedure, 50µl of nuclease-free water was added to the spin column which dissolved the RNA. This was collected by centrifugation at 9,000 rpm for 60 seconds.

### **5.2.7 Analysis of gene expression using quantitative PCR**

cDNA was synthesised according to the methods described previously (Section 2.2.3.2). To determine target gene expression, real-time PCR with custom-designed primers was performed using the Mx3000P<sup>®</sup> QPCR System as described previously (Section 2.2.3.3). The sequences of primers used for target gene amplification are shown in Table 3-1. Calculation of starting concentration was based on standard curves for each target DNA run in parallel, and all the data are presented as fold-change in gene expression after initially being normalised to the housekeeping gene GAPDH and then normalised to an endogenous control in the experiment i.e. to unstretched young NP cells which were assigned a value of 1. Therefore, fold changes in gene expression above 1 suggest an increase in transcription whereas values below 1 indicate a decrease relative to the baseline control i.e. unstretched young NP cells.

## **5.2.8 Statistical Analysis**

Data are presented as Mean  $\pm$  S.E.M, with tissue derived from 5 individual animals. All experiments were performed twice and representative data are presented. Data was tested for normality (Anderson-Darling test). One-way ANOVA plus Dunnett's (Gaussian distribution) or Dunn's (not Gaussian distribution) post hoc test was carried out using GraphPad Prism 5.0 software unless otherwise stated. Differences were considered significant at P values of less than 0.05.



## **5.3 Results**

### **5.3.1 Cell viability did not change after compressive loading**

#### **5.3.1.1 Investigation of cell viability using the live-dead assay**

Using the live-dead assay in conjunction with fluorescence microscopy, it appeared that there was no obvious alteration in cell viability after 10, 30 or 60 minutes of compressive loading, as very few cells stained with the ethidium homodimer (red) (Figure 5-2).

#### **5.3.1.2 Investigation of cell viability using the LDH assay**

To further quantify whether compressive loading increased cell death, cell viability was investigated using the LDH assay. There was no significant alteration in LDH content within the cell culture media after compression (data not shown), suggesting that compressive loading did not change cell viability, either in young NP and OAF cells or mature NP and OAF cells.

### 5.3.3 Characterisation of the IVD cell phenotype in an agarose gel

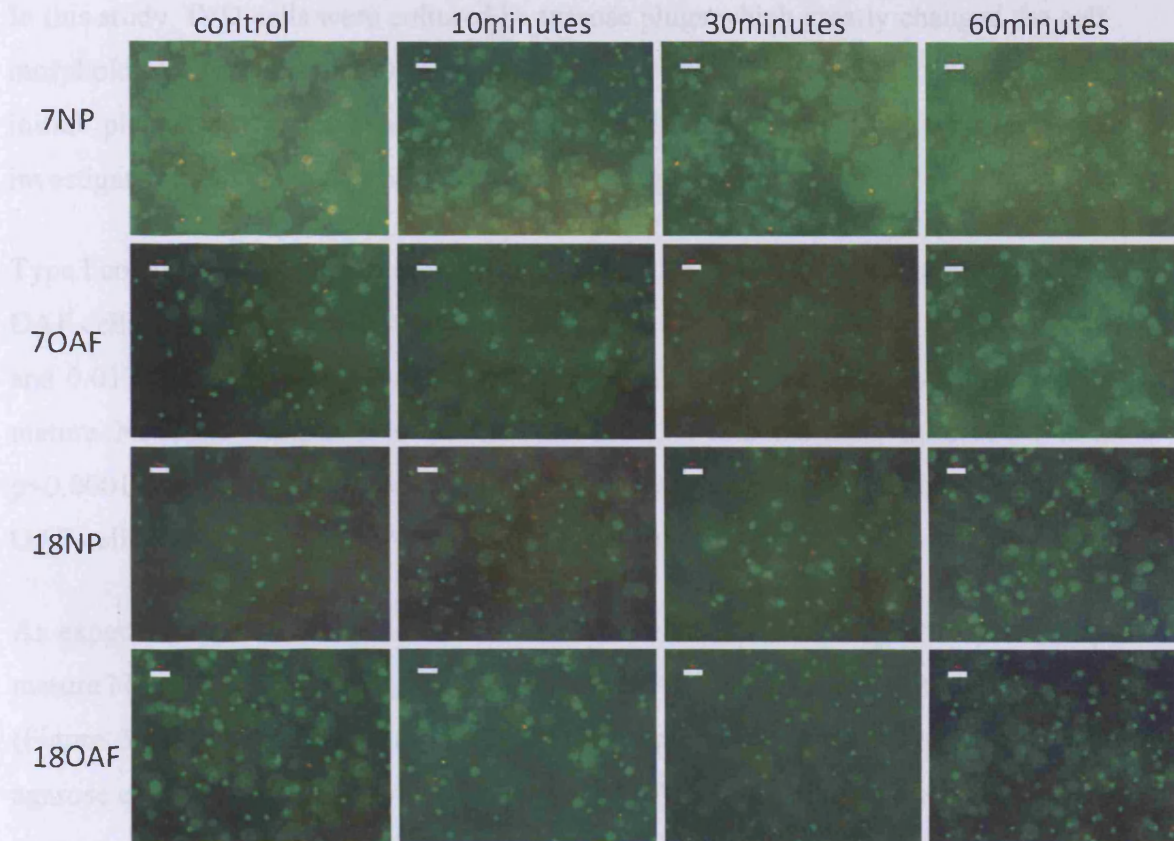


Figure 5-2. Live-dead cell assay results after compressive loading. Intervertebral disc cells cultured in a 3% agarose gel were subjected to a 10% cyclic compressive load at 1Hz for 10, 30 or 60 minutes. Cell viability was investigated using the live-dead assay immediately after loading. Green: live cells; Red: dead cells. Scale bar: 100µm.

### 5.3.2 Characterisation of the IVD cell phenotype in an agarose gel

In this study, IVD cells were cultured in agarose plugs which greatly changed the cell morphology, especially the OAF cells. To ensure both NP and OAF cells kept their initial phenotype, types I and II collagen and aggrecan gene expression were investigated in NP and OAF cells cultured in 3% agarose for 24 hours.

Type I collagen gene expression was 3.7-fold and 1.08-fold higher in young and mature OAF cells when compared with young and mature NP cells (Student's t test,  $p=0.0005$  and  $0.0177$  respectively) (Figure 5-3). More type I collagen mRNA was observed in mature NP cells compared to young NP cells (3.4-fold increase; Student's t test,  $p<0.0001$ ), but no age-related difference was observed between young and mature OAF cells (Student's t test,  $p=0.1719$ ) (Figure 5-3).

As expected, type II collagen levels were 25-fold and 250-fold higher in young and mature NP cells compared to young and mature OAF cells (Student's t test,  $p<0.0001$ ) (Figure 5-3), indicating that the distinct phenotype has been maintained in the 3-D agarose environment. More type II collagen mRNA was observed in young OAF cells compared to mature OAF cells (10-fold increase; Student's t test,  $p=0.0073$ ), but there was no age-related difference in the NP cells (Student's t test,  $p=0.8280$ ) (Figure 5-3).

There was also more aggrecan gene expression in mature NP cells compared to mature OAF cells (4-fold increase; Student's t test,  $p=0.0004$ ), but there was no zonal variation in aggrecan mRNA levels between young NP and young OAF cells (Student's t test,  $p=0.1757$ ) (Figure 5-3). There was more aggrecan mRNA in young OAF cells compared to mature OAF cells (2.5-fold increase; Student's t test,  $p=0.04$ ), but no age-related difference was observed in the NP cells (Student's t test,  $p=0.1072$ ) (Figure 5-3).

Collectively, the increased mRNA expression of type II collagen and aggrecan in NP cells, and the increased expression of type I collagen in OAF cells demonstrated that

the two cell populations maintained their distinct phenotypes when cultured in a 3-D environment i.e. in agarose.

### **5.3.3 The effect of cyclic compressive loading on the organisation and gene expression of F-actin in IVD cells**

#### **5.3.3.1 Compressive loading altered F-actin organisation**

The organisation of F-actin filaments in cells cultured in a 3% agarose gel was investigated using Alexa-488™ conjugated phalloidin (Figure 5-4). Both NP and OAF cells were round or oval when cultured in the agarose. The organisation of F-actin filaments in unloaded young (Figure 5-4A) and mature NP cells (Figure 5-4E) was punctate (red arrow) and distributed throughout the cytoplasm. After 10, 30 or 60 minutes of loading, there was no significant alteration in the architecture of F-actin in young NP cells (Figure 5-4B-D). However, partial pooling of the F-actin filaments within the cytoplasm was observed in mature NP cells after loading (white arrow) (Figure 5-4F-H). In contrast to the NP cells, F-actin filaments within young and mature OAF cells were more fibre-like (yellow arrow), composing a network distributed throughout the cytoplasm (Figure 5-4I-P). There was no age-related difference in F-actin architecture between young (Figure 5-4I-L) and mature OAF cells (Figure 5-4M-P).

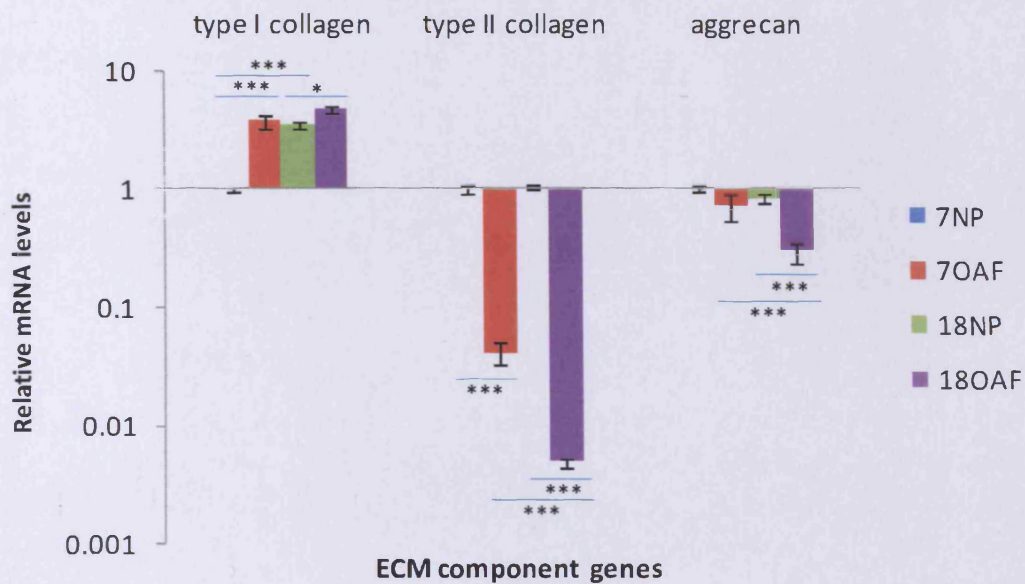
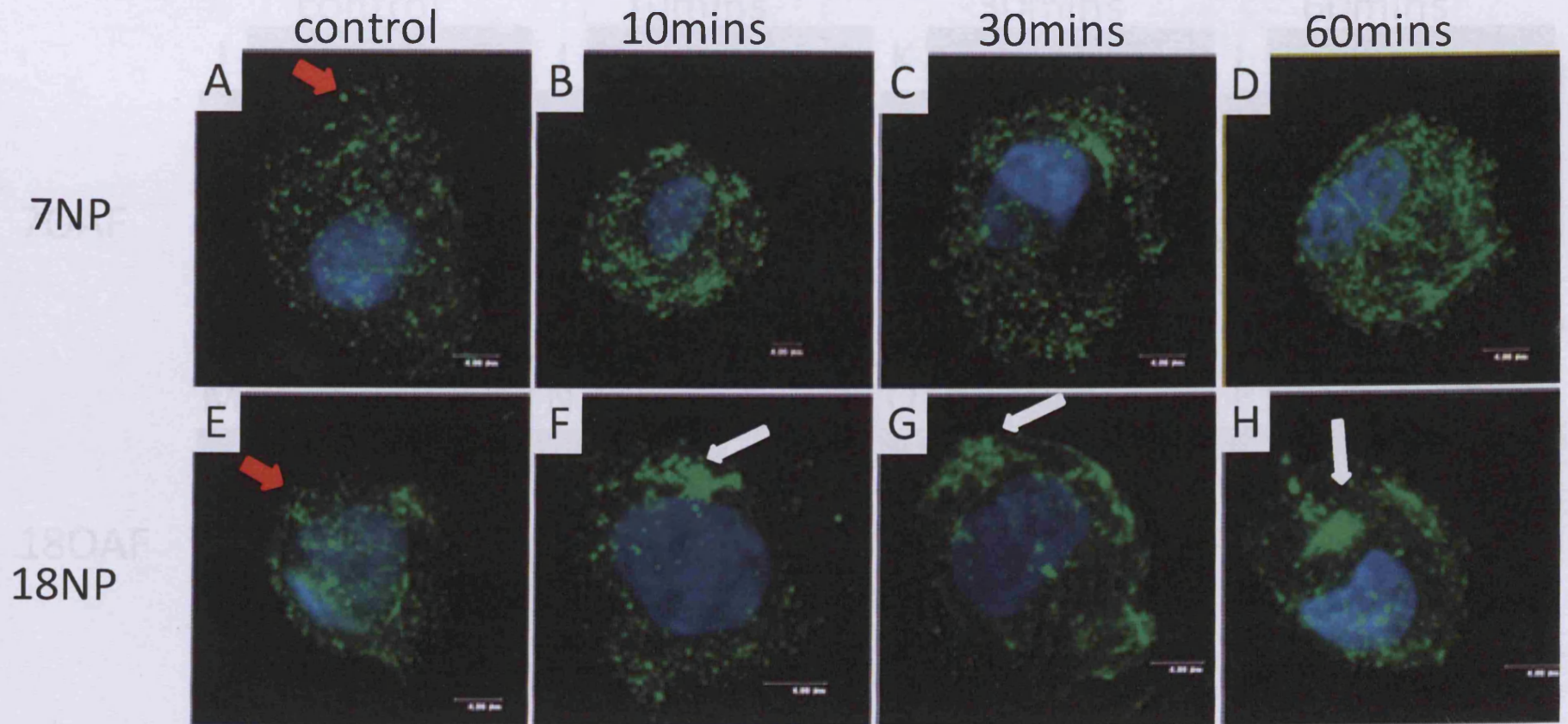


Figure 5-3 Maintenance of NP and OAF phenotypes after seeding cells in a 3-D environment. Intervertebral disc cells were cultured in 3% agarose plugs for 24 hours. Total RNA was extracted and types I and II collagen and aggrecan mRNA expression was determined using real-time PCR. Data was normalised to the housekeeping gene GAPDH and the results were normalised to the young NP control samples. Data are presented as Mean  $\pm$  S.E.M (n=5). \*\*\*:  $p \leq 0.001$ , \*:  $p \leq 0.05$ . Student's t test.

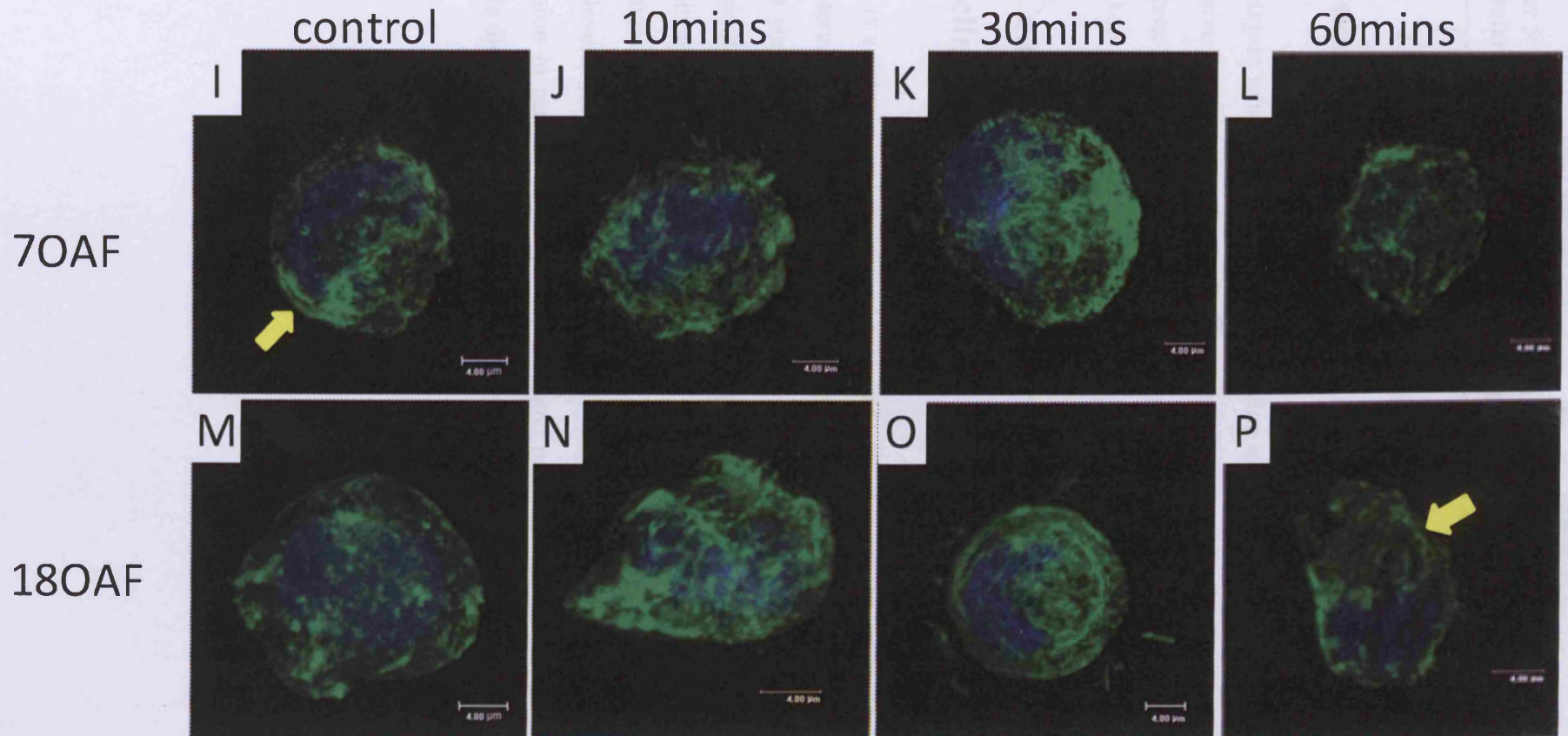
Figure 5-4 The organisation of F-actin filaments within cells subjected to compressive loading. Intervertebral disc cells cultured in a 3% agarose gel were subjected to 10% compressive loading at 1Hz for 10, 30 or 60 minutes. Unloaded cells served as controls. The organisation of F-actin filaments were visualised using Alexa-488™ conjugated phalloidin (green). The nucleus was counterstained with DAPI (blue). Images are presented as 3D reconstructions of serial sections within one cell. Red arrow: punctate staining of F-actin in uncompressed cells. White arrow: partial pooling of F-actin staining in mature NP cells in response to compressive loading. Yellow arrow: fibre-like F-actin staining in OAF cells.

Chapter 5: The effects of cyclic compressive loading on cytoskeletal elements and extracellular matrix metabolism in bovine intervertebral disc cells cultured in agarose

---



Chapter 5: The effects of cyclic compressive loading on cytoskeletal elements and extracellular matrix metabolism in bovine intervertebral disc cells cultured in agarose





### **5.3.3.2 Compressive loading did not change $\beta$ -actin gene expression**

To investigate whether  $\beta$ -actin gene expression was altered in IVD cells subjected to compressive loading, real-time PCR was performed, compressive loading did not alter  $\beta$ -actin gene expression in either young or mature NP cells ( $p>0.05$ ), or in young or mature OAF cells ( $p>0.05$ ) (Data not shown).

### **5.3.4 Compressive loading altered vinculin gene expression in IVD cells**

Vinculin is a cytoskeletal-membrane protein found in focal adhesions, and is involved in the interaction between actin filaments and integrins. Mechanical load induced a small but significant decrease in vinculin gene expression in young NP cells after 10 and 30 minutes ( $p<0.05$ ) (Figure 5-5). In mature NP cells, there was a 1.45-fold decline in vinculin mRNA levels after 10 minutes of loading ( $p<0.05$ ), but this decrease was not significant after 30 or 60 minutes of load ( $p>0.05$ ) (Figure 5-5). In contrast, vinculin mRNA levels were elevated 1.4-fold and 1.6-fold after 30 and 60 minutes of compression in mature OAF cells ( $p<0.05$  and  $p<0.001$  respectively), but the young OAF cells did not appear to alter in response to load ( $p>0.05$ ).

5.3.5 Compressive loading did not change actin related protein gene expression in IVD cells

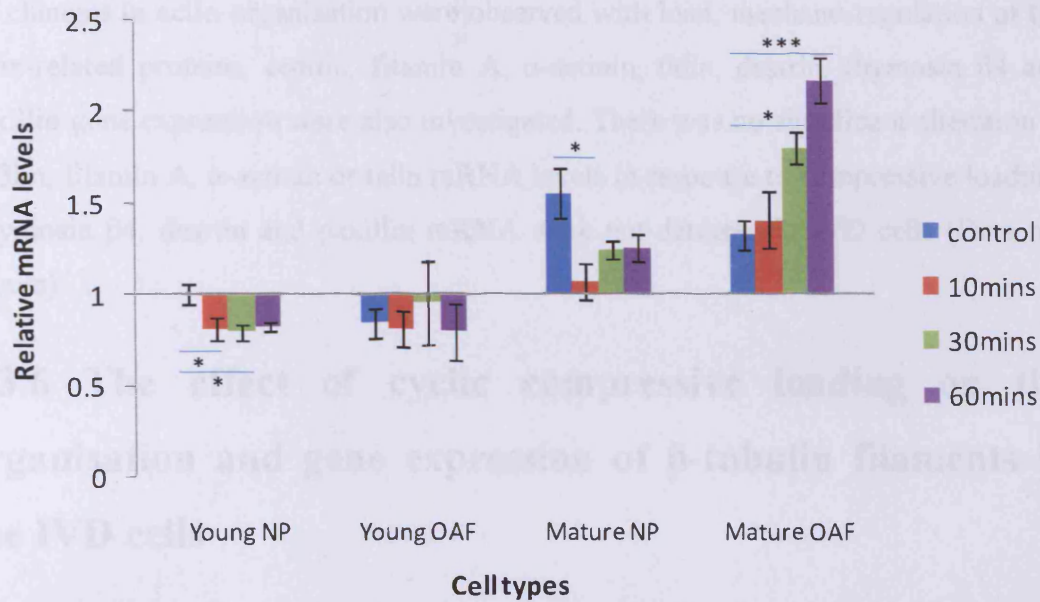


Figure 5-5 Vinculin gene expression in intervertebral disc cells subjected to compressive loading. Intervertebral disc cells cultured in a 3% agarose gel were subjected to 10% compressive loading at 1Hz for 10, 30 or 60 minutes. Unloaded cells were used as controls. Total RNA was extracted and vinculin mRNA levels were determined using real-time PCR. Data were normalised to the housekeeping gene GAPDH and were relative to unloaded young NP cells. Data are presented as Mean  $\pm$  S.E.M (n=5). \*\*\*:  $p < 0.001$ , \*:  $p < 0.05$ .

### **5.3.5 Compressive loading did not change actin-related protein gene expression in IVD cells**

As changes in actin organisation were observed with load, mechano-regulation of the actin-related proteins, cofilin, filamin A,  $\alpha$ -actinin, talin, destrin, thymosin  $\beta$ 4 and paxillin gene expression were also investigated. There was no significant alteration in cofilin, filamin A,  $\alpha$ -actinin or talin mRNA levels in response to compressive loading. Thymosin  $\beta$ 4, destrin and paxillin mRNA were not detected in IVD cells (Data not shown).

### **5.3.6 The effect of cyclic compressive loading on the organisation and gene expression of $\beta$ -tubulin filaments in the IVD cells**

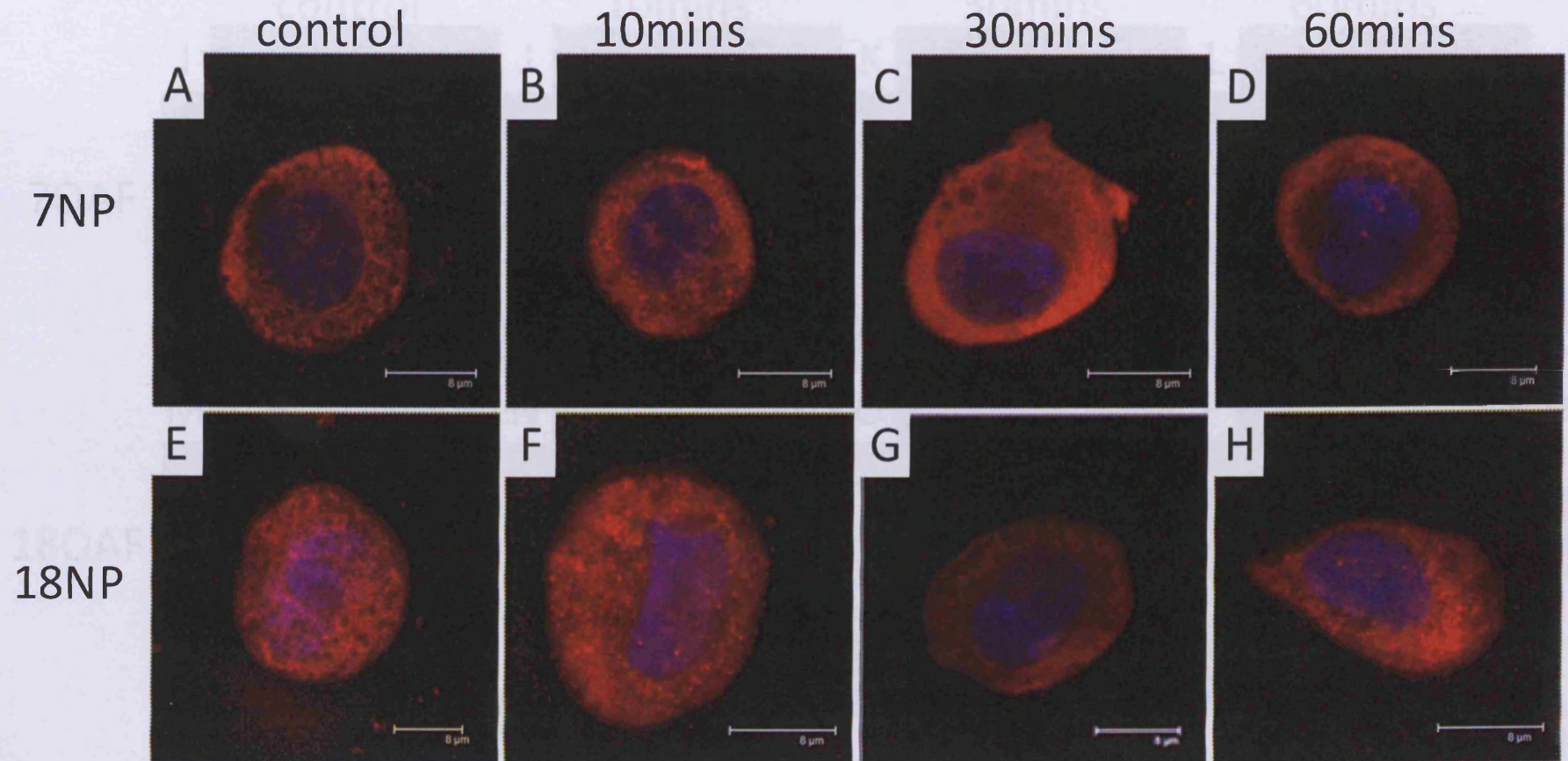
#### **5.3.6.1 Compressive loading did not change $\beta$ -tubulin organisation**

The organisation of  $\beta$ -tubulin filaments was visualised using E7 primary antibody and Alexa-633™ conjugated secondary antibody (Figure 5-6),  $\beta$ -tubulin filaments displayed a dense network, distributed throughout the cytoplasm. There were no significant differences in  $\beta$ -tubulin organisation in NP cells (Figure 5-6A-H) after applying load. Unlike the NP cells, there seemed to be a more organised filament network in young (Figure 5-6L) and mature OAF cells (Figure 5-6P) after applying 60 minutes of compressive loading (white arrow). No age-related difference in  $\beta$ -tubulin architecture was observed between young and mature NP or OAF cells.

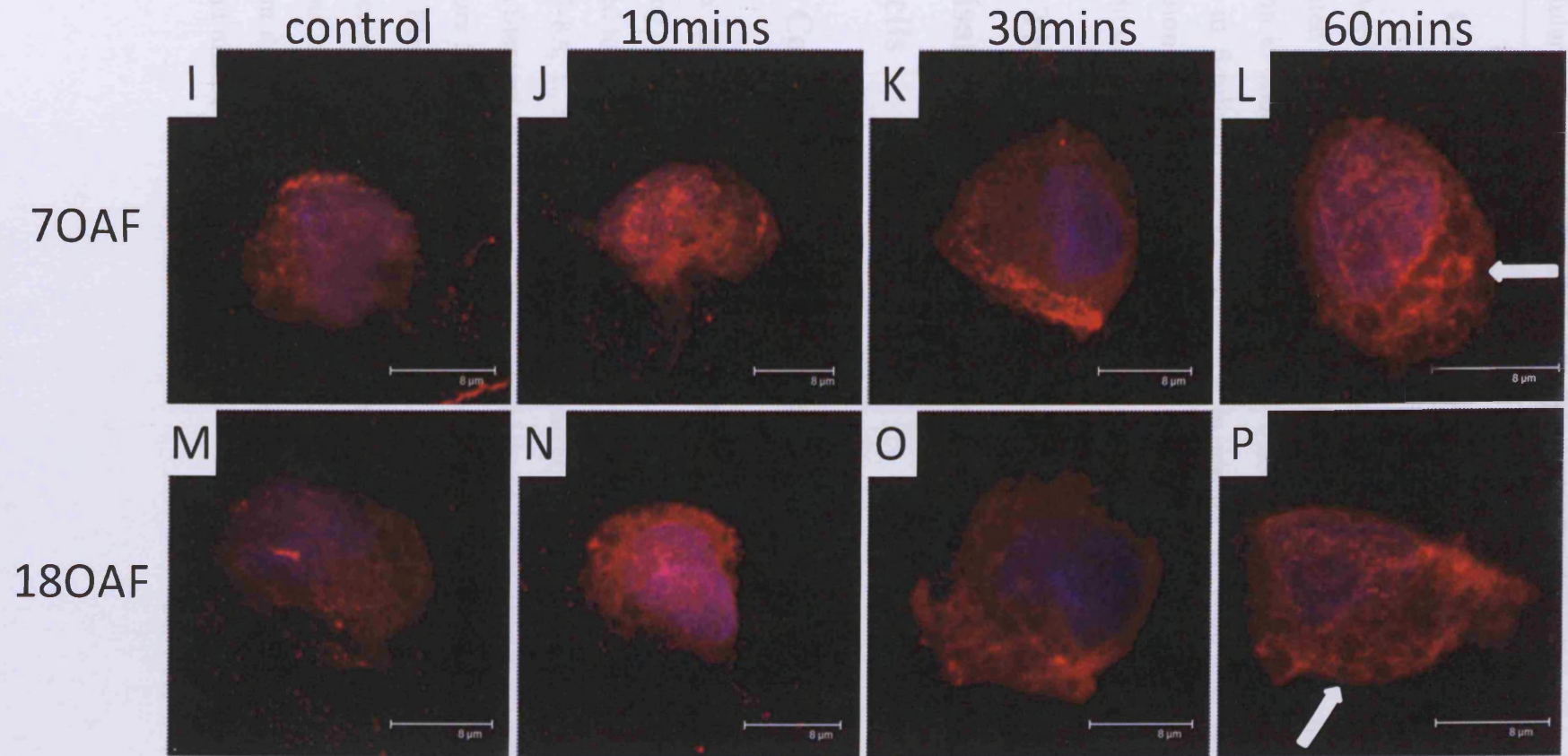
Figure 5-6 The organisation of  $\beta$ -tubulin filaments within cells subjected to compressive loading. Intervertebral disc cells cultured in a 3% agarose gel were subjected to 10% compressive loading at 1Hz for 10, 30 or 60 minutes. Unloaded cells served as controls. The organisation of  $\beta$ -tubulin filaments were visualised using E7 primary antibody with an Alexa-633™ conjugated secondary antibody (red). The nucleus was counterstained with DAPI (blue). Images are presented as 3D reconstructions of serial sections within one cell. White arrow: the organisation of  $\beta$ -tubulin appears to be more organised after compressive loading.

Chapter 5: The effects of cyclic compressive loading on cytoskeletal elements and extracellular matrix metabolism in bovine intervertebral disc cells cultured in agarose

---



Chapter 5: The effects of cyclic compressive loading on cytoskeletal elements and extracellular matrix metabolism in bovine intervertebral disc cells cultured in agarose



### **5.3.6.2 Compressive loading altered $\beta$ -tubulin gene expression**

$\beta$ -tubulin gene expression in IVD cells subjected to compressive loading was also investigated (Figure 5-7). Compressive loading did not change  $\beta$ -tubulin gene expression in young NP and OAF cells ( $p>0.05$ ). There was a small but significant increase in  $\beta$ -tubulin mRNA expression in mature NP cells after 60 minutes of compression ( $p<0.05$ ). In contrast, 30 and 60 minutes of load induced a subtle, but significant decrease in  $\beta$ -tubulin gene expression in mature OAF cells ( $p<0.05$ ).

### **5.3.7 The effect of cyclic compressive loading on the organisation and gene expression of vimentin filaments in the IVD cells**

#### **5.3.7.1 Compressive loading changed vimentin organisation**

Vimentin filaments within cells cultured in a 3% agarose gel were fibre-like, composing a meshwork extending from the nucleus to the cell membrane (Figure 5-8). Compared to the  $\beta$ -tubulin network, the organisation of vimentin in the unloaded cells (Figure 5-8A, E, I & M) was a little bit sparser, with randomly arranged bundles of vimentin filaments extending from one end of the cell membrane to the other end of the cell (Figure 5-8A, I & M, white arrow). After compressive loading, the architecture of vimentin filaments in both NP (Figure 5-8B-D & F-H) and OAF cells (Figure 5-8J-L & N-P) seemed more organised, with finer filaments (yellow arrow) distributed throughout the cytoplasm when compared with the unloaded cells. There was no significant difference in vimentin organisation between NP and OAF cells or between young and mature cells.

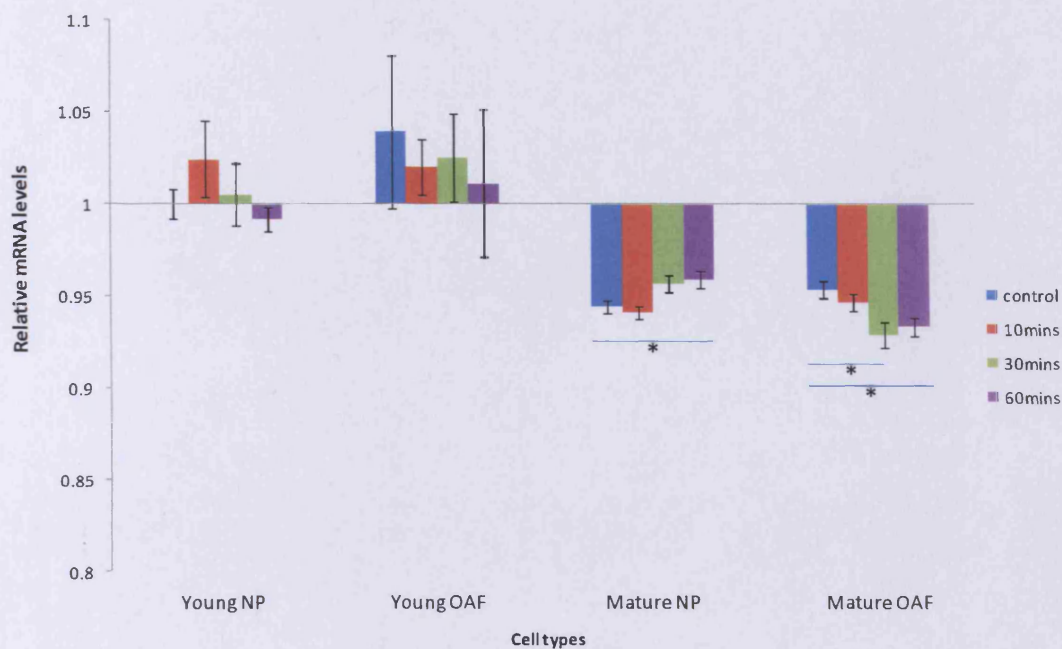


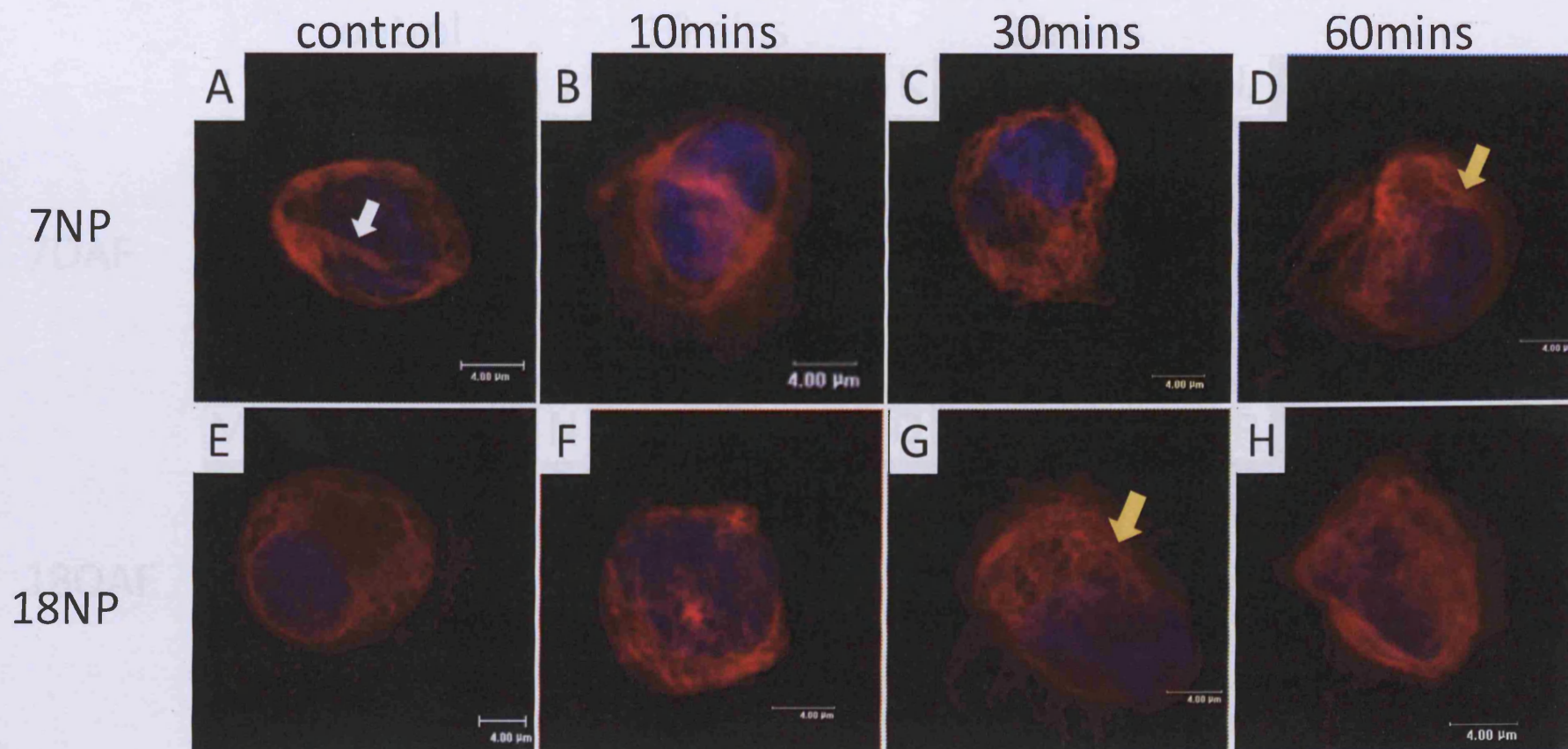
Figure 5-7  $\beta$ -tubulin gene expression in intervertebral disc cells subjected to compressive loading. Intervertebral disc cells cultured in a 3% agarose gel were subjected to 10% compressive loading at 1Hz for 10, 30 or 60 minutes. Unloaded cells were used as controls. Total RNA was extracted and  $\beta$ -tubulin mRNA levels were determined using real-time PCR. Data were normalised to the housekeeping gene GAPDH and were relative to unloaded young NP cells. Data are presented as Mean  $\pm$  S.E.M (n=5). \*: p<0.05.



Figure 5-8 The organisation of vimentin filaments within cells subjected to compressive loading. Intervertebral disc cells cultured in a 3% agarose gel were subjected to 10% compressive loading at 1Hz for 10, 30 or 60 minutes. Unloaded cells served as controls. The organisation of vimentin filaments were visualised using V9 primary antibody with an Alexa-633™ conjugated secondary antibody (red). The nucleus was counterstained with DAPI (blue). Images are presented as 3D reconstructions of serial sections within one cell. White arrow: vimentin bundles extending from one end of the cell membrane to the other end in the control cells. Yellow arrow: compression induces more organised and finer vimentin filaments.

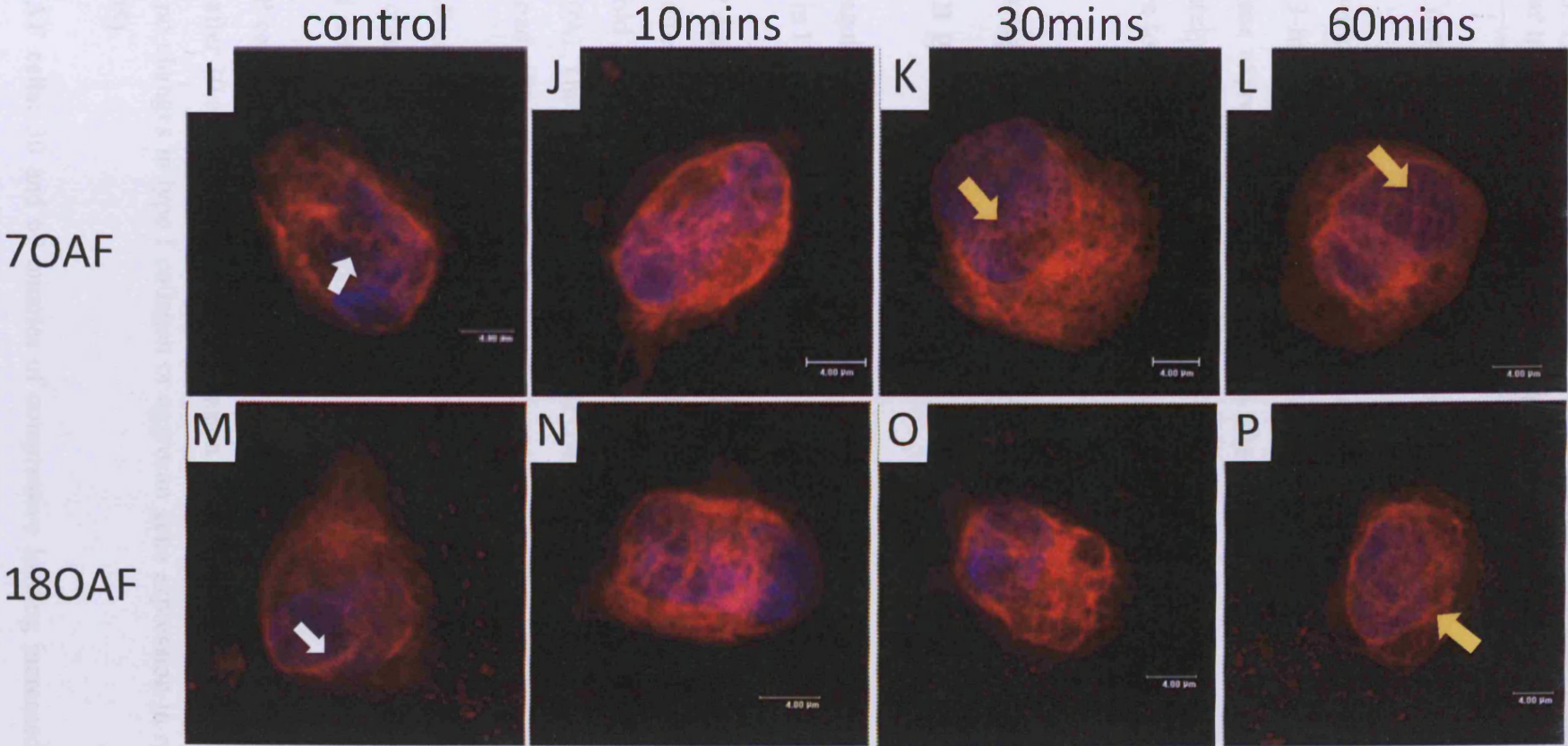
Chapter 5: The effects of cyclic compressive loading on cytoskeletal elements and extracellular matrix metabolism in bovine intervertebral disc cells cultured in agarose

---



Chapter 5: The effects of cyclic compressive loading on cytoskeletal elements and extracellular matrix metabolism in bovine intervertebral disc cells cultured in agarose

---



### 5.3.7.2 Compressive loading altered vimentin gene expression

Compressive loading decreased vimentin gene expression in young NP cells after 60 minutes (1.3-fold;  $p < 0.05$ ) (Figure 5-9). Similarly, there was a significant inhibition of vimentin gene expression in mature NP cells after 30 or 60 minutes of compression (approximately 1.2-fold;  $p < 0.01$ ) (Figure 5-9). For young and mature OAF cells, compressive loading did not change vimentin mRNA levels at any of the time points ( $p > 0.05$ ).

### 5.3.8 Compressive loading altered types I and II collagen and aggrecan gene expression

Mechano-regulation of the ECM components types I and II collagen and aggrecan gene expression in IVD cells was investigated using real-time PCR (Figure 5-10).

**Young NP cells:** there was a small but significant decrease in type I collagen gene expression after 30 minutes of compression ( $P < 0.05$ ) (Figure 5-10A). In contrast, there was a 1.5 fold increase in aggrecan gene expression after 60 minutes of load ( $P < 0.05$ ) (Figure 5-10A). There was no change in type II collagen gene expression in response to any of the loads ( $P > 0.05$ ).

**Young OAF cells:** a 2-fold increase in aggrecan gene expression was observed after 60 minutes of compression ( $P < 0.01$ ) (Figure 5-10B). However, there were no changes in types I or II collagen gene expression at any of the loading time points ( $P > 0.05$ ).

**Mature NP cells:** there was an approximate 1.3-fold increase in type II collagen gene expression after 30 and 60 minutes of compression ( $p < 0.05$ ) (Figure 5-10C). However, there were no changes in type I collagen or aggrecan gene expression in response to load ( $P > 0.05$ ).

**Mature OAF cells:** 30 and 60 minutes of compressive loading increased aggrecan gene expression by almost 3-fold in mature OAF cells ( $p < 0.01$  and  $0.05$  respectively) (Figure 5-10D). However, there was no change in types I or II collagen gene expression in response to compression ( $P > 0.05$ ).

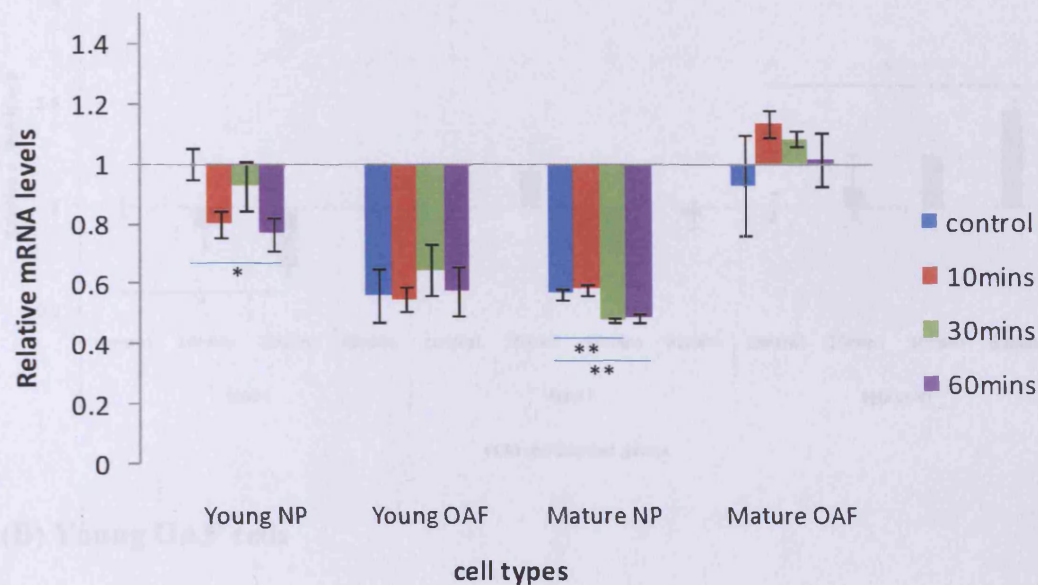
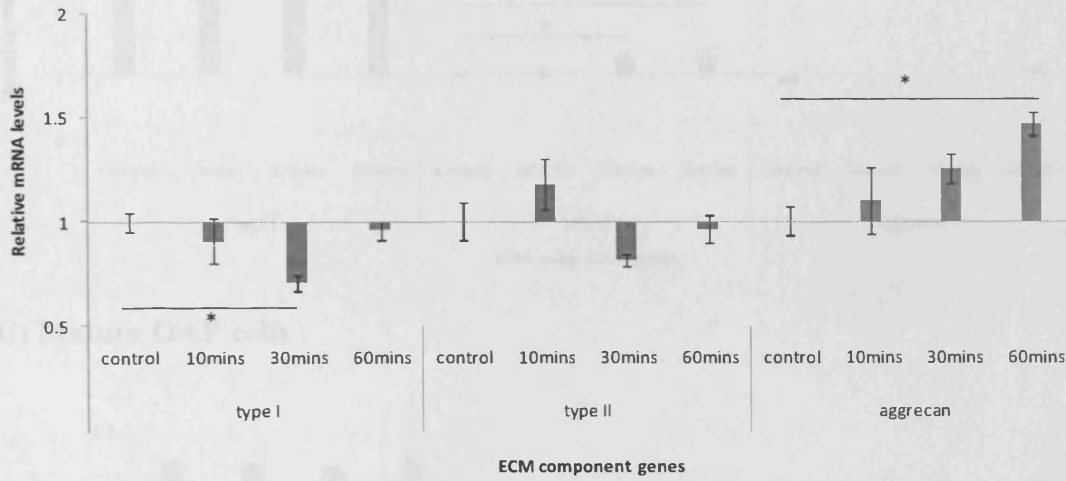


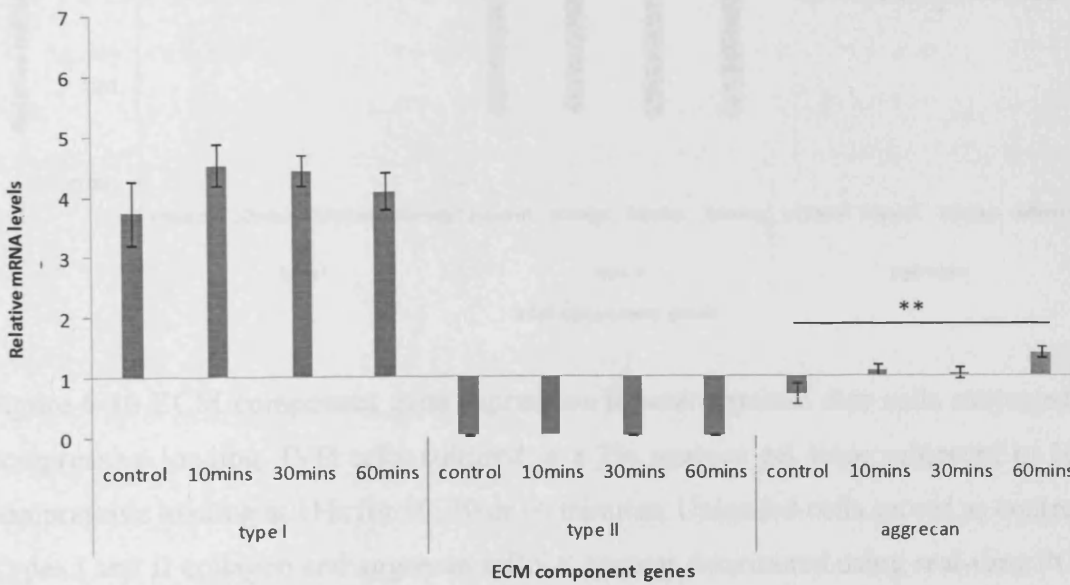
Figure 5-9 Vimentin gene expression in intervertebral disc cells subjected to compressive loading. Intervertebral disc cells cultured in a 3% agarose gel were subjected to 10% compressive loading at 1Hz for 10, 30 or 60 minutes. Unloaded cells were used as controls. Total RNA was extracted and vimentin mRNA content was determined using real-time PCR. Data were normalised to the housekeeping gene GAPDH and were relative to loaded young NP cells. Data are presented as Mean  $\pm$  S.E.M (n=5). \*\*: p<0.01, \*: p<0.05.

(C) Mature NP cells

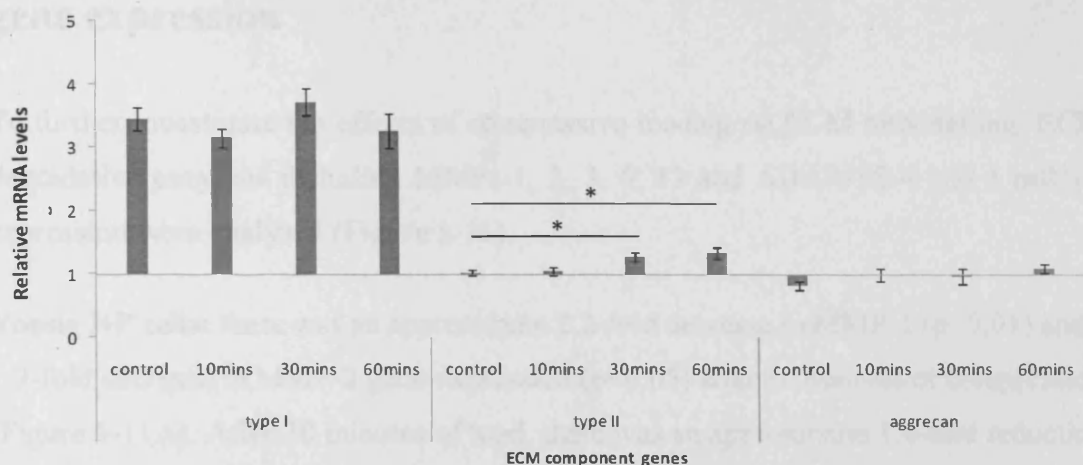
**(A) Young NP cells**



**(B) Young OAF cells**



(C) Mature NP cells



(C) Mature OAF cells

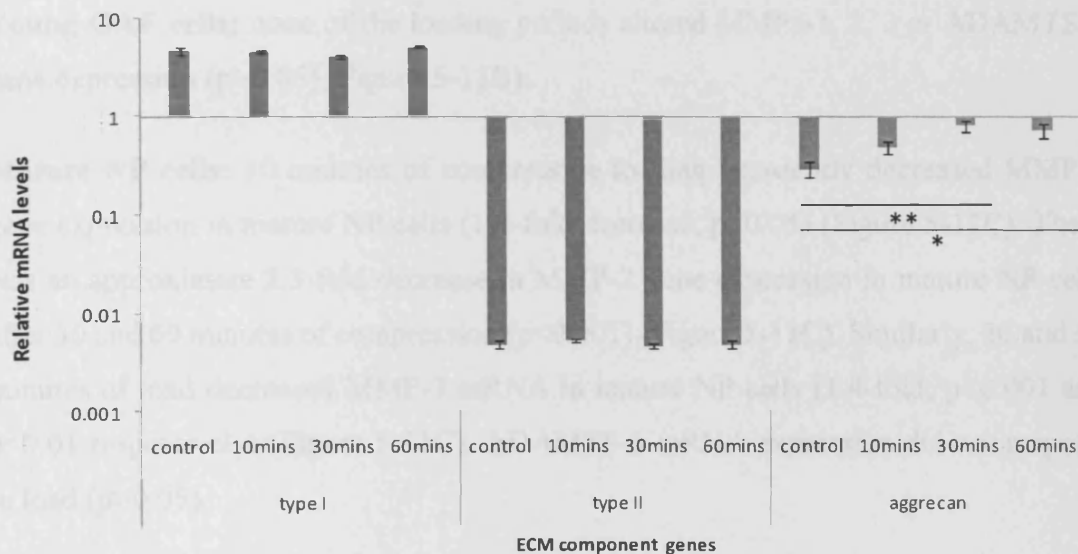


Figure 5-10 ECM component gene expression in intervertebral disc cells subjected to compressive loading. IVD cells cultured in a 3% agarose gel were subjected to 10% compressive loading at 1Hz for 10, 30 or 60 minutes. Unloaded cells served as controls. Types I and II collagen and aggrecan mRNA content determined using real-time PCR. Data were normalised to the housekeeping gene GAPDH and were relative to unloaded young NP cells. Data are presented as Mean  $\pm$  S.E.M (n=5). \*\*: p<0.01, \*: p<0.05. [A] young NP, [B] young OAF, [C] mature NP, [D] mature OAF.

### 5.3.9 Compressive loading altered ECM degradative enzymes gene expression

To further investigate the effects of compressive loading on ECM remodelling, ECM degradative enzymes including MMPs-1, 2, 3, 9, 13 and ADAMTS-4 and 5 mRNA expression were analysed (Figure 5-11).

**Young NP cells:** there was an approximate 2.2-fold decrease in MMP-1 ( $p < 0.01$ ) and a 1.7-fold decrease in MMP-2 gene expression ( $p < 0.05$ ) after 10 minutes of compression (Figure 5-11A). After 30 minutes of load, there was an approximate 1.8-fold reduction in MMP-3 and ADAMTS-5 gene expression ( $p < 0.01$  and  $0.05$  respectively) (Figure 5-11A).

**Young OAF cells:** none of the loading periods altered MMPs-1, 2, 3 or ADAMTS-5 gene expression ( $p > 0.05$ ) (Figure 5-11B).

**Mature NP cells:** 10 minutes of compressive loading transiently decreased MMP-1 gene expression in mature NP cells (1.8-fold decrease;  $p < 0.05$ ) (Figure 5-11C). There was an approximate 2.3-fold decrease in MMP-2 gene expression in mature NP cells after 30 and 60 minutes of compression ( $p < 0.001$ ) (Figure 5-11C). Similarly, 30 and 60 minutes of load decreased MMP-3 mRNA in mature NP cells (1.4-fold;  $p < 0.001$  and  $p < 0.01$  respectively) (Figure 5-11C). ADAMTS-5 mRNA expression did not respond to load ( $p > 0.05$ ).

**Mature OAF cells:** There was a 2-fold decrease in MMP-1 and a 1.3-fold decrease in MMP-3 gene expression after 60 minutes of compression ( $p < 0.05$ ) (Figure 5-11D). In contrast, there was an approximate 1.3-fold increase in MMP-2 gene expression after 30 and 60 minutes of loads ( $p < 0.05$ ) (Figure 5-11D). ADAMTS-5 gene expression did not alter with load.

MMP-9, MMP-13 and ADAMTS-4 gene expression were very low or undetectable in IVD cells (Data not shown).

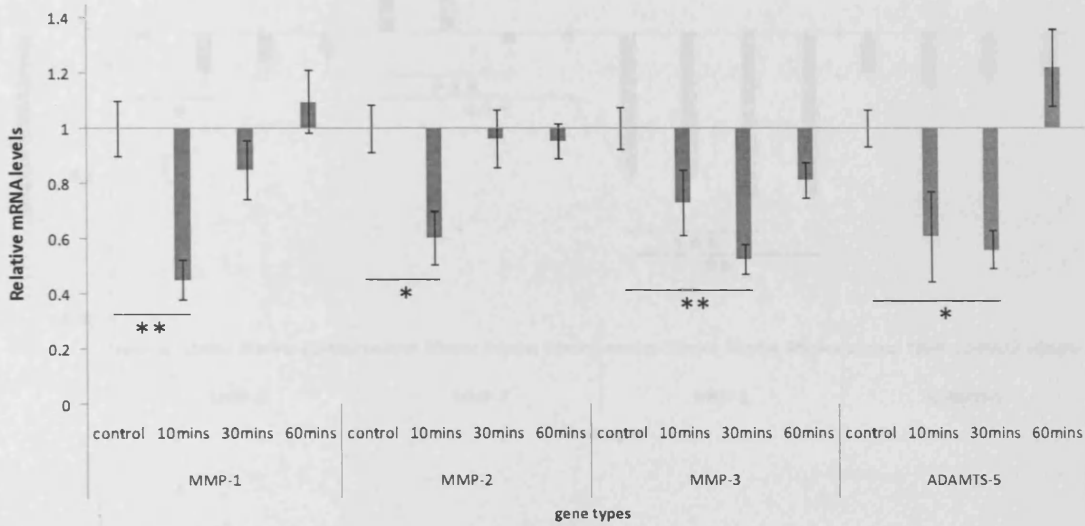


Figure 5-11 ECM degradative enzyme mRNA in intervertebral disc cells subjected to compressive load. IVD cells cultured in a 3% agarose gel were subjected to 10% compressive loading at 1Hz for 10, 30 or 60 minutes. Unloaded cells served as controls. MMP-1, 2, and 3 and ADAMTS-5 mRNA levels were determined using real-time PCR. Data were normalised to the housekeeping gene GAPDH and were relative to unloaded young NP cells. Data are presented as Mean  $\pm$  S.E.M (n=5). \*\*\*:  $p < 0.001$ , \*\*:  $p < 0.01$ , \*:  $p < 0.05$ . [A] young NP, [B] young OAF, [C] mature NP, [D] mature OAF.

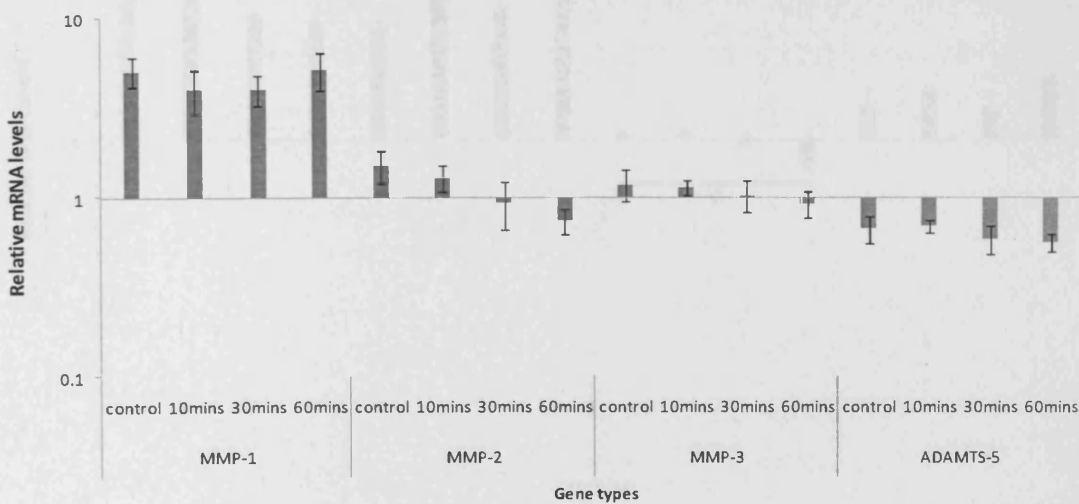
Chapter 5: The effects of cyclic compressive loading on cytoskeletal elements and extracellular matrix metabolism in bovine intervertebral disc cells cultured in agarose

---

(A) Young NP cells



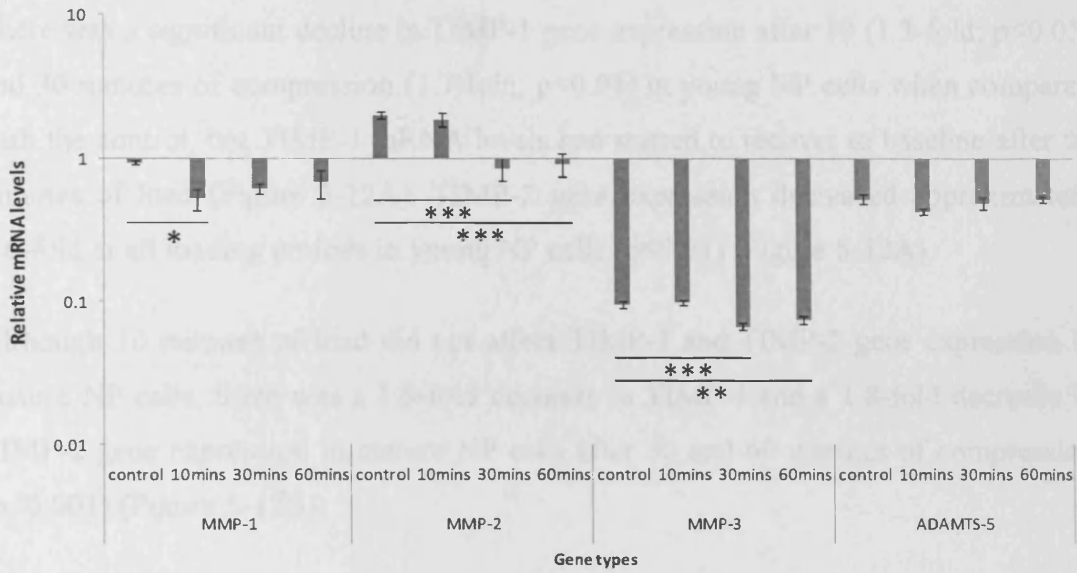
(B) Yong OAF cells



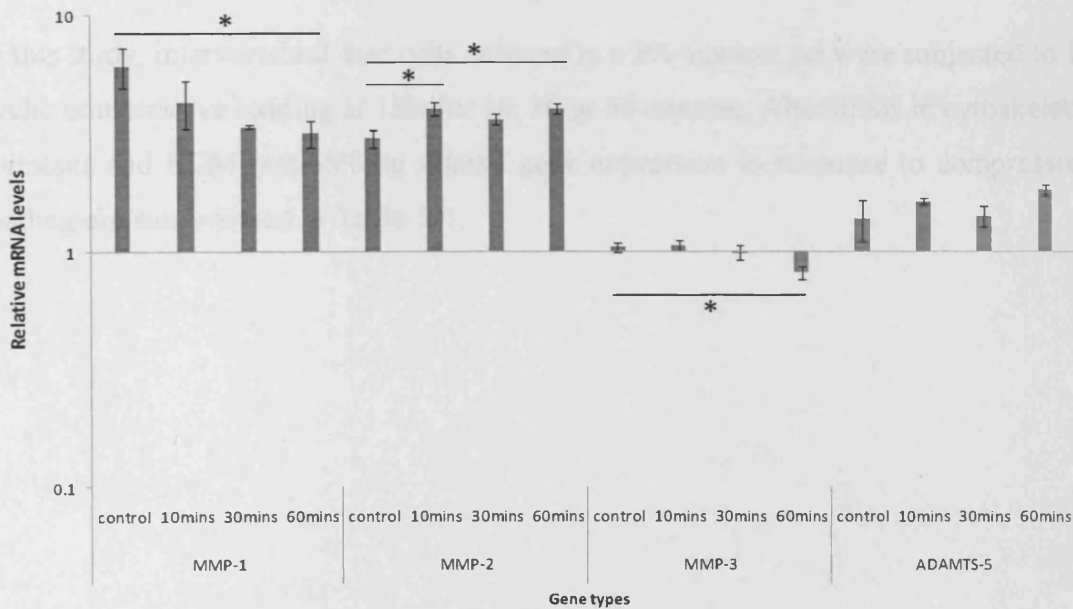
Chapter 5: The effects of cyclic compressive loading on cytoskeletal elements and extracellular matrix metabolism in bovine intervertebral disc cells cultured in agarose

---

(C) Mature NP cells



(D) Mature OAF cells



### **5.3.10 Compressive loading altered TIMP-1 and TIMP-2 gene expression in IVD cells**

There was a significant decline in TIMP-1 gene expression after 10 (1.3-fold;  $p < 0.05$ ) and 30 minutes of compression (1.7-fold;  $p < 0.01$ ) in young NP cells when compared with the control, but TIMP-1 mRNA levels had started to recover to baseline after 60 minutes of load (Figure 5-12A). TIMP-2 gene expression decreased approximately 1.6-fold at all loading periods in young NP cells ( $p < 0.01$ ) (Figure 5-12A).

Although 10 minutes of load did not affect TIMP-1 and TIMP-2 gene expression in mature NP cells, there was a 1.5-fold decrease in TIMP-1 and a 1.8-fold decrease in TIMP-2 gene expression in mature NP cells after 30 and 60 minutes of compression ( $p < 0.001$ ) (Figure 5-12B).

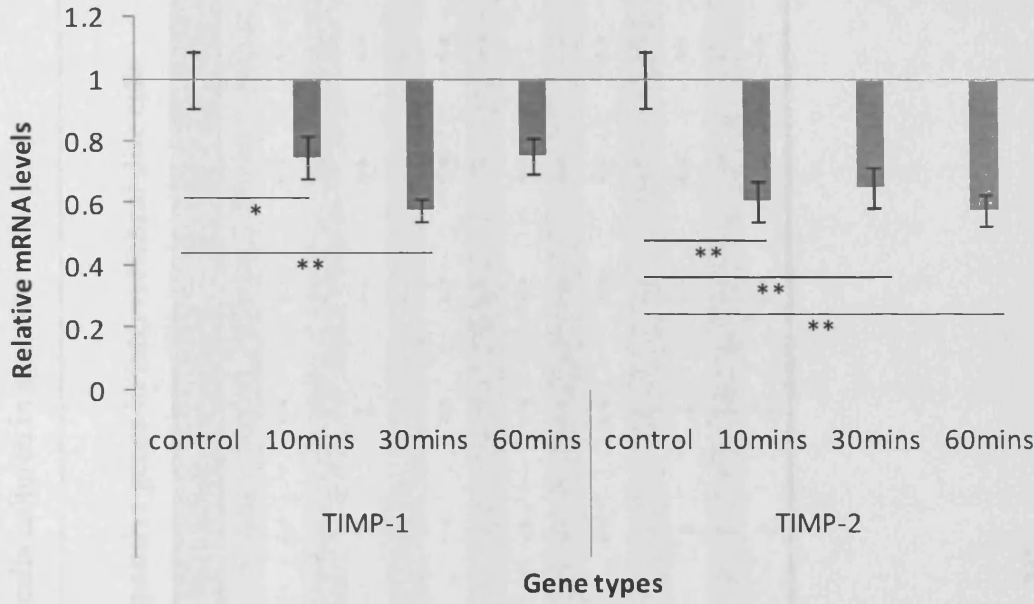
Compressive loading did not affect TIMP-1 or TIMP-2 gene expression in either young or mature OAF cells ( $p > 0.05$ ) (data not shown).

### **5.3.11 Summary**

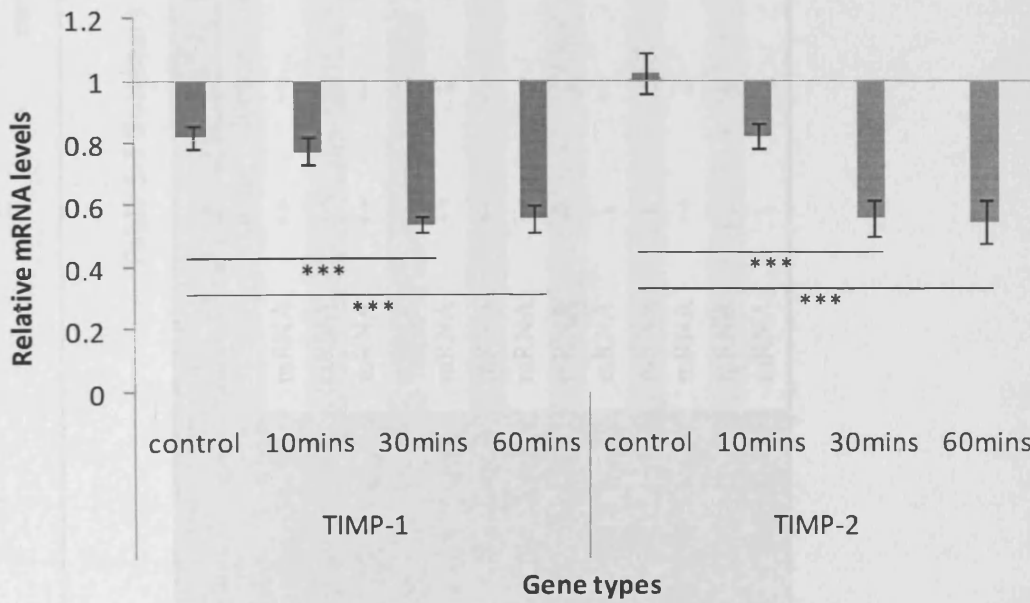
In this study, intervertebral disc cells cultured in a 3% agarose gel were subjected to 10% cyclic compressive loading at 1Hz for 10, 30 or 60 minutes. Alterations in cytoskeletal elements and ECM remodelling related gene expression in response to compressive loading are summarised in Table 5-1.

Figure 5-12 TIMP-1 and TIMP-2 mRNA in intervertebral disc cells subjected to compressive loading. Intervertebral disc cells cultured in a 3% agarose gel were subjected to 10% compressive loading at 1Hz for 10, 30 or 60 minutes. Unloaded cells served as controls. Total RNA was extracted and TIMP-1 and 2 mRNA levels were determined using real-time PCR. Data were normalised to the housekeeping gene GAPDH and were relative to unloaded young NP cells. Data are presented as Mean  $\pm$  S.E.M (n=5). \*\*\*: p<0.001, \*\*: p<0.01, \*: p<0.05. [A] young NP cells, [B] mature NP cells

(A) Young NP cells



(B) Mature NP cells



Chapter 5: The effects of cyclic compressive loading on cytoskeletal elements and extracellular matrix metabolism in bovine intervertebral disc cells cultured in agarose

Table 5-1 Summary of mechanoresponsive genes in intervertebral disc cells

		young NP			mature NP			young OAF			mature OAF		
		10mins	30mins	60mins	10mins	30mins	60mins	10mins	30mins	60mins	10mins	30mins	60mins
<b>β-actin</b>	mRNA	↔	↔	↔	↔	↔	↔	↔	↔	↔	↔	↔	↔
<b>β-tubulin</b>	mRNA	↔	↔	↔	↔	↔	↑	↔	↔	↔	↔	↓	↓
<b>vimentin</b>	mRNA	↔	↔	↓	↔	↓	↓	↔	↔	↔	↔	↔	↔
<b>vinculin</b>	mRNA	↓	↓	↔	↓	↔	↔	↔	↔	↔	↔	↑	↑
<b>type I collagen</b>	mRNA	↔	↓	↔	↔	↔	↔	↔	↔	↔	↔	↔	↔
<b>type II collagen</b>	mRNA	↔	↔	↔	↔	↑	↑	↔	↔	↔	↔	↔	↔
<b>aggrecan</b>	mRNA	↔	↔	↑	↔	↔	↔	↔	↔	↑	↔	↑	↑
<b>ADAMTS-5</b>	mRNA	↔	↓	↔	↔	↔	↔	↔	↔	↔	↔	↔	↔
<b>MMP-1</b>	mRNA	↓	↔	↔	↓	↔	↔	↔	↔	↔	↔	↔	↓
<b>MMP-2</b>	mRNA	↓	↔	↔	↔	↓	↓	↔	↔	↔	↑	↔	↑
<b>MMP-3</b>	mRNA	↔	↓	↔	↔	↓	↓	↔	↔	↔	↔	↔	↓
<b>TIMP-1</b>	mRNA	↓	↓	↔	↔	↓	↓	↔	↔	↔	↔	↔	↔
<b>TIMP-2</b>	mRNA	↓	↓	↓	↔	↓	↓	↔	↔	↔	↔	↔	↔

## 5.4 Discussion

It has been known for a long time that cells, especially chondrocyte-like cells, will differentiate when cultured as a monolayer *in vitro*, which will induce significant alterations in cell morphology and metabolism (Ichimura et al., 1991; Wang et al., 2001; Kluba et al., 2005). Although the cells in this study were not kept for more than two passages during experiments, there were still some alterations to the NP cells, with elongated cell morphology and increased  $\beta$ -actin and type I collagen expression (see Chapter 4). However, those changes were acceptable because the main interest was in the major alterations of the OAF cells in response to stretch. However, it was essential to ensure that NP cells kept their original phenotype in this study because the main objective was to investigate the effects of compressive loading, which is the primary physiological mechanical stimulation in NP, on cytoskeletal element organisation and ECM remodelling. Therefore, cells were seeded into 3% agarose gels and cultured in ITS to maintain the original phenotype of the NP cells.

### 5.4.1 IVD cells remain their phenotypes in 3D culture system

Previous studies have shown that 3D cultures maintain their cell phenotype, and can even reverse differentiation induced by monolayer culture (Wang et al., 2001; Kluba et al., 2005; Chou et al., 2008). However, most of the 3D culture systems for intervertebral disc cells focus on alginate gel (Chiba et al., 1997; Wang et al., 2001; Thonar et al., 2002; Kluba et al., 2005; Shao and Hunter, 2007), which is a viscous gum formed by alginic acid in the presence of calcium ions. An advantage of the alginate culture system is that it is easy to isolate cells from the gel. However, this process takes a relatively long time and involves detachment of the cells and ECM, which might affect gene expression. Some evidence has also shown that the chondrocyte phenotype was altered when cultured in alginate beads (Gregory et al., 1999). In addition, the alginate gel is soft and viscous, therefore when it is compressed, there is not only compressive deformation but also stretching and torsional movement (data not shown), which might affect interpretation of the results. Agarose has often been used for three-dimensional cultures of chondrocytes, a cell type which is similar to NP cells



(LeBaron and Athanasiou, 2000) and recent studies have indicated that it also maintains the intervertebral disc cell phenotype long term (Sato et al., 2001; Gruber et al., 2006). Another important advantage of the agarose culture system is that it is easy to control the displacement when compressive loading is applied due to the stiffness of the agarose gel. Therefore, an agarose gel culture system was used in this study.

The cell phenotypes of NP and OAF cells in agarose constructs were analysed for types I and II collagen as well as aggrecan gene expression using real-time PCR. As expected, there was more type II collagen in NP cells and higher levels of type I collagen in OAF cells, suggesting that the NP and OAF cells kept their phenotypes. There were no zonal differences in aggrecan gene expression between young NP and OAF, which may be because of sample to sample variations in the OAF cells. Another explanation is the alteration in the OAF cell phenotype, as previous studies have shown that seeding OAF cells into agarose promotes aggrecan expression (Gruber et al., 1997; Sato et al., 2001; Gruber et al., 2006). There were no zonal variations in type I collagen gene expression between mature NP and OAF cells, which may be due to the higher variability in mRNA levels. Moreover, previous studies have shown that there was an age-related increase in type I collagen in NP cells (Zhao et al., 2007a). More aggrecan and type II collagen mRNA levels were found in young OAF compared with mature OAF cells, and lower type I collagen gene expression was observed in young NP compared with mature NP cells. All of these results suggest that the zonal and age-related differences in these ECM components observed *in situ* (Chapter 2) were retained in the agarose culture system, indicating its suitability for maintaining IVD cell phenotypes *in vitro*.

Cell viability was investigated after compressive loading was applied. The live-dead assay indicated that cells were evenly distributed in the agarose gel, but there appeared to be some dead cells at the bottom of the gel. This cell death must have occurred when the cells went into the agarose as cell viability was assessed prior to seeding into the agarose gel, using the trypan blue assay and only cells with viability >95% were used for 3D culture. To quantify the cell death rate in agarose after loading, the LDH assay was performed and the results indicated that there was no significant increase in cell death in response to load, which excluded the possibility that the following experimental results were due to increased cell death.

## 5.4.2 Effect of compression on the cytoskeletal elements in IVD cells

Compressive loading is an important mechanical stimulus *in vivo*, especially in the NP of the disc. However, the relationship between compressive loading and the cytoskeleton is largely unknown, as very few studies have been performed. Static compressive loading increases vimentin expression and polymerisation in annulus fibrosus cells cultured in alginate (Chen et al., 2004), suggesting that cytoskeletal elements are involved in mechanotransduction. Alterations in cytoskeletal elements organisation and expression in intervertebral disc cells in response to cyclic compressive strain were therefore investigated. Firstly, the architectures of the cytoskeletal elements F-actin,  $\beta$ -tubulin and vimentin were investigated using confocal microscopy. In contrast to the organisation of IVD cells cultured in monolayer, F-actin was punctate and was distributed beneath the cell membrane in the NP cells cultured in agarose. This kind of organisation is very similar to the architecture of F-actin observed *in situ* (Section 2.3.3.1), further suggesting that the agarose culture system maintains the NP phenotype. However, the organisation of F-actin in the OAF cells was different to that observed *in situ*. The F-actin staining was punctate and fibre-like, but was still localised beneath the cell membrane. This difference in F-actin architecture may arise from the culture system used. NP cells are chondrocyte-like whereas OAF cells are fibroblast-like, which means that the OAF cells are better suited to monolayer culture. In the agarose gel, although the OAF cells had become round or oval, their phenotype still remained fibroblast-like, with high levels of type I collagen and relatively low levels of type II collagen and aggrecan. It may be that F-actin organisation was still fibre-like although the filaments were folded together because of the round or oval appearance of the cells. Interestingly, it seemed that the nuclei of OAF cells maintained their elongated appearance. However, in order to fit into the round or oval shape of the cells, some of the nuclei were folded and displayed a “broad bean-like” shape (Figure 5-4I, K & O).

After compressive loading, there was no alteration in the organisation of F-actin, either in NP or OAF cells, illustrating that F-actin filaments were not sensitive to compressive

loading. This is consistent with the previous results obtained from articular cartilage. However, a recent study performed in chondrocytes cultured in agarose suggested that both static and cyclic compressive loading could induce notable differences in F-actin organisation with a more pronounced punctate distribution when compared with the unloaded control, although the methodology used to quantify the organisation of F-actin filaments is not well addressed (Knight et al., 2006b). The disagreement between these two studies may come from the quantitative analysis used by Knight (Knight et al., 2001). Therefore, to further address whether actin filaments are involved in mechanotransduction,  $\beta$ -actin gene expression was investigated. Consistent with the confocal results, there was no alteration in  $\beta$ -actin gene expression after load, suggesting that actin filaments do not respond to 10% cyclic compression at 1Hz in intervertebral disc cells cultured in agarose. However, recent studies demonstrated that compressive loading transiently induced actin de-polymerisation in chondrocytes cultured in agarose (Campbell et al., 2007), which may not be detected by confocal microscopy. To investigate this further, mRNA levels of actin-associated proteins were quantified in NP and OAF cells subjected to load. These included cofilin, destrin,  $\alpha$ -actinin and gelsolin, but there was no change after 10, 30 or 60 minutes of load, further confirming the results that actin filament organisation is not regulated by a 10% cyclic compressive load (1Hz) in IVD cells cultured in agarose.

Vinculin is a predominant component of focal contacts and is involved in the interaction between F-actin filaments and integrins. The activation of vinculin plays a pivotal role in focal contact formation and actin filament regulation (Zamir and Geiger, 2001). A recent study has shown that mechanical stimulation regulates chondrocyte metabolism through the stretch-activated cation channel; when it was blocked, a significant loss of chondrocyte phenotype was observed, in which vinculin expression and F-actin stress fibres appeared simultaneously (Perkins et al., 2005). Therefore, vinculin can be regarded as a marker for the loss of chondrocyte phenotype. In this study, vinculin expression declined in NP cells after loading, which correlated with the increased type II collagen and aggrecan mRNA levels, suggesting that physiological compressive stimulation can stabilise the chondrocyte-like phenotype of NP cells.

However, in mature OAF cells, there was an increase in vinculin gene expression after loading, which may reflect the distinct OAF phenotype.

Preliminary studies have addressed the relationship between microtubules and compressive loading (Dennerll et al., 1988; Jortikka et al., 2000). However, the effects of compressive loading on the organisation and expression of  $\beta$ -tubulin in IVD cells are still largely unknown. In this study, there appeared to be a more organised filament network in OAF cells after 60 minutes of compressive load, illustrating that the microtubules might respond to load. Further real-time PCR results confirmed this hypothesis, with higher  $\beta$ -tubulin gene expression observed in mature NP cells but lower  $\beta$ -tubulin mRNA levels in mature OAF cells after load. The increased  $\beta$ -tubulin gene levels in NP cells may be caused by increased ECM remodelling. One of the main functions of the microtubules within cells is to transport proteins (Pellegrini and Budman, 2005). Therefore, the increased synthesis of ECM components such as aggrecan and type II collagen (Jortikka et al., 2000; De Croos et al., 2006; Mauck et al., 2007) in cells subjected to compressive load might induce higher microtubule expression to support the increased demands for protein synthesis and transport. Moreover, microtubules can respond to variations in environmental conditions due to the dynamic nature of their assembly /disassembly and may act as mechanotransducers in cells (Morris, 1990). Therefore, the increased  $\beta$ -tubulin gene expression observed here suggests that microtubules are involved in the initiation of mechanotransduction, and thereafter up-regulate expression of ECM genes. This is supported by previous microtubule disruption experiments conducted in heart myocytes (Samuel et al., 1986; Takahashi et al., 1998) and articular cartilage (Jortikka et al., 2000), in which the disruption of microtubules abrogated the alterations of ECM remodelling induced by load.

$\beta$ -tubulin mRNA expression decreased in mature OAF cells after load. Previous studies have indicated that different magnitudes of compressive loading induced distinct ECM remodelling processes (Jortikka et al., 2000). Also, long term static compressive loading decreased the microtubule expression in axons (Nemoto, 1991) and the degree of reduction correlated with the duration and force. Therefore, it is reasonable to hypothesise that the reduction in microtubules may be a result of the type of

compression applied. The mechanical load applied to OAF cells is quite distinct from that on NP cells, as OAF cells mainly experience tension *in vivo*. Therefore, a 10% compressive strain which is physiological for NP cells may be pathological for OAF cells. Moreover, the alteration in OAF cell morphology from an elongated cell to a round or oval appearance in agarose may also change the cells' response to compressive loading.

Interestingly,  $\beta$ -tubulin mRNA was not mechanically-regulated in young NP and OAF cells when compared with their mature counterparts. Previous studies have indicated that  $\beta$ -tubulin decreases in senescent chondrocytes when compared with young cells (Ronot et al., 1988). This suggests that young NP and OAF cells may have a greater microtubule content when compared with mature cells. Therefore, it is reasonable to deduce that the microtubule content in young cells is sufficient to support the increased metabolic demands induced by compressive loading, and that there would be no need to alter  $\beta$ -tubulin expression.

It has been known for a long time that vimentin filaments may be involved in mechanotransduction (Galou et al., 1997; Wang and Stamenovic, 2002; Pekny and Lane, 2007). However, the precise mechanism of how vimentin filaments adapt to compressive load is still largely unknown. In IVD, compressive loading seemed to induce a more organised vimentin architecture, consistent with the preliminary results obtained from articular cartilage, and suggests that vimentin filaments play an important role in mechanotransduction within IVD cells. A reduction in vimentin gene expression was observed in both young and mature NP cells after load, consistent with previous studies performed on chondrocytes (Li et al., 2007a). However, these results contradict a study in IVD cells, in which increased expression of vimentin mRNA as well as increased polymerisation of vimentin subunits were observed in OAF but not NP cells (Chen et al., 2004). The differences may come from the loading regimes that were used. In Chen's study, static compressive loading was applied on IVD cells from 2 to 30 hours, and only 30 hours of loading induced an increase in vimentin gene expression in OAF cells; there was no alteration after 2 and 18 hours of loading. Differences in vimentin gene expression were not analysed in NP cells that had been loaded for less than 2 hours, therefore they might have missed vimentin changes due to

the relatively short half life for gene expression. Another noticeable difference between these two studies is the frequency of loading. In Chen's study, static compressive loading was used whereas 1Hz of cyclic loading was applied in this study. Previous studies have shown that static and cyclic compressive loading have quite different effects on cell metabolism, and there were even opposing biological responses in chondrocytes subjected to static and cyclic compressive loading (Shieh and Athanasiou, 2007; Wang et al., 2007). The mechanism of these diverse effects is not clear, but a recent study showed that nutritional changes might be involved (Huang and Gu, 2008).

### **5.4.3 Effect of compression on ECM remodelling proteases and inhibitors**

To investigate the effects of compressive loading on ECM remodelling, mRNA levels of the aggrecanases (ADAMTS-4 and 5), MMPs (MMP-1, 2, 3, 9, 13) and TIMPs (TIMP-1, 2, 3) were investigated. Due to low expression levels, ADAMTS-4, MMP-9, MMP-13 and TIMP-3 mRNA were not detected. Compressive loading significantly decreased ADAMTS-5 mRNA content in young NP cells after 30 minutes of load, which corresponded with an increase in aggrecan gene expression. This suggests that a 10% cyclic compressive load can stimulate aggrecan synthesis and deposition in young NP cells. This actually coincides with the biological function of proteoglycans in resisting compressive loading. ADAMTS-5 mRNA was not mechanoresponsive in mature NP cells, suggesting that maturity may slow down the ability of cell to respond.

Zonal variations in ADAMTS-5 gene expression were observed. Higher ADAMTS-5 mRNA levels were detected in young NP cells compared with young OAF cells, which is consistent with the distribution of proteoglycan in IVD *in vivo*, suggesting that the expression of aggrecanase correlates with proteoglycan content. An age-related decrease in ADAMTS-5 mRNA was observed in NP cells which is also consistent with the fact that proteoglycan content in the NP decreases with age (Roughley et al., 2006b).

MMP-1 is a major collagenase which degrades collagen *in vivo*. A transient decrease in MMP-1 gene expression was observed after 10 minutes of loading, but this decline recovered to baseline after 30 minutes and remained unchanged even after 60 minutes of mechanical stimulation. This suggests that a 10% cyclic load can inhibit catabolic gene expression, thereby promoting ECM accumulation.

As with MMP-1, compressive loading also decreased MMP-3 gene expression in NP cells, but not in OAF cells, further supporting the MMP-1 data. Previous studies have investigated the effects of load on IVD cells *in vivo* using a mouse tail model, whereby compressive loading was shown to promote MMP-3 expression (Maclean et al., 2004; MacLean et al., 2005; MacLean et al., 2008). However, the deformation of the disc height induced after 1 hour of loading was 46% (MacLean et al., 2005), much higher than the 10% strain used in this study. Therefore, the increased MMP-3 expression is likely to be induced by non-physiological and potentially damaging compressive load. Similarly, this increased MMP-3 gene expression was also observed in cartilage tissue when subjected to 50% injurious compressive loading (Lee et al., 2005), further suggesting that the biological responses of cells to compressive loading are magnitude-dependent.

MMP-2 is a gelatinase and its main function is to digest denatured collagens (gelatins). Previous studies have shown that compressive loading increased MMP-2 gene expression in articular cartilage (Gosset et al., 2008) and intervertebral disc tissue (MacLean et al., 2008), suggesting that MMP-2 may contribute to load-induced catabolic events. The magnitude of load on IVD was 1MPa, which induced a 46% depression of disc height (MacLean et al., 2005), which, as discussed above, is not a physiological strain compared with the strain applied on human IVD (Botsford et al., 1994; Cheung et al., 2003), and can be regarded as an injurious load. In this study, a 10% compressive strain decreased MMP-2 gene expression in young and mature NP cells. This is consistent with the reduction in MMP-1 and MMP-3 gene expression observed, indicating that physiological loading inhibits catabolism in disc cells, and promotes ECM accumulation. Compressive loading did not change MMP-2 mRNA levels in young OAF cells; however, it significantly increased MMP-2 gene expression in mature OAF cells, illustrating the effects of maturity on disc cell metabolism. These

distinct biological responses in MMP-2 gene expression may suggest a possible mechanism of disc degeneration induced by ageing.

TIMPs are the major inhibitors of MMPs and aggrecanases *in vivo*, and the ratio between the expression of TIMPs and MMPs and ADAMTSs significantly influences the ECM remodelling process. In this study, compressive loading decreased both TIMP-1 and TIMP-2 gene expression in young and mature NP cells, but did not change mRNA expression in their OAF counterparts. These results correlate with the MMP gene expression data, suggesting that compressive loading decreases the ECM turnover rate in NP cells. As increased aggrecan, but decreased type I collagen expression was observed in NP cells, the decline in ECM catabolism induced by loading would promote accumulation of aggrecan which is the major ECM component that resists compressive loading *in vivo*. For mature OAF cells, there was no alteration in TIMPs-1 and -2 expression in response to compressive loading, although an increase in MMP-2 expression in mature OAF cells was observed. This would eventually induce catabolism in mature OAF cells, which as stated above, may contribute to the disc degeneration.

## 5.5 Conclusion

The effects of physiological compressive loading (10%, 1Hz) on the organisation and expression of cytoskeletal elements as well as markers of ECM metabolism in IVD cells cultured in agarose were investigated. Key findings were that:

- Cells retain their phenotype in a 3-D environment.
- 10% compressive loading did not change the architecture or gene expression of actin filaments in IVD cells.
- Decreased vinculin gene expression was found in NP cells subjected to compressive loading, but no alteration was observed in OAF cells after loading.
- There appeared to be a more organised  $\beta$ -tubulin network in IVD cells after load. Compressive loading increased  $\beta$ -tubulin mRNA levels in mature NP cells but decreased  $\beta$ -tubulin gene expression in mature OAF cells.



- There appeared to be a more organised network of vimentin filaments in cells after load, but there was less vimentin gene expression in young and mature NP cells after compression.
- Compressive loading increased type II and aggrecan gene expression but decreased type I collagen expression in NP cells.
- Compressive loading decreased MMPs (MMPs-1, 2 and 3), ADAMTS-5 and TIMPs (TIMPs-1 and 2) gene expression in both young and mature NP cells.

Taken together, there was an increase in type II collagen and aggrecan gene expression in NP cells, but a decrease in ECM degrading enzymes, promoting anabolism in these cells, suggestive of a beneficial effect of physiological compressive loading on homeostasis in NP cells. In contrast to the NP cells, OAF cells had a lower reactivity to compressive loading, reflecting their distinct cell phenotype and mechanical features. Alterations in the organisation and gene expression of  $\beta$ -tubulin and vimentin were also observed in IVD cells after loading, suggesting that  $\beta$ -tubulin and vimentin filaments may be involved in mechanotransduction events. Moreover, the diverse biological response of mature OAF cells subjected to loading illustrates that maturity is an important influencing factor for IVD cell metabolism, especially in response to compressive loads.

# CHAPTER 6.

GENERAL DISCUSSION

It has been known for a long time that disc degeneration is the leading cause of low back pain. However, the precise mechanism of disc degeneration is still largely unknown. It is now becoming clear that the development of disc degeneration is an aberrant, cell mediated process caused by, not a single, but multiple factors including ageing, mechanical stimulation (such as occupation), gender, genetics and nutrition (Hadjipavlou et al., 2008). Ageing and mechanical stimulation are the most important factors contributing to this complex multi-factorial aetiology of IVD degeneration (Adams and Roughley, 2006). Ageing causes inevitable and progressive changes in disc matrix composition; for example the decline in proteoglycan content in the NP of IVD and subsequent loss of water causes redistribution of mechanical loads in the disc. These biomechanical changes will influence cell metabolism and the ECM remodelling process, which again, accelerates changes in matrix composition. Therefore, all of these changes form a positive feedback cycle, eventually causing the irreversible loss of tissue homeostasis and onset of disc degeneration.

During this process, cytoskeletal elements play a pivotal role in the mechanotransduction pathway communicating between the ECM and cell nucleus (Errington et al., 1998; Hayes et al., 1999; Bruehlmann et al., 2002; Chen et al., 2004; Li et al., 2007b). For example, F-actin and  $\beta$ -tubulin filaments in normal chondrocytes have been shown to be altered and become similar in organisation to OA chondrocytes under non-physiological high hydrostatic pressure (24MPa) (Fioravanti et al., 2005). This suggests that the dysregulation of cytoskeletal elements may lead to an abnormal cell phenotype, subsequently causing a loss of tissue homeostasis and onset of disease. Due to the main function of the spine, the IVDs are also subjected to different mechanical stimuli including compressive load, strain and shear (Benjamin and Hillen, 2003). As disc degeneration is also an age-related disease, it may have similar alterations in cytoskeletal element organisation and cell metabolism that have been observed in OA chondrocytes (Fioravanti et al., 2003; Capin-Gutierrez et al., 2004). Therefore, we hypothesise that: (i) An intact cytoskeleton plays an important role in IVD cell mechanotransduction. (ii) As disc degeneration is an age-related disease, there will be differences in the organisation and/or expression of cytoskeletal elements between young and mature IVD cells.

To confirm these hypotheses, cytoskeletal element organisation and expression between young and mature disc tissue and cells were investigated, and the following novel and exciting findings are:

- F-actin filaments are punctate and distributed beneath the cell membrane in both NP and OAF. There is higher  $\beta$ -actin expression in the OAF.
- $\beta$ -tubulin filaments form a meshwork distributed throughout the cytoplasm with more  $\beta$ -tubulin gene and protein expression in the NP.
- Vimentin filaments form a meshwork distributed throughout the cytoplasm with lower vimentin protein content in the OAF.
- There is a decline in vimentin protein, but an increase in partially degraded vimentin in OAF with maturity.

These results suggest that regional and development-related differences exist in cytoskeletal elements in disc cells. The regional variations may arise from the different cell phenotypes and functions of the NP and OAF, which are likely caused by the distinct mechanical environments *in vivo*. Higher  $\beta$ -actin gene and protein expression in the OAF suggests a close relationship between a dynamic actin filament network and strain, which has been shown in other cell types such as chondrocytes (Fioravanti et al., 2003) and fibroblasts (Farsi and Aubin, 1984). The greater expression levels of  $\beta$ -tubulin and vimentin in NP cells indicates that both microtubules and intermediate filaments are more likely to resist compressive loading in disc cells, which is consistent with previous studies in chondrocytes (Lee et al., 2000a; Ohashi et al., 2006). Interestingly, two different vimentin products were observed in IVD tissue, which were not observed in the isolated cells. More intact vimentin expression (58KDa) was observed in young tissue and higher vimentin degradation products (40KDa) in mature tissue. This is consistent with the increased expression of partially degraded vimentin observed in OA chondrocytes (Lambrecht et al., 2008). The precise mechanism of the increased vimentin degradation product is not clear, but it is believed that the cleaved vimentin generally has no N-terminal (Lambrecht et al., 2008), which is essential for vimentin assembly (Traub and Vorgias, 1983). Therefore, the age-related increase in degraded vimentin will decrease the ability of vimentin to assemble to form a network in the cytoplasm, which will disrupt mechano-signalling between the ECM and cell

nucleus, subsequently inducing abnormal cell metabolism and ECM remodelling in response to mechanical stimulation (Lambrecht et al., 2008; Stevens et al., 2008). In future studies, degenerative human disc tissue will be used to further investigate an association of this partially degraded vimentin product with increasing severity of disc degeneration.

Different mechanical stimuli including tension and compression are applied to the IVDs. NP and OAF cells have distinct cell phenotypes which correspond to their distinct mechanical environment *in vivo*. Therefore, the third hypothesis is that: (iii) Differences will exist in the organisation and/or expression levels of cytoskeletal elements in the NP and OAF cells in response to different mechanical stimuli. To confirm this, alterations to these cytoskeletal elements in disc cells subjected to CTS was investigated, and the key findings include:

- NP and OAF cells retain their respective phenotype in monolayer culture.
- Stretch-induced mechano-responses in IVD cells are time and strain-dependent.
- Cyclic tensile strain induces an alteration in F-actin and  $\beta$ -tubulin filament organisation, and regulates the mRNA and protein expression of cytoskeletal components including  $\beta$ -actin,  $\beta$ -tubulin and vimentin.
- Cyclic tensile strain induces increase in cofilin but a decrease in  $\alpha$ -actinin, filamin A and thymosin  $\beta$ 4 gene expression.
- Cyclic tensile strain alters the expression of ECM molecules (type I collagen and aggrecan) and ECM remodelling-related enzymes (ADAMTS-5, MMPs and TIMPs), illustrating an enhanced ECM remodelling in IVD cells after strain.
- OAF cells are more responsive to tensile strain than NP cells.
- Maturity can alter the mechano-responses of mature IVD cells to tensile force compared to young cells.

When dynamic strain is applied to disc cells cultured as a monolayer, more F-actin stress fibres were observed, which is likely induced by rapid turnover of actin filaments as a significant increase in cofilin but a decrease in thymosin  $\beta$ 4 gene expression was observed. Cofilin is an actin binding protein which can sever actin filaments, therefore promote actin depolymerisation but simultaneously provide free barbed ends for actin

polymerisation and nucleation (Ichetovkin et al., 2002). Thymosin  $\beta$ 4 is an actin sequestering protein, which can hold ATP-bound G-actin in a form that is unable to polymerise, therefore the decreased thymosin  $\beta$ 4 transcription (and potential reduction in translation) will generate more ATP-bound G-actin for polymerisation (Atkinson et al., 2004). Taken together, they induce a redistribution of actin filaments in IVD cells to form more stress fibres to increase cell contractility and adapt to the applied strain. The actin-binding activity of cofilin is also regulated by phosphorylation (Lappalainen and Drubin, 1997). When cofilin is phosphorylated, i.e. by LIM kinase, the actin severing activity of cofilin is diminished, which decreases the free actin barbed ends on actin filaments, thereby inhibiting actin polymerisation and slowing down the rate of actin turnover (Theriot, 1997; Bamberg et al., 1999). However, although cofilin mRNA is increased, the effect of CTS on cofilin protein levels and the extent of phosphorylation have not yet been determined in this model system. Previous studies have shown that LIM kinase, the mediator of cofilin phosphorylation, is itself subjected to phosphorylation (Arber et al., 1998; Zhao et al., 2007b), which in turn can be induced by tensile force through a RhoA/Rho-dependent kinase (ROCK) signalling pathway (Sarasa-Renedo et al., 2006; Zhao et al., 2007b). RhoA is a member of the small GTPases that cycles between a GDP-bound inactive state and a GTP-bound active state. The strain-induced activation of RhoA is dependent on  $\beta$ 1 integrin (Takahashi et al., 2003), which is believed to play an important role as a “mechano-sensor” in different cell types including IVD (Choquet et al., 1997; Silver and Siperko, 2003; Chowdhury et al., 2006; Gilchrist et al., 2007; Le Maitre et al., 2009).

Besides actin polymerisation, CTS also altered the transcription of ECM components (type I collagen and aggrecan) and ECM remodelling enzymes (ADAMTS-5, MMPs and TIMPs). Whether these strain-induced alterations are actin dependent is not clear, but a study performed in a rat model indicates that disruption of the actin network can abolish the strain-induced up-regulation of MMP-1 expression in tendon cells (Arnoczky et al., 2004). Moreover, strain-induced tenascin-C synthesis, an ECM glycoprotein mainly distributed in the OAF (Gruber et al., 2002), is dependent on both the intact actin cytoskeleton and RhoA/ROCK signalling pathways (Chapados et al., 2006; Sarasa-Renedo et al., 2006). Therefore, it is reasonable to deduce that the

dynamic F-actin filaments are involved in IVD cell mechanotransduction through integrin-RhoA/ROCK signalling pathways, although this remains to be determined.

Integrins can also trigger other signalling pathways such as mitogen-activated protein kinase (MAPK) (Schmidt et al., 1998) and nuclear factor kappa-light-chain-enhancer of activated B cells (NF- $\kappa$ B) pathways (Xu et al., 1998) within the cells in response to tensile force. The MAPK family consists of extracellular signal-related kinases (ERK1/2), c-Jun N-terminal protein kinase (JNK) and p38 kinases. All of them are involved in strain-induced mechano-responses, i.e. up-regulated MMP-2 expression in muscle cells (Grabellus et al., 2007; Milkiewicz et al., 2007). NF- $\kappa$ B is a protein complex that acts as a transcription factor associated with the ECM remodelling process. Previous studies have shown that NF- $\kappa$ B plays a pivotal role in the strain-induced ECM remodelling process in osteoblasts (Agarwal et al., 2003), and that activation of NF- $\kappa$ B is ERK1/2 dependent (Rubin et al., 2003). It is not clear whether this MAPK-NF- $\kappa$ B mechano-signalling pathway is actin-dependent, but it is thought that it is involved in the long term adaptive response of connective tissue cells to mechanical stress through the auto-/paracrine action of growth factors such as TGF- $\beta$  (Chiquet et al., 2003; Hornberger et al., 2005).

Tension-induced activation of the MAPK pathway is also involved in regulating nitric oxide (NO) expression (Hara et al., 2001; Rubin et al., 2003). NO is an important second messenger molecule involved in many physiological and pathological processes. Previous studies indicated that CTS reduced aggrecan gene expression in IVD cells in a NO dependent manner (Rannou et al., 2003; Benallaoua et al., 2006). More interestingly, a study in osteoblasts has shown that strain-induced NO expression, via the MAPK signalling pathway, requires an intact actin network suggesting that actin does participate in this mechanotransduction pathway (Hara et al., 2001).

Besides the signalling mechanisms described above, tensile force can also activate the voltage operated calcium ( $\text{Ca}^{2+}$ ) channels on cell membranes to induce mechano-responses (Walker et al., 2000; Sheu et al., 2005). However, a very recent study in human umbilical vein endothelial cells has shown that load-induced actin reorganisation may be involved in the activation of  $\text{Ca}^{2+}$  channels (Hayakawa et al.,

2008), further suggesting the pivotal role of actin filaments in strain-induced mechanotransduction.

CTS induces a reorganisation of the  $\beta$ -tubulin filaments, along with a reduction in gene and protein expression, illustrating that the microtubule network may be involved in strain-induced mechanotransduction. Previous studies have shown that tensile strain can increase microtubule assembly (Putnam et al., 2001), and that disruption of the microtubule network abolishes strain-induced regulation of RhoA in aortic smooth muscle cells (Putnam et al., 2003). This suggests that strain-induced activation of the Rho GTPases requires changes in the state of microtubule polymerisation. The precise mechanism of microtubule involvement in mechano-signalling is not clear. However, mechanical stress induced-activation of Src, an integrin associated protein, coincides with the displacement of microtubules (Na et al., 2008; Na and Wang, 2008), suggesting that microtubules are essential structures for transmitting stresses to activate other cytoplasmic proteins in the signalling pathways. Therefore, the observed reorganisation of both the actin and tubulin networks in OAF cells in response to cyclic strain may promote the regulation of RhoA, which further modifies the dynamics of F-actin and  $\beta$ -tubulin turnover to induce downstream signalling through MAPK, NF- $\kappa$ B and further transcriptional events.

In cells subjected to tensile strain, the external mechanical forces are mainly resisted by actin filaments, consequently inducing formation of stress fibres. The decreased expression of  $\beta$ -tubulin suggests that microtubules are also involved in tension-induced mechanotransduction, which is likely caused by the role of cellular ‘pre-stress’ in the process of mechanotransduction (Chiquet et al., 2003). According to the tensegrity model (Ingber et al., 1994), “cellular tensegrity”, which refers to structures with an integrity based on a balance between tension and compression, a cell is only able to sense mechanical stimulation at its external surface if it maintains a certain amount of resistance by internal cytoskeletal tension. Therefore, strain-induced mechanotransduction needs at least two cytoskeletal elements: actin filaments which mainly generate tensile force within cells (Kolodney and Wysolmerski, 1992), and microtubules which serve as intracellular struts that counteract actin-generated contraction (Gittes et al., 1993; Howard and Hyman, 2003; Ingber et al., 1994). If any



one of the cytoskeletal elements is disrupted, the cell will lose its pre-stress and will be unable to sense the external mechanical stimulation applied to it. Therefore, F-actin and  $\beta$ -tubulin appear to work together to mediate mechanotransduction.

Strain did not alter the organisation of vimentin in IVD cells, but there was a transient decrease in vimentin gene and protein expression in response to strain, suggesting that vimentin may also be involved in mechanotransduction. Vimentin filaments are believed to act as a cell filler by cross-linking with actin and tubulin filaments to comprise a dense network for mechanotransduction (Galou et al., 1997; Pekny and Lane, 2007). Previous studies have shown that vimentin filaments respond to different mechanical stimuli such as torsion (Wang and Stamenovic, 2000), shear (Henrion et al., 1997; Helmke et al., 2003; Loufrani and Henrion, 2008), compression (Eggli et al., 1988; Schnittler et al., 1993; Benjamin et al., 1994; Chen et al., 2004) and stretch (Karjalainen et al., 2003). This may be induced by the dynamic features of the vimentin filaments. There are three separate domains in the vimentin protein: the head, the central helical coiled-coil/rod, and the non-helical tail domain. The N-terminal head domain is the regulatory region affecting the polymerisation of vimentin through phosphorylation (Eriksson et al., 2004). When dephosphorylated, vimentin assembles to form filaments which comprise the network; when phosphorylated, vimentin filaments will disassemble. Therefore, vimentin is an ideal candidate to participate in mechanotransduction due to the dynamic nature of its assembly/disassembly via de/phosphorylation *in vivo*. Vimentin assembly/disassembly is regulated by other kinases such as MAPK, Akt (protein kinase B) and protein kinase C which are themselves known to be activated by mechanical stimulation (Ridge et al., 2005). For example, the translocation of RhoA-binding kinase  $\alpha$  (ROK $\alpha$ ) – a serine/threonine kinase that directly binds to the activated form of RhoA, can act as an effector to promote the reorganisation of actin filaments, but this is only facilitated when the vimentin network disassembles by phosphorylation (Sin et al., 1998).

The alterations induced by stretching were variable and sometimes inconsistent, which may have resulted from the monolayer culture system. Compared to NP cells, OAF cells are more reactive to tensile strain, which is likely induced by the distinct differences in cell phenotype between NP and OAF. NP cells are more

chondrocyte-like, and mainly resist compression *in vivo*. Therefore, alterations in the organisation and expression of cytoskeletal elements and markers of cell metabolism in IVD cells in response to compressive loading were investigated using a 3D culture system. Key findings are:

- Cells retain their phenotype in a 3-D environment.
- Compressive loading changes the architecture of actin filaments, but no alteration in actin gene expression is observed in IVD cells.
- Decreased vinculin gene expression is found in NP cells subjected to compressive loading, but no alteration is observed in OAF cells after loading.
- There appears to be a more organised  $\beta$ -tubulin network in IVD cells after load. Compressive loading increases  $\beta$ -tubulin mRNA levels in mature NP cells but decreases  $\beta$ -tubulin gene expression in mature OAF cells.
- There appears to be a more organised network of vimentin filaments in cells after load, but there is less vimentin gene expression in young and mature NP cells after compression.
- Compressive loading increases type II collagen and aggrecan gene expression but decreases type I collagen expression in NP cells.
- Compressive loading decreases MMPs (MMP-1, 2 and 3), ADAMTS-5 and TIMPs (TIMP-1 and 2) gene expression in both young and mature NP cells.
- NP cells are more responsive to compression compared to OAF cells.
- Maturity alters the mechano-responses of mature IVD cells to compressive loading.

In contrast to the effects of stretch, compressive loading causes partial pooling of the actin filaments, which is consistent with previous studies performed in chondrocytes (Haudenschild et al., 2008a; Haudenschild et al., 2008b), suggesting actin filaments reorganise when loads are applied. However, no alterations in the expression of actin-binding proteins such as cofilin and thymosin  $\beta$ 4 are observed in IVD cells, although previous studies in chondrocytes have shown that compression can up-regulate both thymosin  $\beta$ 4 (Blain et al., 2002; Blain et al., 2003) and cofilin gene expression (Campbell et al., 2007). This may be caused by the different cell type and mechanical load applied. Recent studies have shown that compression, as with

stretching, can activate RhoA signalling, which in turn induces a reorganisation of actin filaments in chondrocytes (Haudenschild et al., 2008a). Moreover, compression induced NO synthesis is also dependent on RhoA and actin filaments (Haudenschild et al., 2008b). Therefore, the reorganisation of actin filaments observed in the NP cells may likewise be involved in similar mechanotransduction pathways involving RhoA, but this remains to be determined.

In contrast to the stretch study, there is a significant increase in  $\beta$ -tubulin mRNA levels in response to compression. Similar to the role of F-actin in resisting tensile force in the IVD, compressive loading is mainly resisted by the  $\beta$ -tubulin filaments, which may explain the compression-induced increase in  $\beta$ -tubulin gene expression. Although the synthesis and secretion of proteoglycans and collagen in chondrocytes are microtubule dependent (Blain, 2009), the precise mechanism of microtubule involvement in compression-induced mechanotransduction is poorly understood. However, some studies in chondrocytes have shown that the reorganisation of  $\beta$ -tubulin filaments are involved in the compression-induced displacement and deformation of cellular organelles such as rough endoplasmic reticulum, mitochondria and Golgi apparatus which could lead subsequent alterations in cell metabolism (Lee et al., 2000a; Szafranski et al., 2004; Knight et al., 2006a; Ohashi et al., 2006).

As with the stretching study, a decline in vimentin gene expression was observed in IVD cells in response to compression, suggesting that vimentin filaments are involved in compression-induced mechanotransduction, although whether this decrease is evident the protein level remains to be determined. In IVD cells, static compression increased vimentin gene expression and polymerisation of vimentin subunits (Chen et al., 2004). The mechanism of how vimentin filaments participate in signalling is an emerging area of research. Previous studies have shown that the assembly/disassembly of vimentin networks regulate matrix synthesis such as collagen and proteoglycan at both the mRNA and protein level in chondrocytes (Blain et al., 2006), illustrating that vimentin polymerisation may play an important role. Moreover, the disruption of vimentin networks in chondrocytes also increases the phosphorylation of ERK1/2 (unpublished data from Dr. Emma Blain, Cardiff University). This suggests that due to vimentin's role as a phosphoprotein *in vivo*, the effect of the vimentin network on

matrix synthesis is mediated by de/phosphorylation of downstream signalling molecules, e.g. MAPK and ultimately NF- $\kappa$ B the DNA binding element present in the promoter of both *col2a1* and *aggrecan* genes.

Cytoskeletal elements compose a dense network throughout the whole cytoplasm, establishing a linkage between the ECM and cell nucleus and therefore participate in mechanotransduction (Peyton et al., 2007). When mechanical stress is applied on cells, there is a sub-cellular displacement and reorganisation of the cytoskeleton lattice, transmitting the load to the cell nucleus to induce biological responses to the mechanical stimulus (Alenghat and Ingber, 2002). During this process, all of the cytoskeletal elements are likely to be involved in mechanotransduction. However, results presented here, show for the first time that stretching and compression induce different mechano-responses in the organisation and expression of cytoskeletal elements and on IVD cell metabolism. Moreover, these mechano-responses are different between NP and OAF cells. NP and OAF cells are two distinct cell populations in the IVD. In this study, NP and OAF cells also have different metabolic responses to stretching and compression. NP cells have more reactivity to compressive loading, and OAF cells to tensile force. This is consistent with their respective mechanical environments *in situ*, further illustrating the importance of mechanical stimuli on IVD cell metabolism and tissue homeostasis.

Disc degeneration is an age-related disease and another question that is addressed is whether mechanical stimulation induces similar responses in cytoskeletal element organisation/expression and ECM metabolism in mature IVD cells as it does in young. As expected, maturity does delay the response to stretching in OAF cells; a higher level of strain i.e. 15% is required to produce type I collagen, which in young cells is evident with 10% strain. Interestingly, cyclic strain only increases MMP-1 gene expression in mature NP cells and not in the young, suggesting that the different age-related responses can contribute to “abnormal” ECM remodelling processes in IVD cells, which could increase the potential risk of a loss of tissue homeostasis, and the likelihood of disc degeneration.

There are two drawbacks to these studies. Firstly, cells were cultured as a monolayer on type I collagen when the effects of stretching on IVD cells was investigated. Although

maintenance of the cell phenotypes i.e. types I and II collagen and aggrecan levels are confirmed, there are still some changes in cell morphology and phenotype, especially in the NP cells, which might alter how the cells convert a biomechanical signal into alterations in the cytoskeleton and ECM remodelling molecules. As with all cell culture studies, care should be taken in interpreting the results as the system does not necessarily mimic the biological alterations induced by stretching *in vivo*. However, using both a monolayer and 3D culture system has enabled the potential cellular responses to be delineated. For future studies, a 3D-culture system with a well established ECM would yield more informative results which might better represent the *in vivo* situation. Secondly, the mature disc tissue and cells come from 18 month old bovine tails, which is not comparable with an elderly 80 year old human disc, so the combined effects of ageing and mechanical stimulation are not as significant as expected. However, this does not mean that ageing plays no role in disc degeneration. In future studies, 'old' disc samples (9-10 year old bovine tails) would be more useful. Additionally, human IVD tissue from normal and degenerate discs could be used to repeat these experiments in future studies. Moreover, disrupting specific cytoskeletal elements using chemical agents or siRNA technology could provide direct evidence for the role that the cytoskeleton plays in mechanotransduction induced by different mechanical stimuli.

Understanding how reorganisation of the individual networks induces transcriptional responses would also be necessary. Phospho-protein arrays exist which allow the involvement of kinases and phosphatases to be identified; this would yield valuable information as to which signalling molecules are sensitive to mechanical load in IVD cells, and ultimately elucidate the mechano-responsive pathways activated in IVD cells.

In conclusion, for the first time, this study demonstrates that stretching and compression induce different responses in the organisation and expression of cytoskeletal elements and on IVD cell metabolism. Further, it suggests the specific involvement of cytoskeletal elements including  $\beta$ -actin,  $\beta$ -tubulin and vimentin filaments in mechanotransduction in NP and OAF cells. Ageing is an important influencing factor for mechanotransduction in IVD cells, as the cells' response to

mechanical load is delayed or even reversed in mature IVD tissue. Further studies are needed to elucidate the precise signalling mechanisms of the specific cytoskeletal elements in mechanotransduction, which will provide valuable information for finding diagnostic markers and new treatment strategies to alleviate IVD degeneration.

# BIBLIOGRAPHY

## Bibliography

---

**Acaroglu, E. R., Iatridis, J. C., Setton, L. A., Foster, R. J., Mow, V. C. and Weidenbaum, M.** (1995). Degeneration and aging affect the tensile behavior of human lumbar anulus fibrosus. *Spine* **20**, 2690-701.

**Adams, M. A.** (2004). Biomechanics of back pain. *Acupunct Med* **22**, 178-88.

**Adams, M. A.** (2006). Mechanical function of the lumbosacral spine. In *The biomechanics of back pain*, (ed. S. Wolfaard). Churchill, livingstone: Elsevier.

**Adams, M. A., Dolan, P. and Hutton, W. C.** (1986). The stages of disc degeneration as revealed by discograms. *J Bone Joint Surg Br* **68**, 36-41.

**Adams, M. A., Freeman, B. J., Morrison, H. P., Nelson, I. W. and Dolan, P.** (2000). Mechanical initiation of intervertebral disc degeneration. *Spine* **25**, 1625-36.

**Adams, M. A. and Hutton, W. C.** (1982). Prolapsed intervertebral disc. A hyperflexion injury 1981 Volvo Award in Basic Science. *Spine* **7**, 184-91.

**Adams, M. A. and Hutton, W. C.** (1985). Gradual disc prolapse. *Spine* **10**, 524-31.

**Adams, M. A., McNally, D. S. and Dolan, P.** (1996). 'Stress' distributions inside intervertebral discs. The effects of age and degeneration. *J Bone Joint Surg Br* **78**, 965-72.

**Adams, M. A. and Roughley, P. J.** (2006). What is intervertebral disc degeneration, and what causes it? *Spine* **31**, 2151-61.

**Adams, P., Eyre, D. R. and Muir, H.** (1977). Biochemical aspects of development and ageing of human lumbar intervertebral discs. *Rheumatol Rehabil* **16**, 22-9.

**Agarwal, S., Long, P., Gassner, R., Piesco, N. P. and Buckley, M. J.** (2001). Cyclic tensile strain suppresses catabolic effects of interleukin-1beta in fibrochondrocytes from the temporomandibular joint. *Arthritis Rheum* **44**, 608-17.

**Agarwal, S., Long, P., Seyedain, A., Piesco, N., Shree, A. and Gassner, R.** (2003). A central role for the nuclear factor-kappaB pathway in anti-inflammatory and proinflammatory actions of mechanical strain. *Faseb J* **17**, 899-901.

**Aguiar, D. J., Johnson, S. L. and Oegema, T. R.** (1999). Notochordal cells interact with nucleus pulposus cells: regulation of proteoglycan synthesis. *Exp Cell Res* **246**, 129-37.

**Aigner, T., Gresk-otter, K. R., Fairbank, J. C., von der Mark, K. and Urban, J. P.** (1998). Variation with age in the pattern of type X collagen expression in normal and scoliotic human intervertebral discs. *Calcif Tissue Int* **63**, 263-8.



## Bibliography

---

**Alenghat, F. J. and Ingber, D. E.** (2002). Mechanotransduction: all signals point to cytoskeleton, matrix, and integrins. *Sci STKE* **2002**, PE6.

**Amour, A., Slocombe, P. M., Webster, A., Butler, M., Knight, C. G., Smith, B. J., Stephens, P. E., Shelley, C., Hutton, M., Knauper, V. et al.** (1998). TNF-alpha converting enzyme (TACE) is inhibited by TIMP-3. *FEBS Lett* **435**, 39-44.

**Anderson, D. G. and Tannoury, C.** (2005). Molecular pathogenic factors in symptomatic disc degeneration. *Spine J* **5**, 260S-266S.

**Antoniou, J., Steffen, T., Nelson, F., Winterbottom, N., Hollander, A. P., Poole, R. A., Aebi, M. and Alini, M.** (1996). The human lumbar intervertebral disc: evidence for changes in the biosynthesis and denaturation of the extracellular matrix with growth, maturation, ageing, and degeneration. *J Clin Invest* **98**, 996-1003.

**Aota, Y., An, H. S., Imai, Y., Thonar, E. J., Muehleman, C. and Masuda, K.** (2006). Comparison of cellular response in bovine intervertebral disc cells and articular chondrocytes: effects of lipopolysaccharide on proteoglycan metabolism. *Cell Tissue Res* **326**, 787-93.

**Arber, S., Barbayannis, F. A., Hanser, H., Schneider, C., Stanyon, C. A., Bernard, O. and Caroni, P.** (1998). Regulation of actin dynamics through phosphorylation of cofilin by LIM-kinase. *Nature* **393**, 805-9.

**Armstrong, D. G. and Jude, E. B.** (2002). The role of matrix metalloproteinases in wound healing. *J Am Podiatr Med Assoc* **92**, 12-8.

**Arner, E. C.** (2002). Aggrecanase-mediated cartilage degradation. *Curr Opin Pharmacol* **2**, 322-9.

**Arnoczky, S. P., Tian, T., Lavagnino, M. and Gardner, K.** (2004). Ex vivo static tensile loading inhibits MMP-1 expression in rat tail tendon cells through a cytoskeletally based mechanotransduction mechanism. *J Orthop Res* **22**, 328-33.

**Atkinson, S. J., Hosford, M. A. and Molitoris, B. A.** (2004). Mechanism of actin polymerization in cellular ATP depletion. *J Biol Chem* **279**, 5194-9.

**Ayad S, W. J. B.** (1986). Biochemistry of the intervertebral disc. In *The lumbar spine and back pain*, (ed. M. I. V. Jayson), pp. 100-137. London: Churchill Livingstone.

**Bamburg, J. R., McGough, A. and Ono, S.** (1999). Putting a new twist on actin: ADF/cofilins modulate actin dynamics. *Trends Cell Biol* **9**, 364-70.

**Barros, E. M., Rodrigues, C. J., Rodrigues, N. R., Oliveira, R. P., Barros, T. E. and Rodrigues, A. J., Jr.** (2002). Aging of the elastic and collagen fibers in the human cervical interspinous ligaments. *Spine J* **2**, 57-62.

## Bibliography

---

**Baschong, W., Sutterlin, R. and Aebi, U.** (1997). Punch-wounded, fibroblast populated collagen matrices: a novel approach for studying cytoskeletal changes in three dimensions by confocal laser scanning microscopy. *Eur J Cell Biol* **72**, 189-201.

**Battie, M. C., Videman, T. and Parent, E.** (2004). Lumbar disc degeneration: epidemiology and genetic influences. *Spine* **29**, 2679-90.

**Bayliss, M. T.** (1992). Biochemistry of the intervertebral disc. In *The lumbar spine and back pain*, (ed. 4), pp. 111-31. London: Churchill living stone.

**Beard, H. K., Roberts, S. and O'Brien, J. P.** (1981). Immunofluorescent staining for collagen and proteoglycan in normal and scoliotic intervertebral discs. *J Bone Joint Surg Br* **63B**, 529-34.

**Beard, H. K., Ryvar, R., Brown, R. and Muir, H.** (1980). Immunochemical localization of collagen types and proteoglycan in pig intervertebral discs. *Immunology* **41**, 491-501.

**Benallaoua, M., Richette, P., Francois, M., Tsagris, L., Revel, M., Corvol, M., Poiraudou, S., Savouret, J. F. and Rannou, F.** (2006). Modulation of proteoglycan production by cyclic tensile stretch in intervertebral disc cells through a post-translational mechanism. *Biorheology* **43**, 303-10.

**Benjamin, M., Archer, C. W. and Ralphs, J. R.** (1994). Cytoskeleton of cartilage cells. *Microsc Res Tech* **28**, 372-7.

**Benjamin, M. and Hillen, B.** (2003). Mechanical influences on cells, tissues and organs - 'Mechanical Morphogenesis'. *Eur J Morphol* **41**, 3-7.

**Benjamin, M. and Ralphs, J. R.** (2004). Biology of fibrocartilage cells. *Int Rev Cytol* **233**, 1-45.

**Berry, C. C., Shelton, J. C., Bader, D. L. and Lee, D. A.** (2003). Influence of external uniaxial cyclic strain on oriented fibroblast-seeded collagen gels. *Tissue Eng* **9**, 613-24.

**Bertram, H., Steck, E., Zimmerman, G., Chen, B., Carstens, C., Nerlich, A. and Richter, W.** (2006). Accelerated intervertebral disc degeneration in scoliosis versus physiological ageing develops against a background of enhanced anabolic gene expression. *Biochem Biophys Res Commun* **342**, 963-72.

**Blain, E. J.** (2009). Involvement of the cytoskeletal elements in articular cartilage homeostasis and pathology. *Int J Exp Pathol* **90**, 1-15.

**Blain, E. J., Gilbert, S. J., Hayes, A. J. and Duance, V. C.** (2006). Disassembly of the vimentin cytoskeleton disrupts articular cartilage chondrocyte homeostasis. *Matrix Biol* **25**, 398-408.

## Bibliography

---

**Blain, E. J., Mason, D. J. and Duance, V. C. (2002).** The effect of thymosin beta4 on articular cartilage chondrocyte matrix metalloproteinase expression. *Biochem Soc Trans* **30**, 879-82.

**Blain, E. J., Mason, D. J. and Duance, V. C. (2003).** The effect of cyclical compressive loading on gene expression in articular cartilage. *Biorheology* **40**, 111-7.

**Bondeson, J., Wainwright, S., Hughes, C. and Caterson, B. (2008).** The regulation of the ADAMTS4 and ADAMTS5 aggrecanases in osteoarthritis: a review. *Clin Exp Rheumatol* **26**, 139-45.

**Boos, N., Weissbach, S., Rohrbach, H., Weiler, C., Spratt, K. F. and Nerlich, A. G. (2002).** Classification of age-related changes in lumbar intervertebral discs: 2002 Volvo Award in basic science. *Spine* **27**, 2631-44.

**Botsford, D. J., Esses, S. I. and Ogilvie-Harris, D. J. (1994).** In vivo diurnal variation in intervertebral disc volume and morphology. *Spine* **19**, 935-40.

**Bovenzi, M. and Hulshof, C. T. (1999).** An updated review of epidemiologic studies on the relationship between exposure to whole-body vibration and low back pain (1986-1997). *Int Arch Occup Environ Health* **72**, 351-65.

**Brew, K., Dinakarpanian, D. and Nagase, H. (2000).** Tissue inhibitors of metalloproteinases: evolution, structure and function. *Biochim Biophys Acta* **1477**, 267-83.

**Broberg, K. B. (1983).** On the mechanical behaviour of intervertebral discs. *Spine* **8**, 151-65.

**Brown, M. C. and Turner, C. E. (2004).** Paxillin: adapting to change. *Physiol Rev* **84**, 1315-39.

**Brown, M. D. and Hudlicka, O. (2003).** Modulation of physiological angiogenesis in skeletal muscle by mechanical forces: involvement of VEGF and metalloproteinases. *Angiogenesis* **6**, 1-14.

**Brown, M. J., Hallam, J. A., Colucci-Guyon, E. and Shaw, S. (2001).** Rigidity of circulating lymphocytes is primarily conferred by vimentin intermediate filaments. *J Immunol* **166**, 6640-6.

**Bruehlmann, S. B., Rattner, J. B., Matyas, J. R. and Duncan, N. A. (2002).** Regional variations in the cellular matrix of the annulus fibrosus of the intervertebral disc. *J Anat* **201**, 159-71.

**Buckwalter, J. A., Cooper, R. R. and Maynard, J. A. (1976).** Elastic fibers in human intervertebral discs. *J Bone Joint Surg Am* **58**, 73-6.

## Bibliography

---

**Burgeson, R. E. and Hollister, D. W.** (1979). Collagen heterogeneity in human cartilage: identification of several new collagen chains. *Biochem Biophys Res Commun* **87**, 1124-31.

**Campbell, J. J., Blain, E. J., Chowdhury, T. T. and Knight, M. M.** (2007). Loading alters actin dynamics and up-regulates cofilin gene expression in chondrocytes. *Biochem Biophys Res Commun* **361**, 329-34.

**Cantarella, G., Cantarella, R., Caltabiano, M., Risuglia, N., Bernardini, R. and Leonardi, R.** (2006). Levels of matrix metalloproteinases 1 and 2 in human gingival crevicular fluid during initial tooth movement. *Am J Orthod Dentofacial Orthop* **130**, 568 e11-6.

**Capin-Gutierrez, N., Talamas-Rohana, P., Gonzalez-Robles, A., Lavallo-Montalvo, C. and Kouri, J. B.** (2004). Cytoskeleton disruption in chondrocytes from a rat osteoarthrotic (OA) -induced model: its potential role in OA pathogenesis. *Histol Histopathol* **19**, 1125-32.

**Cappello, R., Bird, J. L., Pfeiffer, D., Bayliss, M. T. and Dudhia, J.** (2006). Notochordal cell produce and assemble extracellular matrix in a distinct manner, which may be responsible for the maintenance of healthy nucleus pulposus. *Spine* **31**, 873-82; discussion 883.

**Caterson, B., Hughes, C. E., Roughley, P. and Mort, J. S.** (1995). Anabolic and catabolic markers of proteoglycan metabolism in osteoarthritis. *Acta Orthop Scand Suppl* **266**, 121-4.

**Chakrabarti, S. and Patel, K. D.** (2005). Matrix metalloproteinase-2 (MMP-2) and MMP-9 in pulmonary pathology. *Exp Lung Res* **31**, 599-621.

**Chapados, R., Abe, K., Ihida-Stansbury, K., McKean, D., Gates, A. T., Kern, M., Merklinger, S., Elliott, J., Plant, A., Shimokawa, H. et al.** (2006). ROCK controls matrix synthesis in vascular smooth muscle cells: coupling vasoconstriction to vascular remodeling. *Circ Res* **99**, 837-44.

**Chen, J., Yan, W. and Setton, L. A.** (2004). Static compression induces zonal-specific changes in gene expression for extracellular matrix and cytoskeletal proteins in intervertebral disc cells in vitro. *Matrix Biol* **22**, 573-83.

**Cheung, J. T., Zhang, M. and Chow, D. H.** (2003). Biomechanical responses of the intervertebral joints to static and vibrational loading: a finite element study. *Clin Biomech (Bristol, Avon)* **18**, 790-9.

**Chiba, K., Andersson, G. B., Masuda, K. and Thonar, E. J.** (1997). Metabolism of the extracellular matrix formed by intervertebral disc cells cultured in alginate. *Spine* **22**, 2885-93.

## Bibliography

---

**Chiquet, M., Renedo, A. S., Huber, F. and Fluck, M.** (2003). How do fibroblasts translate mechanical signals into changes in extracellular matrix production? *Matrix Biol* **22**, 73-80.

**Chiquet, M., Tunc-Civelek, V. and Sarasa-Renedo, A.** (2007). Gene regulation by mechanotransduction in fibroblasts. *Appl Physiol Nutr Metab* **32**, 967-73.

**Choquet, D., Felsenfeld, D. P. and Sheetz, M. P.** (1997). Extracellular matrix rigidity causes strengthening of integrin-cytoskeleton linkages. *Cell* **88**, 39-48.

**Chou, A. I., Reza, A. T. and Nicoll, S. B.** (2008). Distinct Intervertebral Disc Cell Populations Adopt Similar Phenotypes in Three-Dimensional Culture. *Tissue Eng Part A* **17**, 17.

**Chowdhury, T. T., Appleby, R. N., Salter, D. M., Bader, D. A. and Lee, D. A.** (2006). Integrin-mediated mechanotransduction in IL-1 beta stimulated chondrocytes. *Biomech Model Mechanobiol* **5**, 192-201.

**Colombini, A., Lombardi, G., Corsi, M. M. and Banfi, G.** (2008). Pathophysiology of the human intervertebral disc. *Int J Biochem Cell Biol* **40**, 837-42.

**Connelly, J. T., Vanderploeg, E. J. and Levenston, M. E.** (2004). The influence of cyclic tension amplitude on chondrocyte matrix synthesis: experimental and finite element analyses. *Biorheology* **41**, 377-87.

**Court, C., Colliou, O. K., Chin, J. R., Liebenberg, E., Bradford, D. S. and Lotz, J. C.** (2001). The effect of static in vivo bending on the murine intervertebral disc. *Spine J* **1**, 239-45.

**Crean, J. K., Roberts, S., Jaffray, D. C., Eisenstein, S. M. and Duance, V. C.** (1997). Matrix metalloproteinases in the human intervertebral disc: role in disc degeneration and scoliosis. *Spine* **22**, 2877-84.

**Critchley, D. R.** (2000). Focal adhesions - the cytoskeletal connection. *Curr Opin Cell Biol* **12**, 133-9.

**Critchley, D. R.** (2004). Cytoskeletal proteins talin and vinculin in integrin-mediated adhesion. *Biochem Soc Trans* **32**, 831-6.

**D'Addario, M., Arora, P. D., Ellen, R. P. and McCulloch, C. A.** (2002). Interaction of p38 and Sp1 in a mechanical force-induced, beta 1 integrin-mediated transcriptional circuit that regulates the actin-binding protein filamin-A. *J Biol Chem* **277**, 47541-50.

**D'Addario, M., Arora, P. D., Ellen, R. P. and McCulloch, C. A.** (2003). Regulation of tension-induced mechanotranscriptional signals by the microtubule network in fibroblasts. *J Biol Chem* **278**, 53090-7.

## Bibliography

---

**D'Addario, M., Arora, P. D., Fan, J., Ganss, B., Ellen, R. P. and McCulloch, C. A.** (2001). Cytoprotection against mechanical forces delivered through beta 1 integrins requires induction of filamin A. *J Biol Chem* **276**, 31969-77.

**De Croos, J. N., Dhaliwal, S. S., Grynepas, M. D., Pilliar, R. M. and Kandel, R. A.** (2006). Cyclic compressive mechanical stimulation induces sequential catabolic and anabolic gene changes in chondrocytes resulting in increased extracellular matrix accumulation. *Matrix Biol* **25**, 323-31.

**del Rio, A., Perez-Jimenez, R., Liu, R., Roca-Cusachs, P., Fernandez, J. M. and Sheetz, M. P.** (2009). Stretching single talin rod molecules activates vinculin binding. *Science* **323**, 638-41.

**Dennerll, T. J., Joshi, H. C., Steel, V. L., Buxbaum, R. E. and Heidemann, S. R.** (1988). Tension and compression in the cytoskeleton of PC-12 neurites. II: Quantitative measurements. *J Cell Biol* **107**, 665-74.

**Devarajan, P., Johnston, J. J., Ginsberg, S. S., Van Wart, H. E. and Berliner, N.** (1992). Structure and expression of neutrophil gelatinase cDNA. Identity with type IV collagenase from HT1080 cells. *J Biol Chem* **267**, 25228-32.

**Deyo, R. A., Mirza, S. K. and Martin, B. I.** (2006). Back pain prevalence and visit rates: estimates from U.S. national surveys, 2002. *Spine* **31**, 2724-7.

**Doege, K. J., Sasaki, M., Kimura, T. and Yamada, Y.** (1991). Complete coding sequence and deduced primary structure of the human cartilage large aggregating proteoglycan, aggrecan. Human-specific repeats, and additional alternatively spliced forms. *J Biol Chem* **266**, 894-902.

**Donohue, P. J., Jahnke, M. R., Blaha, J. D. and Caterson, B.** (1988). Characterization of link protein(s) from human intervertebral-disc tissues. *Biochem J* **251**, 739-47.

**Dours-Zimmermann, M. T. and Zimmermann, D. R.** (1994). A novel glycosaminoglycan attachment domain identified in two alternative splice variants of human versican. *J Biol Chem* **269**, 32992-8.

**Duance, V. C., Crean, J. K., Sims, T. J., Avery, N., Smith, S., Menage, J., Eisenstein, S. M. and Roberts, S.** (1998). Changes in collagen cross-linking in degenerative disc disease and scoliosis. *Spine* **23**, 2545-51.

**Duance, V. C. and Roberts, S.** (2004). The intervertebral disc-structure, composition, and pathology. In *Soft tissue Rheumatology*, pp. 57: Oxford University Press.

**Dunlevy, J. R. and Couchman, J. R.** (1993). Controlled induction of focal adhesion disassembly and migration in primary fibroblasts. *J Cell Sci* **105 ( Pt 2)**, 489-500.

## Bibliography

---

**Durrant, L. A., Archer, C. W., Benjamin, M. and Ralphs, J. R.** (1999). Organisation of the chondrocyte cytoskeleton and its response to changing mechanical conditions in organ culture. *J Anat* **194 ( Pt 3)**, 343-53.

**Ebara, S., Iatridis, J. C., Setton, L. A., Foster, R. J., Mow, V. C. and Weidenbaum, M.** (1996). Tensile properties of nondegenerate human lumbar annulus fibrosus. *Spine* **21**, 452-61.

**Eggl, P. S., Hunziker, E. B. and Schenk, R. K.** (1988). Quantitation of structural features characterizing weight- and less-weight-bearing regions in articular cartilage: a stereological analysis of medial femoral condyles in young adult rabbits. *Anat Rec* **222**, 217-27.

**Eikenberry, E. F., Mendler, M., Bergin, R., Winterhalter, K. H., and Bruckner, P.** (1992). Articular Cartilage and Osteoarthritis, (ed. K. Kuettner, Schleyerbach, R., Peyron, J., and Hascall, V), pp. 133-49. New York: Raven Press, Ltd.

**Erickson, G. R., Northrup, D. L. and Guilak, F.** (2003). Hypo-osmotic stress induces calcium-dependent actin reorganization in articular chondrocytes. *Osteoarthritis Cartilage* **11**, 187-97.

**Eriksson, J. E., He, T., Trejo-Skalli, A. V., Harmala-Brasken, A. S., Hellman, J., Chou, Y. H. and Goldman, R. D.** (2004). Specific in vivo phosphorylation sites determine the assembly dynamics of vimentin intermediate filaments. *J Cell Sci* **117**, 919-32.

**Errington, R. J., Puustjarvi, K., White, I. R., Roberts, S. and Urban, J. P.** (1998). Characterisation of cytoplasm-filled processes in cells of the intervertebral disc. *J Anat* **192 ( Pt 3)**, 369-78.

**Etienne-Manneville, S.** (2004). Actin and microtubules in cell motility: which one is in control? *Traffic* **5**, 470-7.

**Eyre, D. R.** (1979). Biochemistry of the intervertebral disc. *Int Rev Connect Tissue Res* **8**, 227-91.

**Eyre, D. R., Matsui, Y. and Wu, J. J.** (2002). Collagen polymorphisms of the intervertebral disc. *Biochem Soc Trans* **30**, 844-8.

**Eyre, D. R. and Muir, H.** (1976). Types I and II collagens in intervertebral disc. Interchanging radial distributions in annulus fibrosus. *Biochem J* **157**, 267-70.

**Eyre, D. R. and Muir, H.** (1977). Quantitative analysis of types I and II collagens in human intervertebral discs at various ages. *Biochim Biophys Acta* **492**, 29-42.

**Farquharson, C., Lester, D., Seawright, E., Jefferies, D. and Houston, B.** (1999). Microtubules are potential regulators of growth-plate chondrocyte differentiation and hypertrophy. *Bone* **25**, 405-12.

## Bibliography

---

**Farsi, J. M. and Aubin, J. E.** (1984). Microfilament rearrangements during fibroblast-induced contraction of three-dimensional hydrated collagen gels. *Cell Motil* **4**, 29-40.

**Ferguson, S. J. and Steffen, T.** (2003). Biomechanics of the aging spine. *Eur Spine J* **12 Suppl 2**, S97-S103.

**Fioravanti, A., Benetti, D., Coppola, G. and Collodel, G.** (2005). Effect of continuous high hydrostatic pressure on the morphology and cytoskeleton of normal and osteoarthritic human chondrocytes cultivated in alginate gels. *Clin Exp Rheumatol* **23**, 847-53.

**Fioravanti, A., Nerucci, F., Anefeld, M., Collodel, G. and Marcolongo, R.** (2003). Morphological and cytoskeletal aspects of cultivated normal and osteoarthritic human articular chondrocytes after cyclical pressure: a pilot study. *Clin Exp Rheumatol* **21**, 739-46.

**Fleischmajer, R., Perlish, J. S., Burgeson, R. E., Shaikh-Bahai, F. and Timpl, R.** (1990). Type I and type III collagen interactions during fibrillogenesis. *Ann N Y Acad Sci* **580**, 161-75.

**Fleischmajer, R., Timpl, R., Tuderman, L., Raisher, L., Wiestner, M., Perlish, J. S. and Graves, P. N.** (1981). Ultrastructural identification of extension aminopropeptides of type I and III collagens in human skin. *Proc Natl Acad Sci U S A* **78**, 7360-4.

**Frymoyer, J. W. and Cats-Baril, W. L.** (1991). An overview of the incidences and costs of low back pain. *Orthop Clin North Am* **22**, 263-71.

**Fuchs, E. and Cleveland, D. W.** (1998). A structural scaffolding of intermediate filaments in health and disease. *Science* **279**, 514-9.

**Fujita, Y., Duncan, N. A. and Lotz, J. C.** (1997). Radial tensile properties of the lumbar annulus fibrosus are site and degeneration dependent. *J Orthop Res* **15**, 814-9.

**Gal, D., MacDonald, P. C., Porter, J. C., Smith, J. W. and Simpson, E. R.** (1981). Effect of cell density and confluency on cholesterol metabolism in cancer cells in monolayer culture. *Cancer Res* **41**, 473-7.

**Galante, J. O.** (1967). Tensile properties of the human lumbar annulus fibrosus. *Acta Orthop Scand* **100**, Suppl 100:1-91.

**Galou, M., Gao, J., Humbert, J., Mericskay, M., Li, Z., Paulin, D. and Vicart, P.** (1997). The importance of intermediate filaments in the adaptation of tissues to mechanical stress: evidence from gene knockout studies. *Biol Cell* **89**, 85-97.

**Gerstenfeld, L. C., Finer, M. H. and Boedtker, H.** (1985). Altered beta-actin gene expression in phorbol myristate acetate-treated chondrocytes and fibroblasts. *Mol Cell Biol* **5**, 1425-33.



## Bibliography

---

- Gibbons, I. R.** (1981). Cilia and flagella of eukaryotes. *J Cell Biol* **91**, 107s-124s.
- Gilchrist, C. L., Chen, J., Richardson, W. J., Loeser, R. F. and Setton, L. A.** (2007). Functional integrin subunits regulating cell-matrix interactions in the intervertebral disc. *J Orthop Res* **25**, 829-40.
- Goel, V. K., Monroe, B. T., Gilbertson, L. G. and Brinckmann, P.** (1995). Interlaminar shear stresses and laminae separation in a disc. Finite element analysis of the L3-L4 motion segment subjected to axial compressive loads. *Spine* **20**, 689-98.
- Goossens, K., Van Poucke, M., Van Soom, A., Vandesompele, J., Van Zeveren, A. and Peelman, L. J.** (2005). Selection of reference genes for quantitative real-time PCR in bovine preimplantation embryos. *BMC Dev Biol* **5**, 27.
- Gosset, M., Berenbaum, F., Levy, A., Pigenet, A., Thirion, S., Cavadias, S. and Jacques, C.** (2008). Mechanical stress and prostaglandin E(2) synthesis in cartilage. *Biorheology* **45**, 301-20.
- Gotz, W., Barnert, S., Bertagnoli, R., Miosge, N., Kresse, H. and Herken, R.** (1997). Immunohistochemical localization of the small proteoglycans decorin and biglycan in human intervertebral discs. *Cell Tissue Res* **289**, 185-90.
- Grabellus, F., Worm, K. and Schmid, K. W.** (2007). Induction of the matrix metalloproteinase-2 activation system in arteries by tensile stress. Involvement of the p38 MAP-kinase pathway. *Pathol Res Pract* **203**, 135-43.
- Green, T. and Adams, M.** (1993). Tensile properties of the annulus fibrosus. *Eur Spine J* **2**, 203.
- Gregory, K. E., Marsden, M. E., Anderson-MacKenzie, J., Bard, J. B., Bruckner, P., Farjanel, J., Robins, S. P. and Hulmes, D. J.** (1999). Abnormal collagen assembly, though normal phenotype, in alginate bead cultures of chick embryo chondrocytes. *Exp Cell Res* **246**, 98-107.
- Gruber, H. E., Fisher, E. C., Jr., Desai, B., Stasky, A. A., Hoelscher, G. and Hanley, E. N., Jr.** (1997). Human intervertebral disc cells from the annulus: three-dimensional culture in agarose or alginate and responsiveness to TGF-beta1. *Exp Cell Res* **235**, 13-21.
- Gruber, H. E. and Hanley, E. N., Jr.** (1998). Analysis of aging and degeneration of the human intervertebral disc. Comparison of surgical specimens with normal controls. *Spine* **23**, 751-7.
- Gruber, H. E., Hoelscher, G. L., Leslie, K., Ingram, J. A. and Hanley, E. N., Jr.** (2006). Three-dimensional culture of human disc cells within agarose or a collagen sponge: assessment of proteoglycan production. *Biomaterials* **27**, 371-6.

## Bibliography

---

**Gruber, H. E., Ingram, J., Hoelscher, G. L., Norton, H. J. and Hanley, E. N., Jr.** (2007). Cell polarity in the annulus of the human intervertebral disc: morphologic, immunocytochemical, and molecular evidence. *Spine* **32**, 1287-94.

**Gruber, H. E., Ingram, J. A. and Hanley, E. N., Jr.** (2002). Tenascin in the human intervertebral disc: alterations with aging and disc degeneration. *Biotech Histochem* **77**, 37-41.

**Guilak, F.** (1995). Compression-induced changes in the shape and volume of the chondrocyte nucleus. *J Biomech* **28**, 1529-41.

**Guilak, F., Ting-Beall, H. P., Baer, A. E., Trickey, W. R., Erickson, G. R. and Setton, L. A.** (1999). Viscoelastic properties of intervertebral disc cells. Identification of two biomechanically distinct cell populations. *Spine* **24**, 2475-83.

**Hadjipavlou, A. G., Tzermiadianos, M. N., Bogduk, N. and Zindrick, M. R.** (2008). The pathophysiology of disc degeneration: a critical review. *J Bone Joint Surg Br* **90**, 1261-70.

**Handa, T., Ishihara, H., Ohshima, H., Osada, R., Tsuji, H. and Obata, K.** (1997). Effects of hydrostatic pressure on matrix synthesis and matrix metalloproteinase production in the human lumbar intervertebral disc. *Spine* **22**, 1085-91.

**Hara, F., Fukuda, K., Asada, S., Matsukawa, M. and Hamanishi, C.** (2001). Cyclic tensile stretch inhibition of nitric oxide release from osteoblast-like cells is both G protein and actin-dependent. *J Orthop Res* **19**, 126-31.

**Haro, H., Crawford, H. C., Fingleton, B., MacDougall, J. R., Shinomiya, K., Spengler, D. M. and Matrisian, L. M.** (2000). Matrix metalloproteinase-3-dependent generation of a macrophage chemoattractant in a model of herniated disc resorption. *J Clin Invest* **105**, 133-41.

**Haro, H., Shinomiya, K., Murakami, S. and Spengler, D. M.** (1999). Up-regulated expression of matrilysin and neutrophil collagenase in human herniated discs. *J Spinal Disord* **12**, 245-9.

**Hastreiter, D., Ozuna, R. M. and Spector, M.** (2001). Regional variations in certain cellular characteristics in human lumbar intervertebral discs, including the presence of alpha-smooth muscle actin. *J Orthop Res* **19**, 597-604.

**Haudenschild, D. R., D'Lima, D. D. and Lotz, M. K.** (2008a). Dynamic compression of chondrocytes induces a Rho kinase-dependent reorganization of the actin cytoskeleton. *Biorheology* **45**, 219-28.

**Haudenschild, D. R., Nguyen, B., Chen, J., D'Lima, D. D. and Lotz, M. K.** (2008b). Rho kinase-dependent CCL20 induced by dynamic compression of human chondrocytes. *Arthritis Rheum* **58**, 2735-42.

## Bibliography

---

**Hayakawa, K., Tatsumi, H. and Sokabe, M.** (2008). Actin stress fibers transmit and focus force to activate mechanosensitive channels. *J Cell Sci* **121**, 496-503.

**Hayes, A. J., Benjamin, M. and Ralphs, J. R.** (1999). Role of actin stress fibres in the development of the intervertebral disc: cytoskeletal control of extracellular matrix assembly. *Dev Dyn* **215**, 179-89.

**Hayes, A. J., Benjamin, M. and Ralphs, J. R.** (2001). Extracellular matrix in development of the intervertebral disc. *Matrix Biol* **20**, 107-21.

**Heinegard, D., Aspberg, A., Franzen, A. and Lorenzo, P.** (2002). Glycosylated matrix proteins. In *Connective tissue and its heritable disorders: molecular, genetic, and medical aspects*, (ed. S. B. Royce PM), pp. 271-91. New York: Wiley-Liss.

**Hellio Le Graverand, M. P., Ou, Y., Schield-Yee, T., Barclay, L., Hart, D., Natsume, T. and Rattner, J. B.** (2001). The cells of the rabbit meniscus: their arrangement, interrelationship, morphological variations and cytoarchitecture. *J Anat* **198**, 525-35.

**Helmke, B. P., Rosen, A. B. and Davies, P. F.** (2003). Mapping mechanical strain of an endogenous cytoskeletal network in living endothelial cells. *Biophys J* **84**, 2691-9.

**Henrion, D., Terzi, F., Matrougui, K., Duriez, M., Boulanger, C. M., Colucci-Guyon, E., Babinet, C., Briand, P., Friedlander, G., Poitevin, P. et al.** (1997). Impaired flow-induced dilation in mesenteric resistance arteries from mice lacking vimentin. *J Clin Invest* **100**, 2909-14.

**Herrmann, H. and Aebi, U.** (2000). Intermediate filaments and their associates: multi-talented structural elements specifying cytoarchitecture and cytodynamics. *Curr Opin Cell Biol* **12**, 79-90.

**Hickey, D. S. and Hukins, D. W.** (1980). X-ray diffraction studies of the arrangement of collagenous fibres in human fetal intervertebral disc. *J Anat* **131**, 81-90.

**Hilton, R. C. and Ball, J.** (1984). Vertebral rim lesions in dorsolumbar spine. *Ann Rheum Dis* **43**, 856-7.

**Hollander, A. P., Heathfield, T. F., Liu, J. J., Pidoux, I., Roughley, P. J., Mort, J. S. and Poole, A. R.** (1996). Enhanced denaturation of the alpha (II) chains of type-II collagen in normal adult human intervertebral discs compared with femoral articular cartilage. *J Orthop Res* **14**, 61-6.

**Holloway, I., Kayser, M., Lee, D. A., Bader, D. L., Bentley, G. and Knight, M. M.** (2004). Increased presence of cells with multiple elongated processes in osteoarthritic femoral head cartilage. *Osteoarthritis Cartilage* **12**, 17-24.

**Holm, S., Holm, A. K., Ekstrom, L., Karladani, A. and Hansson, T.** (2004). Experimental disc degeneration due to endplate injury. *J Spinal Disord Tech* **17**, 64-71.

## Bibliography

---

**Holm, S., Maroudas, A., Urban, J. P., Selstam, G. and Nachemson, A.** (1981). Nutrition of the intervertebral disc: solute transport and metabolism. *Connect Tissue Res* **8**, 101-19.

**Honda, K., Ohno, S., Tanimoto, K., Ijuin, C., Tanaka, N., Doi, T., Kato, Y. and Tanne, K.** (2000). The effects of high magnitude cyclic tensile load on cartilage matrix metabolism in cultured chondrocytes. *Eur J Cell Biol* **79**, 601-9.

**Hormel, S. E. and Eyre, D. R.** (1991). Collagen in the ageing human intervertebral disc: an increase in covalently bound fluorophores and chromophores. *Biochim Biophys Acta* **1078**, 243-50.

**Hornberger, T. A., Armstrong, D. D., Koh, T. J., Burkholder, T. J. and Esser, K. A.** (2005). Intracellular signaling specificity in response to uniaxial vs. multiaxial stretch: implications for mechanotransduction. *Am J Physiol Cell Physiol* **288**, C185-94.

**Horner, H. A., Roberts, S., Bielby, R. C., Menage, J., Evans, H. and Urban, J. P.** (2002). Cells from different regions of the intervertebral disc: effect of culture system on matrix expression and cell phenotype. *Spine* **27**, 1018-28.

**Horoyan, M., Benoliel, A. M., Capo, C. and Bongrand, P.** (1990). Localization of calcium and microfilament changes in mechanically stressed cells. *Cell Biophys* **17**, 243-56.

**Horst, M. and Brinckmann, P.** (1981). 1980 Volvo award in biomechanics. Measurement of the distribution of axial stress on the end-plate of the vertebral body. *Spine* **6**, 217-32.

**Hsieh, A. H., Wagner, D. R., Cheng, L. Y. and Lotz, J. C.** (2005). Dependence of mechanical behavior of the murine tail disc on regional material properties: a parametric finite element study. *J Biomech Eng* **127**, 1158-67.

**Huang, C. Y. and Gu, W. Y.** (2008). Effects of mechanical compression on metabolism and distribution of oxygen and lactate in intervertebral disc. *J Biomech* **41**, 1184-96.

**Huang, J., Ballou, L. R. and Hasty, K. A.** (2007). Cyclic equibiaxial tensile strain induces both anabolic and catabolic responses in articular chondrocytes. *Gene* **404**, 101-9.

**Hunter, C. J., Matyas, J. R. and Duncan, N. A.** (2003). The notochordal cell in the nucleus pulposus: a review in the context of tissue engineering. *Tissue Eng* **9**, 667-77.

**Hutton, W. C., Elmer, W. A., Boden, S. D., Hyon, S., Toribatake, Y., Tomita, K. and Hair, G. A.** (1999). The effect of hydrostatic pressure on intervertebral disc metabolism. *Spine* **24**, 1507-15.

## Bibliography

---

**Hutton, W. C., Elmer, W. A., Bryce, L. M., Kozłowska, E. E., Boden, S. D. and Kozłowski, M.** (2001). Do the intervertebral disc cells respond to different levels of hydrostatic pressure? *Clin Biomech (Bristol, Avon)* **16**, 728-34.

**Iatridis, J. C., Setton, L. A., Weidenbaum, M. and Mow, V. C.** (1997). Alterations in the mechanical behavior of the human lumbar nucleus pulposus with degeneration and aging. *J Orthop Res* **15**, 318-22.

**Ichetovkin, I., Grant, W. and Condeelis, J.** (2002). Cofilin produces newly polymerized actin filaments that are preferred for dendritic nucleation by the Arp2/3 complex. *Curr Biol* **12**, 79-84.

**Ichimura, K., Tsuji, H., Matsui, H. and Makiyama, N.** (1991). Cell culture of the intervertebral disc of rats: factors influencing culture, proteoglycan, collagen, and deoxyribonucleic acid synthesis. *J Spinal Disord* **4**, 428-36.

**Ingber, D.** (1991). Integrins as mechanochemical transducers. *Curr Opin Cell Biol* **3**, 841-8.

**Ingber, D. E.** (1993). Cellular tensegrity: defining new rules of biological design that govern the cytoskeleton. *J Cell Sci* **104 ( Pt 3)**, 613-27.

**Iscru, D. F., Anghelina, M., Agarwal, S. and Agarwal, G.** (2008). Changes in surface topologies of chondrocytes subjected to mechanical forces: an AFM analysis. *J Struct Biol* **162**, 397-403.

**Ishihara, H., McNally, D. S., Urban, J. P. and Hall, A. C.** (1996). Effects of hydrostatic pressure on matrix synthesis in different regions of the intervertebral disk. *J Appl Physiol* **80**, 839-46.

**Ishihara, H. and Urban, J. P.** (1999). Effects of low oxygen concentrations and metabolic inhibitors on proteoglycan and protein synthesis rates in the intervertebral disc. *J Orthop Res* **17**, 829-35.

**Ishii, Y., Thomas, A. O., Guo, X. E., Hung, C. T. and Chen, F. H.** (2006). Localization and distribution of cartilage oligomeric matrix protein in the rat intervertebral disc. *Spine* **31**, 1539-46.

**Ishikawa, H., Bischoff, R. and Holtzer, H.** (1968). Mitosis and intermediate-sized filaments in developing skeletal muscle. *J Cell Biol* **38**, 538-55.

**Jaasma, M. J., Jackson, W. M. and Keaveny, T. M.** (2006). The effects of morphology, confluency, and phenotype on whole-cell mechanical behavior. *Ann Biomed Eng* **34**, 759-68.

**Janmey, P. A., Euteneuer, U., Traub, P. and Schliwa, M.** (1991). Viscoelastic properties of vimentin compared with other filamentous biopolymer networks. *J Cell Biol* **113**, 155-60.

## Bibliography

---

**Johnson, E. F., Mitchell, R., Berryman, H., Cardoso, S., Ueal, O. and Patterson, D.** (1986). Secretory cells in the nucleus pulposus of the adult human intervertebral disc. A preliminary report. *Acta Anat (Basel)* **125**, 161-4.

**Johnson, W. E. and Roberts, S.** (2003). Human intervertebral disc cell morphology and cytoskeletal composition: a preliminary study of regional variations in health and disease. *J Anat* **203**, 605-12.

**Johnstone, B. and Bayliss, M. T.** (1995). The large proteoglycans of the human intervertebral disc. Changes in their biosynthesis and structure with age, topography, and pathology. *Spine* **20**, 674-84.

**Johnstone, B., Markopoulos, M., Neame, P. and Catterson, B.** (1993). Identification and characterization of glycanated and non-glycanated forms of biglycan and decorin in the human intervertebral disc. *Biochem J* **292** ( Pt 3), 661-6.

**Jortikka, M. O., Parkkinen, J. J., Inkinen, R. I., Karner, J., Jarvelainen, H. T., Nelimarkka, L. O., Tammi, M. I. and Lammi, M. J.** (2000). The role of microtubules in the regulation of proteoglycan synthesis in chondrocytes under hydrostatic pressure. *Arch Biochem Biophys* **374**, 172-80.

**Karjalainen, H. M., Sironen, R. K., Elo, M. A., Kaarniranta, K., Takigawa, M., Helminen, H. J. and Lammi, M. J.** (2003). Gene expression profiles in chondrosarcoma cells subjected to cyclic stretching and hydrostatic pressure. A cDNA array study. *Biorheology* **40**, 93-100.

**Kashiwagi, M., Tortorella, M., Nagase, H. and Brew, K.** (2001). TIMP-3 is a potent inhibitor of aggrecanase 1 (ADAM-TS4) and aggrecanase 2 (ADAM-TS5). *J Biol Chem* **276**, 12501-4.

**Kasra, M., Goel, V., Martin, J., Wang, S. T., Choi, W. and Buckwalter, J.** (2003). Effect of dynamic hydrostatic pressure on rabbit intervertebral disc cells. *J Orthop Res* **21**, 597-603.

**Kasra, M., Merryman, W. D., Loveless, K. N., Goel, V. K., Martin, J. D. and Buckwalter, J. A.** (2006). Frequency response of pig intervertebral disc cells subjected to dynamic hydrostatic pressure. *J Orthop Res* **24**, 1967-73.

**Katsumoto, T., Mitsushima, A. and Kurimura, T.** (1990). The role of the vimentin intermediate filaments in rat 3Y1 cells elucidated by immunoelectron microscopy and computer-graphic reconstruction. *Biol Cell* **68**, 139-46.

**Kaverina, I., Krylyshkina, O., Beningo, K., Anderson, K., Wang, Y. L. and Small, J. V.** (2002). Tensile stress stimulates microtubule outgrowth in living cells. *J Cell Sci* **115**, 2283-91.

**Kim, S. and Coulombe, P. A.** (2007). Intermediate filament scaffolds fulfill mechanical, organizational, and signaling functions in the cytoplasm. *Genes Dev* **21**, 1581-97.

## Bibliography

---

**Kingma, I., van Dieen, J. H., Nicolay, K., Maat, J. J. and Weinans, H. (2000).** Monitoring water content in deforming intervertebral disc tissue by finite element analysis of MRI data. *Magn Reson Med* **44**, 650-4.

**Klein, J. A., Hickey, D. S. and Hukins, D. W. (1983).** Radial bulging of the annulus fibrosus during compression of the intervertebral disc. *J Biomech* **16**, 211-7.

**Klein, J. A. and Hukins, D. W. (1982a).** Collagen fibre orientation in the annulus fibrosus of intervertebral disc during bending and torsion measured by x-ray diffraction. *Biochim Biophys Acta* **719**, 98-101.

**Klein, J. A. and Hukins, D. W. (1982b).** X-ray diffraction demonstrates reorientation of collagen fibres in the annulus fibrosus during compression of the intervertebral disc. *Biochim Biophys Acta* **717**, 61-4.

**Kluba, T., Niemeyer, T., Gaissmaier, C. and Grunder, T. (2005).** Human annulus fibrosus and nucleus pulposus cells of the intervertebral disc: effect of degeneration and culture system on cell phenotype. *Spine* **30**, 2743-8.

**Knight, M. M., Bomzon, Z., Kimmel, E., Sharma, A. M., Lee, D. A. and Bader, D. L. (2006a).** Chondrocyte deformation induces mitochondrial distortion and heterogeneous intracellular strain fields. *Biomech Model Mechanobiol* **5**, 180-91.

**Knight, M. M., Idowu, B. D., Lee, D. A. and Bader, D. L. (2001).** Temporal changes in cytoskeletal organisation within isolated chondrocytes quantified using a novel image analysis technique. *Med Biol Eng Comput* **39**, 397-404.

**Knight, M. M., Toyoda, T., Lee, D. A. and Bader, D. L. (2006b).** Mechanical compression and hydrostatic pressure induce reversible changes in actin cytoskeletal organisation in chondrocytes in agarose. *J Biomech* **39**, 1547-51.

**Korecki, C. L., MacLean, J. J. and Iatridis, J. C. (2008).** Dynamic compression effects on intervertebral disc mechanics and biology. *Spine* **33**, 1403-9.

**Kouri, J. B., Arguello, C., Luna, J. and Mena, R. (1998).** Use of microscopical techniques in the study of human chondrocytes from osteoarthritic cartilage: an overview. *Microsc Res Tech* **40**, 22-36.

**Kreplak, L., Bar, H., Leterrier, J. F., Herrmann, H. and Aebi, U. (2005).** Exploring the mechanical behavior of single intermediate filaments. *J Mol Biol* **354**, 569-77.

**Lahiji, K., Polotsky, A., Hungerford, D. S. and Frondoza, C. G. (2004).** Cyclic strain stimulates proliferative capacity, alpha2 and alpha5 integrin, gene marker expression by human articular chondrocytes propagated on flexible silicone membranes. *In Vitro Cell Dev Biol Anim* **40**, 138-42.

**Lambrecht, S., Verbruggen, G., Verdonk, P. C., Elewaut, D. and Deforce, D. (2008).** Differential proteome analysis of normal and osteoarthritic chondrocytes

## Bibliography

---

reveals distortion of vimentin network in osteoarthritis. *Osteoarthritis Cartilage* **16**, 163-73.

**Langelier, E., Suetterlin, R., Hoemann, C. D., Aebi, U. and Buschmann, M. D.** (2000). The chondrocyte cytoskeleton in mature articular cartilage: structure and distribution of actin, tubulin, and vimentin filaments. *J Histochem Cytochem* **48**, 1307-20.

**Langevin, H. M., Storch, K. N., Cipolla, M. J., White, S. L., Buttolph, T. R. and Taatjes, D. J.** (2006). Fibroblast spreading induced by connective tissue stretch involves intracellular redistribution of alpha- and beta-actin. *Histochem Cell Biol* **125**, 487-95.

**Lappalainen, P. and Drubin, D. G.** (1997). Cofilin promotes rapid actin filament turnover in vivo. *Nature* **388**, 78-82.

**Lazarides, E.** (1980). Intermediate filaments as mechanical integrators of cellular space. *Nature* **283**, 249-256.

**Le Maitre, C. L., Frain, J., Millward-Sadler, J., Fotheringham, A. P., Freemont, A. J. and Hoyland, J. A.** (2009). Altered integrin mechanotransduction in human nucleus pulposus cells derived from degenerated discs. *Arthritis Rheum* **60**, 460-9.

**Le Maitre, C. L., Freemont, A. J. and Hoyland, J. A.** (2004). Localization of degradative enzymes and their inhibitors in the degenerate human intervertebral disc. *J Pathol* **204**, 47-54.

**Le Maitre, C. L., Freemont, A. J. and Hoyland, J. A.** (2006). Human disc degeneration is associated with increased MMP 7 expression. *Biotech Histochem* **81**, 125-31.

**LeBaron, R. G. and Athanasiou, K. A.** (2000). Ex vivo synthesis of articular cartilage. *Biomaterials* **21**, 2575-87.

**LeBaron, R. G., Hook, A., Esko, J. D., Gay, S. and Hook, M.** (1989). Binding of heparan sulfate to type V collagen. A mechanism of cell-substrate adhesion. *J Biol Chem* **264**, 7950-6.

**Lee, A. A., Delhaas, T., McCulloch, A. D. and Villarreal, F. J.** (1999). Differential responses of adult cardiac fibroblasts to in vitro biaxial strain patterns. *J Mol Cell Cardiol* **31**, 1833-43.

**Lee, C. R., Sakai, D., Nakai, T., Toyama, K., Mochida, J., Alini, M. and Grad, S.** (2007a). A phenotypic comparison of intervertebral disc and articular cartilage cells in the rat. *Eur Spine J* **16**, 2174-85.



## Bibliography

---

**Lee, D. A., Knight, M. M., Bolton, J. F., Idowu, B. D., Kayser, M. V. and Bader, D. L. (2000a).** Chondrocyte deformation within compressed agarose constructs at the cellular and sub-cellular levels. *J Biomech* **33**, 81-95.

**Lee, H. S., Millward-Sadler, S. J., Wright, M. O., Nuki, G. and Salter, D. M. (2000b).** Integrin and mechanosensitive ion channel-dependent tyrosine phosphorylation of focal adhesion proteins and beta-catenin in human articular chondrocytes after mechanical stimulation. *J Bone Miner Res* **15**, 1501-9.

**Lee, J. H., Fitzgerald, J. B., Dimicco, M. A. and Grodzinsky, A. J. (2005).** Mechanical injury of cartilage explants causes specific time-dependent changes in chondrocyte gene expression. *Arthritis Rheum* **52**, 2386-95.

**Lee, R. B. and Urban, J. P. (1997).** Evidence for a negative Pasteur effect in articular cartilage. *Biochem J* **321 ( Pt 1)**, 95-102.

**Lee, S. E., Kamm, R. D. and Mofrad, M. R. (2007b).** Force-induced activation of talin and its possible role in focal adhesion mechanotransduction. *J Biomech* **40**, 2096-106.

**Lee, S. H., Derby, R., Chen, Y., Seo, K. S. and Kim, M. J. (2004).** In vitro measurement of pressure in intervertebral discs and annulus fibrosus with and without annular tears during discography. *Spine J* **4**, 614-8.

**Lemaitre, V. and D'Armiento, J. (2006).** Matrix metalloproteinases in development and disease. *Birth Defects Res C Embryo Today* **78**, 1-10.

**Leone, A., Guglielmi, G., Cassar-Pullicino, V. N. and Bonomo, L. (2007).** Lumbar intervertebral instability: a review. *Radiology* **245**, 62-77.

**Li, H., Li, S., Wu, T. J., Xu, Y. and Chen, Y. X. (2007a).** [Early-response of the condylar chondrocyte under cyclic uniaxial compressive stress]. *Zhonghua Kou Qiang Yi Xue Za Zhi* **42**, 529-32.

**Li, S., Duance, V. C. and Blain, E. J. (2007b).** F-actin cytoskeletal organization in intervertebral disc health and disease. *Biochem Soc Trans* **35**, 683-5.

**Liu, G. Z., Ishihara, H., Osada, R., Kimura, T. and Tsuji, H. (2001).** Nitric oxide mediates the change of proteoglycan synthesis in the human lumbar intervertebral disc in response to hydrostatic pressure. *Spine* **26**, 134-41.

**Liu, Y. K., Njus, G., Buckwalter, J. and Wakano, K. (1983).** Fatigue response of lumbar intervertebral joints under axial cyclic loading. *Spine* **8**, 857-65.

**Loeser, R. F. (2002).** Integrins and cell signaling in chondrocytes. *Biorheology* **39**, 119-24.

## Bibliography

---

**Loufrani, L. and Henrion, D.** (2008). Role of the cytoskeleton in flow (shear stress)-induced dilation and remodeling in resistance arteries. *Med Biol Eng Comput* **46**, 451-60.

**Maclean, J. J., Lee, C. R., Alini, M. and Iatridis, J. C.** (2004). Anabolic and catabolic mRNA levels of the intervertebral disc vary with the magnitude and frequency of in vivo dynamic compression. *J Orthop Res* **22**, 1193-200.

**MacLean, J. J., Lee, C. R., Alini, M. and Iatridis, J. C.** (2005). The effects of short-term load duration on anabolic and catabolic gene expression in the rat tail intervertebral disc. *J Orthop Res* **23**, 1120-7.

**MacLean, J. J., Lee, C. R., Grad, S., Ito, K., Alini, M. and Iatridis, J. C.** (2003). Effects of immobilization and dynamic compression on intervertebral disc cell gene expression in vivo. *Spine* **28**, 973-81.

**MacLean, J. J., Roughley, P. J., Monsey, R. D., Alini, M. and Iatridis, J. C.** (2008). In vivo intervertebral disc remodeling: kinetics of mRNA expression in response to a single loading event. *J Orthop Res* **26**, 579-88.

**Majumdar, M. K., Askew, R., Schelling, S., Stedman, N., Blanchet, T., Hopkins, B., Morris, E. A. and Glasson, S. S.** (2007). Double-knockout of ADAMTS-4 and ADAMTS-5 in mice results in physiologically normal animals and prevents the progression of osteoarthritis. *Arthritis Rheum* **56**, 3670-4.

**Maldonado, B. A. and Oegema, T. R., Jr.** (1992). Initial characterization of the metabolism of intervertebral disc cells encapsulated in microspheres. *J Orthop Res* **10**, 677-90.

**Maniadakis, N. and Gray, A.** (2000). The economic burden of back pain in the UK. *Pain* **84**, 95-103.

**Maniotis, A. J., Chen, C. S. and Ingber, D. E.** (1997). Demonstration of mechanical connections between integrins, cytoskeletal filaments, and nucleoplasm that stabilize nuclear structure. *Proc Natl Acad Sci U S A* **94**, 849-54.

**Masuoka, K., Michalek, A. J., MacLean, J. J., Stokes, I. A. and Iatridis, J. C.** (2007). Different effects of static versus cyclic compressive loading on rat intervertebral disc height and water loss in vitro. *Spine* **32**, 1974-9.

**Matsumoto, T., Kawakami, M., Kuribayashi, K., Takenaka, T. and Tamaki, T.** (1999). Cyclic mechanical stretch stress increases the growth rate and collagen synthesis of nucleus pulposus cells in vitro. *Spine* **24**, 315-9.

**Matthews, R. T., Gary, S. C., Zerillo, C., Pratta, M., Solomon, K., Arner, E. C. and Hockfield, S.** (2000). Brain-enriched hyaluronan binding (BEHAB)/brevican cleavage in a glioma cell line is mediated by a disintegrin and metalloproteinase with thrombospondin motifs (ADAMTS) family member. *J Biol Chem* **275**, 22695-703.

## Bibliography

---

**Mauck, R. L., Byers, B. A., Yuan, X. and Tuan, R. S.** (2007). Regulation of cartilaginous ECM gene transcription by chondrocytes and MSCs in 3D culture in response to dynamic loading. *Biomech Model Mechanobiol* **6**, 113-25.

**Meachim, G. and Cornah, M. S.** (1970). Fine structure of juvenile human nucleus pulposus. *J Anat* **107**, 337-50.

**Meir, A., McNally, D. S., Fairbank, J. C., Jones, D. and Urban, J. P.** (2008). The internal pressure and stress environment of the scoliotic intervertebral disc--a review. *Proc Inst Mech Eng [H]* **222**, 209-19.

**Melrose, J., Ghosh, P. and Taylor, T. K.** (2001). A comparative analysis of the differential spatial and temporal distributions of the large (aggrecan, versican) and small (decorin, biglycan, fibromodulin) proteoglycans of the intervertebral disc. *J Anat* **198**, 3-15.

**Melrose, J., Smith, S. M., Appleyard, R. C. and Little, C. B.** (2008). Aggrecan, versican and type VI collagen are components of annular translamellar crossbridges in the intervertebral disc. *Eur Spine J* **17**, 314-24.

**Melrose, J., Smith, S. M., Fuller, E. S., Young, A. A., Roughley, P. J., Dart, A. and Little, C. B.** (2007). Biglycan and fibromodulin fragmentation correlates with temporal and spatial annular remodelling in experimentally injured ovine intervertebral discs. *Eur Spine J* **16**, 2193-205.

**Milkiewicz, M., Mohammadzadeh, F., Ispanovic, E., Gee, E. and Haas, T. L.** (2007). Static strain stimulates expression of matrix metalloproteinase-2 and VEGF in microvascular endothelium via JNK- and ERK-dependent pathways. *J Cell Biochem* **100**, 750-61.

**Millward-Sadler, S. J., Wright, M. O., Lee, H., Nishida, K., Caldwell, H., Nuki, G. and Salter, D. M.** (1999). Integrin-regulated secretion of interleukin 4: A novel pathway of mechanotransduction in human articular chondrocytes. *J Cell Biol* **145**, 183-9.

**Mirza, S. K. and White, A. A., 3rd.** (1995). Anatomy of intervertebral disc and pathophysiology of herniated disc disease. *J Clin Laser Med Surg* **13**, 131-42.

**Mitchison, T., Evans, L., Schulze, E. and Kirschner, M.** (1986). Sites of microtubule assembly and disassembly in the mitotic spindle. *Cell* **45**, 515-27.

**Miyamoto, H., Doita, M., Nishida, K., Yamamoto, T., Sumi, M. and Kurosaka, M.** (2006). Effects of cyclic mechanical stress on the production of inflammatory agents by nucleus pulposus and annulus fibrosus derived cells in vitro. *Spine* **31**, 4-9.

**Mizutani, T., Haga, H. and Kawabata, K.** (2004). Cellular stiffness response to external deformation: tensional homeostasis in a single fibroblast. *Cell Motil Cytoskeleton* **59**, 242-8.

## Bibliography

---

**Morachevskaya, E., Sudarikova, A. and Negulyaev, Y.** (2007). Mechanosensitive channel activity and F-actin organization in cholesterol-depleted human leukaemia cells. *Cell Biol Int* **31**, 374-81.

**Morris, C. E.** (1990). Mechanosensitive ion channels. *J Membr Biol* **113**, 93-107.

**Mudgett, J. S., Hutchinson, N. I., Chartrain, N. A., Forsyth, A. J., McDonnell, J., Singer, II, Bayne, E. K., Flanagan, J., Kawka, D., Shen, C. F. et al.** (1998). Susceptibility of stromelysin 1-deficient mice to collagen-induced arthritis and cartilage destruction. *Arthritis Rheum* **41**, 110-21.

**Mullins, R. D., Heuser, J. A. and Pollard, T. D.** (1998). The interaction of Arp2/3 complex with actin: nucleation, high affinity pointed end capping, and formation of branching networks of filaments. *Proc Natl Acad Sci USA* **95**, 6181-6.

**Murphy, G., Cockett, M. I., Stephens, P. E., Smith, B. J. and Docherty, A. J.** (1987). Stromelysin is an activator of procollagenase. A study with natural and recombinant enzymes. *Biochem J* **248**, 265-8.

**Musch, A.** (2004). Microtubule organization and function in epithelial cells. *Traffic* **5**, 1-9.

**Myers, K. A., Rattner, J. B., Shrive, N. G. and Hart, D. A.** (2007). Osteoblast-like cells and fluid flow: cytoskeleton-dependent shear sensitivity. *Biochem Biophys Res Commun* **364**, 214-9.

**Na, S., Collin, O., Chowdhury, F., Tay, B., Ouyang, M., Wang, Y. and Wang, N.** (2008). Rapid signal transduction in living cells is a unique feature of mechanotransduction. *Proc Natl Acad Sci USA* **105**, 6626-31.

**Na, S. and Wang, N.** (2008). Application of fluorescence resonance energy transfer and magnetic twisting cytometry to quantify mechanochemical signaling activities in a living cell. *Sci Signal* **1**, p11.

**Nachemson, A. and Morris, J. M.** (1964). In Vivo Measurements of Intradiscal Pressure. Discometry, a Method for the Determination of Pressure in the Lower Lumbar Discs. *J Bone Joint Surg Am* **46**, 1077-92.

**Nagase, H. and Kashiwagi, M.** (2003). Aggrecanases and cartilage matrix degradation. *Arthritis Res Ther* **5**, 94-103.

**Nagase, H. and Woessner, J. F., Jr.** (1999). Matrix metalloproteinases. *J Biol Chem* **274**, 21491-4.

**Naito, Z.** (2005). Role of the small leucine-rich proteoglycan (SLRP) family in pathological lesions and cancer cell growth. *J Nippon Med Sch* **72**, 137-45.

**Natarajan, R. N., Williams, J. R. and Andersson, G. B.** (2004). Recent advances in analytical modeling of lumbar disc degeneration. *Spine* **29**, 2733-41.

## Bibliography

---

**Nayal, A., Webb, D. J. and Horwitz, A. F.** (2004). Talin: an emerging focal point of adhesion dynamics. *Curr Opin Cell Biol* **16**, 94-8.

**Neidlinger-Wilke, C., Wurtz, K., Liedert, A., Schmidt, C., Borm, W., Ignatius, A., Wilke, H. J. and Claes, L.** (2005). A three-dimensional collagen matrix as a suitable culture system for the comparison of cyclic strain and hydrostatic pressure effects on intervertebral disc cells. *J Neurosurg Spine* **2**, 457-65.

**Neidlinger-Wilke, C., Wurtz, K., Urban, J. P., Borm, W., Arand, M., Ignatius, A., Wilke, H. J. and Claes, L. E.** (2006). Regulation of gene expression in intervertebral disc cells by low and high hydrostatic pressure. *Eur Spine J* **15 Suppl 3**, S372-8.

**Nemoto, O., Yamagishi, M., Yamada, H., Kikuchi, T. and Takaishi, H.** (1997). Matrix metalloproteinase-3 production by human degenerated intervertebral disc. *J Spinal Disord* **10**, 493-8.

**Nemoto, T.** (1991). [An experimental study on compression neuropathy--changes of the neurofilament and axonal tubulin content detected by enzymatic antibody technique]. *Nippon Seikeigeka Gakkai Zasshi* **65**, 1218-28.

**O'Connell, G. D., Johannessen, W., Vresilovic, E. J. and Elliott, D. M.** (2007). Human internal disc strains in axial compression measured noninvasively using magnetic resonance imaging. *Spine* **32**, 2860-8.

**Oegema, T. R., Jr.** (2002). The role of disc cell heterogeneity in determining disc biochemistry: a speculation. *Biochem Soc Trans* **30**, 839-44.

**Ohashi, T., Hagiwara, M., Bader, D. L. and Knight, M. M.** (2006). Intracellular mechanics and mechanotransduction associated with chondrocyte deformation during pipette aspiration. *Biorheology* **43**, 201-14.

**Okuda, S., Myoui, A., Ariga, K., Nakase, T., Yonenobu, K. and Yoshikawa, H.** (2001). Mechanisms of age-related decline in insulin-like growth factor-I dependent proteoglycan synthesis in rat intervertebral disc cells. *Spine* **26**, 2421-6.

**Omlor, G. W., Lorenz, H., Engelleiter, K., Richter, W., Carstens, C., Kroeber, M. W. and Guehring, T.** (2006). Changes in gene expression and protein distribution at different stages of mechanically induced disc degeneration--an in vivo study on the New Zealand white rabbit. *J Orthop Res* **24**, 385-92.

**Orend, G. and Chiquet-Ehrismann, R.** (2000). Adhesion modulation by antiadhesive molecules of the extracellular matrix. *Exp Cell Res* **261**, 104-10.

**Papageorgiou, A. C. and Rigby, A. S.** (1991). Review of UK data on the rheumatic diseases--7. Low back pain. *Br J Rheumatol* **30**, 208-10.

## Bibliography

---

**Parkkinen, J. J., Lammi, M. J., Inkinen, R., Jortikka, M., Tammi, M., Virtanen, I. and Helminen, H. J.** (1995). Influence of short-term hydrostatic pressure on organization of stress fibers in cultured chondrocytes. *J Orthop Res* **13**, 495-502.

**Patel, K. P., Sandy, J. D., Akeda, K., Miyamoto, K., Chujo, T., An, H. S. and Masuda, K.** (2007). Aggrecanases and aggrecanase-generated fragments in the human intervertebral disc at early and advanced stages of disc degeneration. *Spine* **32**, 2596-603.

**Pearce, R. H. and Grimmer, B. J.** (1983). Target tissue models: the proteoglycans and degeneration of the human intervertebral disc. *J Rheumatol Suppl* **11**, 108-10.

**Pearce, R. H., Grimmer, B. J. and Adams, M. E.** (1987). Degeneration and the chemical composition of the human lumbar intervertebral disc. *J Orthop Res* **5**, 198-205.

**Pekny, M. and Lane, E. B.** (2007). Intermediate filaments and stress. *Exp Cell Res* **313**, 2244-54.

**Pellegrini, F. and Budman, D. R.** (2005). Review: tubulin function, action of antitubulin drugs, and new drug development. *Cancer Invest* **23**, 264-73.

**Pelttari, K., Lorenz, H., Boeuf, S., Templin, M. F., Bischel, O., Goetzke, K., Hsu, H. Y., Steck, E. and Richter, W.** (2008). Secretion of matrix metalloproteinase 3 by expanded articular chondrocytes as a predictor of ectopic cartilage formation capacity in vivo. *Arthritis Rheum* **58**, 467-74.

**Pender, N. and McCulloch, C. A.** (1991). Quantitation of actin polymerization in two human fibroblast sub-types responding to mechanical stretching. *J Cell Sci* **100** ( Pt 1), 187-93.

**Perey, O.** (1957). Fracture of the vertebral end-plate in the lumbar spine; an experimental biochemical investigation. *Acta Orthop Scand Suppl* **25**, 1-101.

**Perkins, G. L., Derfoul, A., Ast, A. and Hall, D. J.** (2005). An inhibitor of the stretch-activated cation receptor exerts a potent effect on chondrocyte phenotype. *Differentiation* **73**, 199-211.

**Perlson, E., Michaelevski, I., Kowalsman, N., Ben-Yaakov, K., Shaked, M., Seger, R., Eisenstein, M. and Fainzilber, M.** (2006). Vimentin binding to phosphorylated Erk sterically hinders enzymatic dephosphorylation of the kinase. *J Mol Biol* **364**, 938-44.

**Peyton, S. R., Ghajar, C. M., Khatiwala, C. B. and Putnam, A. J.** (2007). The emergence of ECM mechanics and cytoskeletal tension as important regulators of cell function. *Cell Biochem Biophys* **47**, 300-20.

## Bibliography

---

**Pfaff, M., Aumailley, M., Specks, U., Knolle, J., Zerwes, H. G. and Timpl, R.** (1993). Integrin and Arg-Gly-Asp dependence of cell adhesion to the native and unfolded triple helix of collagen type VI. *Exp Cell Res* **206**, 167-76.

**Pockert, A. J., Richardson, S. M., Le Maitre, C. L., Lyon, M., Deakin, J. A., Buttle, D. J., Freemont, A. J. and Hoyland, J. A.** (2009). Modified expression of the ADAMTS enzymes and tissue inhibitor of metalloproteinases 3 during human intervertebral disc degeneration. *Arthritis Rheum* **60**, 482-91.

**Pope, M. H., Magnusson, M. and Wilder, D. G.** (1998). Kappa Delta Award. Low back pain and whole body vibration. *Clin Orthop Relat Res*, 241-8.

**Postacchini, F., Bellocchi, M., Ricciardi-Pollini, P. T. and Modesti, A.** (1982). An ultrastructural study of recurrent disc herniation: a preliminary report. *Spine* **7**, 492-7.

**Pritchard, S., Erickson, G. R. and Guilak, F.** (2002). Hyperosmotically induced volume change and calcium signaling in intervertebral disk cells: the role of the actin cytoskeleton. *Biophys J* **83**, 2502-10.

**Pritchard, S. and Guilak, F.** (2004). The role of F-actin in hypo-osmotically induced cell volume change and calcium signaling in annulus fibrosus cells. *Ann Biomed Eng* **32**, 103-11.

**Pullikuth, A. K. and Catling, A. D.** (2007). Scaffold mediated regulation of MAPK signaling and cytoskeletal dynamics: a perspective. *Cell Signal* **19**, 1621-32.

**Putnam, A. J., Cunningham, J. J., Pillemer, B. B. and Mooney, D. J.** (2003). External mechanical strain regulates membrane targeting of Rho GTPases by controlling microtubule assembly. *Am J Physiol Cell Physiol* **284**, C627-39.

**Putnam, A. J., Schultz, K. and Mooney, D. J.** (2001). Control of microtubule assembly by extracellular matrix and externally applied strain. *Am J Physiol Cell Physiol* **280**, C556-64.

**Raffetto, J. D. and Khalil, R. A.** (2008). Matrix metalloproteinases and their inhibitors in vascular remodeling and vascular disease. *Biochem Pharmacol* **75**, 346-59.

**Raif, E. M.** (2008). Effect of cyclic tensile load on the regulation of the expression of matrix metalloproteinases (MMPs -1, -3) and structural components in synovial cells. *J Cell Mol Med* **19**, 19.

**Ralphs, J. R., Benjamin, M. and Thornett, A.** (1991). Cell and matrix biology of the suprapatella in the rat: a structural and immunocytochemical study of fibrocartilage in a tendon subject to compression. *Anat Rec* **231**, 167-77.

## Bibliography

---

**Ralphs, J. R., Waggett, A. D. and Benjamin, M.** (2002). Actin stress fibres and cell-cell adhesion molecules in tendons: organisation in vivo and response to mechanical loading of tendon cells in vitro. *Matrix Biol* **21**, 67-74.

**Rannou, F., Richette, P., Benallaoua, M., Francois, M., Genries, V., Korwin-Zmijowska, C., Revel, M., Corvol, M. and Poiraudau, S.** (2003). Cyclic tensile stretch modulates proteoglycan production by intervertebral disc annulus fibrosus cells through production of nitrite oxide. *J Cell Biochem* **90**, 148-57.

**Ridge, K. M., Linz, L., Flitney, F. W., Kuczmarski, E. R., Chou, Y. H., Omary, M. B., Sznajder, J. I. and Goldman, R. D.** (2005). Keratin 8 phosphorylation by protein kinase C delta regulates shear stress-mediated disassembly of keratin intermediate filaments in alveolar epithelial cells. *J Biol Chem* **280**, 30400-5.

**Roark, E. F., Keene, D. R., Haudenschild, C. C., Godyna, S., Little, C. D. and Argraves, W. S.** (1995). The association of human fibulin-1 with elastic fibers: an immunohistological, ultrastructural, and RNA study. *J Histochem Cytochem* **43**, 401-11.

**Roberts, S., Ayad, S. and Menage, P. J.** (1991a). Immunolocalisation of type VI collagen in the intervertebral disc. *Ann Rheum Dis* **50**, 787-91.

**Roberts, S., Evans, H., Trivedi, J. and Menage, J.** (2006). Histology and pathology of the human intervertebral disc. *J Bone Joint Surg Am* **88 Suppl 2**, 10-4.

**Roberts, S., Menage, J., Duance, V., Wotton, S. and Ayad, S.** (1991b). 1991 Volvo Award in basic sciences. Collagen types around the cells of the intervertebral disc and cartilage end plate: an immunolocalization study. *Spine* **16**, 1030-8.

**Roberts, S., Menage, J., Duance, V. and Wotton, S. F.** (1991c). Type III collagen in the intervertebral disc. *Histochem J* **23**, 503-8.

**Roberts, S., Menage, J. and Urban, J. P.** (1989). Biochemical and structural properties of the cartilage end-plate and its relation to the intervertebral disc. *Spine* **14**, 166-74.

**Rohlmann, A., Graichen, F., Kayser, R., Bender, A. and Bergmann, G.** (2008). Loads on a telemeterized vertebral body replacement measured in two patients. *Spine* **33**, 1170-9.

**Ronot, X., Gaillard-Froger, B., Hainque, B. and Adolphe, M.** (1988). In vitro aging of articular chondrocytes identified by analysis of DNA and tubulin content and relationship to cell size and protein content. *Cytometry* **9**, 436-40.

**Roughley, P., Martens, D., Rantakokko, J., Alini, M., Mwale, F. and Antoniou, J.** (2006a). The involvement of aggrecan polymorphism in degeneration of human intervertebral disc and articular cartilage. *Eur Cell Mater* **11**, 1-7; discussion 7.



## Bibliography

---

**Roughley, P. J.** (2004). Biology of intervertebral disc aging and degeneration: involvement of the extracellular matrix. *Spine* **29**, 2691-9.

**Roughley, P. J., Melching, L. I., Heathfield, T. F., Pearce, R. H. and Mort, J. S.** (2006b). The structure and degradation of aggrecan in human intervertebral disc. *Eur Spine J* **15 Suppl 3**, S326-32.

**Rubenstein, P. A.** (1990). The functional importance of multiple actin isoforms. *Bioessays* **12**, 309-15.

**Rubin, J., Murphy, T. C., Zhu, L., Roy, E., Nanes, M. S. and Fan, X.** (2003). Mechanical strain differentially regulates endothelial nitric-oxide synthase and receptor activator of nuclear kappa B ligand expression via ERK1/2 MAPK. *J Biol Chem* **278**, 34018-25.

**Salter, D. M., Millward-Sadler, S. J., Nuki, G. and Wright, M. O.** (2001). Integrin-interleukin-4 mechanotransduction pathways in human chondrocytes. *Clin Orthop Relat Res*, S49-60.

**Samuel, J. L., Marotte, F., Delcayre, C. and Rappaport, L.** (1986). Microtubule reorganization is related to rate of heart myocyte hypertrophy in rat. *Am J Physiol* **251**, H1118-25.

**Sandy, J. D., Westling, J., Kenagy, R. D., Iruela-Arispe, M. L., Verscharen, C., Rodriguez-Mazaneque, J. C., Zimmermann, D. R., Lemire, J. M., Fischer, J. W., Wight, T. N. et al.** (2001). Versican V1 proteolysis in human aorta in vivo occurs at the Glu441-Ala442 bond, a site that is cleaved by recombinant ADAMTS-1 and ADAMTS-4. *J Biol Chem* **276**, 13372-8.

**Sarasa-Renedo, A., Tunc-Civelek, V. and Chiquet, M.** (2006). Role of RhoA/ROCK-dependent actin contractility in the induction of tenascin-C by cyclic tensile strain. *Exp Cell Res* **312**, 1361-70.

**Sato, K., Kikuchi, S. and Yonezawa, T.** (1999). In vivo intradiscal pressure measurement in healthy individuals and in patients with ongoing back problems. *Spine* **24**, 2468-74.

**Sato, M., Kikuchi, T., Asazuma, T., Yamada, H., Maeda, H. and Fujikawa, K.** (2001). Glycosaminoglycan accumulation in primary culture of rabbit intervertebral disc cells. *Spine* **26**, 2653-60.

**Schmid, T. M. and Linsenmayer, T. F.** (1985). Immunohistochemical localization of short chain cartilage collagen (type X) in avian tissues. *J Cell Biol* **100**, 598-605.

**Schmidt, C., Pommerenke, H., Durr, F., Nebe, B. and Rychly, J.** (1998). Mechanical stressing of integrin receptors induces enhanced tyrosine phosphorylation of cytoskeletally anchored proteins. *J Biol Chem* **273**, 5081-5.

## Bibliography

---

**Schmidt H, Kettler A, Heuer F, Simon U, Claes L and HJ, W.** (2007). Intradiscal pressure, shear strain, and fiber strain in the intervertebral disc under combined loading. *Spine* **32**, 748-55.

**Schmidt, H., Kettler, A., Heuer, F., Simon, U., Claes, L. and Wilke, H. J.** (2007). Intradiscal pressure, shear strain, and fiber strain in the intervertebral disc under combined loading. *Spine* **32**, 748-55.

**Schnittler, H. J., Franke, R. P., Akbay, U., Mrowietz, C. and Drenckhahn, D.** (1993). Improved in vitro rheological system for studying the effect of fluid shear stress on cultured cells. *Am J Physiol* **265**, C289-98.

**Schroder, E. A., Tobita, K., Tinney, J. P., Foldes, J. K. and Keller, B. B.** (2002). Microtubule involvement in the adaptation to altered mechanical load in developing chick myocardium. *Circ Res* **91**, 353-9.

**Schulze, K. J. and Polster, J.** (1979). [Occupational spinal diseases in tractor drivers and farmers]. *Beitr Orthop Traumatol* **26**, 356-62.

**Schwarzer, A. C., Aprill, C. N., Derby, R., Fortin, J., Kine, G. and Bogduk, N.** (1994). The relative contributions of the disc and zygapophyseal joint in chronic low back pain. *Spine* **19**, 801-6.

**Schwingshackl, A., Duszyk, M., Brown, N. and Moqbel, R.** (1999). Human eosinophils release matrix metalloproteinase-9 on stimulation with TNF-alpha. *J Allergy Clin Immunol* **104**, 983-9.

**Scott, J. E., Bosworth, T. R., Cribb, A. M. and Taylor, J. R.** (1994). The chemical morphology of age-related changes in human intervertebral disc glycosaminoglycans from cervical, thoracic and lumbar nucleus pulposus and annulus fibrosus. *J Anat* **184** ( Pt 1), 73-82.

**Searby, N. D., Steele, C. R. and Globus, R. K.** (2005). Influence of increased mechanical loading by hypergravity on the microtubule cytoskeleton and prostaglandin E2 release in primary osteoblasts. *Am J Physiol Cell Physiol* **289**, C148-58.

**Seki, S., Kawaguchi, Y., Chiba, K., Mikami, Y., Kizawa, H., Oya, T., Mio, F., Mori, M., Miyamoto, Y., Masuda, I. et al.** (2005). A functional SNP in CILP, encoding cartilage intermediate layer protein, is associated with susceptibility to lumbar disc disease. *Nat Genet* **37**, 607-12.

**Setton, L. A. and Chen, J.** (2004). Cell mechanics and mechanobiology in the intervertebral disc. *Spine* **29**, 2710-23.

**Shao, X. and Hunter, C. J.** (2007). Developing an alginate/chitosan hybrid fiber scaffold for annulus fibrosus cells. *J Biomed Mater Res A* **82**, 701-10.

**Shelton, L. and Rada, J. S.** (2007). Effects of cyclic mechanical stretch on extracellular matrix synthesis by human scleral fibroblasts. *Exp Eye Res* **84**, 314-22.

## Bibliography

---

**Sheu, S. J., Wu, S. N. and Hu, D. N.** (2005). Stretch-stimulated activity of large conductance calcium-activated potassium channels in human retinal pigment epithelial cells. *J Ocul Pharmacol Ther* **21**, 429-35.

**Shieh, A. C. and Athanasiou, K. A.** (2007). Dynamic compression of single cells. *Osteoarthritis Cartilage* **15**, 328-34.

**Silver, F. H. and Siperko, L. M.** (2003). Mechanosensing and mechanochemical transduction: how is mechanical energy sensed and converted into chemical energy in an extracellular matrix? *Crit Rev Biomed Eng* **31**, 255-331.

**Sin, W. C., Chen, X. Q., Leung, T. and Lim, L.** (1998). RhoA-binding kinase alpha translocation is facilitated by the collapse of the vimentin intermediate filament network. *Mol Cell Biol* **18**, 6325-39.

**Skaggs, D. L., Weidenbaum, M., Iatridis, J. C., Ratcliffe, A. and Mow, V. C.** (1994). Regional variation in tensile properties and biochemical composition of the human lumbar annulus fibrosus. *Spine* **19**, 1310-9.

**Sobajima, S., Shimer, A. L., Chadderdon, R. C., Kompel, J. F., Kim, J. S., Gilbertson, L. G. and Kang, J. D.** (2005). Quantitative analysis of gene expression in a rabbit model of intervertebral disc degeneration by real-time polymerase chain reaction. *Spine J* **5**, 14-23.

**Sowa, G. and Agarwal, S.** (2008). Cyclic Tensile Stress Exerts a Protective Effect on Intervertebral Disc Cells. *Am J Phys Med Rehabil* **17**, 17.

**Stevens, A. L., Wishnok, J. S., Chai, D. H., Grodzinsky, A. J. and Tannenbaum, S. R.** (2008). A sodium dodecyl sulfate-polyacrylamide gel electrophoresis-liquid chromatography tandem mass spectrometry analysis of bovine cartilage tissue response to mechanical compression injury and the inflammatory cytokines tumor necrosis factor alpha and interleukin-1beta. *Arthritis Rheum* **58**, 489-500.

**Stosiek, P., Kasper, M. and Karsten, U.** (1988). Expression of cytokeratin and vimentin in nucleus pulposus cells. *Differentiation* **39**, 78-81.

**Straub, F. B. and Feuer, G.** (1989). Adenosinetriphosphate. The functional group of actin. 1950. *Biochim Biophys Acta* **1000**, 180-95.

**Sun, H. Q., Yamamoto, M., Mejillano, M. and Yin, H. L.** (1999). Gelsolin, a multifunctional actin regulatory protein. *J Biol Chem* **274**, 33179-82.

**Suzuki, K., Enghild, J. J., Morodomi, T., Salvesen, G. and Nagase, H.** (1990). Mechanisms of activation of tissue procollagenase by matrix metalloproteinase 3 (stromelysin). *Biochemistry* **29**, 10261-70.

**Szafranski, J. D., Grodzinsky, A. J., Burger, E., Gaschen, V., Hung, H. H. and Hunziker, E. B.** (2004). Chondrocyte mechanotransduction: effects of compression on

## Bibliography

---

deformation of intracellular organelles and relevance to cellular biosynthesis. *Osteoarthritis Cartilage* **12**, 937-46.

**Sztrolovics, R., Alini, M., Mort, J. S. and Roughley, P. J.** (1999). Age-related changes in fibromodulin and lumican in human intervertebral discs. *Spine* **24**, 1765-71.

**Sztrolovics, R., Alini, M., Roughley, P. J. and Mort, J. S.** (1997). Aggrecan degradation in human intervertebral disc and articular cartilage. *Biochem J* **326 (Pt 1)**, 235-41.

**Takahashi, I., Onodera, K., Sasano, Y., Mizoguchi, I., Bae, J. W., Mitani, H. and Kagayama, M.** (2003). Effect of stretching on gene expression of beta1 integrin and focal adhesion kinase and on chondrogenesis through cell-extracellular matrix interactions. *Eur J Cell Biol* **82**, 182-92.

**Takahashi, M., Tsutsui, H., Tagawa, H., Igarashi-Saito, K., Imanaka-Yoshida, K. and Takeshita, A.** (1998). Microtubules are involved in early hypertrophic responses of myocardium during pressure overload. *Am J Physiol* **275**, H341-8.

**Taylor, J. R.** (1975). Growth of human intervertebral discs and vertebral bodies. *J Anat* **120**, 49-68.

**Theriot, J. A.** (1997). Accelerating on a treadmill: ADF/cofilin promotes rapid actin filament turnover in the dynamic cytoskeleton. *J Cell Biol* **136**, 1165-8.

**Thonar, E., An, H. and Masuda, K.** (2002). Compartmentalization of the matrix formed by nucleus pulposus and annulus fibrosus cells in alginate gel. *Biochem Soc Trans* **30**, 874-8.

**Tortorella, M. D., Burn, T. C., Pratta, M. A., Abbaszade, I., Hollis, J. M., Liu, R., Rosenfeld, S. A., Copeland, R. A., Decicco, C. P., Wynn, R. et al.** (1999). Purification and cloning of aggrecanase-1: a member of the ADAMTS family of proteins. *Science* **284**, 1664-6.

**Towbin, H., Staehelin, T. and Gordon, J.** (1979). Electrophoretic transfer of proteins from polyacrylamide gels to nitrocellulose sheets: procedure and some applications. *Proc Natl Acad Sci USA* **76**, 4350-4.

**Traub, P.** (1995). Intermediate filaments and gene regulation. *Physiol Chem Phys Med NMR* **27**, 377-400.

**Traub, P. and Vorgias, C. E.** (1983). Involvement of the N-terminal polypeptide of vimentin in the formation of intermediate filaments. *J Cell Sci* **63**, 43-67.

**Trout, J. J., Buckwalter, J. A. and Moore, K. C.** (1982). Ultrastructure of the human intervertebral disc: II. Cells of the nucleus pulposus. *Anat Rec* **204**, 307-14.

**Tsuruha, J., Masuko-Hongo, K., Kato, T., Sakata, M., Nakamura, H. and Nishioka, K.** (2001). Implication of cartilage intermediate layer protein in cartilage

## Bibliography

---

destruction in subsets of patients with osteoarthritis and rheumatoid arthritis. *Arthritis Rheum* **44**, 838-45.

**Turner, C. E.** (2000). Paxillin interactions. *J Cell Sci* **113 Pt 23**, 4139-40.

**Urban, J. P. and Roberts, S.** (2003). Degeneration of the intervertebral disc. *Arthritis Res Ther* **5**, 120-30.

**Vale, R. D.** (1987). Intracellular transport using microtubule-based motors. *Annu Rev Cell Biol* **3**, 347-78.

**van Dieen, J. H., van der Veen, A., van Royen, B. J. and Kingma, I.** (2006). Fatigue failure in shear loading of porcine lumbar spine segments. *Spine* **31**, E494-8.

**Van Troys, M., Huyck, L., Leyman, S., Dhaese, S., Vandekerckhove, J. and Ampe, C.** (2008). Ins and outs of ADF/cofilin activity and regulation. *Eur J Cell Biol* **87**, 649-67.

**Vaughan-Thomas, A., Young, R. D., Phillips, A. C. and Duance, V. C.** (2001). Characterization of type XI collagen-glycosaminoglycan interactions. *J Biol Chem* **276**, 5303-9.

**Virtanen, I. M., Song, Y. Q., Cheung, K. M., Ala-Kokko, L., Karppinen, J., Ho, D. W., Luk, K. D., Yip, S. P., Leong, J. C., Cheah, K. S. et al.** (2007). Phenotypic and population differences in the association between CILP and lumbar disc disease. *J Med Genet* **44**, 285-8.

**Waddell, G.** (1991). Low back disability. A syndrome of Western civilization. *Neurosurg Clin N Am* **2**, 719-38.

**Wagner, A. P.** (1989). On the relationships between the rate of cytoskeletal stable assemblies turnover, stability of the differentiated state, development and aging. *J Theor Biol* **138**, 175-84.

**Walker, L. M., Publicover, S. J., Preston, M. R., Said Ahmed, M. A. and El Haj, A. J.** (2000). Calcium-channel activation and matrix protein upregulation in bone cells in response to mechanical strain. *J Cell Biochem* **79**, 648-61.

**Walmsley, R.** (1953). The development and growth of the intervertebral disc. *Edinburgh Med J* **60**, 341-64.

**Walsh, A. J. and Lotz, J. C.** (2004). Biological response of the intervertebral disc to dynamic loading. *J Biomech* **37**, 329-37.

**Wang, D. L., Jiang, S. D. and Dai, L. Y.** (2007). Biologic response of the intervertebral disc to static and dynamic compression in vitro. *Spine* **32**, 2521-8.

## Bibliography

---

**Wang, J., Fan, J., Laschinger, C., Arora, P. D., Kapus, A., Seth, A. and McCulloch, C. A.** (2005). Smooth muscle actin determines mechanical force-induced p38 activation. *J Biol Chem* **280**, 7273-84.

**Wang, J. Y., Baer, A. E., Kraus, V. B. and Setton, L. A.** (2001). Intervertebral disc cells exhibit differences in gene expression in alginate and monolayer culture. *Spine* **26**, 1747-51; discussion 1752.

**Wang, N., Butler, J. P. and Ingber, D. E.** (1993). Mechanotransduction across the cell surface and through the cytoskeleton. *Science* **260**, 1124-7.

**Wang, N. and Stamenovic, D.** (2000). Contribution of intermediate filaments to cell stiffness, stiffening, and growth. *Am J Physiol Cell Physiol* **279**, C188-94.

**Wang, N. and Stamenovic, D.** (2002). Mechanics of vimentin intermediate filaments. *J Muscle Res Cell Motil* **23**, 535-40.

**Wang, Y. L.** (2007). Flux at focal adhesions: slippage clutch, mechanical gauge, or signal depot. *Sci STKE* **2007**, pe10.

**Weiler, C., Nerlich, A. G., Zipperer, J., Bachmeier, B. E. and Boos, N.** (2002). 2002 SSE Award Competition in Basic Science: expression of major matrix metalloproteinases is associated with intervertebral disc degradation and resorption. *Eur Spine J* **11**, 308-20.

**Wenger, K. H., Woods, J. A., Holecek, A., Eckstein, E. C., Robertson, J. T. and Hastly, K. A.** (2005). Matrix remodeling expression in anulus cells subjected to increased compressive load. *Spine* **30**, 1122-6.

**Wenstrup, R. J., Florer, J. B., Brunskill, E. W., Bell, S. M., Chervoneva, I. and Birk, D. E.** (2004). Type V collagen controls the initiation of collagen fibril assembly. *J Biol Chem* **279**, 53331-7.

**Wilke, H., Neef, P., Hinz, B., Seidel, H. and Claes, L.** (2001). Intradiscal pressure together with anthropometric data--a data set for the validation of models. *Clin Biomech (Bristol, Avon)* **16 Suppl 1**, S111-26.

**Wilke, H. J., Neef, P., Caimi, M., Hoogland, T. and Claes, L. E.** (1999). New in vivo measurements of pressures in the intervertebral disc in daily life. *Spine* **24**, 755-62.

**Wilkin, P.** (2009). Are you sitting comfortably? The political economy of the body. *Sociol Health Illn* **31**, 35-50.

**Wu, J. J., Eyre, D. R. and Slayter, H. S.** (1987). Type VI collagen of the intervertebral disc. Biochemical and electron-microscopic characterization of the native protein. *Biochem J* **248**, 373-81.

## Bibliography

---

**Xu, J., Zutter, M. M., Santoro, S. A. and Clark, R. A.** (1998). A three-dimensional collagen lattice activates NF-kappaB in human fibroblasts: role in integrin alpha2 gene expression and tissue remodeling. *J Cell Biol* **140**, 709-19.

**Yang, B. L., Yang, B. B., Erwin, M., Ang, L. C., Finkelstein, J. and Yee, A. J.** (2003). Versican G3 domain enhances cellular adhesion and proliferation of bovine intervertebral disc cells cultured in vitro. *Life Sci* **73**, 3399-413.

**Yoshigi, M., Hoffman, L. M., Jensen, C. C., Yost, H. J. and Beckerle, M. C.** (2005). Mechanical force mobilizes zyxin from focal adhesions to actin filaments and regulates cytoskeletal reinforcement. *J Cell Biol* **171**, 209-15.

**Yu, J., Fairbank, J. C., Roberts, S. and Urban, J. P.** (2005a). The elastic fiber network of the anulus fibrosus of the normal and scoliotic human intervertebral disc. *Spine* **30**, 1815-20.

**Yu, J., Winlove, P. C., Roberts, S. and Urban, J. P.** (2002). Elastic fibre organization in the intervertebral discs of the bovine tail. *J Anat* **201**, 465-75.

**Yu, S. J., Qiu, G. X., Burton, Y., Sandra, R., Cari, W. and Albert, Y.** (2005b). [Expression of integrin alpha5 and actin in the cells of intervertebral disc under cyclic hydrostatic pressure in vitro]. *Zhonghua Wai Ke Za Zhi* **43**, 1605-8.

**Yu, W. H., Yu, S., Meng, Q., Brew, K. and Woessner, J. F., Jr.** (2000). TIMP-3 binds to sulfated glycosaminoglycans of the extracellular matrix. *J Biol Chem* **275**, 31226-32.

**Zamir, E. and Geiger, B.** (2001). Molecular complexity and dynamics of cell-matrix adhesions. *J Cell Sci* **114**, 3583-90.

**Zeiger, A. S. and Layton, B. E.** (2008). Molecular Modeling of the Axial and Circumferential Elastic Moduli of Tubulin. *Biophys J* **11**, 11.

**Zhao, C. Q., Wang, L. M., Jiang, L. S. and Dai, L. Y.** (2007a). The cell biology of intervertebral disc aging and degeneration. *Ageing Res Rev* **6**, 247-61.

**Zhao, X. H., Laschinger, C., Arora, P., Szaszi, K., Kapus, A. and McCulloch, C. A.** (2007b). Force activates smooth muscle alpha-actin promoter activity through the Rho signaling pathway. *J Cell Sci* **120**, 1801-9.

**Zhu, D., Dong, X., Zhu, X., Li, R., Huang, W., Wang, C. and Cui, H.** (2006). [An experimental study on mechanical properties of fiber layers in anulus fibrosus of lumbar intervertebral disc 4,5]. *Sheng Wu Yi Xue Gong Cheng Xue Za Zhi* **23**, 290-4.

**Zhu, Y., McAlinden, A. and Sandell, L. J.** (2001). Type IIA procollagen in development of the human intervertebral disc: regulated expression of the NH(2)-propeptide by enzymic processing reveals a unique developmental pathway. *Dev Dyn* **220**, 350-62.

## Bibliography

---

**Zwicky, R. and Baici, A.** (2000). Cytoskeletal architecture and cathepsin B trafficking in human articular chondrocytes. *Histochem Cell Biol* **114**, 363-72.



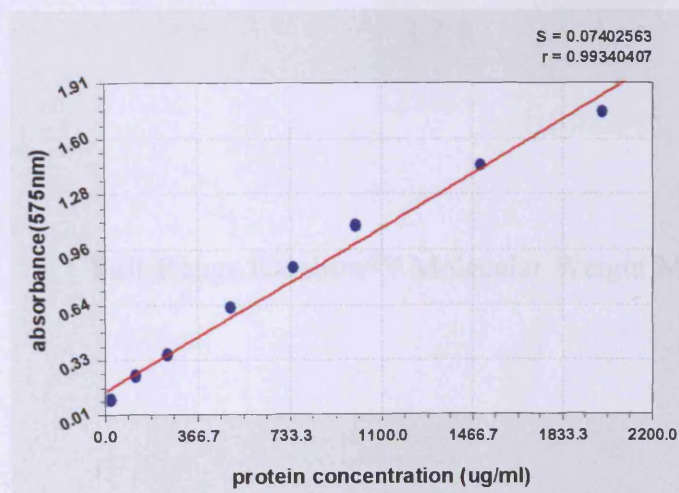
# APPENDICES

## Appendix 1

### BCA Protein Assay System

The BCA protein assay is for colorimetric detection and quantitation of total protein. This method combines the well-known reduction of  $\text{Cu}^{2+}$  to  $\text{Cu}^{1+}$  by protein in an alkaline medium (the biuret reaction) with the highly sensitive and selective colorimetric detection of the cuprous cation ( $\text{Cu}^{1+}$ ) using a unique reagent containing bicinchoninic acid. The purple-colored reaction product of this assay is formed by the chelation of two molecules of BCA with one cuprous ion. This water-soluble complex exhibits a strong absorbance at 562 nm that is nearly linear with increasing protein concentrations over a broad working range (20-2,000  $\mu\text{g/ml}$ ).

A standard curve is generated by plotting the rate changes of absorbance (Y-axis) against concentration of standard samples in  $\mu\text{g ml}^{-1}$  (X-axis). The plot generated should resemble a linear curve from which a linear regression equation can be determined. This allows  $\mu\text{g ml}^{-1}$  values to be read directly from the graph for the unknown supernatant sample concentrations:

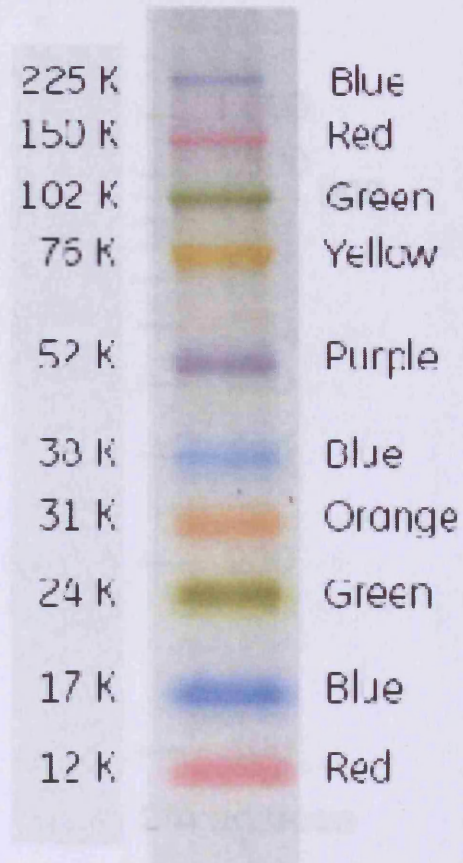


A linear regression equation allows the protein concentration of samples to be determined:

Linear regression equation derived:  $Y=0.14033772+0.00085495292X$

## Appendix 2

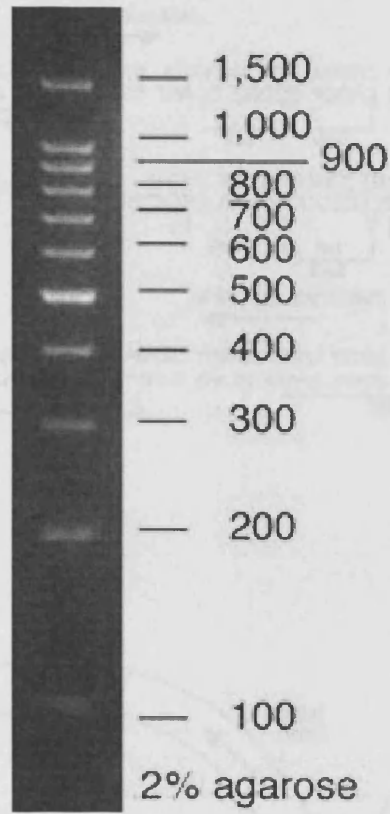
### Protein ladder



Full-Range Rainbow™ Molecular Weight Markers (GE healthcare, U.K.)

## Appendix 3

### DNA ladder

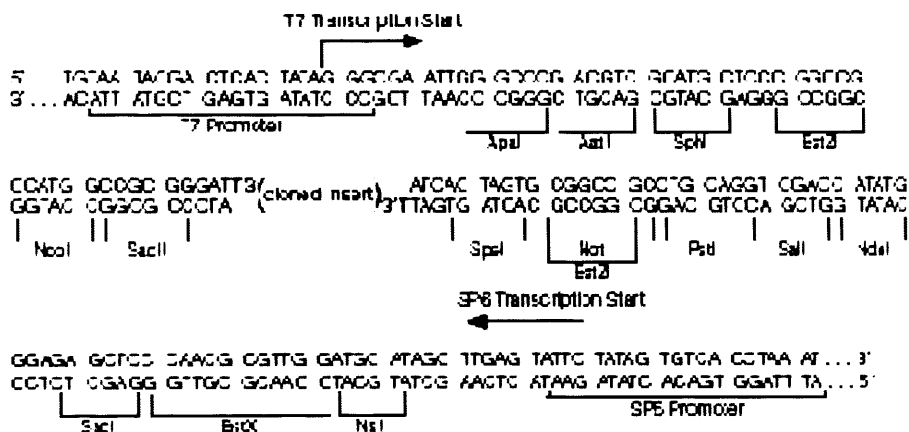


BenchTop 100bp DNA Ladder (Promega, U.K.)

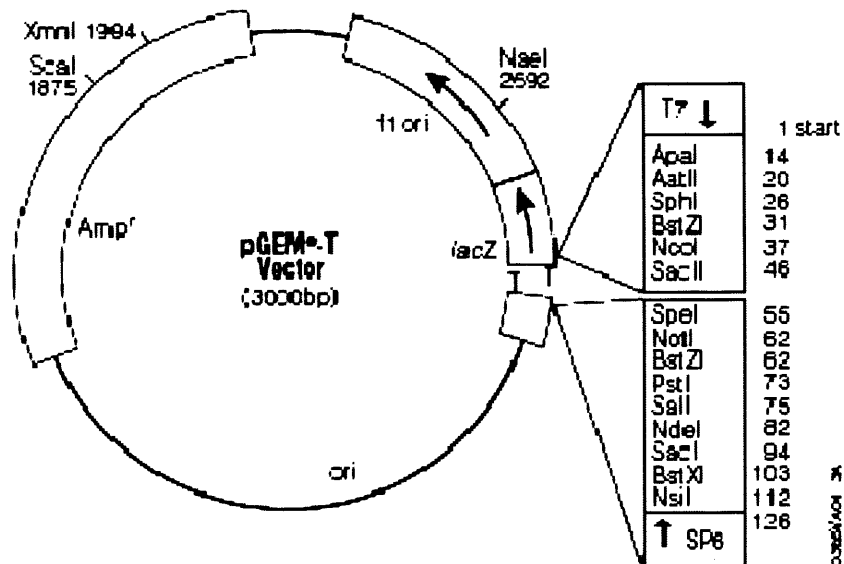
## Appendix 4

### pGEM<sup>®</sup>-T Vector

(A)



(B)



[A] The multiple cloning sequence

[B] map of vector pGEM<sup>®</sup>-T Vector (Promega, U.K.)

# PUBLICATIONS

## Zonal variations in cytoskeletal element organization, mRNA and protein expression in the intervertebral disc

Siyuan Li, Victor C. Duance and Emma J. Blain

Connective Tissue Biology Laboratories, Biomedical Sciences Building, School of Biosciences, Cardiff University, Cardiff, UK

### Abstract

The intervertebral disc is important in maintaining flexibility and dissipating loads applied to the spine. The disc comprises a heterogeneous population of cells, including those of the nucleus pulposus and annulus fibrosus, which are diverse in phenotype, partly due to the different mechanical loads they experience. Several studies have implicated the cytoskeleton in mechanotransduction, but little characterization of the three major cytoskeletal elements – actin, tubulin and vimentin – in the intervertebral disc has been undertaken. In this study we show that there are differences in both the organization and the amounts of these cytoskeletal proteins across the regions of immature bovine intervertebral disc (nucleus pulposus and outer annulus fibrosus), which differs with skeletal maturity. These differences are likely to reflect the diverse mechanical characteristics of the disc regions, and the loads that they experience, i.e. tension in the annulus fibrosus and compression in the nucleus pulposus. Alterations to the organization and amount of cytoskeletal element proteins may change the ability of the cells to respond to mechanical signals, with a loss of tissue homeostasis, suggesting that the cytoskeleton has a potential role in intervertebral disc degeneration.

**Key words** confocal microscopy; cytoskeleton; intervertebral disc; mRNA expression.

### Introduction

The intervertebral disc (IVD) is avascular and alymphatic, and comprises three morphologically distinct zones, namely the nucleus pulposus (NP), the annulus fibrosus [inner (IAF) and outer (OAF)] and the cartilaginous end plate. The IVD has important mechanical functions in maintaining flexibility and dissipating loads applied to the spine. IVD cells exposed to physiological mechanical loads experience complex physical stimuli including compressive, tensile and shear stresses and strains, fluid flows, hydrostatic pressure and osmotic pressure (Weidenbaum et al. 1992; Urban et al. 1993; Iatridis et al. 1996). These physical stimuli are believed to be important regulators of IVD cell metabolism contributing to matrix turnover, both synthesis and degradation, in normal and degenerative discs.

However, it has been reported that the distinct cell populations of the IVD respond differently to compressive loads (Chen et al. 2004; Setton & Chen, 2006; Wang et al. 2007), suggesting that there may be intrinsic differences in the cell types. The IVD comprises a sparse population of

heterogeneous cells; the NP cells resident at the centre of the disc closely resemble chondrocytes, whereas the OAF cells at the periphery of the disc are characteristic of fibroblasts (Errington et al. 1998). In bovine IVDs, the OAF cells have been shown to contain elongated processes containing filamentous F-actin (Errington et al. 1998; Bruehlmann et al. 2002; Li et al. 2007b) and vimentin (Bruehlmann et al. 2002). In the study by Errington et al. (1998), specific cytoskeletal components in the cell processes were hypothesized to play a role in 'sensing' mechanical loads. More recently, it has been demonstrated that the cytoskeleton may play a crucial role in mechanotransduction between the IVD cells and their surrounding extracellular matrix (Hayes et al. 1999; Chen et al. 2004; Li et al. 2007a).

The cytoskeleton, comprising actin microfilaments, tubulin microtubules and vimentin intermediate filaments in the IVD, is fundamental to the dynamic functions of the cell. Collectively, the three major cytoskeletal elements play important roles in cell division, motility, protein trafficking and secretion (Benjamin et al. 1994; Thyberg & Moskalewski, 1999).

Therefore, the activities of the NP and OAF cells of the IVD are likely to be dependent upon their morphology and hence cytoskeletal composition. With the exception of a few studies which have investigated F-actin and vimentin organization in bovine IVD (Errington et al. 1998) and in normal vs. pathological human discs (Johnson & Roberts, 2003) very little is known about the content and organization of the three major cytoskeletal elements in the two

#### Correspondence

V. C. Duance, Connective Tissue Biology Laboratories, Biomedical Sciences Building, School of Biosciences, Cardiff University, Museum Avenue Cardiff, Wales, UK, CF10 3US, UK. T: +44 29 20874111; F: +44 29 20874594; E: duance@cardiff.ac.uk

Accepted for publication 15 September 2008

distinct IVD cell populations, and whether there are differences with skeletal maturity.

The aim of this study was to characterize fully the abundance of the three major cytoskeletal elements – F-actin,  $\beta$ -tubulin and vimentin – in the NP and OAF of immature (7-day-old) and mature (18-month-old) bovine IVDs using a combination of scanning laser confocal microscopy, quantitative PCR and Western blotting to examine, in detail, network organization, mRNA and protein levels. Our study illustrates that there are both zonal (NP vs. OAF) and age-related (7 days vs. 18 months) differences in the cytoskeletal elements of the IVD, which may reflect the diverse phenotypic characteristics of the disc regions.

## Materials and methods

All chemicals were obtained from Sigma (Poole, UK) unless otherwise stated and were of analytical grade or above.

### Source of bovine intervertebral disc

Bovine tails from immature (7-day-old) and skeletally mature (18-month-old) steers were obtained from the abattoir within 6 h of slaughter. The NP and OAF were dissected out of the IVDs (cc1–cc5), snap frozen in liquid nitrogen and stored at  $-80^{\circ}\text{C}$  until required. Dissected NP and OAF from cc1–cc5 discs were pooled per animal and between four and six individual animals were utilized in this study. Accurate dissection of NP from OAF was verified by immunoblotting for type II and type I collagen, respectively (data not shown).

### Analysis of cytoskeletal element organization using confocal microscopy

Frozen cryosections (20  $\mu\text{m}$  thickness) of NP and OAF tissue were taken and fixed in 4% paraformaldehyde. After repeated washes in modified Hanks' balanced salt solution (mHBSS), tissue sections were permeabilized in 5% Triton X-100 and blocked with 10% goat serum prior to overnight incubation with anti-vimentin (V9 clone, 1 : 40) or anti- $\beta$ -tubulin (E7 clone, 1 : 100; Developmental Studies Hybridoma Bank, University of Iowa, Iowa City, IA, USA). Sections were washed extensively and incubated in goat anti-mouse fluorescein isothiocyanate FITC-conjugated secondary antibody (1 : 64) for 1 h. F-actin was stained with Alexa 488™ conjugated phalloidin (1 : 200; Molecular Probes, Invitrogen). Sections were mounted in Vectashield™ containing propidium iodide (10  $\mu\text{g mL}^{-1}$ )

(Vectashield, USA). Sections were examined using a Leica DM6000B upright digital microscope (Leica, Wetzlar, Germany) and controlled by the Leica Control software, set up for dual-channel fluorescence recordings as described previously (Blain et al. 2006). Representative cells were scanned using a 63 $\times$  oil immersion objective with appropriate excitation and emission settings for fluorescein isothiocyanate and propidium iodide. Negative controls, omitting the primary antibody, conducted in parallel were devoid of fluorescent signal (data not shown).

### Analysis of cytoskeletal element gene expression using quantitative PCR

Total RNA was extracted from both NP and OAF of bovine IVDs, and the absolute amounts of cytoskeletal genes expressed by the two cell populations were assessed using quantitative PCR. Tissue (50 mg) was powdered in a liquid-nitrogen cooled Mikro-Dismembrator (Braun Biotech) and 1 mL Trizol™ reagent (Invitrogen, UK) was added directly to the powdered tissue and warmed to room temperature. Following chloroform extraction, samples were precipitated with 70% ethanol and the RNA purified using Qiagen RNeasy™ mini kits according to the manufacturer's protocols (Qiagen, West Sussex, UK). First strand cDNA was synthesized (2  $\mu\text{L}$  RNA per 20  $\mu\text{L}$  reaction volume) using Superscript™ II reverse transcriptase (Invitrogen, Paisley, UK) according to the manufacturer's instructions and as previously described (Blain et al. 2003). Quantitative real-time PCR was performed using the Mx3000P® QPCR System (Stratagene, Edinburgh, UK) with primers designed to the open reading frame of  $\beta$ -actin,  $\beta$ -tubulin and vimentin (Table 1). Calculation of starting concentration was based on standard curves for each target DNA run in parallel. GAPDH was used as an internal reference of housekeeping gene transcription for normalization between different cDNA samples as described previously (Blain et al. 2006).

### Analysis of cytoskeletal element protein expression by Western blotting

Cytoskeletal proteins –  $\beta$ -actin,  $\beta$ -tubulin and vimentin – expressed by the NP and OAF were assessed using Western blotting. Due to the inability to extract sufficient amounts of intracellular proteins direct from the NP tissue, the NP and OAF tissue were subject to a short period of enzymatic digestion to release the cells prior to analysis. Tissue was finely minced and cells extracted from IVD tissue by rapid digestion, over 2 h, using 2.5  $\text{mg mL}^{-1}$  type I collagenase for OAF tissue (Wuertz et al. 2007) and 1  $\text{mg mL}^{-1}$  type II collagenase for NP tissue (Chelberg et al. 1995). Preparations were centrifuged (3000 r.p.m., 10 min), filtered through a cell strainer to

**Table 1** Primer sequences for real-time quantification of cytoskeletal genes

Gene	Primer sequence	Product size (bp)
$\beta$ -actin	Forward: 5'-TTCGAGACCTTCAACACCCC-3'	68*
	Reverse: 5'-GGCCAGAGGCATACAGGGA-3'	
$\beta$ -tubulin	Forward: 5'-GAGGAGGAGGTGGCCTAGAG-3'	175
	Reverse: 5'-GCTTTAATGGTGGTGCTGT-3'	
Vimentin	Forward: 5'-AAGGAAGAGATGGCTCGTCA-3'	164
	Reverse: 5'-TTGGTTTCCTCAGGTTTCAG-3'	

\*Campbell et al. (2007).



remove debris, cell viability confirmed (trypan blue exclusion) and preparations resuspended to yield  $3 \times 10^6$  cells mL<sup>-1</sup>. Total protein concentration was determined using the BCA kit (Pierce, UK) according to manufacturer's instructions, and a direct correlation of cell number and protein concentration was observed for the NP ( $R^2 = 0.968$ ) and OAF cells ( $R^2 = 0.988$ ). Cells were subsequently lysed in 2× sample buffer ( $1 \times 10^6$  cells  $100 \mu\text{L}^{-1}$  [0.06 M Tris pH 6.8, 2% (w/v) SDS, 10% (v/v) glycerol, 0.2% (w/v) bromophenol blue]) (Blain et al. 2001). Protein extracts were reduced with 2.5% (v/v) β-mercaptoethanol and denatured for 30 min at 60 °C. Protein, loaded on an equal cell number basis ( $5 \times 10^5$  cells), was separated on 10% polyacrylamide gels and transferred to PVDF membrane (Millipore, Dundee, UK) at room temperature for 60 min. Membranes were blocked with 3% milk, prior to immunoblotting with specific primary antibodies that recognize β-actin (AC15, 1:100, Abcam, Cambridge, UK), vimentin (V9, 1:400), and β-tubulin (E7, 1:500). Membranes were then incubated with HRP-conjugated sheep anti-mouse secondary antibody (1:10 000) and the HRP signal detected using Hyperfilm® and ECL® detection system (GE Healthcare, Bucks, UK), as described previously (Blain et al. 2006). All Western blots were scanned and differences in the chemiluminescence intensity of digitized bands were assessed using NIH IMAGE software.

### Statistical analysis

Data are presented as mean ± SE, with tissue derived from between four and six individual animals. Data was tested for normality (Anderson–Darling test) and equal variance. One-way analysis of variance (ANOVA) or paired t-test was carried out using SPSS 12.0 software. Differences were considered significant at *P*-values of less than 0.05.

## Results

### Differential F-actin organization and increased β-actin mRNA and protein expression in cells of the outer annulus fibrosus

F-actin organization, mRNA and protein expression were compared in the OAF and NP of young (7-day-old) and skeletally mature (18-month-old) IVDs (Fig. 1). The F-actin network, investigated using Alexa 488™-conjugated phalloidin in conjunction with confocal microscopy, was observed in dense punctate regions throughout the cytoplasm of both young (Fig. 1Ai) and mature (Fig. 1Aii) NP cells. In contrast, F-actin was distributed throughout the cytoplasm extending into the cell processes of young (Fig. 1Aiii) and mature (Fig. 1Aiv) OAF cells. There was no discernible difference in actin architecture between young (Fig. 1Ai,iii) and mature (Fig. 1Aii,iv) populations of IVD cells. To determine whether the zonal variations observed in F-actin distribution were purely organizational or were a consequence of altered gene or protein expression, β-actin mRNA and protein levels were assessed by quantitative PCR (Fig. 1B) and Western blotting (Fig. 1C), respectively. After normalization to the housekeeping gene GAPDH, significantly more β-actin mRNA was observed in the OAF compared with NP in both young ( $P = 0.008$ ) and mature

disc ( $P = 0.025$ ) (Fig. 1B). However, there was no age-related difference in β-actin mRNA levels between young and mature NP ( $P = 0.283$ ) or OAF ( $P = 0.304$ ). As there were zonal variations in β-actin mRNA levels, potential differences in protein expression were also investigated by Western blotting (Fig. 1C). Greater β-actin expression was found in young OAF cells compared with NP cells ( $P = 0.0159$ ) (Fig. 1C). However, there was no zonal variation in β-actin content in mature disc ( $P = 1.00$ ). Additionally, there were no age-related differences in the amount of β-actin protein detected in either NP or OAF cells ( $P = 0.6905$  and  $0.0537$ , respectively) (Fig. 1C).

### Increased β-tubulin mRNA and protein expression in cells of the nucleus pulposus

The architecture of the β-tubulin networks, as well as mRNA and protein expression, were compared in the OAF and NP of young (7-day-old) and skeletally mature IVDs (18-month-old). β-tubulin was observed throughout the cytoplasm in cells from NP and OAF tissue (Fig. 2A). Analysis of the confocal images indicated that there were no obvious differences in β-tubulin organization across the tissue zones or with skeletal maturity (Fig. 2Ai–iv). For completeness, we also investigated the relative amounts of β-tubulin mRNA (Fig. 2B) and protein (Fig. 2C) in the NP and OAF. Significantly more β-tubulin mRNA was detected in NP than in the OAF in both young ( $P = 0.023$ ) and mature IVD ( $P = 0.026$ ; Fig. 2B). However, there was no age-related difference in the expression of β-tubulin mRNA in the OAF ( $P = 0.071$ ) or in the NP ( $P = 0.829$ ). The changes observed at the mRNA level were confirmed at the protein level using Western blotting (Fig. 2C); significantly more β-tubulin protein was detected in NP cells than in OAF cells in both young ( $P = 0.0165$ ) and mature IVD ( $P = 0.0084$ ; Fig. 2C). As with mRNA levels, no age-related differences in β-tubulin protein expression were detected in NP ( $P = 0.114$ ) and OAF cells ( $P = 0.677$ ; Fig. 2C).

### Differential vimentin organization associated with age-related decreases in vimentin mRNA and protein expression in cells of the nucleus pulposus

The architecture of the vimentin intermediate filaments, as well as corresponding mRNA and protein levels were analysed in the NP and OAF of young and skeletally mature bovine IVDs (Fig. 3). Vimentin filaments were observed traversing the cytoplasm from the plasma to the nuclear membrane (Fig. 3A). Vimentin filaments were also observed extending into the cellular processes, especially in OAF cells (Fig. 3Aiii,iv). There was no discernible difference in vimentin architecture between young (Fig. 3Ai,iii) and mature IVD (Fig. 3Aii,iv). However, quantitative mRNA analysis demonstrated appreciably more vimentin mRNA in both young ( $P < 0.001$ ) and mature OAF ( $P = 0.002$ ; Fig. 3B), although

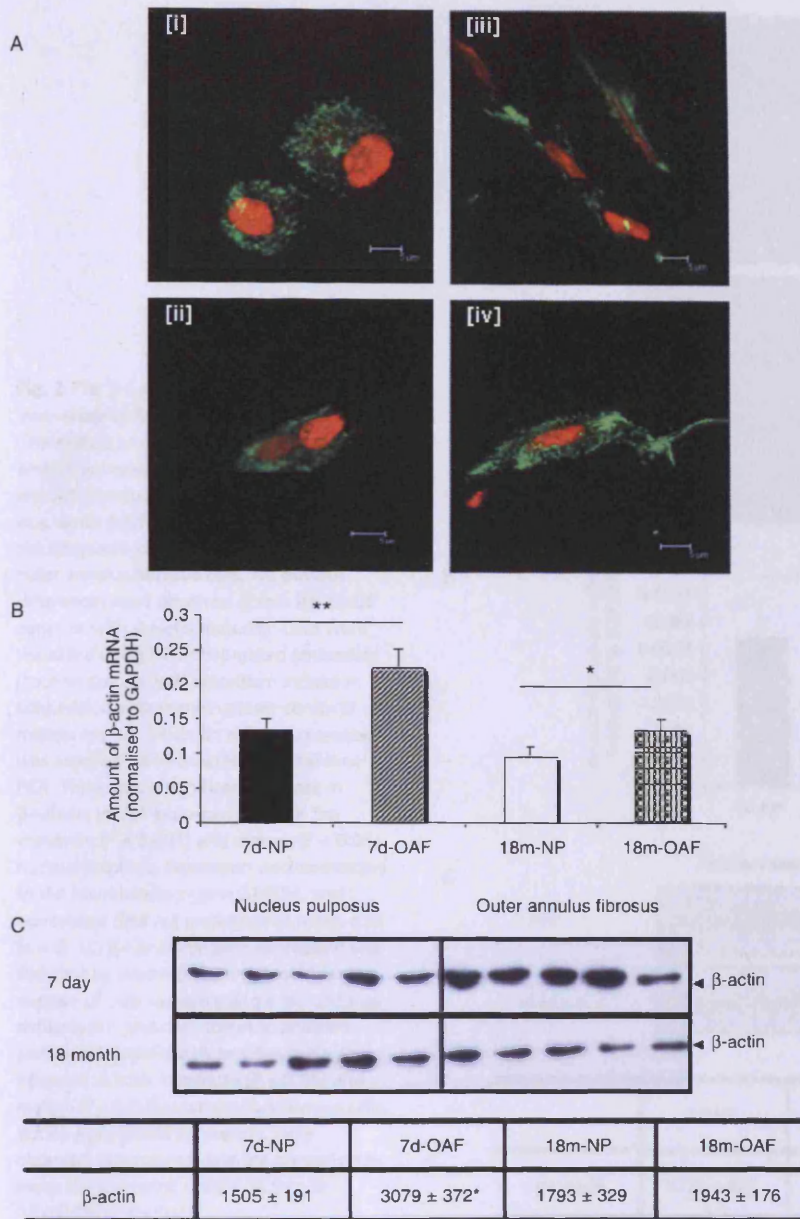


**Fig. 1** The actin cytoskeleton of intervertebral disc. (A) F-actin organization in (i) immature and (ii) mature nucleus pulposus and (iii) immature and (iv) mature outer annulus fibrosus discs. F-actin is predominantly punctate in nucleus pulposus cells, but extends into the processes of the outer annulus fibrosus cells; however, there were no striking differences with skeletal maturity. Cells were visualized using Alexa-488<sup>TM</sup>-phalloidin (counterstained with propidium iodide) in conjunction with scanning laser confocal microscopy.

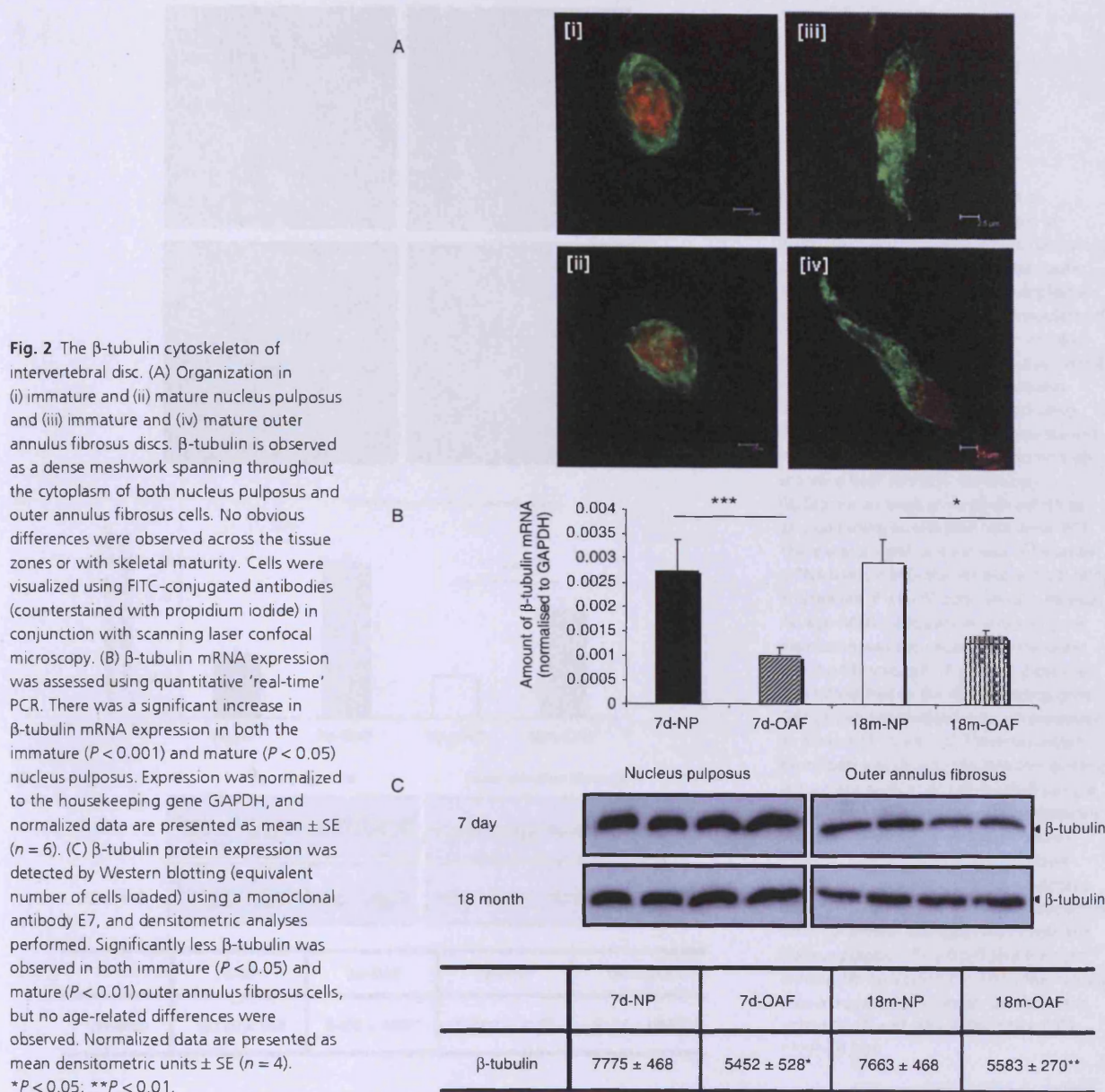
(B)  $\beta$ -actin mRNA expression was assessed using quantitative 'real-time' PCR. There was a significant increase in  $\beta$ -actin mRNA levels in both the immature ( $P < 0.01$ ) and mature ( $P < 0.05$ ) outer annulus fibrosus. Expression was normalized to the housekeeping gene GAPDH, and normalized data are presented as mean  $\pm$  SE ( $n = 6$ ). (C)  $\beta$ -actin protein expression was detected by Western blotting (equivalent number of cells loaded) using a monoclonal antibody AC15, and densitometric analyses performed. Significantly more  $\beta$ -actin was observed in immature outer annulus fibrosus cells ( $P < 0.05$ ), but no differences were observed in the mature disc cell populations. Normalized data are presented as mean densitometric units  $\pm$  SE ( $n = 5$ ). \* $P < 0.05$ ; \*\* $P < 0.01$ .

vimentin gene expression in the OAF decreased with skeletal maturity ( $P = 0.018$ ; Fig. 3B). There was no difference in vimentin mRNA levels in the NP with age ( $P = 0.154$ ). In contrast, Western blotting revealed less vimentin protein in the OAF than in the NP in both young ( $P = 0.0015$ ) and mature IVD ( $P = 0.001$ ; Fig. 3C). An age-related reduction in vimentin protein expression was also evident in both the NP ( $P = 0.007$ ) and the OAF cells ( $P = 0.04$ ; Fig. 3C).

## Discussion

Intervertebral discs, which are important for dissipating loads and providing flexibility to the spine, comprise at

least two distinct cell populations – cells of the NP are 'chondrocyte-like' in morphology, whereas those of the OAF appear 'fibroblast-like'. This likely reflects both the different matrix organization and the different mechanical characteristics of the disc regions (Urban & Roberts, 2003). The NP resists compressive loading, whereas the OAF mainly counteracts tensional forces *in vivo* (Klein et al. 1983). It has previously been hypothesized that the cytoskeleton, which in IVD cells comprises actin microfilaments, tubulin microtubules and vimentin intermediate filaments, can act as a transducer of mechanical signals in tissues including IVD (Chen et al. 2004; Chiquet et al. 2007), bone (Myers et al. 2007) and articular cartilage



(Durrant et al. 1999; Knight et al. 2006; Campbell et al. 2007). Furthermore, the presence/organization of specific cytoskeletal elements may reflect the diverse mechanical functions of these cells.

To date, there has been little characterization of the composition of the three major cytoskeletal elements in the IVD (Errington et al. 1998; Guilak et al. 1999; Bruhlmann et al. 2002; Johnson & Roberts, 2003; Li et al. 2007b), and none directly comparing the cytoskeletal composition of NP and OAF. Therefore, in this present study we have utilized a combination of scanning laser confocal microscopy, quantitative PCR and Western blotting to analyse the organization of and quantify F-actin,  $\beta$ -tubulin and vimentin

of NP and OAF cells *in situ* IVDs. Interestingly, our data demonstrate that the organization, mRNA and protein content of the cytoskeletal elements alter across the IVD, coincident with the two distinct cell populations.

Of the three major cytoskeletal elements, the composition of the actin cytoskeleton is most altered between the NP and OAF of bovine IVDs. F-actin is cytoplasmically punctate in its localization in NP cells. In the OAF, actin filaments are observed extending out into the cell processes, reflecting the fibroblast-like morphology (Dunlevy & Couchman, 1993; Baschong et al. 1997; Pritchard et al. 2002). The distinct localization of F-actin in the NP and OAF is evident in both young and mature IVD. As scanning laser confocal microscopy

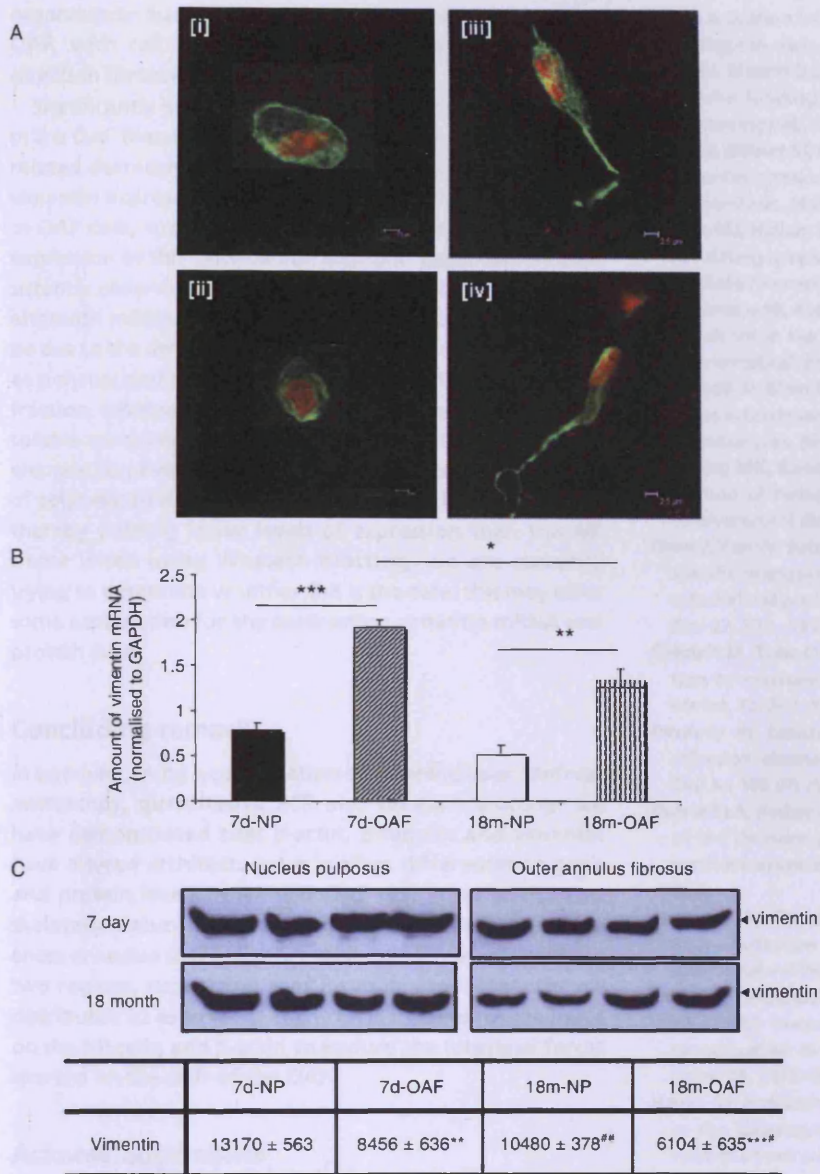


**Fig. 3** The vimentin cytoskeleton of intervertebral disc. (A) Organization in (i) immature and (ii) mature nucleus pulposus, and in (iii) immature and (iv) mature outer annulus fibrosus discs. Vimentin displays an extensive network traversing the cytoplasm of both nucleus pulposus and outer annulus fibrosus cells; vimentin filaments also extend into the processes of the outer annulus fibrosus cells. Cells were visualized using FITC-conjugated antibodies (counterstained with propidium iodide) in conjunction with scanning laser confocal microscopy.

(B) Expression levels of vimentin mRNA as assessed using quantitative 'real-time' PCR. There was a significant increase in vimentin mRNA levels in both the immature ( $P < 0.001$ ) and mature ( $P < 0.01$ ) outer annulus fibrosus. An age-related decrease in vimentin gene expression was also observed in the outer annulus fibrosus cells ( $P < 0.05$ ). Expression was normalized to the housekeeping gene GAPDH, and normalized data are presented as mean  $\pm$  SE ( $n = 6$ ). (C) Vimentin protein expression was detected by Western blotting (equivalent number of cells loaded) using a monoclonal antibody V9, and densitometric analyses performed. Significantly more vimentin was observed in the immature ( $*P < 0.002$ ) and mature nucleus pulposus cells ( $*P < 0.001$ ). An age-related reduction in vimentin protein was observed in both the nucleus pulposus ( $^{\#}P = 0.01$ ) and the outer annulus fibrosus cells ( $^{\#}P < 0.05$ ). Normalized data are presented as mean densitometric units  $\pm$  SE ( $N = 5$ ).  $*P < 0.05$ ;  $**P < 0.01$ ,  $***P < 0.001$ .

can only indicate cell morphology and is not quantitative, both mRNA and protein levels were also analysed to determine whether there were inherent differences in expression levels. Interestingly,  $\beta$ -actin mRNA levels were significantly higher in OAF than in NP cells, irrespective of age. This trend was also reflected in enhanced  $\beta$ -actin protein amounts in the OAF cells; however, this was only true for young IVD and not mature IVD.

To date, the microtubular networks have not been characterized in IVD cells; our study demonstrates that  $\beta$ -tubulin is expressed in cells of the NP and OAF. In both cell populations,  $\beta$ -tubulin forms an extensive meshwork throughout the cytoplasm correlating with its organization in chondrocytes (Blain et al. 2006). In contrast to  $\beta$ -actin, there is significantly more  $\beta$ -tubulin mRNA in NP than in

OAF cells, irrespective of age; this increase in  $\beta$ -tubulin mRNA is also reflected in the increased protein expression.

Vimentin is a highly expressed cytoskeletal protein providing the cell with rigidity; the dense meshwork of filaments supports the cell shape (Brown et al. 2001) and acts to absorb mechanical loads (Kreplak et al. 2005). The vimentin intermediate filaments of the NP were displayed as a dense meshwork that traversed the cytoplasm from the plasma to the nuclear membrane. The organization of vimentin in cells of the NP is characteristic of articular chondrocytes (Postacchini et al. 1982; Durrant et al. 1999; Langelier et al. 2000; Blain et al. 2006) and cells of the meniscus (Hellio Le Graverand et al. 2001). In the OAF, vimentin filaments were observed throughout the cytoplasm as well as extending into the cell processes. This

organization has previously been reported in cells of the OAF, with cell processes parallel to the collagen fibre direction (Bruehlmann et al. 2002).

Significantly higher vimentin mRNA levels were observed in the OAF than in the NP cells, although there was an age-related decrease in the OAF. This age-related reduction in vimentin expression was also evident at the protein level in OAF cells, suggestive of a transcriptional shutdown in expression of this cytoskeletal element. However, we consistently observed more vimentin protein in the NP tissue, although mRNA levels were shown to decrease. This may be due to the dynamic nature of the intermediate filaments, as polymerized vimentin is associated with the insoluble fraction, whereas the depolymerized monomers form the soluble component (Chen et al. 2004). If the cytoskeletal element turnover is more dynamic in OAF cells, the amount of polymerized vimentin may not represent the total amount, thereby yielding lower levels of expression than the NP tissue when using Western blotting; we are currently trying to determine whether this is the case; this may offer some explanation for the contrasting vimentin mRNA and protein data.

## Concluding remarks

In summary, using a combination of scanning laser confocal microscopy, quantitative PCR and Western blotting, we have demonstrated that  $\beta$ -actin,  $\beta$ -tubulin and vimentin have altered architectures as well as differences in gene and protein levels in NP and OAF cells from young and skeletally mature IVD. It is hypothesized that these differences arise due to the distinct mechanical features of these two regions, suggesting that  $\beta$ -tubulin and vimentin are distributed so as to resist the effects of compressive loads on the NP cells, and  $\beta$ -actin to endure the tensional forces exerted on the cells of the OAF.

## Acknowledgements

We would like to acknowledge funding from the EPSRC (Dorothy Hodgkin Postgraduate Award – S.L.) and Arthritis Research Campaign (Grant No. 14874 and 18221: E.J.B.). The E7 monoclonal antibody developed by Michael Klymkowsky was obtained from the Developmental Studies Hybridoma Bank developed under the auspices of the NICHD and maintained by the University of Iowa, Department of Biological Sciences, Iowa City, IA 52242, USA.

## References

- Baschong W, Sutterlin R, Aebi U (1997) Punch-wounded, fibroblast populated collagen matrices: a novel approach for studying cytoskeletal changes in three dimensions by confocal laser scanning microscopy. *Eur J Cell Biol* **72**, 189–201.
- Benjamin M, Archer CW, Ralphs JR (1994) Cytoskeleton of cartilage cells. *Microsc Res Tech* **28**, 372–377.
- Blain EJ, Gilbert SJ, Wardale RJ, Capper SJ, Mason DJ, Duance VC (2001) Up-regulation of matrix metalloproteinase expression and activation following cyclical compressive loading of articular cartilage in vitro. *Arch Biochem Biophys* **396**, 49–55.
- Blain EJ, Mason DJ, Duance VC (2003) The effect of cyclical compressive loading on gene expression in articular cartilage. *Biorheology* **40**, 111–117.
- Blain EJ, Gilbert SJ, Hayes AJ, Duance VC (2006) Disassembly of the vimentin cytoskeleton disrupts articular cartilage chondrocyte homeostasis. *Matrix Biol* **25**, 398–408.
- Brown MJ, Hallam JA, Colucci-Guyon E, Shaw S (2001) Rigidity of circulating lymphocytes is primarily conferred by vimentin intermediate filaments. *J Immunol* **166**, 6640–6646.
- Bruehlmann SB, Rattner JB, Matyas JR, Duncan NA (2002) Regional variations in the cellular matrix of the annulus fibrosus of the intervertebral disc. *J Anat* **201**, 159–171.
- Campbell JJ, Blain EJ, Chowdhury TT, Knight MM (2007) Loading alters actin dynamics and up-regulates cofilin gene expression in chondrocytes. *Biochem Biophys Res Commun* **361**, 329–334.
- Chelberg MK, Banks GM, Geiger DF, Oegema TR, JR (1995) Identification of heterogeneous cell populations in normal human intervertebral disc. *J Anat* **186** (Pt 1), 43–53.
- Chen J, Yan W, Setton LA (2004) Static compression induces zonal-specific changes in gene expression for extracellular matrix and cytoskeletal proteins in intervertebral disc cells in vitro. *Matrix Biol* **22**, 573–583.
- Chiquet M, Tunc-Civelek V, Sarasa-Renedo A (2007) Gene regulation by mechanotransduction in fibroblasts. *Appl Physiol Nutr Metab* **32**, 967–973.
- Dunlevy JR, Couchman JR (1993) Controlled induction of focal adhesion disassembly and migration in primary fibroblasts. *J Cell Sci* **105** (Pt 2), 489–500.
- Durrant LA, Archer CW, Benjamin M, Ralphs JR (1999) Organisation of the chondrocyte cytoskeleton and its response to changing mechanical conditions in organ culture. *J Anat* **194** (Pt 3), 343–353.
- Errington RJ, Puustjarvi K, White IR, Roberts S, Urban JP (1998) Characterisation of cytoplasm-filled processes in cells of the intervertebral disc. *J Anat* **192** (Pt 3), 369–378.
- Guilak F, Ting-Beall HP, Baer AE, Trickey WR, Erickson GR, Setton LA (1999) Viscoelastic properties of intervertebral disc cells. Identification of two biomechanically distinct cell populations. *Spine* **24**, 2475–2483.
- Hayes AJ, Benjamin M, Ralphs JR (1999) Role of actin stress fibres in the development of the intervertebral disc: cytoskeletal control of extracellular matrix assembly. *Dev Dyn* **215**, 179–189.
- Hellio Le Graverand MP, Ou Y, Schield-Yee T, et al. (2001) The cells of the rabbit meniscus: their arrangement, interrelationship, morphological variations and cytoarchitecture. *J Anat* **198**, 525–535.
- Iatridis JC, Weidenbaum M, Setton LA, Mow VC (1996) Is the nucleus pulposus a solid or a fluid? Mechanical behaviors of the nucleus pulposus of the human intervertebral disc. *Spine* **21**, 1174–1184.
- Johnson WE, Roberts S (2003) Human intervertebral disc cell morphology and cytoskeletal composition: a preliminary study of regional variations in health and disease. *J Anat* **203**, 605–612.
- Klein JA, Hickey DS, Hukins DW (1983) Radial bulging of the annulus fibrosus during compression of the intervertebral disc. *J Biomech* **16**, 211–217.
- Knight MM, Toyoda T, Lee DA, Bader DL (2006) Mechanical compression and hydrostatic pressure induce reversible changes in actin cytoskeletal organisation in chondrocytes in agarose. *J Biomech* **39**, 1547–1551.

- Kreplak L, Bar H, Leterrier JF, Herrmann H, Aebi U** (2005) Exploring the mechanical behavior of single intermediate filaments. *J Mol Biol* **354**, 569–577.
- Langelier E, Suetterlin R, Hoemann CD, Aebi U, Buschmann MD** (2000) The chondrocyte cytoskeleton in mature articular cartilage: structure and distribution of actin, tubulin, and vimentin filaments. *J Histochem Cytochem* **48**, 1307–1320.
- Li H, Li S, Wu TJ, Xu Y, Chen YX** (2007a) Early effects of the cyclic uniaxial compressive stress on actin and vimentin of the rat condylar chondrocytes [in Chinese]. *Hua Xi Kou Qiang Yi Xue Za Zhi* **25**, 422–425.
- Li S, Duance VC, Blain EJ** (2007b) F-actin cytoskeletal organization in intervertebral disc health and disease. *Biochem Soc Trans* **35**, 683–685.
- Myers KA, Rattner JB, Shrive NG, Hart DA** (2007) Osteoblast-like cells and fluid flow: cytoskeleton-dependent shear sensitivity. *Biochem Biophys Res Commun* **364**, 214–219.
- Postacchini F, Bellocchi M, Ricciardi-Pollini PT, Modesti A** (1982) An ultrastructural study of recurrent disc herniation: a preliminary report. *Spine* **7**, 492–497.
- Pritchard S, Erickson GR, Guilak F** (2002) Hyperosmotically induced volume change and calcium signaling in intervertebral disk cells: the role of the actin cytoskeleton. *Biophys J* **83**, 2502–2510.
- Setton LA, Chen J** (2006) Mechanobiology of the intervertebral disc and relevance to disc degeneration. *J Bone Joint Surg Am* **88** (Suppl. 2), 52–57.
- Thyberg J, Moskalewski S** (1999) Role of microtubules in the organization of the Golgi complex. *Exp Cell Res* **246**, 263–279.
- Urban JP, Roberts S** (2003) Degeneration of the intervertebral disc. *Arthritis Res Ther* **5**, 120–130.
- Urban JP, Hall AC, Gehl KA** (1993) Regulation of matrix synthesis rates by the ionic and osmotic environment of articular chondrocytes. *J Cell Physiol* **154**, 262–270.
- Wang DL, Jiang SD, Dai LY** (2007) Biologic response of the intervertebral disc to static and dynamic compression in vitro. *Spine* **32**, 2521–2528.
- Weidenbaum M, Foster RJ, Best BA, et al.** (1992) Correlating magnetic resonance imaging with the biochemical content of the normal human intervertebral disc. *J Orthop Res* **10**, 552–561.
- Wuertz K, Urban JP, Klasen J, et al.** (2007) Influence of extracellular osmolarity and mechanical stimulation on gene expression of intervertebral disc cells. *J Orthop Res* **25**, 1513–1522.

# F-actin cytoskeletal organization in intervertebral disc health and disease

S. Li, V.C. Duance<sup>1</sup> and E.J. Blain

Connective Tissue Biology Laboratories, School of Biosciences, Cardiff University, Cardiff CF10 3US, U.K.

## Abstract

The cytoskeleton, which in most cell types, including the intervertebral disc described here, comprises microfilaments, microtubules and intermediate filaments, plays important functions in many fundamental cellular events, including cell division, motility, protein trafficking and secretion. The cytoskeleton is also critical for communication; for example, alterations to the architecture of the F-actin (filamentous actin) cytoskeletal networks can affect communication between the cells and the extracellular matrix, potentially compromising tissue homeostasis. Although there are limited studies to date, this paper aims to review current knowledge on F-actin cytoskeletal element organization in intervertebral disc cells, how F-actin differs with pathology and its implications for mechanotransduction.

## Introduction

IVD (intervertebral disc) degeneration, the leading cause of age-related chronic axial low back pain [1], results in a dramatic change in cell metabolism and ECM (extracellular matrix) turnover of the IVD with age [2–4]. This loss of tissue homeostasis probably results from a change in cell signalling due to alterations in cell–ECM interactions. The IVD comprises three morphologically distinct zones namely the NP (nucleus pulposus) at the centre of the disc in which the resident cells are considered to be ‘chondrocyte-like’, the IAF (inner annulus fibrosus) and the OAF (outer annulus fibrosus), at the periphery of the disc, where the cells are considered to be ‘fibroblast-like’. Variations in cell shape and cytoskeletal element organization have been reported within and between defined zones of the IVD [5].

## F-actin (filamentous actin) cytoskeletal organization in IVD health and disease

Regional variations in the organization of the F-actin cytoskeletal networks across all regions of the disc have been reported previously [5]. As the F-actin cytoskeleton plays such a fundamental role in mechanotransduction between the ECM and IVD cells [6,7], it is likely that dysregulation of the cytoskeletal networks may promote an imbalance in IVD homeostasis favouring a catabolic phenotype which is characteristic of degenerative disc disease. In agreement with the studies of Breuhmann et al. [5], we have also demonstrated a clear difference in F-actin organization between the cells of bovine NP and OAF (Figure 1). Immunofluorescence (Alexa Fluor<sup>®</sup> 488–phalloidin labelling) in conjunction with

confocal microscopy demonstrated an extensive punctate distribution of F-actin throughout the cytoplasm of NP cells (Figure 1A); in comparison, F-actin was localized primarily to the cell processes of the OAF (Figure 1B), as reported previously [5,8]. Unlike others, we have also quantified levels of  $\beta$ -actin mRNA, and, after normalization to GAPDH (glyceraldehyde-3-phosphate dehydrogenase), significantly more  $\beta$ -actin mRNA was observed in OAF compared with NP, in both young and mature disc (Figure 2); this indicates that the differences in F-actin distribution (Figure 1) are also reflected in altered actin levels in these IVD cells.

Although there are zonal differences in  $\beta$ -actin organization and expression in the IVD, we found no age-related changes in  $\beta$ -actin organization between the NP (Figure 1C) and OAF (Figure 1D) or in their mRNA expression (Figure 2). The discs used in this study were obtained from 7-day- and 18-month-old bovine tails where degeneration is not a classical feature. To date, there are no reports of age-related differences in F-actin organization.

However, F-actin organization has been reported to alter dramatically between pathological ‘scoliotic’ and non-pathological human IVD cells. Roberts et al. [3] reported that the cells in the OAF of scoliotic discs were F-actin-positive; F-actin was predominantly absent from ‘normal’ discs [3]. In the same study, F-actin was observed, albeit variably, in the IAF and NP of pathological disc cells, but again was rarely observed in ‘normal’ discs. There was a negative correlation between the frequency of F-actin-positive cells with age in the OAF and IAF/NP [3]. Although one would expect to observe F-actin in ‘normal’ disc, as has been observed in bovine discs (Figure 1) and reported previously [5,8], the lack of F-actin labelling may provide an insight into age-related differences, as the normal discs were generally from donors >70 years old, whereas the pathological discs were from donors <20 years old. Collectively, these disparities in F-actin distribution are likely to contribute to the distinct mechanical characteristics of the two IVD regions.

**Key words:** actin, aging, cytoskeleton, intervertebral disc, mechanotransduction.

**Abbreviations used:** ECM, extracellular matrix; F-actin, filamentous actin; GAPDH, glyceraldehyde-3-phosphate dehydrogenase; IAF, inner annulus fibrosus; IVD, intervertebral disc; NP, nucleus pulposus; OAF, outer annulus fibrosus.

<sup>1</sup>To whom correspondence should be addressed (email [duance@cardiff.ac.uk](mailto:duance@cardiff.ac.uk)).

**Figure 1** | Immunofluorescent localization of F-actin in young (A) NP and (B) OAF, and mature (C) NP and (D) OAF bovine IVD. F-actin was labelled with Alexa Fluor<sup>®</sup> 488-phalloidin and the nuclei were counterstained with propidium iodide. Tissue sections were visualized by confocal microscopy, and the images are three-dimensional reconstructions of serial sections.

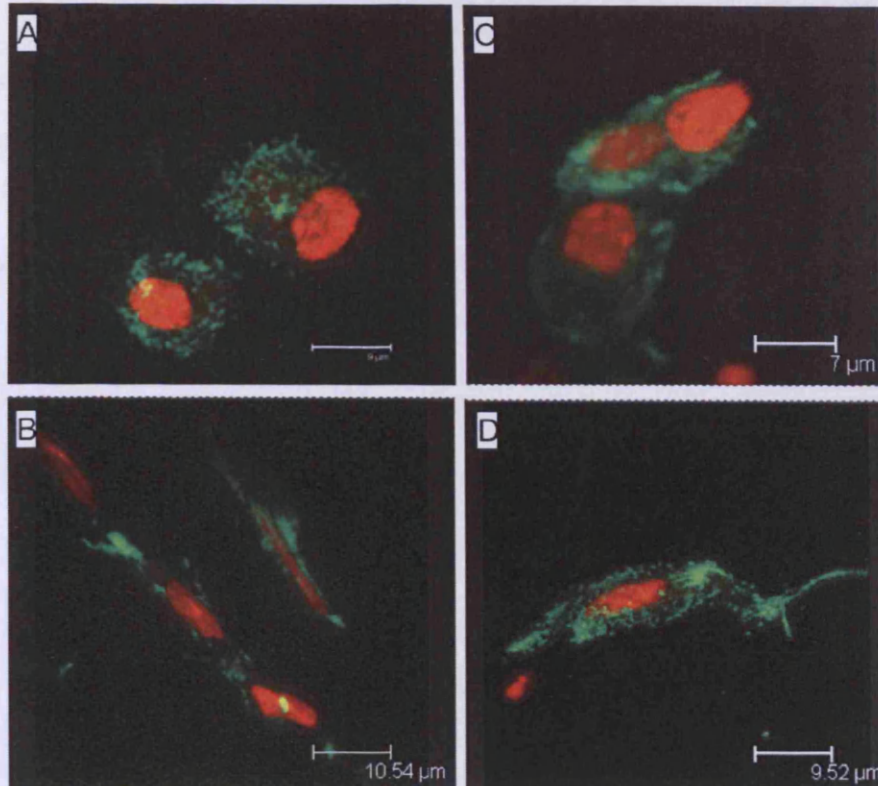
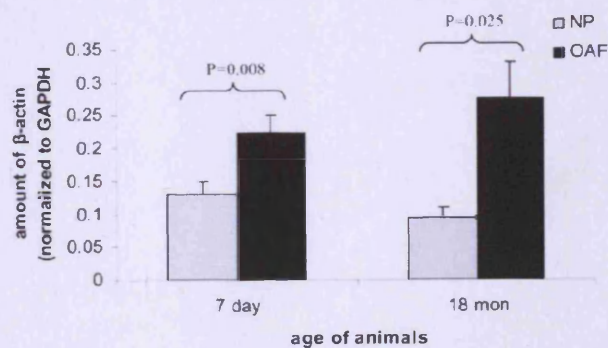


**Figure 2** |  $\beta$ -Actin mRNA expression in the NP and OAF of 7-day- and 18-month-old bovine IVDs, as assessed using quantitative PCR. Data are normalized to the housekeeping gene GAPDH. Results are means  $\pm$  S.E.M. ( $n=6$ ). Significantly more  $\beta$ -actin mRNA was detected in the OAF compared with the NP in both young and mature disc.



functions primarily to withstand tensional forces *in vivo* [9]. The tensile-bearing capacity of the IVD is attributed to the organization of the F-actin networks in the OAF. F-actin is localized to 'cell processes' in the OAF (Figure 1), as reported previously [5,10], which are believed to act as a mechanism for mechanosensing. Our results suggest that F-actin may play a more important role in transducing signals generated by tensile stress compared with compressive stress. Interestingly, F-actin-positive cells were observed more frequently in disc specimens from the convex side of the scoliotic curve, where the cells are under tension, as opposed to the concave side, which is under compression [3]. This coincides with previous studies that demonstrate alterations in the actin cytoskeleton during the cellular response to mechanotransduction. F-actin was shown to reorganize, in cells of the annulus fibrosus, in response to static compression, indicating the role of F-actin in resisting osmotic stress [11].

### Implications of F-actin cytoskeleton in IVD mechanotransduction

Owing to the composition of the disc ECM, the NP functions in resisting compressive loading, whereas the OAF

### Concluding comments

We and others have demonstrated that there are both zonal- and pathology- (and possibly age-) related changes in IVD actin filament organization. Further, we postulate that the significant difference in F-actin organization and expression



between the OAF and NP cells will affect mechanotransduction, leading to a loss of tissue homeostasis as observed in disc pathologies such as scoliosis and age-related degeneration.

We acknowledge funding from the EPSRC (Engineering and Physical Sciences Research Council) (Dorothy Hodgkin Postgraduate Award to S.L.) and Arthritis Research Campaign (grant no. 14874 to E.J.B.).

## References

- 1 Waddell, G. (1991) *Neurosurg. Clin. N. Am.* **2**, 719-738
- 2 Goupille, P., Jayson, M.I., Valat, J.P. and Freemont, A.J. (1998) *Spine* **23**, 1612-1626
- 3 Roberts, S., Caterson, B., Menage, J., Evans, E.H., Jaffray, D.C. and Eisenstein, S.M. (2000) *Spine* **25**, 3005-3013
- 4 Le Maitre, C.L., Freemont, A.J. and Hoyland, J.A. (2004) *J. Pathol.* **204**, 47-54
- 5 Bruehlmann, S.B., Rattner, J.B., Matyas, J.R. and Duncan, N.A. (2002) *J. Anat.* **201**, 159-171
- 6 Hayes, A.J., Benjamin, M. and Ralphs, J.R. (1999) *Dev. Dyn.* **215**, 179-189
- 7 Chen, J., Yan, W. and Setton, L.A. (2004) *Matrix Biol.* **22**, 573-583
- 8 Guilak, F., Ting-Beall, H.P., Baer, A.E., Trickey, W.R., Erickson, G.R. and Setton, L.A. (1999) *Spine* **24**, 2475-2483
- 9 Klein, J.A., Hickey, D.S. and Hukins, D.W. (1983) *J. Biomed. Eng.* **16**, 211-217
- 10 Errington, R.J., Puustjarvi, K., White, I.R., Roberts, S. and Urban, J.P. (1998) *J. Anat.* **192**, 369-378
- 11 Pritchard, S. and Guilak, F. (2004) *Ann. Biomed. Eng.* **32**, 103-111

Received 30 March 2007

